



Quantum chromodynamics and other field theories on the light cone

Stanley J. Brodsky^a, Hans-Christian Pauli^b, Stephen S. Pinsky^c

^a *Stanford Linear Accelerator Center, Stanford University, Stanford, CA 94309, USA*

^b *Max-Planck-Institut für Kernphysik, D-69029 Heidelberg, Germany*

^c *Ohio State University, Columbus, OH 43210, USA*

Received October 1997; editor: R. Petronzio

Contents

1. Introduction	302	4.2. Quantum chromodynamics in 1 + 1 dimensions (KS)	362
2. Hamiltonian dynamics	307	4.3. The Hamiltonian operator in 3 + 1 dimensions (BL)	366
2.1. Abelian gauge theory: quantum electrodynamics	308	4.4. The Hamiltonian matrix and its regularization	376
2.2. Non-abelian gauge theory: Quantum chromodynamics	311	4.5. Further evaluation of the Hamiltonian matrix elements	381
2.3. Parametrization of space–time	313	4.6. Retrieving the continuum formulation	381
2.4. Forms of Hamiltonian dynamics	315	4.7. Effective interactions in 3 + 1 dimensions	385
2.5. Parametrizations of the front form	317	4.8. Quantum electrodynamics in 3 + 1 dimensions	389
2.6. The Poincaré symmetries in the front form	319	4.9. The Coulomb interaction in the front form	393
2.7. The equations of motion and the energy–momentum tensor	322	5. The impact on hadronic physics	395
2.8. The interactions as operators acting in Fock space	327	5.1. Light-cone methods in QCD	395
3. Bound states on the light cone	329	5.2. Moments of nucleons and nuclei in the light-cone formalism	402
3.1. The hadronic eigenvalue problem	330	5.3. Applications to nuclear systems	407
3.2. The use of light-cone wavefunctions	334	5.4. Exclusive nuclear processes	409
3.3. Perturbation theory in the front form	336	5.5. Conclusions	411
3.4. Example 1: The $q\bar{q}$ -scattering amplitude	338	6. Exclusive processes and light-cone wavefunctions	412
3.5. Example 2: Perturbative mass renormalization in QED (KS)	341	6.1. Is PQCD factorization applicable to exclusive processes?	414
3.6. Example 3: The anomalous magnetic moment	345	6.2. Light-cone quantization and heavy particle decays	415
3.7. (1 + 1)-dimensional: Schwinger model (LB)	349	6.3. Exclusive weak decays of heavy hadrons	416
3.8. (3 + 1)-dimensional: Yukawa model	352	6.4. Can light-cone wavefunctions be measured?	418
4. Discretized light-cone quantization	358		
4.1. Why discretized momenta?	360		

QUANTUM CHROMODYNAMICS AND OTHER FIELD THEORIES ON THE LIGHT CONE

Stanley J. BRODSKY^a, Hans-Christian PAULI^b, Stephen S. PINSKY^c

^a*Stanford Linear Accelerator Center, Stanford University, Stanford, CA 94309, USA*

^b*Max-Planck-Institut für Kernphysik, D-69029 Heidelberg, Germany*

^c*Ohio State University, Columbus, OH 43210, USA*



ELSEVIER

AMSTERDAM – LAUSANNE – NEW YORK – OXFORD – SHANNON – TOKYO

7. The light-cone vacuum	419	9.2. Flavor symmetries	450
7.1. Constrained zero modes	419	9.3. Quantum chromodynamics	453
7.2. Physical picture and classification of zero modes	429	9.4. Physical multiplets	454
7.3. Dynamical zero modes	434	10. The prospects and challenges	456
8. Non-perturbative regularization and renormalization	436	Appendix A. General conventions	460
8.1. Tamm–Dancoff Integral equations	437	Appendix B. The Lepage–Brodsky convention (LB)	462
8.2. Wilson renormalization and confinement	442	Appendix C. The Kogut–Soper convention (KS)	463
9. Chiral symmetry breaking	446	Appendix D. Comparing BD- with LB-spinors	465
9.1. Current algebra	447	Appendix E. The Dirac–Bergmann method	466
		References	476

Abstract

In recent years light-cone quantization of quantum field theory has emerged as a promising method for solving problems in the strong coupling regime. The approach has a number of unique features that make it particularly appealing, most notably, the ground state of the free theory is also a ground state of the full theory. We discuss the light-cone quantization of gauge theories from two perspectives: as a calculational tool for representing hadrons as QCD bound states of relativistic quarks and gluons, and also as a novel method for simulating quantum field theory on a computer. The light-cone Fock state expansion of wavefunctions provides a precise definition of the parton model and a general calculus for hadronic matrix elements. We present several new applications of light-cone Fock methods, including calculations of exclusive weak decays of heavy hadrons, and intrinsic heavy-quark contributions to structure functions. A general non-perturbative method for numerically solving quantum field theories, “discretized light-cone quantization”, is outlined and applied to several gauge theories. This method is invariant under the large class of light-cone Lorentz transformations, and it can be formulated such that ultraviolet regularization is independent of the momentum space discretization. Both the bound-state spectrum and the corresponding relativistic light-cone wavefunctions can be obtained by matrix diagonalization and related techniques. We also discuss the construction of the light-cone Fock basis, the structure of the light-cone vacuum, and outline the renormalization techniques required for solving gauge theories within the Hamiltonian formalism on the light cone. © 1998 Elsevier Science B.V. All rights reserved.

PACS: 11.10.Ef; 11.15.Tk; 12.38.Lg; 12.40.Yx

1. Introduction

One of the outstanding central problems in particle physics is the determination of the structure of hadrons such as the proton and neutron in terms of their fundamental quark and gluon degrees of freedom. Over the past 20 years, two fundamentally different pictures of hadronic matter have developed. One, the constituent quark model (CQM) [469], or the quark parton model [144,145], is closely related to experimental observation. The other, quantum chromodynamics (QCD) is based on a covariant non-abelian quantum field theory. The front form of QCD [172] appears to be the only hope of reconciling these two. This elegant approach to quantum field theory is a Hamiltonian gauge-fixed formulation that avoids many of the most difficult problems in the equal-time formulation of the theory. The idea of deriving a front form constituent quark model from QCD actually dates from the early 1970s, and there is a rich literature on the subject [74,119,135,30,6,120,304,305,332,350,87,88,235–237]. The main thrust of this review will be to discuss the complexities that are unique to this formulation of QCD, and other quantum field theories, in varying degrees of detail. The goal is to present a self-consistent framework rather than trying to cover the subject exhaustively. We will attempt to present sufficient background material to allow the reader to see some of the advantages and complexities of light-front field theory. We will, however, not undertake to review all of the successes or applications of this approach. Along the way we clarify some obscure or little-known aspects, and offer some recent results.

The light-cone wavefunctions encode the hadronic properties in terms of their quark and gluon degrees of freedom, and thus all hadronic properties can be derived from them. In the CQM, hadrons are relativistic bound states of a few confined quark and gluon quanta. The momentum distributions of quarks making up the nucleons in the CQM are well-determined experimentally from deep inelastic lepton scattering measurements, but there has been relatively little progress in computing the basic wavefunctions of hadrons from first principles. The bound-state structure of hadrons plays a critical role in virtually every area of particle physics phenomenology. For example, in the case of the nucleon form factors and open charm photoproduction the cross sections depend not only on the nature of the quark currents, but also on the coupling of the quarks to the initial and final hadronic states. Exclusive decay processes will be studied intensively at *B*-meson factories. They depend not only on the underlying weak transitions between the quark flavors, but also the wavefunctions which describe how *B*-mesons and light hadrons are assembled in terms of their quark and gluon constituents. Unlike the leading twist structure functions measured in deep inelastic scattering, such exclusive channels are sensitive to the structure of the hadrons at the amplitude level and to the coherence between the contributions of the various quark currents and multi-parton amplitudes. In electro-weak theory, the central unknown required for reliable calculations of weak decay amplitudes are the hadronic matrix elements. The coefficient functions in the operator product expansion needed to compute many types of experimental quantities are essentially unknown and can only be estimated at this point. The calculation of form factors and exclusive scattering processes, in general, depend in detail on the basic amplitude structure of the scattering hadrons in a general Lorentz frame. Even the calculation of the magnetic moment of a proton requires wavefunctions in a boosted frame. One thus needs a practical computational method for QCD which not only determines its spectrum, but which can provide also the non-perturbative hadronic matrix elements needed for general calculations in hadron physics.

An intuitive approach for solving relativistic bound-state problems would be to solve the gauge-fixed Hamiltonian eigenvalue problem. The natural gauge for light-cone Hamiltonian theories is the light-cone gauge $A^+ = 0$. In this physical gauge the gluons have only two physical transverse degrees of freedom. One imagines that there is an expansion in multi-particle occupation number Fock states. The solution of this problem is clearly a formidable task, and if successful, would allow one to calculate the structure of hadrons in terms of their fundamental degrees of freedom. But even in the case of the simpler abelian quantum theory of electrodynamics very little is known about the nature of the bound-state solutions in the strong-coupling domain. In the non-abelian quantum theory of chromodynamics, a calculation of bound-state structure has to deal with many difficult aspects of the theory simultaneously: confinement, vacuum structure, spontaneous breaking of chiral symmetry (for massless quarks), and describing a relativistic many-body system with unbounded particle number. The analytic problem of describing QCD bound states is compounded not only by the physics of confinement, but also by the fact that the wavefunction of a composite of relativistic constituents has to describe systems of an arbitrary number of quanta with arbitrary momenta and helicities. The conventional Fock state expansion based on equal-time quantization becomes quickly intractable because of the complexity of the vacuum in a relativistic quantum field theory. Furthermore, boosting such a wavefunction from the hadron's rest frame to a moving frame is as complex a problem as solving the bound-state problem itself. In modern textbooks on quantum field theory [242,342], one therefore hardly finds any trace of a Hamiltonian. This reflects the contemporary conviction that the concept of a Hamiltonian is old-fashioned and littered with all kinds of almost intractable difficulties. The presence of the square root operator in the equal-time Hamiltonian approach presents severe mathematical difficulties. Even if these problems could be solved, the eigensolution is only determined in its rest system as noted above.

Actually, the action and the Hamiltonian principle in some sense are complementary, and both have their own virtues. In solvable models they can be translated into each other. In the absence of such, it depends on the kind of problem one is interested in: The action method is particularly suited for calculating cross sections, while the Hamiltonian method is more suited for calculating bound states. Considering composite systems, systems of many constituent particles subject to their own interactions, the Hamiltonian approach seems to be indispensable in describing the connections between the constituent quark model, deep inelastic scattering, exclusive process, etc. In the CQM, one always describes mesons as made of a quark and an anti-quark, and baryons as made of three quarks (or three anti-quarks). These constituents are bound by some phenomenological potential which is tuned to account for the hadron's properties such as masses, decay rates or magnetic moments. The CQM does not display any visible manifestation of spontaneous chiral symmetry breaking; actually, it totally prohibits such a symmetry since the constituent masses are large on a hadronic scale, typically of the order of one-half of a meson mass or one-third of a baryon mass. Standard values are 330 MeV for the up- and down-quark, and 490 MeV for the strange-quark, very far from the "current" masses of a few (tens) MeV. Even the ratio of the up- or down-quark masses to the strange-quark mass is vastly different in the two pictures. If one attempted to incorporate a bound gluon into the model, one would have to assign to it a mass at least of the order of magnitude of the quark mass, in order to limit its impact on the classification scheme. But a gluon mass violates the gauge invariance of QCD.

Fortunately, "light-cone quantization", which can be formulated independent of the Lorentz frame, offers an elegant avenue of escape. The square root operator does not appear, and the

vacuum structure is relatively simple. There is no spontaneous creation of massive fermions in the light-cone quantized vacuum. There are, in fact, many reasons to quantize relativistic field theories at fixed light-cone time. Dirac [123], in 1949, showed that in this so-called “front form” of Hamiltonian dynamics, a maximum number of Poincaré generators become independent of the interaction, including certain Lorentz boosts. In fact, unlike the traditional equal-time Hamiltonian formalism, quantization on a plane tangential to the light cone (“null plane”) can be formulated without reference to a specific Lorentz frame. One can construct an operator whose eigenvalues are the invariant mass squared M^2 . The eigenvectors describe bound states of arbitrary four-momentum and invariant mass M and allow the computation of scattering amplitudes and other dynamical quantities. The most remarkable feature of this approach, however, is the apparent simplicity of the light-cone vacuum. In many theories the vacuum state of the free Hamiltonian is also an eigenstate of the total light-cone Hamiltonian. The Fock expansion constructed on this vacuum state provides a complete relativistic many-particle basis for diagonalizing the full theory. The simplicity of the light-cone Fock representation as compared to that in equal-time quantization is directly linked to the fact that the physical vacuum state has a much simpler structure on the light cone because the Fock vacuum is an exact eigenstate of the full Hamiltonian. This follows from the fact that the total light-cone momentum $P^+ > 0$ and it is conserved. This means that all constituents in a physical eigenstate are directly related to that state, and not to disconnected vacuum fluctuations.

In the Tamm–Dancoff method (TDA) and sometimes also in the method of discretized light-cone quantization (DLCQ), one approximates the field theory by truncating the Fock space. Based on the success of the constituent quark models, the assumption is that a few excitations describe the essential physics and that adding more Fock space excitations only refines the initial approximation. Wilson [455,456] has stressed the point that the success of the Feynman parton model provides hope for the eventual success of the front-form methods.

One of the most important tasks in hadron physics is to calculate the spectrum and the wavefunctions of physical particles from a covariant theory, as mentioned. The method of “discretized light-cone quantization” has precisely this goal. Since its first formulation [354,355] many problems have been resolved but some remain open. To date, DLCQ has proved to be one of the most powerful tools available for solving bound-state problems in quantum field theory [363,68].

Let us review briefly the difficulties. As with conventional non-relativistic many-body theory one starts out with a Hamiltonian. The kinetic energy is a one-body operator and thus simple. The potential energy is at least a two-body operator and thus complicated. One has solved the problem if one has found one or several eigenvalues and eigenfunctions of the Hamiltonian equation. One can always expand the eigenstates in terms of products of single-particle states. These single-particle wavefunctions are solutions of an arbitrary “single-particle Hamiltonian”. In the Hamiltonian matrix for a two-body interaction most of the matrix elements vanish, since a two-body Hamiltonian changes the state of up to two particles. The structure of the Hamiltonian is that one of a finite penta-diagonal block matrix. The dimension within a block, however, is infinite to start with. It is made finite by an artificial cut-off, for example on the single-particle quantum numbers. A finite matrix, however, can be diagonalized on a computer: the problem becomes ‘approximately soluble’. Of course, at the end, one must verify that the physical results are (more or less) insensitive to the cut-off(s) and other formal parameters. Early calculations [353], where this procedure was

actually carried out in one space dimension, showed rapid converge to the exact eigenvalues. The method was successful in generating the exact eigenvalues and eigenfunctions for up to 30 particles. From these early calculations it was clear that discretized plane waves are a manifestly useful tool for many-body problems. In this review we will display the extension of this method (DLCQ) to various quantum field theories [137–140,227,228,258,259,261,264,354,355,358,422,29,272,359–361,392,393].

The first studies of model field theories had disregarded the so-called ‘zero modes’, the space-like constant field components defined in a finite spatial volume (discretization) and quantized at equal light-cone time. But subsequent studies have shown that they can support certain kinds of vacuum structure. The long range phenomena of spontaneous symmetry breaking [206–208,33,382,223,389] as well as the topological structure [259,261] can in fact be reproduced when they are included carefully. The phenomena are realized in quite different ways. For example, spontaneous breaking of Z_2 symmetry ($\phi \rightarrow -\phi$) in the ϕ^4 -theory in $1 + 1$ dimension occurs via a *constrained* zero mode of the scalar field [33]. There the zero mode satisfies a nonlinear constraint equation that relates it to the dynamical modes in the problem. At the critical coupling a bifurcation of the solution occurs [209,210,389,33]. In formulating the theory, one must choose one of them. This choice is analogous to what in the conventional language we would call the choice of vacuum state. These solutions lead to new operators in the Hamiltonian which break the Z_2 symmetry at and beyond the critical coupling. The various solutions contain c -number pieces which produce the possible vacuum expectation values of ϕ . The properties of the strong-coupling phase transition in this model are reproduced, including its second-order nature and a reasonable value for the critical coupling [33,382]. One should emphasize that solving the constraint equations really amounts to determining the Hamiltonian (P^-) and possibly other Poincaré generators, while the wavefunction of the vacuum remains simple. In general, P^- becomes very complicated when the constraint zero modes are included, and this in some sense is the price to pay to have a formulation with a simple vacuum, combined with possibly finite vacuum expectation values. Alternatively, it should be possible to think of discretization as a cutoff which removes states with $0 < p^+ < \pi/L$, and the zero mode contributions to the Hamiltonian as effective interactions that restore the discarded physics. In the light-front power counting à la Wilson it is clear that there will be a huge number of allowed operators.

Quite separately, Kalloniatis et al. [259] have shown that also a *dynamical* zero mode arises in a pure SU(2) Yang–Mills theory in $1 + 1$ dimensions. A complete fixing of the gauge leaves the theory with one degree of freedom, the zero mode of the vector potential A^+ . The theory has a discrete spectrum of zero- P^+ states corresponding to modes of the flux loop around the finite space. Only one state has a zero eigenvalue of the energy P^- , and is the true ground state of the theory. The non-zero eigenvalues are proportional to the length of the spatial box, consistent with the flux loop picture. This is a direct result of the topology of the space. Since the theory considered there was a purely topological field theory, the exact solution was identical to that in the conventional equal-time approach on the analogous spatial topology [217].

Much of the work so far performed has been for theories in $1 + 1$ dimensions. For these theories there is much success to report. Numerical solutions have been obtained for a variety of gauge theories including U(1) and SU(N) for $N = 1, 2, 3$ and 4 [228,227,229,230,272]; Yukawa [182]; and to some extent ϕ^4 [203,204]. A considerable amount of analysis of ϕ^4 [203,204,206–210,214] has been performed and a fairly complete discussion of the Schwinger model has been presented

[137–139,326,210,214,296]. The long-standing problem in reaching high numerical accuracy towards the massless limit has been resolved recently [438].

The extension of this program to physical theories in $3 + 1$ dimensions is a formidable computational task because of the much larger number of degrees of freedom. The amount of work is therefore understandably smaller; however, progress is being made. Analyses of the spectrum and light-cone wavefunctions of positronium in QED_{3+1} have been made by Tang et al. [422] and Krautgärtner et al. [279]. Numerical studies on positronium have provided the Bohr, the fine, and the hyperfine structure with very good accuracy [429]. Currently, Hiller et al. [222] are pursuing a non-perturbative calculation of the lepton anomalous moment in QED using the DLCQ method. Burkardt [79] and, more recently, van de Sande and Dalley [79,437,439,116] have solved gauge theories with transverse dimensions by combining a transverse lattice method with DLCQ, taking up an old suggestion of Bardeen and Pearson [17,18]. Also of interest is recent work of Hollenberg and Witte [225], who have shown how Lanczos tri-diagonalization can be combined with a plaquette expansion to obtain an analytic extrapolation of a physical system to infinite volume. The major problem one faces here is a reasonable definition of an effective interaction including the many-body amplitudes [357,361]. There has been considerable work focusing on the truncations required to reduce the space of states to a manageable level [363,367,368,456]. The natural language for this discussion is that of the renormalization group, with the goal being to understand the kinds of effective interactions that occur when states are removed, either by cutoffs of some kind or by an explicit Tamm–Dancoff truncation. Solutions of the resulting effective Hamiltonian can then be obtained by various means, for example using DLCQ or basis function techniques. Some calculations of the spectrum of heavy quarkonia in this approach have recently been reported [48]. Formal work on renormalization in $3 + 1$ dimensions [339] has yielded some positive results but many questions remain. More recently, DLCQ has been applied to new variants of QCD_{1+1} with quarks in the adjoint representation, thus obtaining color-singlet eigenstates analogous to gluonium states [121, 360,437].

The physical nature of the light-cone Fock representation has important consequences for the description of hadronic states. As to be discussed in greater detail in Sections 3 and 5, one can compute electromagnetic and weak form factors rather directly from an overlap of light-cone wavefunctions $\psi_n(x_i, k_{\perp i}, \lambda_i)$ [131,299,418]. Form factors are generally constructed from hadronic matrix elements of the current $\langle p | j^\mu(0) | p + q \rangle$. In the interaction picture one can identify the fully interacting Heisenberg current J^μ with the free current j^μ at the space-time point $x^\mu = 0$. Calculating matrix elements of the current $j^+ = j^0 + j^3$ in a frame with $q^+ = 0$, only diagonal matrix elements in particle number $n' = n$ are needed. In contrast, in the equal-time theory one must also consider off-diagonal matrix elements and fluctuations due to particle creation and annihilation in the vacuum. In the non-relativistic limit one can make contact with the usual formulas for form factors in Schrödinger many-body theory.

In the case of inclusive reactions, the hadron and nuclear structure functions are the probability distributions constructed from integrals and sums over the absolute squares $|\psi_n|^2$. In the far off-shell domain of large parton virtuality, one can use perturbative QCD to derive the asymptotic fall-off of the Fock amplitudes, which then in turn leads to the QCD evolution equations for distribution amplitudes and structure functions. More generally, one can prove factorization theorems for exclusive and inclusive reactions which separate the hard and soft momentum transfer

regimes, thus obtaining rigorous predictions for the leading power behavior contributions to large momentum transfer cross sections. One can also compute the far off-shell amplitudes within the light-cone wavefunctions where heavy quark pairs appear in the Fock states. Such states persist over a time $\tau \simeq P^+/\mathcal{M}^2$ until they are materialized in the hadron collisions. As we shall discuss in Section 6, this leads to a number of novel effects in the hadroproduction of heavy quark hadronic states [67].

A number of properties of the light-cone wavefunctions of the hadrons are known from both phenomenology and the basic properties of QCD. For example, the endpoint behavior of light-cone wave and structure functions can be determined from perturbative arguments and Regge arguments. Applications are presented in Ref. [70]. There are also correspondence principles. For example, for heavy quarks in the non-relativistic limit, the light-cone formalism reduces to conventional many-body Schrödinger theory. On the other hand, we can also build effective three-quark models which encode the static properties of relativistic baryons. The properties of such wavefunctions are discussed in Section 5.

We will review the properties of vector and axial vector non-singlet charges and compare the space–time with their light-cone realization. We will show that the space–time and light-cone axial currents are distinct; this remark is at the root of the difference between the chiral properties of QCD in the two forms. We show for the free quark model that the front form is chirally symmetric in the SU(3) limit, whether the common mass is zero or not. In QCD chiral symmetry is broken both explicitly and dynamically. This is reflected on the light-cone by the fact that the axial-charges are not conserved even in the chiral limit. Vector and axial-vector charges annihilate the Fock space vacuum and so are bona fide operators. They form an SU(3)⊗SU(3) algebra and conserve the number of quarks and anti-quarks separately when acting on a hadron state. Hence, they classify hadrons, on the basis of their valence structure, into multiplets which are not mass degenerate. This classification however turns out to be phenomenologically deficient. The remedy of this situation is unitary transformation between the charges and the physical generators of the classifying SU(3)⊗SU(3) algebra.

Although we are still far from solving QCD explicitly, it now is the right time to give a presentation of the light-cone activities to a larger community. The front form can contribute to the physical insight and interpretation of experimental results. We therefore will combine a certain amount of pedagogical presentation of canonical field theory with the rather abstract and theoretical questions of most recent advances. The present attempt can neither be exhaustive nor complete, but we have in mind that we ultimately have to deal with the true physical questions of experiment.

We will use two different metrics in this review. The literature is about evenly split in their use. We have, for the most part, used the metric that was used in the original work being reviewed. We label them the LB convention and the KS convention and discuss them in more detail in Section 2 and the appendix.

2. Hamiltonian dynamics

What is a Hamiltonian? Dirac [125] defines the Hamiltonian H as that *operator* whose action on the state vector $|t\rangle$ of a physical system has the same effect as taking the partial derivative with

respect to time t , i.e.

$$H|t\rangle = i \partial/\partial t|t\rangle. \quad (2.1)$$

Its expectation value is a *constant of the motion*, referred to shortly as the “energy” of the system. We will not consider pathological constructs where a Hamiltonian depends explicitly on time. The concept of an energy has developed over many centuries and applies irrespective of whether one deals with the motion of a non-relativistic particle in classical mechanics or with a non-relativistic wavefunction in the Schrödinger equation, and it generalizes almost unchanged to a relativistic and covariant field theory. The Hamiltonian operator P_0 is a constant of the motion which acts as the displacement operator in time $x^0 \equiv t$,

$$P_0|x^0\rangle = i \partial/\partial x^0|x^0\rangle. \quad (2.2)$$

This definition applies also in the front form, where the “Hamiltonian” operator P_+ is a constant of the motion whose action on the state vector,

$$P_+|x^+\rangle = i \partial/\partial x^+|x^+\rangle, \quad (2.3)$$

has the same effect as the partial with respect to “light-cone time” $x^+ \equiv (t + z)$. In this section we elaborate on these concepts and operational definitions to some detail for a relativistic theory, focusing on covariant gauge field theories. For the most part the LB convention is used however many of the results are convention independent.

2.1. Abelian gauge theory: Quantum electrodynamics

The prototype of a field theory is Faraday’s and Maxwell’s electrodynamics [323], which is gauge invariant as first pointed by Weyl [449].

The non-trivial set of Maxwells equations has the four components

$$\partial_\mu F^{\mu\nu} = gJ^\nu. \quad (2.4)$$

The six components of the electric and magnetic fields are collected into the antisymmetric *electromagnetic field tensor* $F^{\mu\nu} \equiv \partial^\mu A^\nu - \partial^\nu A^\mu$ and expressed in terms of the *vector potentials* A^μ describing vector bosons with a strictly vanishing mass. Each component is a real-valued operator function of the three space coordinates $x^k = (x, y, z)$ and of the time $x^0 = t$. The space–time coordinates are arranged into the vector x^μ labeled by the *Lorentz indices* $(\kappa, \lambda, \mu, \nu = 0, 1, 2, 3)$. The Lorentz indices are lowered by the *metric tensor* $g_{\mu\nu}$ and raised by $g^{\mu\nu}$ with $g_{\kappa\mu}g^{\mu\lambda} = \delta_\kappa^\lambda$. These and other conventions are collected in Appendix A. The coupling constant g is related to the dimensionless *fine structure constant* by

$$\alpha = g^2/4\pi\hbar c. \quad (2.5)$$

The antisymmetry of $F^{\mu\nu}$ implies a vanishing four-divergence of the current $J^\nu(x)$, i.e.

$$\partial_\mu J^\mu = 0. \quad (2.6)$$

In the equation of motion, the time derivatives of the vector potentials are expressed as functionals of the fields and their space-like derivatives, which in the present case are of second order in the

time, like $\partial_0 \partial_0 A^\mu = f[A^\nu, J^\mu]$. The Dirac equations

$$(i\gamma^\mu \partial_\mu - m)\Psi = g\gamma^\mu A_\mu \Psi, \quad (2.7)$$

for given values of the vector potentials A_μ , define the time derivatives of the four complex-valued spinor components $\Psi_\alpha(x)$ and their adjoints $\bar{\Psi}_\alpha(x) = \Psi_\beta^\dagger(x)(\gamma^0)_{\beta\alpha}$, and thus of the current $J^\nu \equiv \bar{\Psi}\gamma^\nu\Psi = \bar{\Psi}_\alpha\gamma^\nu_{\alpha\beta}\Psi_\beta$. The mass of the fermion is denoted by m , the four *Dirac matrices* by $\gamma^\mu = (\gamma^\mu)_{\alpha\beta}$. The *Dirac indices* α or β enumerate the components from 1 to 4, doubly occurring indices are implicitly summed over without reference to their lowering or raising.

The combined set of the Maxwell *and* Dirac equations is closed. The combined set of the 12 coupled differential equations in 3 + 1 space–time dimensions is called *quantum electrodynamics* (QED).

The trajectories of physical particles extremalize the *action*. Similarly, the equations of motion in a field theory like Eqs. (2.4) and (2.7) extremalize the *action density*, usually referred to as the *Lagrangian* \mathcal{L} . The Lagrangian of quantum electrodynamics (QED)

$$\mathcal{L} = -\frac{1}{4}F^{\mu\nu}F_{\mu\nu} + \frac{1}{2}[\bar{\Psi}(i\gamma^\mu D_\mu - m)\Psi + \text{h.c.}], \quad (2.8)$$

with the *covariant derivative* $D_\mu = \partial_\mu - igA_\mu$, is a local and hermitean operator, classically a real function of space–time x^μ . This almost empirical fact can be cast into the familiar and canonical *calculus of variation* as displayed in many text books [39,242], whose essentials shall be recalled briefly.

The Lagrangian for QED is a functional of the 12 components $\Psi_\alpha(x)$, $\bar{\Psi}_\alpha(x)$, $A_\mu(x)$ and their space–time derivatives. Denoting them collectively by $\phi_r(x)$ and $\partial_\mu\phi_r(x)$ one has thus $\mathcal{L} = \mathcal{L}[\phi_r, \partial_\mu\phi_r]$. Crucial is that \mathcal{L} depends on space–time only through the fields. Independent variation of the action with respect to ϕ_r and $\partial_\mu\phi_r$,

$$\delta_\phi \int dx^0 dx^1 dx^2 dx^3 \mathcal{L}(x) = 0, \quad (2.9)$$

results in the 12 *equations of motion*, the *Euler equations*

$$\partial_\kappa \pi_r^\kappa - \delta\mathcal{L}/\delta\phi_r = 0 \quad \text{with } \pi_r^\kappa[\phi] \equiv \delta\mathcal{L}/\delta(\partial_\kappa\phi_r), \quad (2.10)$$

for $r = 1, 2, \dots, 12$. The *generalized momentum fields* $\pi_r^\kappa[\phi]$ are introduced here for convenience and later use, with the argument $[\phi]$ usually suppressed except when useful to emphasize the field in question. The Euler equations symbolize the most compact form of equations of motion. Indeed, the variation with respect to the vector potentials

$$\delta\mathcal{L}/\delta(\partial_\kappa A_\lambda) \equiv \pi^{\kappa\lambda}[A] = -F^{\kappa\lambda} \quad \text{and} \quad \delta\mathcal{L}/\delta A_\lambda \equiv gJ^\lambda = g\bar{\Psi}\gamma^\lambda\Psi \quad (2.11)$$

yields straightforwardly the Maxwell equations (2.4), and varying with respect to the spinors

$$\pi_\alpha^\kappa[\psi] \equiv \frac{\delta\mathcal{L}}{\delta(\partial_\kappa\Psi_\alpha)} = \frac{i}{2}\bar{\Psi}_\beta\gamma^\kappa_{\beta\alpha}, \quad \frac{\delta\mathcal{L}}{\delta\Psi_\alpha} = -\frac{i}{2}\partial_\mu\bar{\Psi}_\beta\gamma^\mu_{\beta\alpha} + g\bar{\Psi}_\beta\gamma^\mu_{\beta\alpha}A_\mu - m\bar{\Psi}_\alpha \quad (2.12)$$

and its adjoints give the Dirac equations (2.7).

The canonical formalism is particularly suited for discussing the symmetries of a field theory. According to a theorem of Noether [242,346] every continuous symmetry of the Lagrangian is associated with a four-current whose four-divergence vanishes. This in turn implies a *conserved*

charge as a constant of motion. Integrating the current J^μ in Eq. (2.6) over a three-dimensional surface of a hypersphere, embedded in four-dimensional space–time, generates a conserved charge. The surface element $d\omega_\lambda$ and the (finite) volume Ω are defined most conveniently in terms of the totally antisymmetric tensor $\varepsilon_{\lambda\mu\nu\rho}$ ($\varepsilon_{0123} = 1$):

$$d\omega_\lambda = \frac{1}{3!} \varepsilon_{\lambda\mu\nu\rho} dx^\mu dx^\nu dx^\rho, \quad \Omega = \int d\omega_0 = \int dx^1 dx^2 dx^3, \quad (2.13)$$

respectively. Integrating Eq. (2.6) over the hyper-surface specified by $x^0 = \text{const.}$ then reads

$$\frac{\partial}{\partial x^0} \int_\Omega dx^1 dx^2 dx^3 J^0(x) + \int_\Omega dx^1 dx^2 dx^3 \left[\frac{\partial}{\partial x^1} J^1(x) + \frac{\partial}{\partial x^2} J^2(x) + \frac{\partial}{\partial x^3} J^3(x) \right] = 0. \quad (2.14)$$

The terms in the square bracket reduce to surface terms which vanish if the boundary conditions are carefully defined. Under that proviso the charge

$$Q = \int d\omega_0 J^0(x) = \int_\Omega dx^1 dx^2 dx^3 J^0(x^0, x^1, x^2, x^3) \quad (2.15)$$

is independent of time x^0 and a constant of the motion.

Since \mathcal{L} is frame-independent, there must be ten conserved four-currents. Here they are

$$\partial_\lambda T^{\lambda\nu} = 0 \quad \partial_\lambda J^{\lambda,\mu\nu} = 0, \quad (2.16)$$

where the *energy–momentum* $T^{\lambda\nu}$ and the *boost–angular–momentum* stress tensor $J^{\lambda,\mu\nu}$ are respectively,

$$T^{\lambda\nu} = \pi_r^\lambda \partial^\nu \phi_r - g^{\lambda\nu} \mathcal{L}, \quad J^{\lambda,\mu\nu} = x^\mu T^{\lambda\nu} - x^\nu T^{\lambda\mu} + \pi_r^\lambda \Sigma_{rs}^{\mu\nu} \phi_s. \quad (2.17)$$

As a consequence the Lorentz group has ten “conserved charges”, the ten constants of the motion

$$P^\nu = \int_\Omega d\omega_0 (\pi_r^0 \partial^\nu \phi_r - g^{0\nu} \mathcal{L}), \quad (2.18)$$

$$M^{\mu\nu} = \int_\Omega d\omega_0 (x^\mu T^{0\nu} - x^\nu T^{0\mu} + \pi_r^0 \Sigma_{rs}^{\mu\nu} \phi_s(x)),$$

the 4 components of *energy–momentum* and the 6 *boost–angular* momenta, respectively. The first two terms in $M^{\mu\nu}$ correspond to the orbital and the last term to the spin part of angular momentum. The spin part Σ is either

$$\Sigma_{\alpha\beta}^{\mu\nu} = \frac{1}{4} [\gamma^\mu, \gamma^\nu]_{\alpha\beta} \quad \text{or} \quad \Sigma_{\rho\sigma}^{\mu\nu} = g_\rho^\mu g_\sigma^\nu - g_\sigma^\mu g_\rho^\nu, \quad (2.19)$$

depending on whether ϕ_r refers to spinor or to vector fields, respectively. In the latter case, we substitute $\pi_r^\lambda \rightarrow \pi^{\rho\lambda} = \delta\mathcal{L}/\delta(\partial_\lambda A_\rho)$ and $\phi_s \rightarrow A^\sigma$. Inserting Eqs. (2.11) and (2.12) one gets for gauge theory the familiar expressions [39]

$$J^{\lambda,\mu\nu} = x^\mu T^{\lambda\nu} - x^\nu T^{\lambda\mu} + \frac{1}{8i} \bar{\Psi} (\gamma^\lambda [\gamma^\mu, \gamma^\nu] + [\gamma^\nu, \gamma^\mu] \gamma^\lambda) \Psi + A^\mu F^{\lambda\nu} - A^\nu F^{\lambda\mu}. \quad (2.20)$$

The symmetries will be discussed further in Section 2.6.

In deriving the energy–momentum stress tensor one might overlook that $\pi_r^\lambda[\phi]$ does *not necessarily* commute with $\partial^\mu \phi_r$. As a rule, one therefore should symmetrize in the boson and

anti-symmetrize in the fermion fields, i.e.

$$\begin{aligned}\pi_r^\lambda[\phi]\partial^\mu\phi_r &\rightarrow \frac{1}{2}(\pi_r^\lambda[\phi]\partial^\mu\phi_r + \partial^\mu\phi_r\pi_r^\lambda[\phi]), \\ \pi_r^\lambda[\psi]\partial^\mu\psi_r &\rightarrow \frac{1}{2}(\pi_r^\lambda[\psi]\partial^\mu\psi_r - \partial^\mu\psi_r\pi_r^\lambda[\psi]),\end{aligned}\quad (2.21)$$

respectively, but this will be done only implicitly.

The Lagrangian \mathcal{L} is invariant under local gauge transformations, in general described by a unitary and space–time-dependent matrix operator $U^{-1}(x) = U^\dagger(x)$. In QED, the dimension of this matrix is 1 with the most general form $U(x) = e^{-igA(x)}$. Its elements form the abelian group $U(1)$, hence abelian gauge theory. If one substitutes the spinor and vector fields in $F^{\mu\nu}$ and $\bar{\Psi}_\alpha D_\mu \Psi_\beta$ according to

$$\tilde{\Psi}_\alpha = U\Psi_\alpha, \quad \tilde{A}_\mu = UA_\mu U^\dagger + (i/g)(\partial_\mu U)U^\dagger, \quad (2.22)$$

one verifies their invariance under this transformation, as well as that of the whole Lagrangian. The Noether current associated with this symmetry is the J^μ of Eq. (2.11).

A straightforward application of the variational principle, Eqs. (2.11) and (2.12), does not yield immediately manifestly gauge invariant expressions. Rather one gets

$$T^{\mu\nu} = F^{\mu\kappa}\partial^\nu A_\kappa + \frac{1}{2}[\bar{\Psi}i\gamma^\mu\partial^\nu\Psi + \text{h.c.}] - g^{\mu\nu}\mathcal{L}. \quad (2.23)$$

However, using the Maxwell equations one derives the identity

$$F^{\mu\kappa}\partial^\nu A_\kappa = F^{\mu\kappa}F_\kappa^\nu + gJ^\mu A^\nu + \partial_\kappa(F^{\mu\kappa}A^\nu). \quad (2.24)$$

Inserting that into the former gives

$$T^{\mu\nu} = F^{\mu\kappa}F_\kappa^\nu + \frac{1}{2}[i\bar{\Psi}\gamma^\mu D^\nu\Psi + \text{h.c.}] - g^{\mu\nu}\mathcal{L} + \partial_\kappa(F^{\mu\kappa}A^\nu). \quad (2.25)$$

All explicit gauge dependence resides in the last term in the form of a four-divergence. One can thus write

$$T^{\mu\nu} = F^{\mu\kappa}F_\kappa^\nu + \frac{1}{2}[i\bar{\Psi}\gamma^\mu D^\nu\Psi + \text{h.c.}] - g^{\mu\nu}\mathcal{L}, \quad (2.26)$$

which together with energy–momentum

$$P^\nu = \int_\Omega d\omega_0(F^{0\kappa}F_\kappa^\nu - g^{0\nu}\mathcal{L} + \frac{1}{2}[i\bar{\Psi}\gamma^0 D^\nu\Psi + \text{h.c.}]) \quad (2.27)$$

is manifestly gauge-invariant.

2.2. Non-abelian gauge theory: Quantum chromodynamics

For the gauge group $SU(3)$, one replaces each local gauge field $A^\mu(x)$ by the 3×3 matrix $A^\mu(x)$,

$$A^\mu \rightarrow (A^\mu)_{cc'} = \frac{1}{2} \begin{pmatrix} \frac{1}{\sqrt{3}}A_8^\mu + A_3^\mu & A_1^\mu - iA_2^\mu & A_4^\mu - iA_5^\mu \\ A_1^\mu + iA_2^\mu & \frac{1}{\sqrt{3}}A_8^\mu - A_3^\mu & A_6^\mu - iA_7^\mu \\ A_4^\mu + iA_5^\mu & A_6^\mu + iA_7^\mu & -\frac{2}{\sqrt{3}}A_8^\mu \end{pmatrix}. \quad (2.28)$$

This way one moves from quantum electrodynamics to *quantum chromodynamics* with the eight real-valued *color vector potentials* A_a^μ enumerated by the *gluon index* $a = 1, \dots, 8$. These matrices

are all *hermitean* and *traceless* since the trace can always be absorbed into an abelian U(1) gauge theory. They belong thus to the class of *special unitary* 3×3 matrices SU(3). In order to make sense of expressions like $\bar{\Psi}A^\mu\Psi$ the *quark fields* $\Psi(x)$ must carry a *color index* $c = 1,2,3$ which are usually suppressed as are the Dirac indices in the color triplet spinor $\Psi_{c,\alpha}(x)$.

More generally for SU(N), the vector potentials A^μ are hermitian and traceless $N \times N$ matrices. All such matrices can be parametrized $A^\mu \equiv T_{cc'}^a A_a^\mu$. The color index c (or c') runs now from 1 to n_c , and correspondingly the gluon index a (or r, s, t) from 1 to $n_c^2 - 1$. Both are implicitly summed, with no distinction of lowering or raising them. The color matrices $T_{cc'}^a$ obey

$$[T^r, T^s]_{cc'} = if^{rsa}T_{cc'}^a, \quad \text{Tr}(T^r T^s) = \frac{1}{2}\delta_r^s. \quad (2.29)$$

The *structure constants* f^{rst} are tabulated in the literature [242,342,343] for SU(3). For SU(2) they are the totally antisymmetric tensor ε_{rst} , since $T^a = \frac{1}{2}\sigma^a$ with σ^a being the Pauli matrices. For SU(3), the T^a are related to the Gell–Mann matrices λ^a by $T^a = \frac{1}{2}\lambda^a$. The gauge-invariant Lagrangian density for QCD or SU(N) is

$$\begin{aligned} \mathcal{L} &= -\frac{1}{2}\text{Tr}(F^{\mu\nu}F_{\mu\nu}) + \frac{1}{2}[\bar{\Psi}(i\gamma^\mu D_\mu - m)\Psi + \text{h.c.}] \\ &= -\frac{1}{4}F_a^{\mu\nu}F_{\mu\nu}^a + \frac{1}{2}[\bar{\Psi}(i\gamma^\mu D_\mu - m)\Psi + \text{h.c.}], \end{aligned} \quad (2.30)$$

in analogy to Eq. (2.8). The unfamiliar factor of 2 is because of the trace convention in Eq. (2.29). The mass matrix $m = m\delta_{cc'}$ is diagonal in color space. The matrix notation is particularly suited for establishing gauge invariance according to Eq. (2.22) with the unitary operators U now being $N \times N$ matrices, hence *non-abelian* gauge theory. The latter fact generates an extra term in the *color-electro-magnetic* fields

$$F^{\mu\nu} \equiv \partial^\mu A^\nu - \partial^\nu A^\mu + ig[A^\mu, A^\nu],$$

or

$$F_a^{\mu\nu} \equiv \partial^\mu A_a^\nu - \partial^\nu A_a^\mu - gf^{ars}A_r^\mu A_s^\nu, \quad (2.31)$$

but such that $F^{\mu\nu}$ remains antisymmetric in the Lorentz indices. The covariant derivative *matrix* finally is $D_{cc'}^\mu = \delta_{cc'}\partial^\mu + igA_{cc'}^\mu$. The variational derivatives are now

$$\delta\mathcal{L}/\delta(\partial_\kappa A_r^\lambda) = -F_r^{\kappa\lambda}, \quad \delta\mathcal{L}/\delta A_r^\lambda = -gJ_r^\lambda \quad \text{with } J_r^\lambda = \bar{\Psi}\gamma^\lambda T^a\Psi + f^{ars}F_r^{\lambda\kappa}A_\kappa^s, \quad (2.32)$$

in analogy to Eq. (2.11), and yield the *color-Maxwell equations*

$$\partial_\mu F^{\mu\nu} = gJ^\nu \quad \text{with } J^\nu = \bar{\Psi}\gamma^\nu T^a\Psi T^a + (1/i)[F^{\nu\kappa}, A_\kappa]. \quad (2.33)$$

The *color-Maxwell current* is *conserved*,

$$\partial_\mu J^\mu = 0. \quad (2.34)$$

Note that the color-fermion current $j_a^\mu = \bar{\Psi}\gamma^\nu T^a\Psi$ is *not trivially conserved*. The variational derivatives with respect to the spinor fields like Eq. (2.12) give correspondingly the color-Dirac equations

$$(i\gamma^\mu D_\mu - m)\Psi = 0. \quad (2.35)$$

Everything proceeds in analogy with QED. The color-Maxwell equations allow for the identity

$$F_a^{\mu\kappa}\partial^\nu A_\kappa^a = F_a^{\mu\kappa}F_{\kappa,a}^\nu + gJ_a^\mu A_a^\nu + gf^{ars}F_a^{\mu\kappa}A_r^\nu A_\kappa^s + \partial_\kappa(F_a^{\mu\kappa}A_a^\nu). \quad (2.36)$$

The energy–momentum stress tensor becomes

$$T^{\mu\nu} = 2\text{Tr}(\mathbf{F}^{\mu\kappa}\mathbf{F}_\kappa^\nu) + \frac{1}{2}[i\bar{\Psi}\gamma^\mu\mathbf{D}^\nu\Psi + \text{h.c.}] - g^{\mu\nu}\mathcal{L} - 2\partial_\kappa\text{Tr}(\mathbf{F}^{\mu\kappa}\mathbf{A}^\nu). \quad (2.37)$$

Leaving out the four divergence, $T^{\mu\nu}$ is manifestly gauge-invariant,

$$T^{\mu\nu} = 2\text{Tr}(\mathbf{F}^{\mu\kappa}\mathbf{F}_\kappa^\nu) + \frac{1}{2}[i\bar{\Psi}\gamma^\mu\mathbf{D}^\nu\Psi + \text{h.c.}] - g^{\mu\nu}\mathcal{L} \quad (2.38)$$

as are the generalized momenta [245]

$$P^\nu = \int_\Omega d\omega_0(2\text{Tr}(\mathbf{F}^{0\kappa}\mathbf{F}_\kappa^\nu) - g^{0\nu}\mathcal{L} + \frac{1}{2}[i\bar{\Psi}\gamma^0\mathbf{D}^\nu\Psi + \text{h.c.}]). \quad (2.39)$$

Note that all this holds for SU(N), in fact it holds for $d + 1$ dimensions.

2.3. Parametrization of space–time

Let us review some aspects of canonical field theory. The Lagrangian determines both the equations of motion and the constants of motion. The equations of motion are differential equations. Solving differential equations one must give initial data. On a hypersphere in four-space, characterized by a fixed initial “time” $x^0 = 0$, one assumes to know all necessary field components $\phi_r(x_0^0, \underline{x})$. The goal is then to generate the fields for all space–time by means of the differential equations of motion.

Equivalently, one can propagate the initial configurations forward or backward in time with the Hamiltonian. In a classical field theory, particularly one in which every field ϕ_r has a conjugate momentum $\pi_r[\phi] \equiv \pi_r^0[\phi]$, see Eq. (2.10), one gets from the constant of motion P_0 to the Hamiltonian P_0 by substituting the velocity fields $\partial_0\phi_r$ with the canonically conjugate momenta π_r , thus $P_0 = P_0[\phi, \pi]$. Equations of motion are then given in terms of the classical Poisson brackets [186],

$$\partial_0\phi_r = \{P_0, \phi_r\}_{\text{cl}}, \quad \partial_0\pi_r = \{P_0, \pi_r\}_{\text{cl}}. \quad (2.40)$$

They are discussed in greater details in Appendix E. Following Dirac [125–127], the transition to an operator formalism like quantum mechanics is consistently achieved by replacing the classical Poisson brackets of two functions A and B by the “quantum Poisson brackets”, the commutators of two operators A and B

$$\{A, B\}_{\text{cl}} \rightarrow (1/i\hbar)[A, B]_{x^0=y^0}, \quad (2.41)$$

and correspondingly by the anti-commutator for two fermionic fields. Particularly, one substitutes the basic Poisson bracket

$$\{\phi_r(x), \pi_s(y)\}_{\text{cl}} = \delta_{rs}\delta^{(3)}(\underline{x} - \underline{y}) \quad (2.42)$$

by the basic commutator

$$(1/i\hbar)[\phi_r(x), \pi_s(y)]_{x^0=y^0} = \delta_{rs}\delta^{(3)}(\underline{x} - \underline{y}). \quad (2.43)$$

The time derivatives of the operator fields are then given by the Heisenberg equations, see Eq. (2.57).

In gauge theory like QED and QCD, one cannot proceed so straightforwardly as in the above canonical procedure, for two reasons: (1) Not all of the fields have a conjugate momentum, that is not all of them are independent; (2) Gauge theory has redundant degrees of freedom. There are plenty of conventions how one can ‘fix the gauge’. It suffices to say for the moment that ‘canonical quantization’ applies only for the independent fields. In Appendix E we will review the Dirac–Bergman procedure for handling dependent degrees of freedom, or for ‘quantizing under constraint’.

Thus far time t and space \underline{x} was treated as if they were completely separate issues. But in a covariant theory, time and space are only different aspects of four-dimensional space–time. One can however generalize the concepts of space and of time in an operational sense. One can define ‘space’ as that hypersphere in four-space on which one chooses the initial field configurations in accord with microcausality. The remaining, the fourth coordinate can be thought of being kind of normal to the hypersphere and understood as ‘time’. Below we shall speak of space-like and time-like coordinates, correspondingly.

These concepts can be grasped more formally by conveniently introducing generalized coordinates \tilde{x}^ν . Starting from a baseline parametrization of space–time like the above x^μ [39] with a given metric tensor $g^{\mu\nu}$ whose elements are all zero except $g^{00} = 1$, $g^{11} = -1$, $g^{22} = -1$, and $g^{33} = -1$, one parametrizes space–time by a certain functional relation

$$\tilde{x}^\nu = \tilde{x}^\nu(x^\mu). \quad (2.44)$$

The freedom in choosing $\tilde{x}^\nu(x^\mu)$ is restricted only by the condition that the inverse $x^\mu(\tilde{x}^\nu)$ exists as well. The transformation conserves the arc length; thus $(ds)^2 = g_{\mu\nu}dx^\mu dx^\nu = \tilde{g}_{\kappa\lambda}d\tilde{x}^\kappa d\tilde{x}^\lambda$. The metric tensors for the two parametrizations are then related by

$$\tilde{g}_{\kappa\lambda} = (\partial x^\mu / \partial \tilde{x}^\kappa) g_{\mu\nu} (\partial x^\nu / \partial \tilde{x}^\lambda). \quad (2.45)$$

The two four-volume elements are related by the Jacobian $\mathcal{J}(\tilde{x}) = \|\partial x / \partial \tilde{x}\|$, particularly $d^4x = \mathcal{J}(\tilde{x})d^4\tilde{x}$. We shall keep track of the Jacobian only implicitly. The three-volume element $d\omega_0$ is treated correspondingly.

All the above considerations must be independent of this reparametrization. The fundamental expressions like the Lagrangian can be expressed in terms of either x or \tilde{x} . There is however one subtle point. By matter of convenience, one defines the hypersphere as that locus in four-space on which one sets the “initial conditions” at the same “initial time”, or on which one “quantizes” the system correspondingly in a quantum theory. The hypersphere is thus defined as that locus in four-space with the same value of the “time-like” coordinate \tilde{x}^0 , i.e. $\tilde{x}^0(x^0, \underline{x}) = \text{const}$. Correspondingly, the remaining coordinates are called ‘space-like’ and denoted by the spatial three-vector $\tilde{\mathbf{x}} = (\tilde{x}^1, \tilde{x}^2, \tilde{x}^3)$. Because of the (in general) more complicated metric, cuts through the four-space characterized by $\tilde{x}^0 = \text{const}$ are quite different from those with $\tilde{x}_0 = \text{const}$. In generalized coordinates the covariant and contravariant indices can have rather different interpretation, and one must be careful with the lowering and rising of the Lorentz indices. For example, only $\partial_0 = \partial / \partial \tilde{x}^0$ is a ‘time derivative’ and only P_0 a “Hamiltonian”, as opposed to ∂^0 and P^0 which in general are completely different objects. The actual choice of $\tilde{x}(x)$ is a matter of preference and convenience.

2.4. Forms of Hamiltonian dynamics

Obviously, one has many possibilities to parametrize space–time by introducing some generalized coordinates $\tilde{x}(x)$. But one should exclude all those which are accessible by a Lorentz transformation. Those are included anyway in a covariant formalism. This limits considerably the freedom and excludes, for example, almost all rotation angles. Following Dirac [123] there are no more than three basically different parametrizations. They are illustrated in Fig. 1, and cannot be mapped on each other by a Lorentz transform. They differ by the hypersphere on which the fields are initialized, and correspondingly one has different “times”. Each of these space–time parametrizations has thus its own Hamiltonian, and correspondingly Dirac [123] speaks of the three *forms of Hamiltonian dynamics*: The *instant form* is the familiar one, with its hypersphere given by $t = 0$. In the *front form* the hypersphere is a tangent plane to the light cone. In the *point form* the time-like coordinate is identified with the eigentime of a physical system and the hypersphere has a shape of a hyperboloid.

Which of the three forms should be preferred? The question is difficult to answer, in fact it is ill-posed. In principle, all three forms should yield the same physical results, since physics should not depend on how one parametrizes the space (and the time). If it depends on it, one has made a mistake. But usually one adjusts parametrization to the nature of the physical problem to simplify the amount of practical work. Since one knows so little on the typical solutions of a field theory, it might well be worth the effort to admit also other than the conventional “instant” form.

The bulk of research on field theory implicitly uses the instant form, which we do not even attempt to summarize. Although it is the conventional choice for quantizing field theory, it has

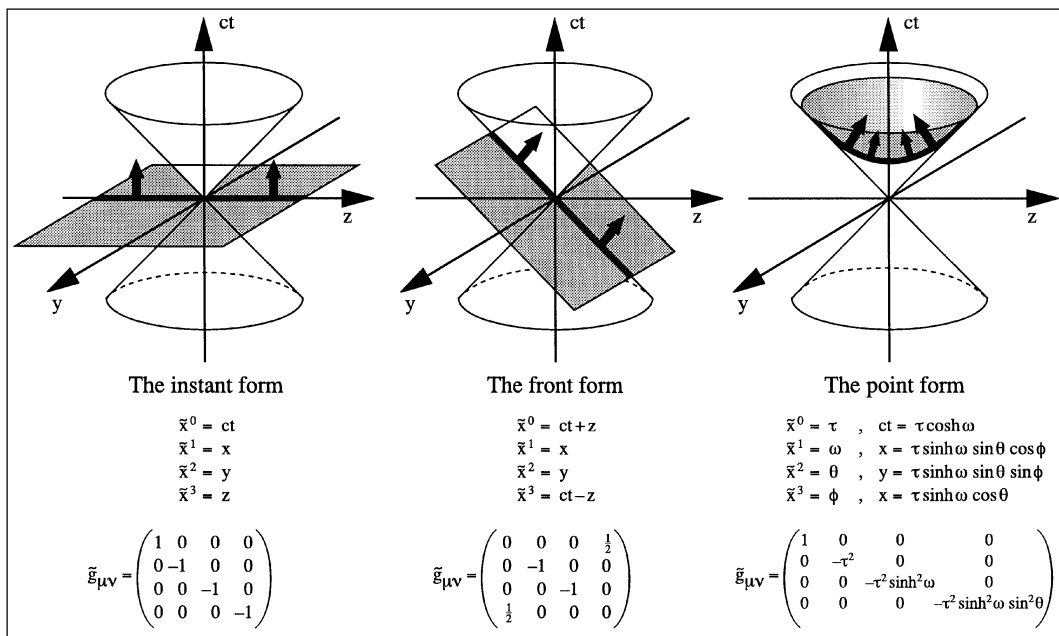


Fig. 1. Dirac’s three forms of Hamiltonian dynamics.

many practical disadvantages. For example, given the wavefunctions of an n -electron atom at an initial time $t = 0$, $\psi_n(\mathbf{x}_i, t = 0)$, one can use the Hamiltonian H to evolve $\psi_n(\mathbf{x}_i, t)$ to later times t . However, an experiment which specifies the initial wavefunction would require the simultaneous measurement of the positions of all of the bounded electrons. In contrast, determining the initial wavefunction at fixed light-cone time $\tau = 0$ only requires an experiment which scatters one plane-wave laser beam, since the signal reaching each of the n electrons, along the light front, at the same light-cone time $\tau = t_i + z_i/c$.

A reasonable choice of $\tilde{x}(x)$ is restricted by microcausality: a light signal emitted from any point on the hypersphere must not cross the hypersphere. This holds for the instant or for the point form, but the front form seems to be in trouble. The light cone corresponds to light emitted from the origin and touches the front form hypersphere at $(x, y) = (0, 0)$. A signal carrying actually information moves with the group velocity always smaller than the phase velocity c . Thus, if no information is carried by the signal, points on the light cone are unable to communicate. Only when solving problems in one-space and one-time dimension, the front form initializes fields only on the characteristic. Whether this generates problems for pathological cases like massless bosons (or fermions) is still under debate.

Comparatively little work is done in the point form [154,192,405]. Stech and collaborators [192] have investigated the free particle, by analyzing the Klein–Gordon and the Dirac equation. As it turns out, the orthonormal functions spanning the Hilbert space for these cases are rather difficult to work with. Their addition theorems are certainly more complicated than the simple plane-wave states applicable in the instant or the front form.

The front form has a number of advantages which we will review in this article. Dirac's legacy had been forgotten and re-invented several times, thus the approach carries names as different as *infinite-momentum frame*, *null-plane quantization*, *light-cone quantization*, or most unnecessarily *light-front quantization*. In the essence these are the same.

The infinite-momentum frame first appeared in the work of Fubini and Furlan [153] in connection with current algebra as the limit of a reference frame moving with almost the speed of light. Weinberg [448] asked whether this limit might be more generally useful. He considered the infinite-momentum limit of the old-fashioned perturbation diagrams for scalar meson theories and showed that the vacuum structure of these theories simplified in this limit. Later Susskind [414,415] showed that the infinities which occur among the generators of the Poincaré group when they are boosted to a fast-moving reference frame can be scaled or subtracted out consistently. The result is essentially a change of the variables. Susskind used the new variables to draw attention to the (two-dimensional) Galilean subgroup of the Poincaré group. He pointed out that the simplified vacuum structure and the non-relativistic kinematics of theories at infinite momentum might offer potential-theoretic intuition in relativistic quantum mechanics. Bardakci and Halpern [16] further analyzed the structure of the theories at infinite momentum. They viewed the infinite-momentum limit as a change of variables from the laboratory time t and space coordinate z to a new “time” $\tau = (t + z)/\sqrt{2}$ and a new “space” $\zeta = (t - z)/\sqrt{2}$. Chang and Ma [92] considered the Feynman diagrams for a ϕ^3 -theory and quantum electrodynamics from this point of view and were able to demonstrate the advantage of their approach in several illustrative calculations. Kogut and Soper [274] have examined the formal foundations of quantum electrodynamics in the infinite-momentum frame, and interpret the infinite-momentum limit as the change of variables thus avoiding limiting procedures. The time-ordered perturbation series of the S-matrix is due to them, see also

[40,41,406,274,275]. Drell et al. [130–133] have recognized that the formalism could serve as kind of natural tool for formulating the quark-parton model.

Independent of and almost simultaneous with the infinite-momentum frame is the work on null plane quantization by Leutwyler [302,303], Klauder et al. [273], and by Rohrlich [390]. In particular, they have investigated the stability of the so-called “little group” among the Poincaré generators [304–307]. Leutwyler recognized the utility of defining quark wavefunctions to give an unambiguous meaning to concepts used in the parton model.

The later developments using the infinite-momentum frame have displayed that the naming is somewhat unfortunate since the total momentum is finite and since the front form needs no particular Lorentz frame. Rather it is *frame-independent* and covariant. *Light-Cone Quantization* seemed to be more appropriate. Casher [91] gave the first construction of the light-cone Hamiltonian for non-Abelian gauge theory and gave an overview of important considerations in light-cone quantization. Chang et al. [93–96] demonstrated the equivalence of light-cone quantization with standard covariant Feynman analysis. Brodsky et al. [53] calculated one-loop radiative corrections and demonstrated renormalizability. Light-cone Fock methods were used by Lepage and Brodsky in the analysis of exclusive processes in QCD [297–300,62,345]. In all of this work there was no citation of Dirac’s work. It did reappear first in the work of Pauli and Brodsky [354,355], who explicitly diagonalize a light-cone Hamiltonian by the method of *discretized light-cone quantization*, see also Section 4. *Light-front* quantization appeared first in the work of Harindranath and Vary [203,204] adopting the above concepts without change. Franke and collaborators [14,146–148,385], Karmanov [267,268], and Pervushin [369] have also done important work on light-cone quantization. Comprehensive reviews can be found in [300,62,66,250,72,185,80].

2.5. Parametrizations of the front form

If one were free to parametrize the front form, one would choose it most naturally as a *real rotation* of the coordinate system, with an angle $\varphi = \pi/4$. The “time-like” coordinate would then be $x^+ = \tilde{x}^0$ and the “space-like” coordinate $x^- = \tilde{x}^3$, or collectively

$$\begin{pmatrix} x^+ \\ x^- \end{pmatrix} = \frac{1}{\sqrt{2}} \begin{pmatrix} 1 & -1 \\ 1 & 1 \end{pmatrix} \begin{pmatrix} x^0 \\ x^3 \end{pmatrix}, \quad g_{\alpha\beta} = \begin{pmatrix} 0 & 1 \\ 1 & 0 \end{pmatrix}. \quad (2.46)$$

The metric tensor $g^{\mu\nu}$ obviously transforms according to Eq. (2.45), and the Jacobian for this transformation is unity.

But this has not what has been done, starting way back with Bardakci and Halpern [16] and continuing with Kogut and Soper [274]. Their definition corresponds to a rotation of the coordinate system by $\varphi = -\pi/4$ and an *reflection* of x^- . The Kogut–Soper convention (KS) [274] is thus:

$$\begin{pmatrix} x^+ \\ x^- \end{pmatrix} = \frac{1}{\sqrt{2}} \begin{pmatrix} 1 & 1 \\ 1 & -1 \end{pmatrix} \begin{pmatrix} x^0 \\ x^3 \end{pmatrix}, \quad g_{\alpha\beta} = \begin{pmatrix} 0 & 1 \\ 1 & 0 \end{pmatrix}. \quad (2.47)$$

see also Appendix C. It is often convenient to distinguish longitudinal Lorentz indices α or β (+, -) from the transversal ones i or j (1,2), and to introduce transversal vectors by

$x_{\perp} = (x^1, x^2)$. The KS-convention is particularly suited for theoretical work, since the raising and lowering of the Lorentz indices is simple. With the totally antisymmetric symbol

$$\varepsilon_{+12}^+ = 1, \quad \text{thus} \quad \varepsilon_{+12-} = 1, \quad (2.48)$$

the volume integral becomes

$$\int d\omega_+ = \int dx^- d^2x_{\perp} = \int dx_+ d^2x_{\perp}. \quad (2.49)$$

One should emphasize that $\partial_+ = \partial^-$ is a time-like derivative $\partial/\partial x^+ = \partial/\partial x_-$ as opposed to $\partial_- = \partial^+$, which is a space-like derivative $\partial/\partial x^- = \partial/\partial x_+$. Correspondingly, $P_+ = P^-$ is the Hamiltonian which propagates in the light-cone time x^+ , while $P_- = P^+$ is the longitudinal space-like momentum.

In much of the practical work, however, one is bothered with the $\sqrt{2}$'s scattered all over the place. At the expense of having various factors of 2, this is avoided in the Lepage–Brodsky (LB) convention [299]:

$$\begin{pmatrix} x^+ \\ x^- \end{pmatrix} = \begin{pmatrix} 1 & 1 \\ 1 & -1 \end{pmatrix} \begin{pmatrix} x^0 \\ x^3 \end{pmatrix} \quad \text{thus} \quad g^{\alpha\beta} = \begin{pmatrix} 0 & 2 \\ 2 & 0 \end{pmatrix}, \quad g_{\alpha\beta} = \begin{pmatrix} 0 & \frac{1}{2} \\ \frac{1}{2} & 0 \end{pmatrix}, \quad (2.50)$$

see also Appendix B. Here, $\partial_+ = \frac{1}{2}\partial^-$ is a time-like and $\partial_- = \frac{1}{2}\partial^+$ a space-like derivative. The Hamiltonian is $P_+ = \frac{1}{2}P^-$, and $P_- = \frac{1}{2}P^+$ is the longitudinal momentum. With the totally antisymmetric symbol

$$\varepsilon_{+12}^+ = 1 \quad \varepsilon_{+12-} = \frac{1}{2}, \quad (2.51)$$

the volume integral becomes

$$\int d\omega_+ = \frac{1}{2} \int dx^- d^2x_{\perp} = \int dx_+ d^2x_{\perp}. \quad (2.52)$$

We will use both the LB-convention and the KS-convention in this review, and indicate in each section which convention we are using.

The transition from the instant form to the front form is quite simple: In all the equations found in Sections 2.1 and 2.2 one has to substitute the “0” by the “+” and the “3” by the “−”. Take as an example the QED four-momentum in Eq. (2.27) to get

$$\begin{aligned} P_v &= \int_{\Omega} d\omega_0 \left(F^{0\kappa} F_{\kappa v} + \frac{1}{4} g_v^0 F^{\kappa\lambda} F_{\kappa\lambda} + \frac{1}{2} [i\bar{\Psi}\gamma^0 D_v \Psi + \text{h.c.}] \right), \\ P_v &= \int_{\Omega} d\omega_+ \left(F^{+\kappa} F_{\kappa v} + \frac{1}{4} g_v^+ F^{\kappa\lambda} F_{\kappa\lambda} + \frac{1}{2} [i\bar{\Psi}\gamma^+ D_v \Psi + \text{h.c.}] \right), \end{aligned} \quad (2.53)$$

also in KS-convention. The instant and the front form look thus almost identical. However, after having worked out the Lorentz algebra, the expressions for the instant and front-form

Hamiltonians are drastically different:

$$\begin{aligned}
 P_0 &= \frac{1}{2} \int_{\Omega} d\omega_0 (\mathbf{E}^2 + \mathbf{B}^2) + \frac{1}{2} \int_{\Omega} d\omega_0 [i\bar{\Psi}\gamma^+ D_0 \Psi + \text{h.c.}], \\
 P_+ &= \frac{1}{2} \int_{\Omega} d\omega_+ (E_{\parallel}^2 + B_{\parallel}^2) + \frac{1}{2} \int_{\Omega} d\omega_+ [i\bar{\Psi}\gamma^+ D_+ \Psi + \text{h.c.}],
 \end{aligned}
 \tag{2.54}$$

for the instant and the front-form energy, respectively. In the former one has to deal with all three components of the electric and the magnetic field, in the latter only with two of them, namely with the longitudinal components $E_{\parallel} = \frac{1}{2} F^{+-} = E_z$ and $B_{\parallel} = F^{12} = B_z$. Correspondingly, energy–momentum for non-abelian gauge theory is

$$\begin{aligned}
 P_v &= \int_{\Omega} d\omega_0 (F_a^{0\kappa} F_{\kappa v}^a + \frac{1}{4} g_v^0 F_a^{\kappa\lambda} F_{\kappa\lambda}^a + \frac{1}{2} [i\bar{\Psi}\gamma^0 T^a D_v^a \Psi + \text{h.c.}]), \\
 P_v &= \int_{\Omega} d\omega_+ (F_a^{+\kappa} F_{\kappa v}^a + \frac{1}{4} g_v^+ F_a^{\kappa\lambda} F_{\kappa\lambda}^a + \frac{1}{2} [i\bar{\Psi}\gamma^+ T^a D_v^a \Psi + \text{h.c.}]).
 \end{aligned}
 \tag{2.55}$$

These expressions are exact but not yet very useful, and we shall come back to them in later sections. But they are good enough to discuss their symmetries in general.

2.6. The Poincaré symmetries in the front form

The algebra of the four-energy–momentum $P^\mu = p^\mu$ and four-angular–momentum $M^{\mu\nu} = x^\mu p^\nu - x^\nu p^\mu$ for free particles [19,400,433,450] with the basic commutator $(1/i\hbar)[x^\mu, p_\nu] = \delta_\nu^\mu$ is

$$\begin{aligned}
 (1/i\hbar)[P^\rho, M^{\mu\nu}] &= g^{\rho\mu} P^\nu - g^{\rho\nu} P^\mu, & (1/i\hbar)[P^\rho, P^\mu] &= 0, \\
 (1/i\hbar)[M^{\rho\sigma}, M^{\mu\nu}] &= g^{\rho\nu} M^{\sigma\mu} + g^{\sigma\mu} M^{\rho\nu} - g^{\rho\mu} M^{\sigma\nu} - g^{\sigma\nu} M^{\rho\mu}.
 \end{aligned}
 \tag{2.56}$$

It is postulated that the generalized momentum operators satisfy the same commutator relations. They form thus a group and act as propagators in the sense of the Heisenberg equations

$$\begin{aligned}
 (1/i\hbar)[P^\nu, \phi_r(x)] &= i\partial^\nu \phi_r(x) \\
 (1/i\hbar)[M^{\mu\nu}, \phi_r(x)] &= (x^\mu \partial^\nu - x^\nu \partial^\mu) \phi_r(x) + \Sigma_{rs}^{\mu\nu} \phi_s.
 \end{aligned}
 \tag{2.57}$$

Their validity for the front form was verified by Chang et al. [94–96], and partially even before that by Kogut and Soper [274]. Leutwyler and others have made important contributions [302–307]. The ten constants of motion P^μ and $M^{\mu\nu}$ are observables, thus hermitean operators with real eigenvalues. It is advantageous to construct representations in which the constants of motion are diagonal. The corresponding Heisenberg equations, for example, become then almost trivial. But one cannot diagonalize all ten constants of motion simultaneously because they do not commute. One has to make a choice.

The commutation relations, Eq. (2.56), define a group. The group is isomorphic to the Poincaré group, to the ten 4×4 matrices which generate an arbitrary inhomogeneous Lorentz

transformation. The question of how many and which operators can be diagonalized simultaneously turns out to be identical to the problem of classifying all irreducible unitary transformations of the Poincaré group. According to Dirac [123] one cannot find more than seven mutually commuting operators.

It is convenient to discuss the structure of the Poincaré group [400,433] in terms of the Pauli–Lubansky vector $V^\kappa \equiv \varepsilon^{\kappa\lambda\mu\nu} P_\lambda M_{\mu\nu}$, with $\varepsilon^{\kappa\lambda\mu\nu}$ being the totally antisymmetric symbol in 4 dimensions. V is orthogonal to the generalized momenta, $P_\mu V^\mu = 0$, and obeys the algebra

$$(1/i\hbar)[V^\kappa, P^\mu] = 0, \quad (1/i\hbar)[V^\kappa, M^{\mu\nu}] = g^{\kappa\nu} V^\mu - g^{\kappa\mu} V^\nu, \quad (1/i\hbar)[V^\kappa, V^\lambda] = \varepsilon^{\kappa\lambda\mu\nu} V_\mu P_\nu. \quad (2.58)$$

The two group invariants are the operator for the invariant mass-squared $M^2 = P^\mu P_\mu$ and the operator for intrinsic spin-squared $V^2 = V^\mu V_\mu$. They are Lorentz scalars and commute with all generators P^μ and $M^{\mu\nu}$, as well as with all V^μ . A convenient choice of the six mutually commuting operators is therefore for the front form:

- (1) the invariant mass squared, $M^2 = P^\mu P_\mu$,
- (2–4) the three space-like momenta, P^+ and \mathbf{P}_\perp ,
- (5) the total spin squared, $S^2 = V^\mu V_\mu$,
- (6) one component of V , say V^+ , called S_z .

There are other equivalent choices. In constructing a representation which diagonalizes simultaneously the six mutually commuting operators one can proceed consecutively, in principle, by diagonalizing one after the other. At the end, one will have realized the old dream of Wigner [450] and of Dirac [123] to classify physical systems with the quantum numbers of the irreducible representations of the Poincaré group.

Inspecting the definition of boost-angular-momentum $M_{\mu\nu}$ in Eq. (2.18) one identifies which components are dependent on the interaction and which are not. Dirac [123,126] calls them complicated and simple, or dynamic and kinematic, or Hamiltonians and momenta, respectively. In the instant form, the three components of the boost vector $K_i = M_{i0}$ are dynamic, and the three components of angular momentum $J_i = \varepsilon_{ijk} M_{jk}$ are kinematic. The cyclic symbol ε_{ijk} is 1, if the space-like indices ijk are in cyclic order, and zero otherwise.

As noted already by Dirac [123], the front form is special in having four kinematic components of $M_{\mu\nu}$ (M_{+-} , M_{12} , M_{1-} , M_{2-}) and only two dynamic ones (M_{+1} and M_{+2}). One checks this directly from the defining equation (2.18). Kogut and Soper [274] discuss and interpret them in terms of the above boosts and angular momenta. They introduce the transversal vector \mathbf{B}_\perp with components

$$\mathbf{B}_{\perp 1} = M_{+1} = (1/\sqrt{2})(K_1 + J_2), \quad \mathbf{B}_{\perp 2} = M_{+2} = (1/\sqrt{2})(K_2 - J_1). \quad (2.59)$$

In the front form they are kinematic and boost the system in x - and y -direction, respectively. The kinematic operators

$$M_{12} = J_3, \quad M_{+-} = K_3 \quad (2.60)$$

rotate the system in the x - y plane and boost it in the longitudinal direction, respectively. In the front form one deals thus with seven mutually commuting operators [123]

$$M_{+-}, \mathbf{B}_\perp \quad \text{and all } P^\mu, \quad (2.61)$$

instead of the six in the instant form. The remaining two Poincaré generators are combined into a transversal angular-momentum vector \mathbf{S}_\perp with

$$S_{\perp 1} = M_{1-} = (1/\sqrt{2})(K_1 - J_2), \quad S_{\perp 2} = M_{2-} = (1/\sqrt{2})(K_2 + J_1). \quad (2.62)$$

They are both dynamical, but commute with each other and M^2 . They are thus members of a dynamical subgroup [274], whose relevance has yet to be exploited.

Thus, one can diagonalize the light-cone energy P^- within a Fock basis where the constituents have fixed total P^+ and \mathbf{P}_\perp . For convenience, we shall define a “light-cone Hamiltonian” as the operator

$$H_{\text{LC}} = P^\mu P_\mu = P^- P^+ - \mathbf{P}_\perp^2, \quad (2.63)$$

so that its eigenvalues correspond to the invariant mass spectrum M_i of the theory. The boost invariance of the eigensolutions of H_{LC} reflects the fact that the boost operators K_3 and \mathbf{B}_\perp are kinematical. In fact, one can boost the system to an “intrinsic frame” in which the transversal momentum vanishes

$$\mathbf{P}_\perp = \mathbf{0} \quad \text{thus } H_{\text{LC}} = P^- P^+. \quad (2.64)$$

In this frame, the longitudinal component of the Pauli–Lubansky vector reduces to the longitudinal angular momentum $J_3 = J_z$, which allows for considerable reduction of the numerical work [429]. The transformation to an arbitrary frame with finite values of \mathbf{P}_\perp is then trivially performed.

The above symmetries imply the very important aspect of the front form that both the Hamiltonian and all amplitudes obtained in light-cone perturbation theory (graph by graph!) are manifestly invariant under a large class of Lorentz transformations:

(1) boosts along the 3-direction: and $p^+ \rightarrow C_\parallel p^+$, $\mathbf{p}_\perp \rightarrow \mathbf{p}_\perp$,

$$\mathbf{p}_\perp p^- \rightarrow C_\parallel^{-1} p^-$$

(2) transverse boosts: $p^+ \rightarrow p^+$, $\mathbf{p}_\perp \rightarrow \mathbf{p}_\perp + p^+ \mathbf{C}_\perp$,

$$p^- \rightarrow p^- + 2\mathbf{p}_\perp \cdot \mathbf{C}_\perp + p^+ \mathbf{C}_\perp^2$$

(3) rotations in the x - y plane: $p^+ \rightarrow p^+$, $\mathbf{p}_\perp^2 \rightarrow \mathbf{p}_\perp^2$.

All of these hold for every single-particle momentum p^μ , and for any set of dimensionless c -numbers C_\parallel and \mathbf{C}_\perp . It is these invariances which also lead to the frame independence of the Fock state wave functions.

If a theory is rotational invariant, then each eigenstate of the Hamiltonian which describes a state of non-zero mass can be classified in its rest frame by its spin eigenvalues

$$\begin{aligned} J^2 |P^0 = M, \mathbf{P} = \mathbf{0}\rangle &= s(s+1) |P^0 = M, \mathbf{P} = \mathbf{0}\rangle, \\ J_z |P^0 = M, \mathbf{P} = \mathbf{0}\rangle &= s_z |P^0 = M, \mathbf{P} = \mathbf{0}\rangle. \end{aligned} \quad (2.65)$$

This procedure is more complicated in the front form since the angular momentum operator does not commute with the invariant mass-squared operator M^2 . Nevertheless, Hornbostel [228–230] constructs light-cone operators

$$\begin{aligned} \mathcal{J}^2 &= \mathcal{J}_3^2 + \mathcal{J}_\perp^2, \quad \text{with } \mathcal{J}_3 = J_3 + \varepsilon_{ij} B_{\perp i} P_{\perp j} / P^+, \\ \mathcal{J}_{\perp k} &= (1/M) \varepsilon_{k\ell} (S_{\perp \ell} P^+ - B_{\perp \ell} P^- - K_3 P_{\perp \ell} + \mathcal{J}_{3\varepsilon_{\ell m}} P_{\perp m}), \end{aligned} \quad (2.66)$$

which, in principle, could be applied to an eigenstate $|P^+, \mathbf{P}_\perp\rangle$ to obtain the rest frame spin quantum numbers. This is straightforward for \mathcal{J}_3 since it is kinematical; in fact, $\mathcal{J}_3 = J_3$ in a frame with $\mathbf{P}_\perp = \mathbf{0}_\perp$. However, \mathcal{J}_\perp is dynamical and depends on the interactions. Thus, it is generally difficult to explicitly compute the total spin of a state using light-cone quantization. Some of the aspects have been discussed by Coester [106] and collaborators [105,102]. A practical and simple way has been applied by Trittman [429]. Diagonalizing the light-cone Hamiltonian in the intrinsic frame for $J_z \neq 0$, he can ask for J_{\max} , the maximum eigenvalue of J_z within a numerically degenerate multiplet of mass-squared eigenvalues. The total ‘spin J ’ is then determined by $J = 2J_{\max} + 1$, as to be discussed in Section 4. But more work on this question is certainly necessary, as well as on the discrete symmetries like parity and time reversal and their quantum numbers for a particular state, see also Hornbostel [228–230]. One needs the appropriate language for dealing with spin in highly relativistic systems.

2.7. The equations of motion and the energy–momentum tensor

Energy–momentum for gauge theory had been given in Eq. (2.55). They contain time derivatives of the fields which can be eliminated using the equations of motion.

The color-Maxwell equations are given in Eq. (2.33). They are four (sets of) equations for determining the four (sets of) functions A_a^μ . One of the equations of motion is removed by fixing the gauge and we choose the light-cone gauge [22]

$$A_a^+ = 0. \quad (2.67)$$

Two of the equations of motion express the time derivatives of the two transversal components A_\perp^a in terms of the other fields. Since the front-form momenta in Eq. (2.55) do not depend on them, we discard them here. The fourth is the analogue of the Coulomb equation or of the Gauss’ law in the instant form, particularly $\partial_\mu F_a^{\mu+} = gJ_a^+$. In the light-cone gauge the color-Maxwell charge density J_a^+ is independent of the vector potentials, and the Coulomb equation reduces to

$$-\partial^+ \partial_- A_a^- - \partial^+ \partial_i A_{\perp a}^i = gJ_a^+. \quad (2.68)$$

This equation involves only (light-cone) space derivatives. Therefore, it can be satisfied only, if one of the components is a functional of the others. There are subtleties involved in actually doing this, in particular one has to cope with the ‘zero mode problem’, see for example [358]. Disregarding this here, one inverts the equation by

$$A_+^a = \tilde{A}_+^a + (g/(i\partial^+)^2)J_a^+. \quad (2.69)$$

For the free case ($g = 0$), A^- reduces to \tilde{A}^- . Following Lepage and Brodsky [299], one can collect all components which survive the limit $g \rightarrow 0$ into the ‘free solution’ \tilde{A}_a^μ , defined by

$$\tilde{A}_+^a = -(1/\partial^+) \partial_i A_{\perp a}^i, \quad \text{thus } \tilde{A}_a^\mu = (0, \mathbf{A}_{\perp a}, \tilde{A}_a^+). \quad (2.70)$$

Its four-divergence vanishes by construction and the Lorentz condition $\partial_\mu \tilde{A}_a^\mu = 0$ is satisfied as an operator. As a consequence, \tilde{A}_a^μ is purely transverse. The inverse space derivatives $(i\partial^+)^{-1}$ and $(i\partial^+)^{-2}$ are actually Green’s functions. Since they depend only on x^- , they are comparatively simple, much simpler than in the instant form where $(\nabla^2)^{-1}$ depends on all three space-like coordinates.

The color-Dirac equations are defined in Eq. (2.35) and are used here to express the time derivatives $\partial_+ \Psi$ as function of the other fields. After multiplication with $\beta = \gamma^0$ they read explicitly

$$(i\gamma^0\gamma^+ T^a D_+^a + i\gamma^0\gamma^- T^a D_-^a + i\alpha_\perp^i T^a D_{\perp i}^a)\Psi = m\beta\Psi, \quad (2.71)$$

with the usual $\alpha^k = \gamma^0\gamma^k$, $k = 1,2,3$. In order to isolate the time derivative one introduces the projectors $\Lambda_\pm = \Lambda^\pm$ and projected spinors $\Psi_\pm = \Psi^\pm$ by

$$\Lambda_\pm = \frac{1}{2}(1 \pm \alpha^3), \quad \Psi_\pm = \Lambda_\pm \Psi. \quad (2.72)$$

Note that the raising or lowering of the projector labels \pm is irrelevant. The $\gamma^0\gamma^\pm$ are obviously related to the Λ^\pm , but differently in the KS- and LB-convention

$$\gamma^0\gamma^\pm = 2\Lambda_{\text{LB}}^\pm = \sqrt{2}\Lambda_{\text{KS}}^\pm. \quad (2.73)$$

Multiplying the color-Dirac equation once with Λ^+ and once with Λ^- , one obtains a coupled set of spinor equations

$$\begin{aligned} 2i\partial_+ \Psi_+ &= (m\beta - i\alpha_\perp^i T^a D_{\perp i}^a)\Psi_- + 2gA_+^a T^a \Psi_+, \\ 2i\partial_- \Psi_- &= (m\beta - i\alpha_\perp^i T^a D_{\perp i}^a)\Psi_+ + 2gA_-^a T^a \Psi_-. \end{aligned} \quad (2.74)$$

Only the first of them involves a time derivative. The second is a constraint, similar to the above in the Coulomb equation. With the same proviso in mind, one defines

$$\Psi_- = (1/2i\partial_-)(m\beta - i\alpha_\perp^i T^a D_{\perp i}^a)\Psi_+. \quad (2.75)$$

Substituting this into the former, the time derivative is

$$2i\partial_+ \Psi_+ = 2gA_+^a T^a \Psi_+ + (m\beta - i\alpha_\perp^i T^a D_{\perp i}^a)(1/2i\partial_-)(m\beta - i\alpha_\perp^i T^a D_{\perp i}^a)\Psi_+. \quad (2.76)$$

Finally, in analogy to the color-Maxwell case, one can conveniently introduce the free spinors $\tilde{\Psi} = \tilde{\Psi}_+ + \tilde{\Psi}_-$ by

$$\tilde{\Psi} = \Psi_+ + (m\beta - i\alpha_\perp^i \partial_{\perp i})(1/2i\partial_-)\Psi_+. \quad (2.77)$$

Contrary to the full spinor see, for example, Eq. (2.75), $\tilde{\Psi}$ is independent of the interaction. To get the corresponding relations for the KS-convention, one substitutes the “2” by “ $\sqrt{2}$ ” in accord with Eq. (2.73).

The front-form Hamiltonian according to Eq. (2.55) is

$$P_+ = \int_\Omega d\omega_+ \left(F^{+\kappa} F_{\kappa+} + \frac{1}{4} F_a^{\kappa\lambda} F_{\kappa\lambda}^a + \frac{1}{2} [i\tilde{\Psi}\gamma^+ T^a D_+^a \Psi + \text{h.c.}] \right). \quad (2.78)$$

Expressing it as a functional of the fields will finally lead to Eq. (2.89) below, but despite the straightforward calculation we display explicitly the intermediate steps. Consider first the energy density of the color-electro-magnetic fields $\frac{1}{4} F^{\kappa\lambda} F_{\kappa\lambda} + F^{+\kappa} F_{\kappa+}$. Conveniently defining the abbreviations

$$B_a^{\mu\nu} = f^{abc} A_b^\mu A_c^\nu, \quad \chi_a^\mu = f^{abc} \partial^\mu A_b^\nu A_c^\nu, \quad (2.79)$$

the field tensors in Eq. (2.31) are rewritten as $F_a^{\mu\nu} = \partial^\mu A_a^\nu - \partial^\nu A_a^\mu - gB_a^{\mu\nu}$ and typical tensor contractions become

$$\frac{1}{4}F_a^{\mu\nu}F_{\mu\nu} = \partial^\mu A_a^\nu \partial_\mu A_a^\nu - \partial^\mu A_a^\nu \partial_\nu A_a^\mu + 2\chi_a^\mu A_a^\mu + \frac{1}{2}g^2 B_a^{\mu\nu} B_{\mu\nu}. \quad (2.80)$$

Using $F^{\alpha\kappa}F_{\alpha\kappa} = 2F^{+\kappa}F_{+\kappa}$, the color-electro-magnetic energy density

$$\frac{1}{4}F^{\kappa\lambda}F_{\kappa\lambda} + F^{+\kappa}F_{\kappa+} = \frac{1}{4}F^{\kappa\lambda}F_{\kappa\lambda} - \frac{1}{2}F^{\kappa\alpha}F_{\kappa\alpha} = \frac{1}{4}F^{\kappa i}F_{\kappa i} - \frac{1}{4}F^{\kappa\alpha}F_{\kappa\alpha} = \frac{1}{4}F^{ij}F_{ij} - \frac{1}{4}F^{\alpha\beta}F_{\alpha\beta} \quad (2.81)$$

separates completely into a longitudinal (α, β) and a transversal contribution (i, j) [358]; see also Eq. (2.54). Substituting A_+ by Eq. (2.69), the color-electric and color-magnetic parts become

$$\begin{aligned} \frac{1}{4}F^{\alpha\beta}F_{\beta\alpha} &= \frac{1}{2}\partial^+ A_+ \partial^+ A_+ = \frac{1}{2}g^2 J^+ (1/(i\partial^+)^2) J^+ + \frac{1}{2}(\partial_i A_{\perp}^i)^2 + gJ^+ \tilde{A}_+, \\ \frac{1}{4}F^{ij}F_{ij} &= \frac{1}{4}g^2 B^{ij}B_{ij} - \frac{1}{2}(\partial_i A_{\perp}^i)^2 + \chi^i A_i + \frac{1}{2}A^i(\partial^i \partial_i) A_j, \end{aligned} \quad (2.82)$$

respectively. The role of the different terms will be discussed below. The color-quark energy density is evaluated in the LB-convention. With $i\bar{\Psi}\gamma^+ D_+^a T^a \Psi = i\Psi^\dagger \gamma^0 \gamma^+ D_+^a T^a \Psi$ and the projectors of Eq. (2.72) one gets first $i\bar{\Psi}\gamma^+ D_+^a T^a \Psi = i\sqrt{2}\Psi^\dagger_+ D_+^a T^a \Psi_+$. Direct substitution of the time derivatives in Eq. (2.76) then gives

$$i\bar{\Psi}\gamma^+ D_+^a T^a \Psi = \tilde{\Psi}^\dagger_+(m\beta - i\alpha_{\perp}^j D_{\perp j}^a T^a)(1/\sqrt{2}i\partial_-)(m\beta - i\alpha_{\perp}^j D_{\perp j}^b T^b)\Psi_+. \quad (2.83)$$

Isolating the interaction in the covariant derivatives $iT^a D_\mu^a = i\partial_\mu - gT^a A_\mu^a$ produces

$$\begin{aligned} i\bar{\Psi}\gamma^+ D_+^a T^a \Psi &= g\tilde{\Psi}^\dagger_+ \alpha_{\perp}^j A_{\perp j}^a T^a \tilde{\Psi}_- + g\tilde{\Psi}^\dagger_- \alpha_{\perp}^j A_{\perp j}^a T^a \tilde{\Psi}_+ \\ &+ (g^2/\sqrt{2})\Psi^\dagger_+ \alpha_{\perp}^j A_{\perp j}^a T^a \frac{1}{i\partial_-} \alpha_{\perp}^i A_{\perp i}^b T^b \Psi_+ \\ &+ (1/\sqrt{2})\Psi^\dagger_+(m\beta - i\alpha_{\perp}^j \partial_{\perp j})(1/i\partial_-)(m\beta - i\alpha_{\perp}^i \partial_{\perp i})\Psi_+. \end{aligned} \quad (2.84)$$

Introducing \tilde{j}_a^μ as the color-fermion part of the total current \tilde{J}_a^μ , that is

$$\tilde{j}_a^\mu(x) = \tilde{\Psi}\gamma^\mu T^a \tilde{\Psi} \quad \text{with} \quad \tilde{J}_a^\mu(x) = \tilde{j}_a^\mu(x) + \tilde{\chi}_a^\mu(x), \quad (2.85)$$

one notes that $J_a^+ = \tilde{J}_a^+$ when comparing with the defining equation (2.77). For the transversal parts holds obviously

$$\tilde{j}_{\perp a}^i = \tilde{\Psi}^\dagger \alpha_{\perp}^i T^a \tilde{\Psi} = \tilde{\Psi}^\dagger_+ \alpha_{\perp}^i T^a \tilde{\Psi}_- + \tilde{\Psi}^\dagger_- \alpha_{\perp}^i T^a \tilde{\Psi}_+. \quad (2.86)$$

With $\gamma^+ \gamma^+ = 0$ one finds

$$\begin{aligned} \tilde{\Psi}\gamma^\mu \tilde{A}_{\mu\gamma^+} \gamma^v \tilde{A}_v \tilde{\Psi} &= \tilde{\Psi}\gamma_{\perp}^i \tilde{A}_{\perp i\gamma^+} \gamma^i \tilde{A}_{\perp i} \tilde{\Psi} = \tilde{\Psi}^\dagger \alpha_{\perp}^i \tilde{A}_{\perp i\gamma^+} \gamma^0 \alpha_{\perp}^j \tilde{A}_{\perp j} \tilde{\Psi} \\ &= \sqrt{2}\tilde{\Psi}^\dagger_+ \alpha_{\perp}^i \tilde{A}_{\perp i} \alpha_{\perp}^i \tilde{A}_{\perp i} \tilde{\Psi}_+, \end{aligned} \quad (2.87)$$

see also [300]. The covariant time derivative of the dynamic spinors Ψ_α is therefore

$$i\bar{\Psi}\gamma^+ D_+^a T^a \Psi = g\tilde{j}_{\perp}^i \tilde{A}_{\perp i} + \frac{1}{2}g^2 \tilde{\Psi}\gamma^\mu \tilde{A}_\mu (\gamma^+ / i\partial^+) \gamma^v \tilde{A}_v \tilde{\Psi} + \frac{1}{2}\tilde{\Psi}\gamma^+ ((m^2 - \nabla_{\perp}^2) / i\partial^+) \tilde{\Psi} \quad (2.88)$$

in terms of the fields \tilde{A}_μ and $\tilde{\Psi}_\alpha$. One finds the same expression in LB-convention. Since it is a hermitean operator, one can add Eqs. (2.82) and (2.88) to finally get the front-form Hamiltonian as a sum of five terms,

$$\begin{aligned}
P_+ = & \frac{1}{2} \int dx_+ d^2x_\perp \left(\tilde{\Psi} \gamma^+ \frac{m^2 + (i\nabla_\perp)^2}{i\partial^+} \tilde{\Psi} + \tilde{A}_a^\mu (i\nabla_\perp)^2 \tilde{A}_\mu^a \right) + g \int dx_+ d^2x_\perp \tilde{J}_a^\mu \tilde{A}_\mu^a \\
& + \frac{g^2}{4} \int dx_+ d^2x_\perp \tilde{B}_a^{\mu\nu} \tilde{B}_{\mu\nu}^a + \frac{g^2}{2} \int dx_+ d^2x_\perp \tilde{J}_a^+ \frac{1}{(i\partial^+)^2} \tilde{J}_a^+ \\
& + \frac{g^2}{2} \int dx_+ d^2x_\perp \tilde{\Psi} \gamma^\mu T^a \tilde{A}_\mu^a \frac{\gamma^+}{i\partial^+} (\gamma^\nu T^b \tilde{A}_\nu^b \tilde{\Psi}) .
\end{aligned} \tag{2.89}$$

Only the first term survives the limit $g \rightarrow 0$, hence $P^- \rightarrow \tilde{P}^-$, referred to as the free part of the Hamiltonian. For completeness, the space-like components of energy–momentum as given in Eq. (2.55) become

$$\begin{aligned}
P_k = & \int dx_+ d^2x_\perp (F^{+\kappa} F_{\kappa k} + i\tilde{\Psi} \gamma^+ T^a D_k^a \Psi) \\
= & \int dx_+ d^2x_\perp (\tilde{\Psi} \gamma^+ i\partial_k \tilde{\Psi} + \tilde{A}_a^\mu \partial^+ \partial_k \tilde{A}_\mu^a) \quad \text{for } k = 1, 2, - .
\end{aligned} \tag{2.90}$$

Inserting the free solutions as given below in Eq. (2.100), one gets for $\tilde{P}^\mu = (P^+, \mathbf{P}_\perp, \tilde{P}^-)$

$$\tilde{P}^\mu = \sum_{\lambda, c, f} \int dp^+ d^2p_\perp p^\mu (\tilde{a}^\dagger(q) \tilde{a}(q) + \tilde{b}^\dagger(q) \tilde{b}(q) + \tilde{d}^\dagger(q) \tilde{d}(q)) , \tag{2.91}$$

in line with expectation: In momentum representation the momenta \tilde{P}^μ are diagonal operators. Terms depending on the coupling constant are interactions and in general are non-diagonal operators in Fock space.

Eqs. (2.89) and (2.90) are quite generally applicable:

- They hold both in the Kogut–Soper and Lepage–Brodsky convention.
- They hold for arbitrary non-abelian gauge theory $SU(N)$.
- They hold therefore also for QCD ($N = 3$) and are manifestly invariant under color rotations.
- They hold for abelian gauge theory (QED), formally by replacing the color matrices $T_{c,c'}^a$ with the unit matrix and by setting to zero the structure constants f^{abc} , thus $B^{\mu\nu} = 0$ and $\chi^\mu = 0$.
- They hold for 1 time dimension and arbitrary $d + 1$ space dimensions, with $i = 1, \dots, d$. Only what has to be adjusted is the volume integral $\int dx_+ d^2x_\perp$.
- They thus hold also for the popular toy models in $1 + 1$ dimensions.
- Last but not least, they hold for the ‘dimensionally reduced models’ of gauge theory, formally by setting the transversal derivatives of the free fields to zero, that is $\partial_\perp \tilde{\Psi}_\alpha = 0$ and $\partial_\perp \tilde{A}_\mu = 0$.

Most remarkable, however, is that the relativistic Hamiltonian in Eq. (2.89) is *additive* [274] in the “kinetic” and the “potential” energy, very much like a non-relativistic Hamiltonian

$$H = T + U . \tag{2.92}$$

In this respect, the front form is distinctly different from the conventional instant form. With $H \equiv P_+$ the *kinetic energy*

$$T = \tilde{P}_+ = \frac{1}{2} \int dx_+ d^2x_\perp \left(\tilde{\Psi} \gamma^+ \frac{m^2 + (i\nabla_\perp)^2}{i\partial^+} \tilde{\Psi} + \tilde{A}_a^\mu (i\nabla_\perp)^2 \tilde{A}_\mu^a \right) \quad (2.93)$$

is the only term surviving the limit $g \rightarrow 0$ in Eq. (2.89). The *potential energy* U is correspondingly the sum of the four terms

$$U = V + W_1 + W_2 + W_3. \quad (2.94)$$

Each of them has a different origin and interpretation. The *vertex interaction*

$$V = g \int dx_+ d^2x_\perp \tilde{J}_a^\mu \tilde{A}_\mu^a \quad (2.95)$$

is the light-cone analogue of the $J_\mu A^\mu$ -structures known from covariant theories, particularly electrodynamics. It generates three-point vertices describing bremsstrahlung and pair creation. However, since \tilde{J}^μ contains also the pure gluon part $\tilde{\chi}^\mu$, it includes the three-point-gluon vertices as well. The *four-point-gluon interactions*

$$W_1 = \frac{g^2}{2} \int dx_+ d^2x_\perp \tilde{B}_a^{\mu\nu} \tilde{B}_{\mu\nu}^a \quad (2.96)$$

describe the four-point-gluon vertices. They are typical for non-abelian gauge theory and come only from the color-magnetic fields in Eq. (2.82). The *instantaneous-gluon interaction*

$$W_2 = \frac{g^2}{2} \int dx_+ d^2x_\perp \tilde{J}_a^+ \frac{1}{(i\partial^+)^2} \tilde{J}_a^+ \quad (2.97)$$

is the light-cone analogue of the Coulomb energy, having the same structure (density-propagator-density) and the same origin, namely Gauss' equation (2.69). W_3 describes quark–quark, gluon–gluon, and quark–gluon instantaneous-gluon interactions. The last term, finally, is the *instantaneous-fermion interaction*

$$W_3 = \frac{g^2}{2} \int dx_+ d^2x_\perp \tilde{\Psi} \gamma^\mu T^a \tilde{A}_{\mu; i\partial^+}^a \gamma^\nu T^b \tilde{A}_\nu^b \tilde{\Psi}. \quad (2.98)$$

It originates from the light-cone specific decomposition of Dirac's equation (2.74) and has no counterpart in conventional theories. The present formalism is however more symmetric: The instantaneous gluons and the instantaneous fermions are partners. This has some interesting consequences, as we shall see below. Actually, the instantaneous interactions were seen first by Kogut and Soper [274] in the time-dependent analysis of the scattering amplitude as remnants of choosing the light-cone gauge.

One should carefully distinguish the above front-form Hamiltonian H from the light-cone Hamiltonian H_{LC} , defined in Eqs. (2.63) and (2.64) as the operator of invariant mass-squared. The former is the time-like component of a four-vector and therefore frame-dependent. The latter is a Lorentz scalar and therefore independent of the frame. The former is covariant, the latter invariant under Lorentz transformations, particularly under boosts. The two are related to each

other by multiplying H with a number, the eigenvalue of $2P^+$:

$$H_{\text{LC}} = 2P^+ H. \quad (2.99)$$

The above discussion and interpretation of H applies therefore also to H_{LC} . Note that matrix elements of the ‘‘Hamiltonian’’ have the dimension $\langle \text{energy} \rangle^2$.

2.8. The interactions as operators acting in Fock space

In Section 2.7 the energy–momentum four-vector P_μ was expressed in terms of the free fields. One inserts them into the expressions for the interactions and integrates over configuration space. The free fields are

$$\begin{aligned} \tilde{\Psi}_{\alpha f}(x) &= \sum_\lambda \int \frac{d^3 p^+ d^2 p_\perp}{\sqrt{2p^+(2\pi)^3}} (\tilde{b}(q) u_\alpha(p, \lambda) e^{-ipx} + \tilde{d}^\dagger(q) v_\alpha(p, \lambda) e^{+ipx}), \\ \tilde{A}_\mu^a(x) &= \sum_\lambda \int \frac{d^3 p^+ d^2 p_\perp}{\sqrt{2p^+(2\pi)^3}} (\tilde{a}(q) \varepsilon_\mu(p, \lambda) e^{-ipx} + \tilde{a}^\dagger(q) \varepsilon_\mu^*(p, \lambda) e^{+ipx}), \end{aligned} \quad (2.100)$$

where the properties of the u_α , v_α and ε_μ are given in the appendices and where

$$[\tilde{a}(q), \tilde{a}^\dagger(q')] = \{\tilde{b}(q), \tilde{b}^\dagger(q')\} = \{\tilde{d}(q), \tilde{d}^\dagger(q')\} = \delta(p^+ - p'^+) \delta^{(2)}(\mathbf{p}_\perp - \mathbf{p}'_\perp) \delta_\lambda^{\lambda'} \delta_c^c \delta_{f'}^{f'}. \quad (2.101)$$

Doing that in detail is quite laborious. We therefore restrict ourselves here to a few instructive examples, the vertex interaction V , the instantaneous-gluon interaction W_2 and the instantaneous-fermion interaction W_3 .

According to Eq. (2.95) the fermionic contribution to the vertex interaction is

$$\begin{aligned} V_f &= g \int dx_+ d^2 x_\perp \tilde{j}_a^\mu \tilde{A}_\mu^a = g \int dx_+ d^2 x_\perp \tilde{\Psi}(x) \gamma^\mu T^a \tilde{\Psi}(x) \tilde{A}_\mu^a(x) \Big|_{x^+ = 0} \\ &= \frac{g}{\sqrt{(2\pi)^3}} \sum_{\lambda_1, \lambda_2, \lambda_3} \sum_{c_1, c_2, a_3} \int \frac{d^3 p_1^+ d^2 p_{\perp 1}}{\sqrt{2p_1^+}} \int \frac{d^3 p_2^+ d^2 p_{\perp 2}}{\sqrt{2p_2^+}} \int \frac{d^3 p_3^+ d^2 p_{\perp 3}}{\sqrt{2p_3^+}} \int \frac{dx_+ d^2 x_\perp}{(2\pi)^3} [(\tilde{b}^\dagger(q_1) \bar{u}_\alpha(p_1, \lambda_1) e^{+ip_1 x} \\ &\quad + \tilde{d}(q_1) \bar{v}_\alpha(p_1, \lambda_1) e^{-ip_1 x}) T_{c_1, c_2}^{a_3} \gamma_{\alpha\beta}^\mu (\tilde{d}^\dagger(q_2) v_\beta(p_2, \lambda_2) e^{+ip_2 x} + \tilde{b}(q_2) u_\beta(p_2, \lambda_2) e^{-ip_2 x})] \\ &\quad \times (\tilde{a}^\dagger(q_3) \varepsilon_\mu^*(p_3, \lambda_3) e^{+ip_3 x} + \tilde{a}(q_3) \varepsilon_\mu(p_3, \lambda_3) e^{-ip_3 x}). \end{aligned} \quad (2.102)$$

The integration over configuration space produces essentially Dirac delta–functions in the single particle momenta, which reflect momentum conservation:

$$\int \frac{dx_+}{2\pi} e^{ix_+(\sum_j p_j^+)} = \delta\left(\sum_j p_j^+\right), \quad \int \frac{d^2 x_\perp}{(2\pi)^3} e^{-ix_\perp(\sum_j \mathbf{p}_{\perp j})} = \delta^{(2)}\left(\sum_j \mathbf{p}_{\perp j}\right). \quad (2.103)$$

Note that the sum of these single-particle momenta is essentially the sum of the particle momenta minus the sum of the hole momenta. Consequently, if a particular term has *only creation or only destruction operators* as in

$$b^\dagger(q_1) d^\dagger(q_2) a^\dagger(q_3) \delta(p_1^+ + p_2^+ + p_3^+) \simeq 0,$$

its contribution vanishes since the light-cone longitudinal momenta p^+ are all positive and cannot add to zero. The case that they are exactly equal to zero is excluded by the regularization procedures discussed below in Section 4. As a consequence, all energy diagrams which generate the vacuum fluctuations in the usual formulation of quantum field theory are absent from the outset in the front form.

The purely fermionic part of the *instantaneous-gluon interaction* given by Eq. (2.97) becomes, respectively,

$$\begin{aligned}
W_{2,f} &= \frac{g^2}{2} \int dx_+ d^2x_\perp \tilde{j}_a^+ \frac{1}{(i\partial^+)^2} \tilde{j}_a^+ = \frac{g^2}{2} \int dx_+ d^2x_\perp \bar{\Psi}(x) \gamma^+ T^a \tilde{\Psi}(x) \frac{1}{(i\partial^+)^2} \bar{\Psi}(x) \gamma^+ T^a \tilde{\Psi}(x) |_{x^+ = 0}. \\
W_{2,f} &= \frac{g^2}{2(2\pi)^3} \sum_{\lambda_j} \sum_{c_1, c_2, c_3, c_4} \int \frac{dp_1^+ d^2p_{\perp 1}}{\sqrt{2p_1^+}} \int \frac{dp_2^+ d^2p_{\perp 2}}{\sqrt{2p_2^+}} \int \frac{dp_3^+ d^2p_{\perp 3}}{\sqrt{2p_3^+}} \int \frac{dp_4^+ d^2p_{\perp 4}}{\sqrt{2p_4^+}} \\
&\quad \times \int \frac{dx_+ d^2x_\perp}{(2\pi)^3} [(\tilde{b}^\dagger(q_1) \bar{u}_\alpha(p_1, \lambda_1) e^{+ip_1x} + \tilde{d}(q_1) \bar{v}_\alpha(p_1, \lambda_1) e^{-ip_1x}) T_{c_1, c_2}^a \\
&\quad \times \gamma_{\alpha\beta}^+(\tilde{d}^\dagger(q_2) v_\alpha(p_2, \lambda_2) e^{+ip_2x} + \tilde{b}(q_2) u_\alpha(p_2, \lambda_2) e^{-ip_2x})] \\
&\quad \times \frac{1}{(i\partial^+)^2} [(\tilde{b}^\dagger(q_3) \bar{u}_\alpha(p_3, \lambda_3) e^{+ip_3x} + \tilde{d}(q_3) \bar{v}_\alpha(p_3, \lambda_3) e^{-ip_3x}) T_{c_3, c_4}^a \\
&\quad \times \gamma_{\alpha\beta}^+(\tilde{d}^\dagger(q_4) v_\beta(p_4, \lambda_4) e^{+ip_4x} + \tilde{b}(q_4) u_\beta(p_4, \lambda_4) e^{-ip_4x})]. \tag{2.104}
\end{aligned}$$

By the same reason as discussed above, there will be no contributions from terms with only creation or only destruction operators. The instantaneous-fermion interaction, finally, becomes according to Eq. (2.98),

$$\begin{aligned}
W_3 &= \frac{g^2}{2} \int dx_+ d^2x_\perp \bar{\Psi} \gamma^\mu T^a \tilde{A}_{\mu i\partial^+}^a \gamma^+ (\gamma^\nu T^b \tilde{A}_\nu^b \tilde{\Psi}) \\
&= \frac{g^2}{2(2\pi)^3} \sum_{\lambda_j} \sum_{c_1, a_2, a_3, c_4} \int \frac{dp_1^+ d^2p_{\perp 1}}{\sqrt{2p_1^+}} \int \frac{dp_2^+ d^2p_{\perp 2}}{\sqrt{2p_2^+}} \int \frac{dp_3^+ d^2p_{\perp 3}}{\sqrt{2p_3^+}} \int \frac{dp_4^+ d^2p_{\perp 4}}{\sqrt{2p_4^+}} \\
&\quad \times \int \frac{dx_+ d^2x_\perp}{(2\pi)^3} [(\tilde{b}^\dagger(q_1) \bar{u}(p_1, \lambda_1) e^{+ip_1x} + \tilde{d}(q_1) \bar{v}(p_1, \lambda_1) e^{-ip_1x}) T_{c_1, c}^{a_2} \\
&\quad \times \gamma^\mu (\tilde{a}^\dagger(q_2) \varepsilon_\mu^*(p_2, \lambda_2) e^{+ip_2x} + \tilde{a}(q_2) \varepsilon_\mu(p_2, \lambda_2) e^{-ip_2x}) \\
&\quad \times \frac{1}{i\partial^+} (\tilde{a}^\dagger(q_3) \varepsilon_\nu^*(p_3, \lambda_3) e^{+ip_3x} + \tilde{a}(q_3) \varepsilon_\nu(p_3, \lambda_3) e^{-ip_3x}) T_{c, c_4}^{a_3} \\
&\quad \times \gamma^\nu (\tilde{d}^\dagger(q_4) v(p_4, \lambda_4) e^{+ip_4x} + \tilde{b}(q_4) u(p_4, \lambda_4) e^{-ip_4x})]. \tag{2.105}
\end{aligned}$$

Each of the instantaneous interactions types has primarily $2^4 - 2 = 14$ individual contributions, which will not be enumerated in all detail. In Section 4 complete tables of all interactions will be tabulated in their final normal ordered form, that is with all creation operators are to the left of the destruction operators. All instantaneous interactions like those shown above are four-point interactions and the creation and destruction operators appear in a natural order. According to Wick's theorem this "time-ordered" product equals to the normal ordered product plus the sum of

all possible pairwise contractions. The fully contracted interactions are simple c -numbers which can be omitted due to vacuum renormalization. The one-pair contracted operators, however, cannot be thrown away and typically have a structure like

$$I(q)\tilde{b}^\dagger(q)\tilde{b}(q). \quad (2.106)$$

Due to the properties of the spinors and polarization functions u_α , v_α and ε_μ they become diagonal operators in momentum space. The coefficients $I(q)$ are kind of mass terms and have been labeled as “self-induced inertias” [354]. Even if they formally diverge, they are part of the operator structure of field theory, and therefore should not be discarded but need careful regularization. In Section 4 they will be tabulated as well.

3. Bound states on the light cone

In principle, the problem of computing for quantum chromodynamics the spectrum and the corresponding wavefunctions can be reduced to diagonalizing the light-cone Hamiltonian. Any hadronic state must be an eigenstate of the light-cone Hamiltonian, thus a bound state of mass M , which satisfies $(M^2 - H_{\text{LC}})|M\rangle = 0$. Projecting the Hamiltonian eigenvalue equation onto the various Fock states $\langle q\bar{q}|$, $\langle q\bar{q}g|$... results in an infinite number of coupled integral eigenvalue equations. Solving these equations is equivalent to solving the field theory. The light-cone Fock basis is a very physical tool for discussing these theories because the vacuum state is simple and the wavefunctions can be written in terms of relative coordinates which are frame-independent. In terms of the Fock-space wavefunction, one can give exact expressions for the form factors and structure functions of physical states. As an example we evaluate these expressions with a perturbative wavefunction for the electron and calculate the anomalous magnetic moment of the electron.

In order to lay down the groundwork for upcoming non-perturbative studies, it is indispensable to gain control over the perturbative treatment. We devote therefore a section to the perturbative treatment of quantum electrodynamics and gauge theory on the light cone. Light-cone perturbation theory is really Hamiltonian perturbation theory, and we give the complete set of rules which are the analogues of the Feynman rules. We shall demonstrate in a selected example, that one gets the same covariant and gauge-invariant scattering amplitude as in Feynman theory. We also shall discuss one-loop renormalization of QED in the Hamiltonian formalism.

Quantization is done in the light-cone gauge, and the light-cone time-ordered perturbation theory is developed in the null-plane Hamiltonian formalism. For gauge-invariant quantities, this is very loosely equivalent to the use of Feynman diagrams together with an integration over p^- by residues [426,427]. The one-loop renormalization of QED quantized on the null plane looks very different from the standard treatment. In addition to not being manifestly covariant, x^+ -ordered perturbation theory is fraught with singularities, even at tree level. The origin of these unusual, “spurious”, infrared divergences is not a mystery. Consider, for example, a free particle whose transverse momentum $\mathbf{p}_\perp = (p^1, p^2)$ is fixed, and whose third component p^3 is cut at some momentum Λ . Using the mass-shell relation, $p^- = (m^2 + \mathbf{p}_\perp^2)/2p^+$, one sees that p^+ has a lower bound proportional to Λ^{-1} . Hence, the light-cone spurious infrared divergences are simply a manifestation of space–time ultraviolet divergences. A great deal of work is continuing on how to treat these divergences in a self-consistent manner [456]. Bona fide infrared divergences are of

course also present, and can be taken care of as usual by giving the photon a small mass, consistent with light-cone quantization [406].

As a matter of practical experience, and quite opposed to the instant form of the Hamiltonian approach, one gets reasonable results even if the infinite number of integral is equations truncated. The Schwinger model is particularly illustrative because in the instant form this bound state has a very complicated structure in terms of Fock states while in the front form the bound state consists of a single electron–positron pair. One might hope that a similar simplification occurs in QCD. The Yukawa model is treated here in Tamm–Dancoff truncation in $3 + 1$ dimensions [182,373,374]. This model is particularly important because it features a number of the renormalization problems inherent to the front form, and it motivates the approach of Wilson to be discussed later.

3.1. The hadronic eigenvalue problem

The first step is to find a language in which one can represent hadrons in terms of relativistic confined quarks and gluons. The Bethe–Salpeter formalism [37,312] has been the central method for analyzing hydrogenic atoms in QED, providing a completely covariant procedure for obtaining bound-state solutions. However, calculations using this method are extremely complex and appear to be intractable much beyond the ladder approximation. It also appears impractical to extend this method to systems with more than a few constituent particles. A review can be found in Ref. [312].

An intuitive approach for solving relativistic bound-state problems would be to solve the Hamiltonian eigenvalue problem

$$H|\Psi\rangle = \sqrt{M^2 + \mathbf{P}^2}|\Psi\rangle \quad (3.1)$$

for the particle’s mass, M , and wavefunction, $|\Psi\rangle$. Here, one imagines that $|\Psi\rangle$ is an expansion in multi-particle occupation number Fock states, and that the operators H and \mathbf{P} are second-quantized Heisenberg operators. Unfortunately, this method, as described by Tamm and Dancoff [117,421], is complicated by its non-covariant structure and the necessity to first understand its complicated vacuum eigensolution over all space and time. The presence of the square-root operator also presents severe mathematical difficulties. Even if these problems could be solved, the eigensolution is only determined in its rest system ($\mathbf{P} = 0$); determining the boosted wavefunction is as complicated as diagonalizing H itself.

In principle, the front-form approach works in the same way. One aims at solving the Hamiltonian eigenvalue problem

$$H|\Psi\rangle = \frac{M^2 + \mathbf{P}_\perp^2}{2P^+}|\Psi\rangle, \quad (3.2)$$

which for several reasons is easier: Contrary to P_z the operator P^+ is positive, having only positive eigenvalues. The square-root operator is absent, and the boost operators are kinematic, see Section 2.6. As discussed there, in both the instant and the front form, the eigenfunctions can be labeled with six numbers, the six eigenvalues of the invariant mass M , of the three space-like momenta P^+ , \mathbf{P}_\perp , and of the generalized total spin-squared S^2 and its longitudinal projection S_z , that is

$$|\Psi\rangle = |\Psi; M, P^+, \mathbf{P}_\perp, S^2, S_z; h\rangle. \quad (3.3)$$

states with $P^+ = 0$ built on zero-mode massless gluon quanta [189], but as discussed in Section 7, the physical vacuum is *still far simpler* than is usual.

Since $k_i^+ > 0$ and $P^+ > 0$, one can define boost-invariant longitudinal momentum fractions

$$x_i = \frac{k_i^+}{P^+} \quad \text{with } 0 < x_i < 1, \quad (3.9)$$

and adjust the notation. All particles in a Fock state $|\mu_n\rangle = |n : x_i, \mathbf{k}_{\perp i}, \lambda_i\rangle$ have then four-momentum

$$k_i^\mu \equiv (k^+, \mathbf{k}_\perp, k^-)_i = \left(x_i P^+, \mathbf{k}_{\perp i}, \frac{m_i^2 + k_{\perp i}^2}{x_i P^+} \right) \quad \text{for } i = 1, \dots, N_n, \quad (3.10)$$

and are “on shell”, $(k^\mu k_\mu)_i = m_i^2$. Also the Fock state is “on shell” since one can interpret

$$\left(\sum_{i=1}^{N_n} k_i^- \right) P^+ - \mathbf{P}_\perp^2 = \sum_{i=1}^{N_n} \left(\frac{(\mathbf{k}_{\perp i} + x_i \mathbf{P}_\perp)^2 + m_i^2}{x} \right) - \mathbf{P}_\perp^2 = \sum_{i=1}^{N_n} \left(\frac{k_{\perp i}^2 + m^2}{x} \right)_i \quad (3.11)$$

as its free invariant mass squared $\tilde{M}^2 = \tilde{\mathbf{P}}^\mu \tilde{\mathbf{P}}_\mu$. There is some confusion over the terms “on-shell” and “off-shell” in the literature [367]. The single-particle states are on-shell, as mentioned, but the Fock states μ_n are off the energy shell since \tilde{M} in general is different from the bound-state mass M which appears in Eq. (3.2). In the intrinsic frame ($\mathbf{P}_\perp = \mathbf{0}$), the values of x_i and $\mathbf{k}_{\perp i}$ are constrained by

$$\sum_{i=1}^{N_n} x_i = 1, \quad \sum_{i=1}^{N_n} \mathbf{k}_{\perp i} = \mathbf{0}, \quad (3.12)$$

because of Eq. (3.8). The phase-space differential $d[\mu_n]$ depends on how one normalizes the single-particle states. In the convention where commutators are normalized to a Dirac δ -function, the phase-space integration is

$$\int d[\mu_n] \dots = \sum_{\lambda_i \in n} \int [dx_i d^2 k_{\perp i}] \dots, \quad \text{with} \quad (3.13)$$

$$[dx_i d^2 k_{\perp i}] = \delta\left(1 - \sum_{j=1}^{N_n} x_j\right) \delta^{(2)}\left(\sum_{j=1}^{N_n} \mathbf{k}_{\perp j}\right) dx_1 \dots dx_{N_n} d^2 k_{\perp 1} \dots d^2 k_{\perp N_n}.$$

The additional Dirac δ -functions account for the constraints (3.12). The eigenvalue equation (3.2) therefore stands for an infinite set of coupled integral equations

$$\sum_{n'} \int [d\mu'_{n'}] \langle n : x_i, \mathbf{k}_{\perp i}, \lambda_i | H | n' : x'_i, \mathbf{k}'_{\perp i}, \lambda'_i \rangle \Psi_{n'/h}(x'_i, \mathbf{k}'_{\perp i}, \lambda'_i) = \frac{M^2 + \mathbf{P}_\perp^2}{2P^+} \Psi_{n/h}(x_i, \mathbf{k}_\perp, \lambda_i) \quad (3.14)$$

for $n = 1, \dots, \infty$. The major difficulty is not primarily the large number of coupled integral equations, but rather that the above equations are ill-defined for very large values of the transversal momenta (“ultraviolet singularities”) and for values of the longitudinal momenta close to the endpoints $x \sim 0$ or $x \sim 1$ (“endpoint singularities”). One often has to introduce cut-offs Λ , to regulate the theory in some convenient way, and subsequently to renormalize it at a particular

mass or momentum scale Q . The corresponding wavefunction will be indicated by corresponding upper scripts,

$$\Psi_{n/h}^{(A)}(x_i, \mathbf{k}_\perp, \lambda_i) \quad \text{or} \quad \Psi_{n/h}^{(Q)}(x_i, \mathbf{k}_\perp, \lambda_i). \quad (3.15)$$

Consider a pion in QCD with momentum $P = (P^+, \mathbf{P}_\perp)$ as an example. It is described by

$$|\pi : P\rangle = \sum_{n=1}^{\infty} \int d[\mu_n] |n : x_i P^+, \mathbf{k}_{\perp i} + x_i \mathbf{P}_\perp, \lambda_i\rangle \Psi_{n/\pi}(x_i, \mathbf{k}_{\perp i}, \lambda_i), \quad (3.16)$$

where the sum is over all Fock space sectors of Eq. (3.7). The ability to specify wavefunctions simultaneously in any frame is a special feature of light-cone quantization. The light-cone wavefunctions $\Psi_{n/\pi}$ do not depend on the total momentum, since x_i is the longitudinal momentum fraction carried by the i^{th} parton and $\mathbf{k}_{\perp i}$ is its momentum “transverse” to the direction of the meson; both of these are frame-independent quantities. They are the probability amplitudes to find a Fock state of bare particles in the physical pion.

More generally, consider a meson in SU(N). The kernel of the integral equation (3.14) is illustrated in Fig. 2 in terms of the block matrix $\langle n : x_i, \mathbf{k}_{\perp i}, \lambda_i | H | n' : x'_i, \mathbf{k}'_{\perp i}, \lambda'_i \rangle$. The structure of this matrix depends of course on the way one has arranged the Fock space, see Eq. (3.7). Note that most of the block matrix elements vanish due to the nature of the light-cone interaction as defined in

n	Sector	1 q \bar{q}	2 gg	3 q \bar{q} g	4 q \bar{q} q \bar{q}	5 ggg	6 q \bar{q} gg	7 q \bar{q} q \bar{q} g	8 q \bar{q} q \bar{q} q \bar{q}	9 gggg	10 q \bar{q} ggg	11 q \bar{q} q \bar{q} gg	12 q \bar{q} q \bar{q} q \bar{q} g	13 q \bar{q} q \bar{q} q \bar{q} q \bar{q}
1	q \bar{q}				
2	gg			
3	q \bar{q} g							
4	q \bar{q} q \bar{q}	
5	ggg
6	q \bar{q} gg								.				.	.
7	q \bar{q} q \bar{q} g
8	q \bar{q} q \bar{q} q \bar{q}			
9	gggg
10	q \bar{q} ggg
11	q \bar{q} q \bar{q} gg
12	q \bar{q} q \bar{q} q \bar{q} g			
13	q \bar{q} q \bar{q} q \bar{q} q \bar{q}		

Fig. 2. The Hamiltonian matrix for a SU(N)-meson. The matrix elements are represented by energy diagrams. Within each block they are all of the same type: either vertex, fork or seagull diagrams. Zero matrices are denoted by a dot (\cdot). The single gluon is absent since it cannot be color neutral.

Eq. (2.94). The vertex interaction in Eq. (2.95) changes the particle number by one, while the instantaneous interactions in Eqs. (2.96), (2.97) and (2.98) change the particle number only up to two.

3.2. The use of light-cone wavefunctions

The infinite set of integral equations (3.14) is difficult if not impossible to solve. But given the light-cone wavefunctions $\Psi_{n/h}(x_i, \mathbf{k}_{\perp i}, \lambda_i)$, one can compute any hadronic quantity by convolution with the appropriate quark and gluon matrix elements. In many cases of practical interest it suffices to know less information than the complete wavefunction. As an example consider

$$G_{a/h}(x, Q) = \sum_n \int d[\mu_n] |\Psi_{n/h}^{(Q)}(x_i, \mathbf{k}_{\perp i}, \lambda_i)|^2 \sum_i \delta(x - x_i). \quad (3.17)$$

$G_{a/h}$ is a function of one variable, characteristic for a particular hadron, and depends parametrically on the typical scale Q . It gives the probability to find in that hadron a particle with longitudinal momentum fraction x , irrespective of the particle type, and irrespective of its spin, color, flavor or transversal momentum \mathbf{k}_{\perp} . Because of wavefunction normalization the integrated probability is normalized to one.

One can ask also for conditional probabilities, for example, for the probability to find a quark of a particular flavor f and its momentum fraction x , but again irrespective of the other quantum numbers. Thus,

$$G_{f/h}(x; Q) = \sum_n \int d[\mu_n] |\Psi_{n/h}^{(Q)}(x_i, \mathbf{k}_{\perp i}, \lambda_i)|^2 \sum_i \delta(x - x_i) \delta_{i,f}. \quad (3.18)$$

The conditional probability is *not normalized*, even if one sums over all flavors. Such probability functions can be measured. For exclusive cross sections, one often needs only the probability amplitudes of the valence part

$$\Phi_{f/h}(x; Q) = \sum_n \int d[\mu_n] \Psi_{n/h}^{(Q)}(x_i, \mathbf{k}_{\perp i}, \lambda_i) \sum_i \delta(x - x_i) \delta_{i,f} \delta_{n,\text{valence}} \Theta(\mathbf{k}_{\perp i}^2 \leq Q^2). \quad (3.19)$$

Here, the transverse momenta are integrated up to momentum transfer Q^2 .

The leading-twist structure functions measured in deep-inelastic lepton scattering are immediately related to the above light-cone probability distributions by

$$2MF_1(x, Q) = \frac{F_2(x, Q)}{x} \approx \sum_f e_f^2 G_{f/p}(x, Q). \quad (3.20)$$

This follows from the observation that deep-inelastic lepton scattering in the Bjorken-scaling limit occurs if x_{bj} matches the light-cone fraction of the struck quark with charge e_f . However, the light cone wavefunctions contain much more information for the final state of deep-inelastic scattering, such as the multi-parton distributions, spin and flavor correlations, and the spectator jet composition.

One of the most remarkable simplicities of the light-cone formalism is that one can write down the exact expressions for the electro-magnetic form factors. In the interaction picture, one can

equate the full Heisenberg current to the free (quark) current $J^\mu(0)$ described by the free Hamiltonian at $x^+ = 0$. As was first shown by Drell and Yan [133], it is advantageous to choose a special coordinate frame to compute form factors, structure functions, and other current matrix elements at space-like photon momentum. One then has to examine only the J^+ component to get form factors like

$$F_{S \rightarrow S'}(q^2) = \langle P', S' | J^+ | P, S \rangle \quad \text{with } q_\mu = P'_\mu - P_\mu. \quad (3.21)$$

This holds for any (composite) hadron of mass M , and any initial or final spins S [133,56]. In the Drell frame, as illustrated in Fig. 3, the photon's momentum is transverse to the momentum of the incident hadron and the incident hadron can be directed along the z -direction, thus

$$P^\mu = \left(P^+, \mathbf{0}_\perp, \frac{M^2}{P^+} \right), \quad q^\mu = \left(0, \mathbf{q}_\perp, \frac{2q \cdot P}{P^+} \right). \quad (3.22)$$

With such a choice the four-momentum transfer is $-q_\mu q^\mu \equiv Q^2 = \mathbf{q}_\perp^2$, and the quark current can neither create pairs nor annihilate the vacuum. This is distinctly different from the conventional treatment, where there are contributions from terms in which the current is annihilated by the vacuum, as illustrated in Fig. 4. Front-form kinematics allow to trivially boost the hadron's four-momentum from P to P' , and therefore the space-like form factor for a hadron is just a sum of overlap integrals analogous to the corresponding non-relativistic formula [133]

$$F_{S \rightarrow S'}(Q^2) = \sum_n \sum_f e_f \int d[\mu_n] \Psi_{n,S'}^*(x_i, \mathbf{l}_{\perp i}, \lambda_i) \Psi_{n,S}(x_i, \mathbf{k}_{\perp i}, \lambda_i). \quad (3.23)$$

Here e_f is the charge of the struck quark, and

$$\mathbf{l}_{\perp i} \equiv \begin{cases} \mathbf{k}_{\perp i} - x_i \mathbf{q}_\perp + \mathbf{q}_\perp & \text{for the struck quark,} \\ \mathbf{k}_{\perp i} - x_i \mathbf{q}_\perp & \text{for all other partons.} \end{cases} \quad (3.24)$$

This is particularly simple for a spin-zero hadron like a pion. Notice that the transverse momenta appearing as arguments of the first wavefunction correspond not to the actual momenta carried by the partons but to the actual momenta minus $x_i \mathbf{q}_\perp$, to account for the motion of the final hadron. Notice also that $\mathbf{l}_{\perp i}$ and $\mathbf{k}_{\perp i}$ become equal as $\mathbf{q}_\perp \rightarrow 0$, and that $F_\pi \rightarrow 1$ in this limit due to

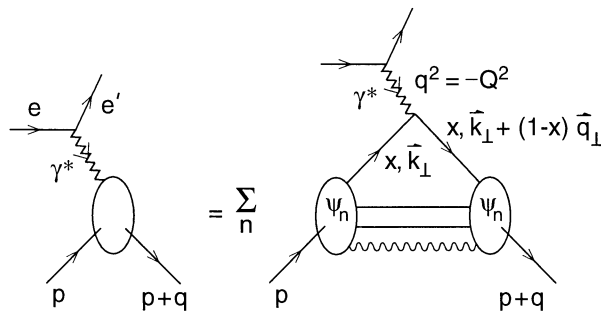


Fig. 3. Calculation of the form factor of a bound state from the convolution of light-cone Fock amplitudes. The result is exact if one sums over all Ψ_n .

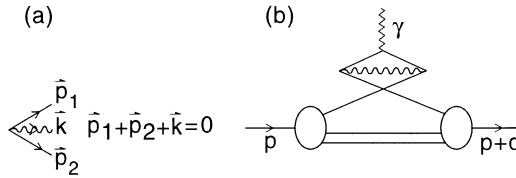


Fig. 4. (a) Illustration of a vacuum creation graph in time-ordered perturbation theory. A corresponding contribution to the form factor of a bound state is shown in (b).

wavefunction normalization. In most of the cases it suffices to treat the problem in perturbation theory.

3.3. Perturbation theory in the front form

The light-cone Green’s functions $\tilde{G}_{fi}(x^+)$ are the probability amplitudes that a state starting in Fock state $|i\rangle$ ends up in Fock state $|f\rangle$ a (light-cone) time x^+ later

$$\langle f | \tilde{G}(x^+) | i \rangle = \langle f | e^{-iP^+x^+} | i \rangle = \langle f | e^{-iHx^+} | i \rangle = i \int \frac{d\varepsilon}{2\pi} e^{-i\varepsilon x^+} \langle f | G(\varepsilon) | i \rangle. \tag{3.25}$$

The Fourier transform $\langle f | G(\varepsilon) | i \rangle$ is usually called the resolvent of the Hamiltonian H [333], i.e.

$$\langle f | G(\varepsilon) | i \rangle = \left\langle f \left| \frac{1}{\varepsilon - H + i0_+} \right| i \right\rangle = \left\langle f \left| \frac{1}{\varepsilon - H_0 - U + i0_+} \right| i \right\rangle. \tag{3.26}$$

Separating the Hamiltonian $H = H_0 + U$ according to Eq. (2.92) into a free part H_0 and an interaction U , one can expand the resolvent into the usual series

$$\begin{aligned} \langle f | G(\varepsilon) | i \rangle = & \left\langle f \left| \frac{1}{\varepsilon - H_0 + i0_+} + \frac{1}{\varepsilon - H_0 + i0_+} U \frac{1}{\varepsilon - H_0 + i0_+} \right. \right. \\ & \left. \left. + \frac{1}{\varepsilon - H_0 + i0_+} U \frac{1}{\varepsilon - H_0 + i0_+} U \frac{1}{\varepsilon - H_0 + i0_+} + \dots \right| i \right\rangle. \end{aligned} \tag{3.27}$$

The rules for x^+ -ordered perturbation theory follow immediately when the resolvent of the free Hamiltonian $(\varepsilon - H_0)^{-1}$ is replaced by its spectral decomposition.

$$\frac{1}{\varepsilon - H_0 + i0_+} = \sum_n \int d[\mu_n] |n : k_i^+, \mathbf{k}_{\perp i}, \lambda_i\rangle \frac{1}{\varepsilon - \sum_i ((k_{\perp i}^2 + m^2)/2k_i^+) + i0_+} \langle n : k_i^+, \mathbf{k}_{\perp i}, \lambda_i|. \tag{3.28}$$

The sum becomes a sum over all states n intermediate between two interactions U .

To calculate then $\langle f | G(\varepsilon) | i \rangle$ perturbatively, all x^+ -ordered diagrams must be considered, the contribution from each graph computed according to the rules of old-fashioned Hamiltonian perturbation theory [274,299]:

1. Draw all topologically distinct x^+ -ordered diagrams.
2. Assign to each line a momentum k^μ , a helicity λ , as well as color and flavor, corresponding to a single-particle on-shell, with $k^\mu k_\mu = m^2$. With fermions (electrons or quark) associate a spinor

$u_\alpha(k, \lambda)$, with antifermions $v_\alpha(k, \lambda)$, and with vector bosons (photons or gluons) a polarization vector $\varepsilon_\mu(k, \lambda)$. These are given explicitly in Appendices B and C.

- For each vertex include factor V as given in Fig. 5 for QED and Fig. 6 for QCD, with further tables given in Section 4. To convert incoming into outgoing lines or vice versa replace

$$u \leftrightarrow v, \quad \bar{u} \leftrightarrow -\bar{v}, \quad \varepsilon \leftrightarrow \varepsilon^*$$

in any of these vertices (see also items 8,9, and 10).

- For each intermediate state there is a factor

$$\frac{1}{\varepsilon - \sum_i ((k_\perp^2 + m^2)/2k^+)_i + i0_+},$$

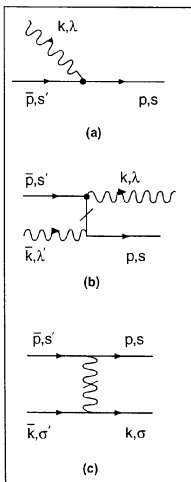
where $\varepsilon = \tilde{P}_{in+}$ is the incident light-cone energy.

- To account for three-momentum conservation include for each intermediate state the delta functions $\delta(P^+ - \sum_i k_i^+)$ and $\delta^{(2)}(\mathbf{P}_\perp - \sum_i \mathbf{k}_{\perp i})$.
- Integrate over each internal k with the weight

$$\int d^2k_\perp dk^+ \frac{\theta(k^+)}{(2\pi)^{3/2}}$$

and sum over internal helicities (and colors for gauge theories).

- Include a factor -1 for each closed fermion loop, for each fermion line that both begins and ends in the initial state, and for each diagram in which fermion lines are interchanged in either of the initial or final states.
- Imagine that every internal line is a sum of a “dynamic” and an “instantaneous” line, and draw all diagrams with 1,2,3, ... instantaneous lines.
- Two consecutive instantaneous interactions give a vanishing contribution.

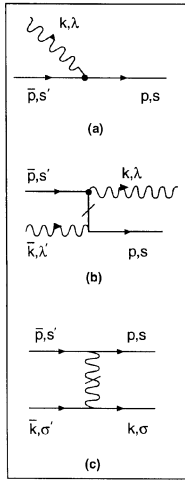


$$V = \frac{e}{(2\pi)^{3/2}} \frac{\bar{u}(\bar{p}, s') \not{\varepsilon}^*(k, \lambda) u(p, s)}{\sqrt{2\bar{p}^+} \sqrt{2k^+} \sqrt{2p^+}}$$

$$W_f = \frac{e^2}{(2\pi)^3} \frac{\bar{u}(\bar{p}, s') \not{\varepsilon}^*(\bar{k}, \lambda') \gamma^+ \not{\varepsilon}(k, \lambda) u(p, s)}{\sqrt{2\bar{p}^+} \sqrt{2\bar{k}^+} 2(\bar{k}^+ - p^+) \sqrt{2k^+} \sqrt{2p^+}}$$

$$W_b = -\frac{e^2}{(2\pi)^3} \frac{\bar{u}(\bar{p}, s') \gamma^+ u(p, s)}{\sqrt{2\bar{p}^+} \sqrt{2p^+}} \frac{1}{2(\bar{p}^+ - p^+)^2} \frac{\bar{u}(\bar{k}, \sigma') \gamma^+ u(k, \sigma)}{\sqrt{2\bar{k}^+} \sqrt{2k^+}}$$

Fig. 5. A few selected matrix elements of the QED front-form Hamiltonian $H = P_+$ in KS-convention.



$$\begin{aligned}
 V &= \frac{g}{(2\pi)^{3/2}} \frac{\bar{u}(\bar{p}, s')}{\sqrt{2\bar{p}^+}} \not{\epsilon}^*(k, \lambda) \frac{u(p, s)}{\sqrt{2p^+}} T_{c\bar{p}c p}^{a_k} \\
 W_f &= \frac{g^2}{(2\pi)^3} \frac{\bar{u}(\bar{p}, s')}{\sqrt{2\bar{p}^+}} \not{\epsilon}^*(\bar{k}, \lambda') \frac{T_{c\bar{p},c}^{a_{\bar{k}}} \gamma^+ T_{c,c p}^{a_k}}{2(\bar{k}^+ - p^+)} \not{\epsilon}(k, \lambda) \frac{u(p, s)}{\sqrt{2p^+}} \\
 W_b &= -\frac{g^2}{(2\pi)^3} \frac{\bar{u}(\bar{p}, s') \gamma^+ u(p, s)}{\sqrt{2\bar{p}^+} \sqrt{2p^+}} \frac{T_{c\bar{p},c}^{a_{\bar{k}}} T_{c,c p}^{a_k}}{(\bar{p}^+ - p^+)^2} \frac{\bar{u}(\bar{k}, \sigma') \gamma^+ u(k, \sigma)}{\sqrt{2\bar{k}^+} \sqrt{2k^+}}
 \end{aligned}$$

Fig. 6. A few selected matrix elements of the QCD front form Hamiltonian $H = P_+$ in LB-convention.

10. For the instantaneous fermion lines use the factor W_f in Fig. 5 or Fig. 6, or the corresponding tables in Section 4. For the instantaneous boson lines use the factor W_b .

The light-cone Fock state representation can thus be used advantageously in perturbation theory. The sum over intermediate Fock states is equivalent to summing all x^+ -ordered diagrams and integrating over the transverse momentum and light-cone fractions x . Because of the restriction to positive x , diagrams corresponding to vacuum fluctuations or those containing backward-moving lines are eliminated.

3.4. Example 1: The $q\bar{q}$ -scattering amplitude

The simplest application of the above rules is the calculation of the electron–muon scattering amplitude to lowest non-trivial order. But the quark–antiquark scattering is only marginally more difficult. We thus imagine an initial (q, \bar{q}) -pair with different flavors $f \neq \bar{f}$ to be scattered off each other by exchanging a gluon.

Let us treat this problem as a pedagogical example to demonstrate the rules. Rule 1: There are two time-ordered diagrams associated with this process. In the first one the gluon is emitted by the quark and absorbed by the antiquark, and in the second it is emitted by the antiquark and absorbed by the quark. For the first diagram, we assign the momenta required in rule 2 by giving explicitly the initial and final Fock states

$$|q, \bar{q}\rangle = \frac{1}{\sqrt{n_c}} \sum_{c=1}^{n_c} b_{c f}^\dagger(k_q, \lambda_q) d_{c \bar{f}}^\dagger(k_{\bar{q}}, \lambda_{\bar{q}}) |0\rangle, \quad (3.29)$$

$$|q', \bar{q}'\rangle = \frac{1}{\sqrt{n_c}} \sum_{c=1}^{n_c} b_{c f}^\dagger(k'_q, \lambda'_q) d_{c \bar{f}}^\dagger(k'_{\bar{q}}, \lambda'_{\bar{q}}) |0\rangle, \quad (3.30)$$

respectively. Note that both states are invariant under $SU(n_c)$. The usual color singlets of QCD are obtained by setting $n_c = 3$. The intermediate state

$$|q', \bar{q}, g\rangle = \sqrt{\frac{2}{n_c^2 - 1}} \sum_{c=1}^{n_c} \sum_{c'=1}^{n_c} \sum_{a=1}^{n_c^2 - 1} T_{c,c'}^a b_{c'f}^\dagger(k'_q, \lambda'_q) d_{cf}^\dagger(k_{\bar{q}}, \lambda_{\bar{q}}) a_a^\dagger(k_g, \lambda_g) |0\rangle, \quad (3.31)$$

has “a gluon in flight”. Under that impact, the quark has changed its momentum (and spin), while the antiquark as a spectator is still in its initial state. At the second vertex, the gluon in flight is absorbed by the antiquark, the latter acquiring its final values $(k'_{\bar{q}}, \lambda'_{\bar{q}})$. Since the gluons longitudinal momentum is positive, the diagram allows only for $k_q^+ < k_q^+$. Rule 3 requires at each vertex the factors

$$\langle q, \bar{q} | V | q', \bar{q}, g \rangle = \frac{g}{(2\pi)^{3/2}} \sqrt{\frac{n_c^2 - 1}{2n_c}} \frac{[\bar{u}(k_q, \lambda_q) \gamma^\mu \varepsilon_\mu(k_g, \lambda_g) u(k'_q, \lambda'_q)]}{\sqrt{2k_q^+} \sqrt{2k_g^+} \sqrt{2k_q^+}}, \quad (3.32)$$

$$\langle q', \bar{q}, g | V | q', \bar{q}' \rangle = \frac{g}{(2\pi)^{3/2}} \sqrt{\frac{n_c^2 - 1}{2n_c}} \frac{[\bar{u}(k_{\bar{q}}, \lambda_{\bar{q}}) \gamma^\nu \varepsilon_\nu^*(k_g, \lambda_g) u(k'_{\bar{q}}, \lambda'_{\bar{q}})]}{\sqrt{2k_{\bar{q}}^+} \sqrt{2k_g^+} \sqrt{2k_{\bar{q}}^+}}, \quad (3.33)$$

respectively. If one works with color neutral Fock states, all color structure reduces to an overall factor C , with $C^2 = (n_c^2 - 1)/2n_c$. This factor is the only difference between QCD and QED for this example. For QCD $C^2 = \frac{4}{3}$ and for QED $C^2 = 1$. Rule 4 requires the energy denominator $1/\Delta E$. With the initial energy

$$\varepsilon = \tilde{P}_+ = \frac{1}{2} \tilde{P}^- = (k_q + k_{\bar{q}})_+ = \frac{1}{2} (k_q + k_{\bar{q}})^-,$$

the energy denominator

$$2\Delta E = (k_q + k_{\bar{q}})^- - (k_g + k'_q + k_{\bar{q}})^- = -Q^2/k_g^+ \quad (3.34)$$

can be expressed in terms of the Feynman four-momentum transfers

$$Q^2 = k_g^+(k_g + k'_q - k_q)^-, \quad \bar{Q}^2 = k_g^+(k_g + k_{\bar{q}} - k'_{\bar{q}})^-. \quad (3.35)$$

Rule 5 requires two Dirac-delta functions, one at each vertex, to account for conservation of three-momentum. One of them is removed by the requirement of rule 6, namely to integrate over all intermediate internal momenta and the other remains in the final equation (3.43). The momentum of the exchanged gluon is thus fixed by the external legs of the graph. Rule 6 requires that one sums over the gluon helicities. The polarization sum gives

$$d_{\mu\nu}(k_g) \equiv \sum_{\lambda_g} \varepsilon_\mu(k_g, \lambda_g) \varepsilon_\nu^*(k_g, \lambda_g) = -g_{\mu\nu} + (k_{g,\mu} \eta_\nu + k_{g,\nu} \eta_\mu) / k_g^k \eta_k, \quad (3.36)$$

see Appendix B. The null vector η^μ has the components [299]

$$\eta^\mu = (\eta^+, \boldsymbol{\eta}_\perp, \eta^-) = (0, \mathbf{0}_\perp, 2), \quad (3.37)$$

and thus the properties $\eta^2 \equiv \eta^\mu \eta_\mu = 0$ and $k\eta = k^+$. In light-cone gauge, we find for the η -dependent terms

$$\left(\sum_{\lambda_g} \langle q, \bar{q} | V | q', \bar{q}, g \rangle \langle q', \bar{q}, g | V | q', \bar{q}' \rangle \right)_n = \frac{(gC)^2}{(2\pi)^3} \frac{1}{2k_g^+ (k_g\eta)} \times \left\{ \frac{[\bar{u}(q)\gamma_\mu k_g^\mu u(q')]}{\sqrt{4k_q^+ k_q'^+}} \frac{[\bar{u}(\bar{q})\gamma_\nu \eta^\nu u(\bar{q}')] }{\sqrt{4k_{\bar{q}}^+ k_{\bar{q}}'^+}} + \frac{[\bar{u}(q)\gamma_\mu \eta^\mu u(q')]}{\sqrt{4k_q^+ k_q'^+}} \frac{[\bar{u}(\bar{q})\gamma_\nu k_g^\nu u(\bar{q}')] }{\sqrt{4k_{\bar{q}}^+ k_{\bar{q}}'^+}} \right\}. \quad (3.38)$$

Next, we introduce four-vectors like $l_q^\mu = (k_g + k_q - k_q')^\mu$. Since its three-components vanish by momentum conservation, l_q^μ must be proportional to the null vector η^μ . With Eq. (3.35) one gets

$$l_q^\mu = (k_g + k_q - k_q')^\mu = (Q^2/2k_g^+)\eta^\mu, \quad l_{\bar{q}}^\mu = (k_g + k_{\bar{q}} - k_{\bar{q}}')^\mu = (\bar{Q}^2/2k_g^+)\eta^\mu. \quad (3.39)$$

The well-known property of the Dirac spinors, $(k_q - k_q')^\mu [\bar{u}(k_q, \lambda_q)\gamma_\mu u(k_q', \lambda_q')] = 0$, yields then

$$[\bar{u}(q)\gamma_\mu k_g^\mu u(q')] = [\bar{u}(q)\gamma_\mu \eta^\mu u(q')] Q^2/2k_g^+ = [\bar{u}(q)\gamma^+ u(q')] Q^2/2k_g^+,$$

and Eq. (3.38) becomes

$$\left(\sum_{\lambda_g} \langle q, \bar{q} | V | q', \bar{q}, g \rangle \langle q', \bar{q}, g | V | q', \bar{q}' \rangle \right)_n = \frac{(gC)^2}{(2\pi)^3} \frac{Q^2}{2(k_g^+)^3} \frac{[\bar{u}(q)\gamma^+ u(q')]}{\sqrt{4k_q^+ k_q'^+}} \frac{[\bar{u}(\bar{q})\gamma^+ u(\bar{q}')] }{\sqrt{4k_{\bar{q}}^+ k_{\bar{q}}'^+}}. \quad (3.40)$$

Including the $g_{\mu\nu}$ contribution, the diagram of second order in V gives thus

$$V \frac{1}{\bar{P}_+ - H_0} V = \frac{g^2 C^2}{(2\pi)^3} \frac{[\bar{u}(k_q, \lambda_q)\gamma^\mu u(k_q', \lambda_q')]}{\sqrt{4k_q^+ k_q'^+}} \frac{1}{Q^2} \frac{[\bar{u}(k_{\bar{q}}, \lambda_{\bar{q}})\gamma_\mu u(k_{\bar{q}}', \lambda_{\bar{q}}')]}{\sqrt{4k_{\bar{q}}^+ k_{\bar{q}}'^+}} - \frac{g^2 C^2}{(2\pi)^3} \frac{[\bar{u}(k_q, \lambda_q)\gamma^+ u(k_q', \lambda_q')]}{\sqrt{4k_q^+ k_q'^+}} \frac{1}{(k_g^+)^2} \frac{[\bar{u}(k_{\bar{q}}, \lambda_{\bar{q}})\gamma^+ u(k_{\bar{q}}', \lambda_{\bar{q}}')]}{\sqrt{4k_{\bar{q}}^+ k_{\bar{q}}'^+}}, \quad (3.41)$$

up to the delta functions, and a step function $\Theta(k_q'^+ \leq k_q^+)$, which truncates the final momenta k'^+ . Evaluating the second time ordered diagram, one gets the same result up to the step function $\Theta(k_q'^+ \geq k_q^+)$. Using

$$\Theta(k_q'^+ \leq k_q^+) + \Theta(k_q'^+ \geq k_q^+) = 1,$$

the final sum of all time-ordered diagrams to order g^2 is Eq. (3.41). One proceeds with rule 8, by including consecutively the instantaneous lines. In the present case, there is only one. From Fig. 5 we find

$$\langle q, \bar{q} | W_b | q', \bar{q}' \rangle = \frac{g^2 C^2}{(2\pi)^3} \frac{[\bar{u}(k_q, \lambda_q)\gamma^+ u(k_q', \lambda_q')]}{\sqrt{4k_q^+ k_q'^+}} \frac{1}{(k_q^+ - k_q'^+)^2} \frac{[\bar{u}(k_{\bar{q}}, \lambda_{\bar{q}})\gamma^+ u(k_{\bar{q}}', \lambda_{\bar{q}}')]}{\sqrt{4k_{\bar{q}}^+ k_{\bar{q}}'^+}}. \quad (3.42)$$

Finally, adding up all contributions up to order g^2 , the $q\bar{q}$ -scattering amplitude becomes

$$W + V \frac{1}{\bar{P}_+ - H_0} V = \frac{(gC)^2}{(2\pi)^3} \frac{(-1)}{(k_q - k_{\bar{q}})^2} [\bar{u}(k_q, \lambda_q)\gamma^\mu u(k_q', \lambda_q')] [\bar{u}(k_{\bar{q}}, \lambda_{\bar{q}})\gamma_\mu u(k_{\bar{q}}', \lambda_{\bar{q}}')] \times \frac{1}{\sqrt{k_q^+ k_{\bar{q}}^+ k_q'^+ k_{\bar{q}}'^+}} \delta(P^+ - P'^+) \delta^{(2)}(\mathbf{P}_\perp - \mathbf{P}'_\perp). \quad (3.43)$$

The instantaneous diagram W is thus cancelled exactly against a corresponding term in the diagram of second order in the vertex interaction V . Their sum gives the correct second-order result.

3.5. Example 2: Perturbative mass renormalization in QED (KS)

As an example for light-cone perturbation theory we follow here the work of Mustaki et al. [339,372] to calculate the second-order mass renormalization of the electron and the renormalization constants Z_2 and Z_3 in the KS convention.

Since all particles are on-shell in light-cone time-ordered perturbation theory, the electron wavefunction renormalization Z_2 must be obtained separately from the mass renormalization δm . At order e^2 , one finds three contributions. First, the perturbation expansion

$$T = W + V(1/(p_+ - H_0))V \quad (3.44)$$

yields a second-order contribution in V , as shown in Fig. 7a. The initial (or final) electron four momentum is denoted by

$$p^\mu = (p^+, \mathbf{p}_\perp, (p_\perp^2 + m^2)/2p^+). \quad (3.45)$$

Second and finally, one has first-order contributions from W_f and W_g , corresponding to Fig. 7b and Fig. 7c. In the literature [354,422,66] these two-point vertices have been called “seagulls” or “self-induced inertias”.

One has to calculate the transition matrix amplitude $T_{pp}\delta_{s,\sigma} = \langle p, s | T | p, \sigma \rangle$ between a free electron states with momentum and spin (p, s) and one with momentum and spin (p, σ) . The

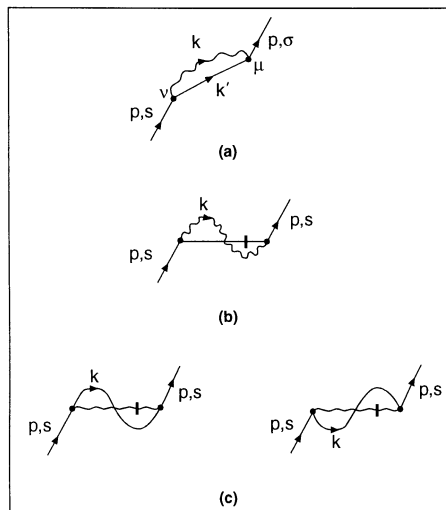


Fig. 7. One loop self-energy correction for the electron. Time flows upward in these diagrams.

normalization of states as in Eq. (3.3) was thus far

$$\langle p', s' | p, s \rangle = \delta(p^+ - p'^+) \delta^2(p_\perp - p'_\perp) \delta_{s, s'}, \quad (3.46)$$

but for an invariant normalization it is better to use $\langle \tilde{p}, s | \equiv \sqrt{2p^+} \langle p, s |$. Then one finds,

$$2m\delta m \delta_{s\sigma} \equiv T_{\tilde{p}\tilde{p}} = 2p^+ T_{pp} \Rightarrow \delta m \delta_{s\sigma} = (p^+/m) T_{pp}. \quad (3.47)$$

The other momenta appearing in Fig. 7a are

$$k = (k^+, \mathbf{k}_\perp, k_\perp^2/2k^+), \quad (3.48)$$

$$k' = \left(p^+ - k^+, \frac{(p_\perp - k_\perp)^2 + m^2}{2(p^+ - k^+)}, \mathbf{p}_\perp - \mathbf{k}_\perp \right). \quad (3.49)$$

Using the above rules to calculate T_{pp} , one obtains for the contribution from Fig. 7a,

$$\delta m_a \delta_{s\sigma} = e^2 \frac{1}{m} \sum_{\lambda, s'} \int \frac{d^2 k_\perp}{(4\pi)^3} \int_0^{p^+} dk^+ \frac{[\bar{u}(p, \sigma) \not{\epsilon}^*(k, \lambda) u(k', s')][\bar{u}(k', s') \not{\epsilon}(k, \lambda) u(p, s)]}{k^+(p^+ - k^+)(p^- - k^- - k'^-)}. \quad (3.50)$$

It can be shown that

$$[\bar{u}(p, \sigma) \gamma^\mu (k' + m) \gamma^\nu u(p, s)] d_{\mu\nu}(k) = 4\delta_{s\sigma} \left[\left(\frac{2p^+}{k^+} + \frac{k^+}{p^+ - k^+} \right) (p \cdot k) - m^2 \right], \quad (3.51)$$

which leads to the expression given below for δm_a . For Fig. 7b, one gets, using the rule for the instantaneous fermion,

$$\begin{aligned} \delta m_b &= e^2 \frac{p^+}{2m} \sum_\lambda \int \frac{d^2 k_\perp}{(2\pi)^3} \int_0^{+\infty} dk^+ \frac{\bar{u}(p, s) \not{\epsilon}^*(k, \lambda) \gamma^+ \not{\epsilon}(k, \lambda) u(p, \sigma)}{2p^+ 2k^+ 2(p^+ - k^+)} \\ &= e^2 \frac{p^+}{2m} \int \frac{d^2 k_\perp}{(2\pi)^3} \int_0^{+\infty} \frac{dk^+}{k^+(p^+ - k^+)}. \end{aligned} \quad (3.52)$$

For Fig. 7c one finds,

$$\begin{aligned} \delta m_c &= \frac{e^2 p^+}{2m} \sum_s \int \frac{d^2 k_\perp}{(2\pi)^3} \int_0^{+\infty} dk^+ \frac{\bar{u}(p, s) \gamma^+ \left[\frac{u(k, s) \bar{u}(k, s)}{\sqrt{2p^+}} - \frac{v(k, s) \bar{v}(k, s)}{2(p^+ + k^+)^2} \right] \gamma^+ u(p, \sigma)}{2k^+ \left[\frac{2(p^+ - k^+)^2}{\sqrt{2p^+}} - \frac{2(p^+ + k^+)^2}{\sqrt{2p^+}} \right]} \\ &= \frac{e^2 p^+}{2m} \int \frac{d^2 k_\perp}{(2\pi)^3} \left[\int_0^{+\infty} \frac{dk^+}{(p^+ - k^+)^2} - \int_0^{+\infty} \frac{dk^+}{(p^+ + k^+)^2} \right]. \end{aligned} \quad (3.53)$$

These integrals have potential singularities at $k^+ = 0$ and $k^+ = p^+$, as well as an ultra-violet divergence in k_\perp . To regularize them, we introduce in a first step small cut-offs α and β :

$$\alpha < k^+ < p^+ - \beta, \quad (3.54)$$

and get rid of the pole at $k^+ = p^+$ in δm_b and δm_c by a principal value prescription. One then obtains

$$\begin{aligned}\delta m_a &= \frac{e^2}{2m} \int \frac{d^2 k_\perp}{(2\pi)^3} \left[\int_0^{p^+} \frac{dk^+ m^2}{k^+ p \cdot k} - 2 \left(\frac{p^+}{\alpha} - 1 \right) - \ln \left(\frac{p^+}{\beta} \right) \right], \\ \delta m_b &= \frac{e^2}{2m} \int \frac{d^2 k_\perp}{(2\pi)^3} \ln \left(\frac{p^+}{\alpha} \right), \\ \delta m_c &= \frac{e^2}{m} \int \frac{d^2 k_\perp}{(2\pi)^3} \left(\frac{p^+}{\alpha} - 1 \right),\end{aligned}\tag{3.55}$$

where

$$p \cdot k = \frac{m^2(k^+)^2 + (p^+)^2 k_\perp^2}{2p^+ k^+}.\tag{3.56}$$

Adding these three contributions yields

$$\delta m = \frac{e^2}{2m} \int \frac{d^2 k_\perp}{(2\pi)^3} \left[\int_0^{p^+} \frac{dk^+ m^2}{k^+ p \cdot k} + \ln \left(\frac{\beta}{\alpha} \right) \right].\tag{3.57}$$

Note the cancelation of the most singular infrared divergence.

To complete the calculation, we present two possible regularization procedures:

1. *Transverse dimensional regularization.* The dimension of transverse space, d , is continued from its physical value of 2 to $2 + \varepsilon$ and all integrals are replaced by

$$\int d^2 k_\perp \rightarrow (\mu^2)^\varepsilon \int d^d k_\perp,\tag{3.58}$$

using $\varepsilon = 1 - d/2$ as a small quantity. One thus gets

$$\begin{aligned}(\mu^2)^\varepsilon \int d^d k_\perp (k_\perp^2)^\alpha &= 0 \quad \text{for } \alpha \geq 0, \\ (\mu^2)^\varepsilon \int d^d k_\perp \frac{1}{k_\perp^2 + M^2} &= \left(\frac{\mu^2}{M^2} \right)^\varepsilon \frac{\pi}{\varepsilon}, \\ (\mu^2)^\varepsilon \int d^d k_\perp \frac{1}{(k_\perp^2 + M^2)^2} &= \left(\frac{\mu^2}{M^2} \right)^\varepsilon \frac{\pi}{M^2}, \\ (\mu^2)^\varepsilon \int d^d k_\perp \frac{k_\perp^2}{k_\perp^2 + M^2} &= - \left(\frac{\mu^2}{M^2} \right)^\varepsilon \frac{\pi M^2}{\varepsilon}.\end{aligned}\tag{3.59}$$

In this method, α and β in Eq. (3.57) are treated as constants. Dimensional regularization gives zero for the logarithmic term, and for the remainder

$$\delta m = \frac{e^2 m}{(2\pi)^3} \int_0^1 dx \int \frac{d^2 k_\perp}{k_\perp^2 + m^2 x^2},\tag{3.60}$$

with $x \equiv (k^+/p^+)$, the above integral yields

$$\delta m = e^2 m / 8\pi^2 \varepsilon \quad (3.61)$$

as the final result.

2. *Cut-offs*. In this method [299,422,66], one restricts the momenta of any intermediate Fock state by means of the invariant condition

$$\tilde{P}^2 = \sum_i \left(\frac{m^2 + k_{\perp}^2}{x} \right)_i \leq \Lambda^2, \quad (3.62)$$

where \tilde{P} is the free total four-momentum of the intermediate state, and where Λ is a large cut-off. Furthermore, one assumes that all transverse momenta are smaller than a certain cut-off Λ_{\perp} , with

$$\Lambda_{\perp} \ll \Lambda. \quad (3.63)$$

In the case of Fig. 5a, Eq. (3.62) reads

$$\frac{k_{\perp}^2}{k^+} + \frac{(p_{\perp} - k_{\perp})^2 + m^2}{p^+ - k^+} < \Lambda' \quad \text{with } \Lambda' \equiv \frac{\Lambda^2 + p_{\perp}^2}{p^+}. \quad (3.64)$$

Hence

$$\alpha = \frac{k_{\perp}^2}{\Lambda'}, \quad \beta = \frac{(p_{\perp} - k_{\perp})^2 + m^2}{\Lambda'} \Rightarrow \frac{\beta}{\alpha} = \frac{(p_{\perp} - k_{\perp})^2 + m^2}{k_{\perp}^2}. \quad (3.65)$$

In Ref. [339] it is shown that

$$\int d^2 k_{\perp} \ln\left(\frac{\beta}{\alpha}\right) = \int d^2 k_{\perp} \int_0^{p^+} \frac{dk^+}{p^+} \frac{m^2}{p \cdot k}. \quad (3.66)$$

Now

$$\delta m = \frac{e^2}{2m} \int \frac{d^2 k_{\perp}}{(2\pi)^3} \int_0^{p^+} dk^+ \frac{m^2}{p \cdot k} \left(\frac{1}{p^+} + \frac{1}{k^+} \right). \quad (3.67)$$

Upon integration, and dropping the finite part, one finds

$$\delta m = (3e^2 m / 16\pi^2) \ln(\Lambda_{\perp}^2 / m^2), \quad (3.68)$$

which is of the same form as the standard result [39]. Since δm is not by itself a measurable quantity, there is no contradiction in finding different results. Note that the seagulls are necessary for obtaining the conventional result.

Finally, the wavefunction renormalization Z_2 , at order e^2 , is given by

$$1 - Z_2 = \sum_m' \frac{|\langle p|V|m\rangle|^2}{(p_+ - \tilde{P}_{+,m})^2}, \quad (3.69)$$

where $\tilde{P}_{+,m}$ is the free total energy of the intermediate state m . Note that this expression is the same as one of the contributions to δm , except that here the denominator is squared. One has thus

$$\begin{aligned} (1 - Z_2)\delta_{s\sigma} &= \frac{e^2}{p^+} \int \frac{d^2 k_\perp}{(4\pi)^3} \int_0^{p^+} \frac{dk^+}{k^+(p^+ - k^+)} \frac{\bar{u}(p,\sigma)\gamma^\mu(\gamma^\alpha k'_\alpha + m)\gamma^\nu u(p,s)d_{\mu\nu}(k)}{(p^- - k^- - k'^-)^2} \\ &= \frac{e^2 \delta_{s\sigma}}{(2\pi)^3} \int_0^1 dx \int \frac{d^2 k_\perp}{k_\perp^2 + m^2 x^2} \left[\frac{2(1-x)k_\perp^2}{x(k_\perp^2 + m^2 x^2)} + x \right], \end{aligned} \quad (3.70)$$

which is the same result as that obtained by Kogut and Soper [274]. Naturally, this integral is both infrared and ultraviolet divergent. Using the above rules, one gets

$$Z_2(p^+) = 1 + \frac{e^2}{8\pi^2 \varepsilon} \left[\frac{3}{2} - 2 \ln\left(\frac{p^+}{\alpha}\right) \right] + \frac{e^2}{(2\pi)^2} \ln\left(\frac{p^+}{\alpha}\right) \left[1 - 2 \ln\left(\frac{\mu}{m}\right) - \ln\left(\frac{p^+}{\alpha}\right) \right], \quad (3.71)$$

where μ^2 is the scale introduced by dimensional regularization. Note that Z_2 has an unusual dependence on the longitudinal momentum, not found in the conventional instant form. But this may vary with the choice of regularization. A similar p^+ dependence was found for scalar QED by Thorn [426,427].

In Ref. [339,340] the full renormalization of front-form QED was carried out to the one-loop level. Electron and photon mass corrections were evaluated, as well as the wavefunction renormalization constants Z_2 and Z_3 , and the vertex correction Z_1 . One feature that distinguishes the front-form from the instant-form results is that the ultraviolet-divergent parts of Z_1 and Z_2 exhibit momentum dependence. For physical quantities such as the renormalized charge e_R , this momentum dependence cancels due to the Ward identity $Z_1(p^+, p'^+) = \sqrt{Z_2(p^+)Z_2(p'^+)}$. On the other hand, momentum-dependent renormalization constants imply non-local counter terms. Given that the tree-level Hamiltonian is non-local in x^- , it is actually not surprising to find counter terms exhibiting non-locality. As mentioned in Ref. [456], the power counting works differently here in the front than in the instant form. This is already indicated by the presence of four-point interactions in the Hamiltonian. The momentum dependence in Z_1 and Z_2 is another manifestation of unusual power counting laws. It will be interesting to apply them systematically in the case of QED. Power counting alone does not provide information about cancelation of divergences between diagrams. It is therefore important to gain more insight into the mechanism of cancelation in cases where one does expect this to occur as in the calculation of the electron mass shift.

3.6. Example 3: The anomalous magnetic moment

The anomalous magnetic moment of the electron had been calculated in the front form by Brodsky et al. [53], using the method of alternating denominators. Its calculation is a transparent example of calculating electro-magnetic form factors for both elementary and composite systems [41,56] as presented in Section 3.2 and for applying light-cone perturbation theory. Langnau and Burkardt [76,77,291,292] have calculated the anomalous magnetic moment at very strong coupling, by combining this method with discretized light-cone quantization, see below. We choose light-cone coordinates corresponding to the Drell frame, Eq. (3.14), and denote as in the preceding section the electron's four-momentum and spin with (p, s) . In line with Eq. (3.21), the Dirac and

Pauli form factors can be identified from the spin-conserving and spin-flip current matrix elements:

$$\mathcal{M}_{\uparrow\uparrow}^+ = \left\langle p + q, \uparrow \left| \frac{J^+(0)}{p^+} \right| p, \uparrow \right\rangle = 2F_1(q^2), \quad (3.72)$$

$$\mathcal{M}_{\uparrow\downarrow}^+ = \left\langle p + q, \uparrow \left| \frac{J^+(0)}{p^+} \right| p, \downarrow \right\rangle = -2(q_1 - iq_2) \frac{F_2(q^2)}{2M}, \quad (3.73)$$

where \uparrow corresponds to positive spin projection $s_z = +\frac{1}{2}$ along the z -axis. The mass of the composite system M is of course the physical mass m of the lepton. The interaction of the current $J^+(0)$ conserves the helicity of the struck constituent fermion $(\bar{u}_{\lambda'} \gamma^+ u_{\lambda})/k_+ = 2\delta_{\lambda\lambda'}$. Thus, one has from Eqs. (3.23), (3.72) and (3.73)

$$F_1(q^2) = \frac{1}{2} \mathcal{M}_{\uparrow\uparrow}^+ = \sum_j e_j \int [d\mu_n] \psi_{p^+q, \uparrow}^{*n}(x, k_{\perp}, \lambda) \psi_{p, \uparrow}^{(n)}(x, k_{\perp}, \lambda), \quad (3.74)$$

$$-\left(\frac{q_1 - iq_2}{2M}\right) F_2(q^2) = \frac{1}{2} \mathcal{M}_{\uparrow\downarrow}^+ = \sum_j e_j \int [d\mu_n] \psi_{p^+q, \uparrow}^{*n}(x, k_{\perp}, \lambda) \psi_{p, \downarrow}^{(n)}(x, k_{\perp}, \lambda). \quad (3.75)$$

In this notation, the summation over all contributing Fock states (n) and helicities (λ) is assumed, and the reference to single-particle states i in the Fock states is suppressed. Momentum conservation is used to eliminate the explicit reference to the momentum of the struck lepton in Eq. (3.24). Finally, the leptons wavefunction directed along the final direction $p + q$ in the current matrix element is denoted as

$$\psi_{p^+q, s_z}^{(n)}(x, \mathbf{k}_{\perp}, \lambda) = \Psi_{n/e(p+q, s_z)}(x_i, \mathbf{k}_{\perp i}, \lambda_i).$$

One recalls that $F_1(q^2)$ evaluated in the limit $q^2 \rightarrow 0$ with $F_1 \rightarrow 1$ is equivalent to wavefunction normalization

$$\int [d\mu] \psi_{p^+}^* \psi_{p^+} = 1, \quad \int [d\mu] \psi_{p\downarrow}^* \psi_{p\downarrow} = 1. \quad (3.76)$$

The anomalous moment $a = F_2(0)/F_1(0)$ can be determined from the coefficient linear in $q_1 - iq_2$ from $\psi_{p^+q}^*$ in Eq. (3.75). Since according to Eq. (3.24)

$$\frac{\partial}{\partial q_{\perp}} \psi_{p^+q}^* \equiv - \sum_{i \neq j} x_i \frac{\partial}{\partial k_{\perp i}} \psi_{p^+q}^*, \quad (3.77)$$

one can, after integration by parts, write explicitly

$$\frac{a}{M} = - \sum_j e_j \int [d\mu_n] \sum_{i \neq j} \psi_{p^+}^* x_i \left(\frac{\partial}{\partial k_1} + \frac{i\partial}{\partial k_2} \right)_i \psi_{p\downarrow}. \quad (3.78)$$

The anomalous moment can thus be expressed in terms of a local matrix element at zero momentum transfer (see also with Section 5 below). It should be emphasized that Eq. (3.78) is exact, valid for the anomalous element of actually *any* spin- $\frac{1}{2}$ -system.

As an example for the above perturbative formalism, one can evaluate the electron’s anomalous moment to order α [53]. In principle, one would have to account for all x^+ -ordered diagrams as displayed in Fig. 8. But most of them do not contribute, because either the vacuum fluctuation graphs vanish in the front form or they vanish because of using the Drell frame. Only the diagram in the upper-left corner of Fig. 8 contributes the two electron–photon Fock states with spins $|\frac{1}{2}\lambda_e, \lambda_\gamma\rangle = |-\frac{1}{2}, 1\rangle$ and $|\frac{1}{2}, -1\rangle$:

$$\psi_{p\downarrow} = \frac{e/\sqrt{x}}{M^2 - \frac{k_\perp^2 + \lambda^2}{x} - \frac{k_\perp^2 + \hat{m}^2}{1-x}} \times \begin{cases} \sqrt{2} \frac{(k_1 - ik_2)}{x} & \text{for } |-\frac{1}{2}\rangle \rightarrow |-\frac{1}{2}, 1\rangle, \\ \sqrt{2} \frac{M(1-x) - \hat{m}}{1-x} & \text{for } |-\frac{1}{2}\rangle \rightarrow |\frac{1}{2}, -1\rangle, \end{cases} \quad (3.79)$$

$$\psi_{p\uparrow}^* = \frac{e/\sqrt{x}}{M^2 - \frac{k_\perp^2 + \lambda^2}{x} - \frac{k_\perp^2 + \hat{m}^2}{1-x}} \times \begin{cases} -\sqrt{2} \frac{M(1-x) - \hat{m}}{1-x} & \text{for } |-\frac{1}{2}, 1\rangle \rightarrow |\frac{1}{2}\rangle, \\ -\sqrt{2} \frac{(k_1 - ik_2)}{x} & \text{for } |\frac{1}{2}, -1\rangle \rightarrow |\frac{1}{2}\rangle. \end{cases} \quad (3.80)$$

The quantities to the left of the curly bracket in Eqs. (3.79) and (3.80) are the matrix elements of

$$\frac{\bar{u}(p+k, \lambda)}{(p^+ - k^+)^{1/2}} \gamma^\mu \varepsilon_\mu^*(k, \lambda'') \frac{u(p, \lambda')}{(p^+)^{1/2}}, \quad \frac{\bar{u}(p, \lambda)}{(p^+)^{1/2}} \gamma^\mu \varepsilon_\mu(k, \lambda'') \frac{u(p-k, \lambda')}{(p^+ - k^+)^{1/2}},$$

respectively, where $k^\mu \varepsilon_\mu(k, \lambda) = 0$ and in light-cone gauge $\varepsilon^+(k, \lambda) = 0$. In LB-convention holds $\varepsilon_\perp(\mathbf{k}_\perp, \lambda) \rightarrow \varepsilon_\perp(\mathbf{k}_\perp, \pm) = \pm (1/\sqrt{2})(\hat{x} \pm i\hat{y})$, see also Appendix B [41]. For the sake of generality, we let the intermediate lepton and boson have mass \hat{m} and \tilde{m} , respectively. Substituting (3.79) and (3.80) into Eq. (3.78), one finds that only the $|-\frac{1}{2}, 1\rangle$ intermediate state actually contributes to a ,

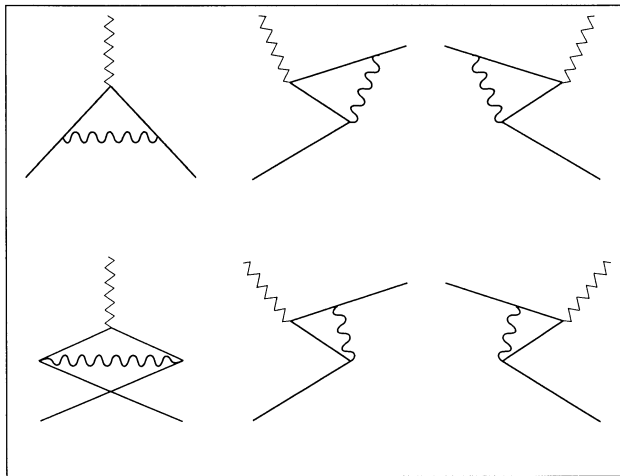


Fig. 8. Time-ordered contributions to the electron’s anomalous magnetic moment. In light-cone quantization with $q^+ = 0$, only the upper-left graph needs to be computed to obtain the Schwinger result.

since terms which involve differentiation of the denominator of $\psi_{p\downarrow}$ cancel. One thus gets [56]

$$a = 4Me^2 \int_0^1 \frac{d^2 k_{\perp}}{16\pi^3} dx \frac{[\hat{m} - (1-x)M]/x(1-x)}{[M^2 - (k_{\perp}^2 + \hat{m}^2)/(1-x) - (k_{\perp}^2 + \tilde{m}^2)/x]^2},$$

$$= \frac{\alpha}{\pi} \int_0^1 dx \frac{M[\hat{m} - M(1-x)]x(1-x)}{\hat{m}^2 x + \tilde{m}^2(1-x) - M^2 x(1-x)}, \quad (3.81)$$

which, in the case of QED ($\hat{m} = M, \tilde{m} = 0$) gives the Schwinger result $a = \alpha/2\pi$ [53]. As compared to Schwinger the above is an almost trivial calculation.

The general result Eq. (3.78) can also be written in matrix form

$$\frac{a}{2M} = - \sum_j e_j \int [dx d^2 k_{\perp}] \psi^* \mathbf{S}_{\perp} \cdot \mathbf{L}_{\perp} \psi, \quad (3.82)$$

where \mathbf{S}_{\perp} is the spin operator for the total system and \mathbf{L}_{\perp} is the generator of ‘‘Galilean’’ transverse boosts [41] on the light cone, i.e. $\mathbf{S}_{\perp} \cdot \mathbf{L}_{\perp} = (S_+ L_- + S_- L_+)/2$ where $S_{\pm} = (S_1 \pm iS_2)$ is the spin-ladder operator and

$$L_{\pm} = \sum_{i \neq j} x_i \left(\frac{\partial}{\partial k_i} \mp \frac{\partial}{\partial k_{2i}} \right) \quad (3.83)$$

(summed over spectators) in the analog of the angular momentum operator $\mathbf{r} \times \mathbf{p}$. Eq. (3.78) can also be written simply as an expectation value in impact space.

The results given in Eqs. (3.74), (3.75) and (3.78) may also be convenient for calculating the anomalous moments and form factors of hadrons in quantum chromodynamics directly from the quark and gluon wavefunctions $\psi(x, \mathbf{k}_{\perp}, \lambda)$. These wavefunctions can also be used to calculate the structure functions and distribution amplitudes which control large momentum transfer inclusive and exclusive processes. The charge radius of a composite system can also be written in the form of a local, forward matrix element:

$$\left. \frac{\partial F_1(q^2)}{\partial q^2} \right|_{q^2=0} = - \sum_j e_j \int [dx d^2 k_{\perp}] \psi_{p,\uparrow}^* \left(\sum_{i \neq j} x_i \frac{\partial}{\partial k_{\perp i}} \right)^2 \psi_{p,\uparrow}. \quad (3.84)$$

We thus find that, in general, any Fock state $|n\rangle$ which couples to both ψ_{\uparrow}^* and ψ_{\downarrow} will give a contribution to the anomalous moment. Notice that because of rotational symmetry in the \hat{x} - and \hat{y} -direction, the contribution to $a = F_2(0)$ in Eq. (3.78) always involves the form $(a, b = 1, \dots, n)$

$$M \sum_{i \neq j} \psi_{\uparrow}^* x_i \frac{\partial}{\partial k_{\perp i}} \psi_{\downarrow} \sim \mu M \rho(\mathbf{k}_{\perp}^a \cdot \mathbf{k}_{\perp}^b), \quad (3.85)$$

compared to the integral (3.76) for wavefunction normalization which has terms of order

$$\psi_{\uparrow}^* \psi_{\uparrow} \sim \mathbf{k}_{\perp}^a \cdot \mathbf{k}_{\perp}^b \rho(\mathbf{k}_{\perp}^a \cdot \mathbf{k}_{\perp}^b), \quad \mu^2 \rho(\mathbf{k}_{\perp}^a \cdot \mathbf{k}_{\perp}^b). \quad (3.86)$$

Here ρ is a rotationally invariant function of the transverse momenta and μ is a constant with dimensions of mass. Thus, by order of magnitude

$$a = \mathcal{O}(\mu M / (\mu^2 + \langle \mathbf{k}_{\perp}^2 \rangle)) \quad (3.87)$$

summed and weighted over the Fock states. In the case of a renormalizable theory, the only parameters μ with the dimension of mass are fermion masses. In super-renormalizable theories, μ can be proportional to a coupling constant g with dimension of mass.

In the case where all the mass-scale parameters of the composite state are of the same order of magnitude, we obtain $a = \mathcal{O}(MR)$ as in Eq. (3.13), where $R = \langle \mathbf{k}_\perp^2 \rangle^{-1/2}$ is the characteristic size of the Fock state. On the other hand, in theories where $\mu^2 \ll \langle \mathbf{k}_\perp^2 \rangle$, we obtain the quadratic relation $a = \mathcal{O}(\mu MR^2)$. Thus, composite models for leptons can avoid conflict with the high-precision QED measurements in several ways.

- There can be strong cancellations between the contribution of different Fock states.
- The parameter μ can be minimized. For example, in a renormalizable theory this can be accomplished by having the bound state of light fermions and heavy bosons. Since $\mu \geq M$, we then have $a \geq \mathcal{O}(M^2 R^2)$.
- If the parameter μ is of the same order as the other mass scales in the composite state, then we have a linear condition $a = \mathcal{O}(MR)$.

3.7. (1 + 1)-dimensional: Schwinger model (LB)

Quantum electrodynamics in one-space and one-time dimension (QED₁₊₁) with massless charged fermions is known as the Schwinger model. It is one of the very few models of field theory which can be solved analytically [311,401,402,108–110]. The charged particles are confined because the Coulomb interaction in one-space dimension is linear in the relative distance, and there is only one physical particle, a massive neutral scalar particle with no self-interactions. The Fock-space content of the physical states depends crucially on the coordinate system and on the gauge. It is only in the front form that a simple constituent picture emerges [34,326,317]. It is the best example of the type of simplification that people hope will occur for QCD in physical space–time. Recent studies of similar model with massive fermion and for non-abelian theory where the fermion is in the fundamental and adjoint representation show however that many properties are unique to the Schwinger model [193,347].

The Schwinger model in Hamiltonian front-form field theory was studied first by Bergknoff [34]. The description here follows him closely, as well as Perry's recent lectures [367]. There is an extensive literature on this subject: DLCQ [137,460], lattice gauge theory [113], light-front integral equations [315], and light-front Tamm-Dancoff approaches [338] have used the model for testing the various methods.

Bergknoff showed that the physical boson in the Schwinger model in light-cone gauge is a pure electron–positron state. This is an amazing result in a strong-coupling theory of massless bare particles, and it illustrates how a constituent picture may arise in QCD. The kinetic energy vanishes in the massless limit, and the potential energy is minimized by a wavefunction that is flat in momentum space. One might expect that since a linear potential produces a state that is as localized as possible in position space.

Consider first the massive Schwinger model. The finite fermion mass m is a parameter to be set to zero, later. The Lagrangian for the theory takes the same form as the QED Lagrangian, Eq. (2.8). Again one works in the light-cone gauge $A^+ = 0$, and uses the same projection operators \mathcal{A}_\pm as in

Section 2. The analogue of Eq. (2.74) becomes now simply

$$i\partial^- \psi_+ = -im\psi_- + eA^- \psi_+, \quad i\partial^+ \psi_- = im\psi_- . \quad (3.88)$$

The equation for ψ_+ involves the light-front time derivative ∂^- , so ψ_+ is a dynamical degree of freedom that must be quantized. On the other hand, the equation for ψ_- involves only spatial derivatives, so ψ_- is a constrained degree of freedom that should be eliminated in favor of ψ_+ . Formally,

$$\psi_- = (m/\partial^+) \psi_+ . \quad (3.89)$$

It is necessary to specify boundary condition in order to invert the operator ∂^+ . If we had not chosen a finite mass for the fermions then both ψ_+ and ψ_- would be independent degrees of freedom and we would have to specify initial conditions for both. Furthermore, in the front form, it has only been possible to calculate the condensate $\langle 0|\psi\bar{\psi}|0\rangle$ for the Schwinger model by identifying it as the coefficient of the linear term in the mass expansion of matrix element of the currents [34]. Due to the gauge, one component is fixed to $A^+ = 0$, but the other component A^- of the gauge field is also a constrained degree of freedom. It can be formally eliminated by the light-cone analogue of Gauss's law:

$$A^- = - (4e/(\partial^+)^2) \psi_+^\dagger \psi_+ . \quad (3.90)$$

One is left with a single dynamical degree of freedom, ψ_+ , which is canonically quantized at $x^+ = 0$,

$$\{\psi_+(x^-), \psi_+^\dagger(y^-)\} = A_+ \delta(x^- - y^-) \quad (3.91)$$

similar to what was done in QED. The field operator at $x^+ = 0$, expanded in terms of the free particle creation and annihilation operators, takes the very simple form

$$\psi_+(x^-) = \int_{k^+ > 0} \frac{dk^+}{4\pi} [b_k e^{-ik \cdot x} + d_k^\dagger e^{ik \cdot x}] \quad \text{with } \{d_k, d_p^\dagger\} = \{b_k, b_p^\dagger\} = 4\pi \delta(k^+ - p^+) . \quad (3.92)$$

The canonical Hamiltonian $H = P_+ = \frac{1}{2}P^-$ is divided into the three parts,

$$H = H_0 + H'_0 + V' . \quad (3.93)$$

These Fock-space operators are obtained by inserting the free fields in Eq. (3.92) into the canonical expressions in Eq. (2.89). The free part of the Hamiltonian becomes

$$H_0 = \int_{k > 0} \frac{dk}{8\pi} \left(\frac{m^2}{k} \right) (b_k^\dagger b_k + d_k^\dagger d_k) . \quad (3.94)$$

H'_0 is the one-body operator which is obtained by normal ordering the interaction, i.e.

$$H'_0 = \frac{e^2}{4\pi} \int_{k > 0} \frac{dk}{4\pi} \int_{p > 0} dp \left(\frac{1}{(k-p)^2} - \frac{1}{(k+p)^2} \right) (b_k^\dagger b_k + d_k^\dagger d_k) . \quad (3.95)$$

The divergent momentum integral is regulated by the momentum cut-off, $|k-p| > \varepsilon$. One finds

$$H'_0 = \frac{e^2}{2\pi} \int \frac{dk}{4\pi} \left(\frac{1}{\varepsilon} - \frac{1}{k} + \mathcal{O}(\varepsilon) \right) (b_k^\dagger b_k + d_k^\dagger d_k) . \quad (3.96)$$

The normal-ordered interaction is

$$V' = 4\pi e^2 \int \frac{dk_1}{4\pi} \dots \frac{dk_4}{4\pi} \delta(k_1 + k_2 - k_3 - k_4) \left\{ \frac{2}{(k_1 - k_3)^2} b_1^\dagger d_2^\dagger d_4 b_3 \right. \\ \left. + \frac{2}{(k_1 + k_2)^2} b_1^\dagger d_2^\dagger d_3 b_4 - \frac{1}{(k_1 - k_3)^2} (b_1^\dagger b_2^\dagger b_3 b_4 + d_1^\dagger d_2^\dagger d_3 d_4) + \dots \right\}. \quad (3.97)$$

The interactions that involve the creation or annihilation of electron–positron pairs are not displayed. The first term in V' is the electron–positron interaction. The longitudinal momentum cut-off requires $|k_1 - k_3| > \varepsilon$ and leads to the potential

$$v(x^-) = 4q_1 q_2 \int_{-\infty}^{\infty} \frac{dk}{4\pi} \theta(|k| - \varepsilon) e^{-ikx^-/2} = q_1 q_2 \left[\frac{2}{\pi\varepsilon} - |x^-| + \mathcal{O}(\varepsilon) \right]. \quad (3.98)$$

This potential contains a linear Coulomb potential that we expect in two dimensions, but it also contains a divergent constant, being negative for unlike charges and positive for like charges.

In charge neutral states the infinite constant in V' is *exactly* canceled by the divergent “mass” term in H_0 . This Hamiltonian assigns an infinite energy to states with net charge, and a finite energy as, $\varepsilon \rightarrow 0$, to charge zero states. This does not imply that charged particles are confined, but that the linear potential prevents charged particles from moving to arbitrarily large separation except as charge-neutral states.

One should emphasize that even though the interaction between charges is long-ranged, there are no van der Waals forces in 1 + 1 dimensions. It is a simple geometrical calculation to show that all long-range forces between two neutral states cancel exactly. This does not happen in higher dimensions, and if we use long-range two-body operators to implement confinement we must also find many-body operators that cancel the strong long-range van der Waals interactions.

Given the complete Hamiltonian in normal-ordered form we can study bound states. A powerful tool for getting started is the variational wavefunction. In this case, one can begin with a state that contains a single electron–positron pair

$$|\Psi(P)\rangle = \int_0^P \frac{dp}{4\pi} \phi(p) b_p^\dagger d_{P-p}^\dagger |0\rangle. \quad (3.99)$$

The normalization of this state is $\langle \Psi(P') | \Psi(P) \rangle = 4\pi P \delta(P' - P)$. The expectation value of the one-body operators in the Hamiltonian is

$$\langle \Psi | H_0 + H'_0 | \Psi \rangle = \frac{1}{2P} \int \frac{dk}{4\pi} \left[\frac{m^2 - e^2/\pi}{k} + \frac{m^2 - e^2/\pi}{P - k} + \frac{2e^2}{\pi\varepsilon} \right] |\phi(k)|^2, \quad (3.100)$$

and the expectation value of the normal-ordered interaction is

$$\langle \Psi | V' | \Psi \rangle = -\frac{e^2}{P} \int' \frac{dk_1}{4\pi} \frac{dk_2}{4\pi} \left[g \frac{1}{(k_1 - k_2)^2} + \frac{1}{P^2} \right] \phi^*(k_1) \phi(k_2). \quad (3.101)$$

The prime on the last integral indicates that the range of integration in which $|k_1 - k_2| < \varepsilon$ must be removed. By expanding the integrand about $k_1 = k_2$, one can easily confirm that the $1/\varepsilon$ divergences cancel.

The easiest case to study is the massless Schwinger model. With $m = 0$, the energy is minimized when

$$\phi(k) = \sqrt{4\pi}. \quad (3.102)$$

The invariant-mass squared, $M^2 = 2PH$, becomes then finally

$$M^2 = e^2/\pi. \quad (3.103)$$

This type of simple analysis can be used to show that *this electron–positron state is actually the exact ground state of the theory* with momentum P , and that bound states do not interact with one another [367].

It is intriguing that for massless fermions, the massive bound state is a simple bound state of an electron and a positron when the theory is formulated in the front form using the light-cone gauge. This is not true in other gauges and coordinate systems. This happens because the charges screen one another perfectly, and this may be the way a constituent picture emerge in QCD. On the other hand there are many differences between two and four dimensions. In two dimensions, for example, the coupling has the dimension of mass making it natural for the bound state mass to be proportional to coupling in the massless limit. On the other hand, in four dimensions the coupling is dimensionless and the bound states in a four-dimensional massless theory must acquire a mass through dimensional transmutations. A simple model of how this might happen is discussed in the renormalization of the Yukawa model and in some simple models in the section on renormalization.

3.8. (3 + 1)-dimensional: Yukawa model

Our ultimate aim is to study the bound-state problem in QCD. However light-front QCD is plagued with divergences arising from both small longitudinal momentum and large transverse momentum. To gain experience with the novel renormalization programs that this requires, it is useful to study a simpler model. The two-fermion bound-state problem in the 3 + 1 light-front Yukawa model has many of the non-perturbative problems of QCD while still being tractable in the Tamm–Dancoff approximation. This section follows closely the work in Refs. [182,373,374]. The problems that were encountered in this calculation are typical of any (3 + 1)-dimensional non-perturbative calculation and laid the basis for Wilson’s current light-front program [451,452,456,364–366] which will be briefly discussed in the section on renormalization.

The light-front Tamm–Dancoff method (LFTD) is Tamm–Dancoff truncation of the Fock space in light-front quantum field theory and was proposed [363,422] to overcome some of the problems in the equal-time Tamm–Dancoff method [68]. In this approach, one introduces a longitudinal momentum cut-off ε to remove all the troublesome vacuum diagrams. The bare vacuum state is then an eigenstate of the Hamiltonian. One can also introduce a transverse momentum cut-off Λ to regulate ultraviolet divergences. Of course, the particle truncation and momentum cut-offs spoil Lorentz symmetries. In a properly renormalized theory, one has to remove the cut-off dependence from the observables and recover the lost Lorentz symmetries. One has avoided the original vacuum problem but now the construction of a properly renormalized Hamiltonian is a nontrivial problem. In particular, the light-front Tamm–Dancoff approximation breaks rotational invariance with respect to the two transverse directions. This is visible in the spectrum which does not exhibit

the degeneracy associated with the total angular momentum multiplets. It is seen that renormalization has sufficient flexibility to restore the degeneracy.

Retaining only two-fermion and two-fermion, one-boson states one obtains a two-fermion bound-state problem in the lowest-order Tamm–Dancoff truncation. This is accomplished by eliminating the three-body-sector algebraically which leaves an integral equation for the two-body state. This bound state equation has both divergent self-energy and divergent one-boson exchange contributions. In the renormalization of the one-boson exchange divergences the self-energy corrections are ignored. Related work can be found in Refs. [176,279,459].

Different counter terms are introduced to renormalize the divergences associated with one-boson exchange. The basis for these counter terms is easily understood, and uses a momentum space slicing called the high–low analysis. It was introduced by Wilson [454] and is discussed in detail for a simple one-dimensional model in the section on renormalization.

To remove the self-energy divergences one first introduces a sector-dependent mass counter term which removes the quadratic divergence. The remaining logarithmic divergence is removed by a redefinition of the coupling constant. Here one faces the well-known problem of triviality: For a fixed renormalized coupling the bare coupling becomes imaginary beyond a certain ultraviolet cut-off. This was probably seen first in the Lee model [293] and then in meson–nucleon scattering using the equal-time Tamm–Dancoff method [114].

The canonical light-front Hamiltonian for the (3 + 1)-dimensional Yukawa model is given by

$$P^- = \frac{1}{2} \int dx^- d^2x_\perp [2i\psi^\dagger \partial^+ \psi_- + m_B^2 \phi^2 + \partial_\perp \phi \cdot \partial_\perp \phi]. \tag{3.104}$$

The equations of motion are used to express ψ_- in terms of ψ_+ , i.e.

$$\psi_- = (1/i\partial^+) [i\alpha_\perp \cdot \partial_\perp + \beta(m_F + g\phi)] \psi_+. \tag{3.105}$$

For simplicity, the two fermions are taken to be of different flavors, one denoted by b_σ and the other by B_σ . We divide the Hamiltonian P^- into P_{free}^- and P_{int}^- , where

$$P_{\text{free}}^- = \int [d^3k] \frac{m_B^2 + k^2}{k^+} a^\dagger(k)a(k) + \sum_\sigma \int [d^3k] \frac{m_F^2 + k^2}{k^+} [b_\sigma^\dagger(k)b_\sigma(k) + B_\sigma^\dagger(k)B_\sigma(k)], \tag{3.106}$$

$$P_{\text{int}}^- = g \sum_{\sigma_1, \sigma_2} \int [d^3k_1] \int [d^3k_2] \int [d^3k_3] 2(2\pi)^3 \delta^3(k_1 - k_2 - k_3) \\ \times [(b_{\sigma_1}^\dagger(k_1)b_{\sigma_2}(k_2) + B_{\sigma_1}^\dagger(k_1)B_{\sigma_2}(k_2))a(k_3)\bar{u}_{\sigma_1}(k_1)u_{\sigma_2}(k_2) + (b_{\sigma_2}^\dagger(k_2)b_{\sigma_1}(k_1) \\ + B_{\sigma_2}^\dagger(k_2)B_{\sigma_1}(k_1))a^\dagger(k_3)\bar{u}_{\sigma_2}(k_2)u_{\sigma_1}(k_1)]. \tag{3.107}$$

Note that the instantaneous interaction was dropped from P_{int}^- for simplicity. The fermion number 2 state that is an eigenstate of P^- with momentum P and helicity σ is denoted as $|\Psi(P, \sigma)\rangle$. The wavefunction is normalized in the truncated Fock space, with

$$\langle \Psi(P', \sigma') | \Psi(P, \sigma) \rangle = 2(2\pi)^3 P^+ \delta^3(P - P') \delta_{\sigma\sigma'}.$$

In the lowest-order Tamm–Dancoff truncation one has

$$|\Psi(P, \sigma)\rangle = \sum_{\sigma_1 \sigma_2} \int [d^3 k_1] \int [d^3 k_2] \Phi_2(P, \sigma | k_1 \sigma_1, k_2 \sigma_2) b_{\sigma_1}^\dagger(k_1) B_{\sigma_2}^\dagger(k_2) |0\rangle \\ + \sum_{\sigma_1 \sigma_2} \int [d^3 k_1] \int [d^3 k_2] \int [d^3 k_3] \Phi_3(P, \sigma | k_1 \sigma_1, k_2 \sigma_2, k_3) b_{\sigma_1}^\dagger(k_1) B_{\sigma_2}^\dagger(k_2) a^\dagger(k_3) |0\rangle,$$

where Φ_2 is the two-particle and Φ_3 the three-particle amplitude, and where $|0\rangle$ is the vacuum state. For notational convenience, one introduces the amplitudes Ψ_2 and Ψ_3 by

$$\Phi_2(P, \sigma | k_1 \sigma_1, k_2 \sigma_2) = 2(2\pi)^3 P^+ \delta^3(P - k_1 - k_2) \sqrt{x_1 x_2} \Psi_2^{\sigma_1 \sigma_2}(\kappa_1 x_1, \kappa_2 x_2), \quad (3.108)$$

$$\Phi_3(P, \sigma | k_1 \sigma_1, k_2 \sigma_2, k_3) = 2(2\pi)^3 P^+ \delta^3(P - \Sigma k_i) \sqrt{x_1 x_2 x_3} \Psi_3^{\sigma_1 \sigma_2}(\kappa_1 x_1, \kappa_2 x_2, \kappa_3 x_3). \quad (3.109)$$

As usual, the intrinsic variables are x_i and $\kappa_i = \kappa_{\perp i}$:

$$k_i^\mu = \left(x_i P^+, \kappa_{\perp i}, \frac{\kappa_{\perp i}^2 + m^2}{x_i P^+} \right),$$

with $\sum_i x_i = 1$ and $\sum_i \kappa_{\perp i} = 0$. By projecting the eigenvalue equation

$$(P^+ P^- - P_\perp^2) |\Psi\rangle = M^2 |\Psi\rangle \quad (3.110)$$

onto a set of free Fock states, one obtains two coupled integral equations:

$$\left[M^2 - \frac{m_F^2 + (\kappa_1)^2}{x_1} - \frac{m_F^2 + (\kappa_1)^2}{x_2} \right] \Psi_2^{\sigma_1 \sigma_2}(\kappa_1, x_1) \\ = \frac{g}{2(2\pi)^3} \sum_{s_1} \int \frac{dy_1 d^2 q_1}{\sqrt{(x_1 - y_1) x_1 y_1}} \Psi_3^{s_1 \sigma_2}(q_1, y_1; \kappa_2, x_2) \bar{u}_{\sigma_1}(\kappa_1, x_1) u_{s_1}(q_1, y_1) \\ + \frac{g}{2(2\pi)^3} \sum_{s_2} \int \frac{dy_2 d^2 q_2}{\sqrt{(x_2 - y_2) x_2 y_2}} \Psi_3^{\sigma_1 s_2}(\kappa_1, x_1; q_2, y_2) \bar{u}_{\sigma_2}(\kappa_2, x_2) u_{s_2}(q_2, y_2) \quad (3.111)$$

and

$$\left[M^2 - \frac{m_F^2 + (\kappa_1)^2}{x_1} - \frac{m_F^2 + (\kappa_2)^2}{x_2} - \frac{m_B^2 + (\kappa_1 + \kappa_2)^2}{x_3} \right] \Psi_3^{\sigma_1 \sigma_2}(\kappa_1, x_1; \kappa_2, x_2) \\ = g \sum_{s_1} \frac{\Psi_2^{s_1 \sigma_2}(-\kappa_2, x_1 + x_3)}{\sqrt{x_3 x_1 (x_1 + x_3)}} \bar{u}_{\sigma_1}(\kappa_1, x_1) u_{s_1}(-\kappa_2, x_1 + x_3) \\ + g \sum_{s_2} \frac{\Psi_2^{\sigma_1 s_2}(\kappa_1, x_1)}{\sqrt{x_3 x_2 (x_3 + x_2)}} \bar{u}_{\sigma_2}(\kappa_2, x_2) u_{s_2}(-\kappa_1, x_2 + x_3). \quad (3.112)$$

After eliminating Ψ_3 one ends up with an integral equation for Ψ_2 and the eigenvalue M^2 :

$$M^2 \Psi_2^{\sigma_1, \sigma_2}(\kappa, x) = \left(\frac{m_F^2 + \kappa^2}{x(1-x)} + [\text{SE}] \right) \Psi_2^{\sigma_1, \sigma_2}(\kappa, x) + \frac{\alpha}{4\pi^2} \sum_{s_1, s_2} \int dy d^2q K(\kappa, x; q, y; \omega)_{\sigma_1, \sigma_2; s_1, s_2} \Psi_2^{s_1, s_2}(q, y) + \text{counterterms}, \quad (3.113)$$

where $\alpha = g^2/4\pi$ is the fine structure constant. The absorption of the boson on the same fermion gives rise to the self-energy term [SE], the one by the other fermion generates an effective interaction, or the boson-exchange kernel K ,

$$K(\kappa, x; q, y; \omega)_{\sigma_1, \sigma_2; s_1, s_2} = \frac{[\bar{u}(\kappa, x; \sigma_1)u(q, y; s_1)][\bar{u}(-\kappa, 1-x; \sigma_2)u(-q, 1-y; s_2)]}{(a + 2(\kappa \cdot q))\sqrt{x(1-x)y(1-y)}}, \quad (3.114)$$

with

$$a = |x-y| \left\{ \omega - \frac{1}{2} \left[\frac{m_F^2 + k^2}{x(1-x)} + \frac{m_F^2 + q^2}{y(1-y)} \right] \right\} - m_B^2 + 2m_F^2 - \frac{m_F^2 + k^2}{2} \left[\frac{y}{x} + \frac{1-y}{1-x} \right] - \frac{m_F^2 + q^2}{2} \left[\frac{x}{y} + \frac{1-x}{1-y} \right], \quad (3.115)$$

with $k = |\kappa|$ and $\omega \equiv M^2$. Possible counter terms will be discussed below.

Since $\sigma = \uparrow, \downarrow$ one faces thus $4 \times 4 = 16$ coupled integral equations in the three variables x and κ_{\perp} . But the problem is simplified considerably by exploiting the rotational symmetry around the z -axis. Let us demonstrate that shortly. By Fourier transforming over the angle ϕ , one introduces first states Φ with good total spin-projection $S_z = \sigma_1 + \sigma_2 \equiv m$,

$$\Psi_2^{\sigma_1, \sigma_2}(\kappa, x) = \sum_m \frac{e^{im\phi}}{\sqrt{2\pi}} \Phi_{\sigma_1, \sigma_2}(k, x; m) \quad (3.116)$$

and uses that second to redefine the kernel:

$$V(k, x, m; q, y, m'; M^2)_{\sigma_1, \sigma_2; s_1, s_2} = \int \frac{d\phi d\phi'}{2\pi} e^{-im\phi} e^{im'\phi'} K(k, \phi, x; q, \phi', y; M^2)_{\sigma_1, \sigma_2; s_1, s_2}. \quad (3.117)$$

The ϕ -integrals can be done analytically. Now, recall that neither S_z nor L_z is conserved; only $J_z = S_z + L_z$ is a good quantum number. In the two-particle sector of spin- $\frac{1}{2}$ particles the spin projections are limited to $|S_z| \leq 1$, and thus, for J_z given, one has to consider only the four amplitudes $\Phi_{\uparrow\uparrow}(k, x; J_z - 1)$, $\Phi_{\uparrow\downarrow}(k, x; J_z)$, $\Phi_{\downarrow\uparrow}(k, x; J_z)$, and $\Phi_{\downarrow\downarrow}(k, x; J_z + 1)$. Rotational symmetry allows thus to reduce the number of coupled equations from 16 to 4, and the number of integration variables from 3 to 2. Finally, one always can add and subtract the states, introducing

$$\begin{aligned} \Phi_r^{\pm}(k, x) &= (1/\sqrt{2})(\Phi_{\uparrow\uparrow}(k, x; J_z - 1) \pm \Phi_{\downarrow\downarrow}(k, x; J_z + 1)), \\ \Phi_s^{\pm}(k, x) &= (1/\sqrt{2})(\Phi_{\uparrow\downarrow}(k, x; J_z) \pm \Phi_{\downarrow\uparrow}(k, x; J_z)). \end{aligned} \quad (3.118)$$

The integral equations couple the sets (t^-, s^+) and (t^+, s^-) . For $J_z = 0$, the “singlet” and the “triplet” states uncouple completely, and one has to solve only two pairs of two coupled integral equations. In a way, these reductions are quite natural and straightforward, and have been applied independently also by Krautgärtner et al. [279] and most recently by Trittman and Pauli [429].

Next, let us discuss the structure of the *integrand* in Eq. (3.113) and analyze eventual divergences. Restrict first to $J_z = 0$, and consider $[\bar{u}(x, \kappa; \sigma_1)u(y, q; s_1)]$ for large q , taken from the tables in Section 4. They are such that the kernel K becomes independent of $|q|$ in the limit $|q| \rightarrow \infty$. Thus, unless Φ vanishes faster than $|q|^{-2}$, the q -integral potentially diverges. In fact, introducing an ultraviolet cut-off Λ to regularize the $|q|$ -dependence, the integrals involving the singlet wavefunctions Φ_s^\pm diverge logarithmically with Λ . In the $J_z = 1$ sector one must solve a system of four coupled integral equations. One finds that the kernel $V_{\uparrow\uparrow, \downarrow\downarrow}$ approaches the same limit $-f(x, y)$ as q becomes large relative to k . All other kernels fall off faster with q . For higher values of J_z , the integrand converges since the wavefunctions fall-off faster than $|q|^{-2}$. Counter terms are therefore needed only for $J_z = 0$ and $J_z = \pm 1$. These boson-exchange counter terms have no analogue in equal-time perturbation theory, and will be discussed below.

These integral equations are solved numerically, using Gauss–Legendre quadratures to evaluate the q and y integrals. Note that the eigenvalue M^2 appears on both the left- and right-hand side of the integral equation. One handles this by choosing some “starting point” value ω on the r.h.s. By solving the resulting matrix eigenvalue problem one obtains the eigenvalue $M^2(\omega)$. Taking that as the new starting point value, one iterates the procedure until $M^2(\omega) = \omega$ is numerically fulfilled sufficiently well.

For the parameter values $1 \leq \alpha \leq 2$ and $2 \leq m_F/m_B \leq 4$ one finds only two stable bound states, one for each $|J_z| \leq 1$. In the corresponding wavefunctions, one observes a dominance of the spin-zero configuration $S_z = 0$. The admixture from higher values of L_z increases gradually with increasing α , but the predominance of $L_z = 0$ persists also when counter terms are included in the calculation. With the above parameter choice no bound states have been found numerically for $J_z > 1$. They start to appear only when α is significantly increased.

The above bound-state equations are regularized. How are they renormalized? In the section on renormalization, below, we shall show in simple one-dimensional models that it is possible to add counter terms to the integral equation of this type that completely remove all the cut-off dependence from both the wavefunctions and the bound-state spectrum. In these one-dimensional models the finite part of the counter term contains an arbitrary dimensionful scale μ and an associated arbitrary constant. In two-dimensional models the arbitrary constant becomes an arbitrary function. The analysis presented here is based on the methods used in the one-dimensional models. It is convenient to subdivide the study of these counter terms into two categories. One is called the asymptotic counter terms, and the other is called the perturbative counter terms.

Studies of the simple models and the general power counting arguments show that integral equations should be supplemented by a counter term of the form,

$$G(\Lambda) \int q \, dq \, dy \, F(x, y) \phi(q, y). \quad (3.119)$$

For the Yukawa model one has not been able to solve for $G(\Lambda) F(x, y)$ exactly such that it removes all that cut-off dependence. One can, however, estimate $G(\Lambda) F(x, y)$ perturbatively. The

lowest-order perturbative counter terms, those of order α^2 , correspond to the box graphs in the integral equation. They are thus called the “box counter terms” (BCT). Applying it to the Yukawa model, one finds that the integral equation should be modified according to

$$V(k, x; q, y; \omega) \rightarrow V(k, x; q, y; \omega) - V^{\text{BCT}}(x, y). \quad (3.120)$$

$V^{\text{BCT}}(x, y)$ contains an undetermined parameter ‘ C ’. Redoing the bound-state mass calculations with this counter term one finds that the cut-off independence of the solutions is greatly reduced. Thus, one has an (almost) finite calculation involving arbitrary parameters, C for each sector. Adjusting the C ’s allows us to move eigenvalues around only in a limited way. It is possible however to make the $J_z = 1$ state degenerate with either of the two $J_z = 0$ states. The splitting among the two $J_z = 0$ states remains small.

One can also eliminate divergences non-perturbatively by subtracting the large transverse momentum limit of the kernel. We call this type of counter term as the asymptotic counter term. In the Yukawa model one is only able to employ such counter terms in the $J_z = 0$ sector. One then has

$$V(k, x; q, y; M^2)^{s^+, s^+} \rightarrow V(k, x; q, y; M^2)^{s^+, s^+} + f(x, y), \quad (3.121)$$

$$V(k, x; q, y; M^2)^{s^-, s^-} \rightarrow V(k, x; q, y; M^2)^{s^-, s^-} - f(x, y). \quad (3.122)$$

One can find an extra interaction allowed by power counting in the LC-Hamiltonian that would give rise to more terms. One finds that with the asymptotic counter term the cut-off dependence has been eliminated for the $(t -, s +)$ states and improved for the $(t +, s -)$ states. We also find that this counter term modifies the large k behavior of the amplitudes $\Phi(k, x)$ making them fall off faster than before.

The asymptotic counter term, as it stands, does not include any arbitrary constants that can be tuned to renormalize the theory to some experimental input. This differs from the case with the box counter term where such a constant appeared. One may, however, add an adjustable piece which in general involves an arbitrary function of longitudinal momenta. This is motivated by the simple models discussed in the section on renormalization. One replaces

$$f(x, y) \rightarrow f(x, y) - G_\mu / (1 + \frac{1}{6} G_\mu \ln(A/\mu)) \quad (3.123)$$

G_μ and the scale μ are not independent. A change in μ can be compensated by adjusting G_μ such that $(1/G_\mu) - \frac{1}{6} \ln(\mu) = \text{constant}$. This ‘constant’ is arbitrary and plays the role of the constant “ C ” in the box counter term. One finds that by adjusting the constant a much wider range of possible eigenvalues can be covered, compared to the situation with the box counter term.

Consider now the effects of the self-energy term [SE]. Note that in the bound state problem the self-energy is a function of the bound state energy M^2 . The most severe ultraviolet divergence in $[\text{SE}]_{(M^2)}$ is a quadratical divergence. One eliminates this divergence by subtracting at the threshold $M^2 = M_0^2 \equiv (m_F^2 + k^2)/(x(1-x))$

$$[\text{SE}]_{(M^2)} \rightarrow [\text{SE}]_{(M^2)} - [\text{SE}]_{(M_0^2)} \equiv g^2(M^2 - M_0^2)\sigma_{(M^2)}. \quad (3.124)$$

$\sigma_{(M^2)}$ is still logarithmically divergent. The remaining logarithmically divergent piece corresponds to wavefunction renormalization of the two fermion lines. One finds

$$\sigma_{\log\text{div. part}} = \left(\frac{\partial[\text{SE}]}{\partial M^2} \right)_{\log\text{div.}} \equiv -W(A) \quad (3.125)$$

One can absorb this divergence into a new definition of the coupling constant. After the subtraction (but ignoring all “boson-exchange” counter terms) the integral equation becomes

$$(M^2 - M_0^2)\Psi_{2^{\sigma_1\sigma_2}}(\mathbf{k}, x) = \frac{\alpha}{4\pi^2}[\text{BE}] + \frac{\alpha}{4\pi^2}(M^2 - M_0^2)\sigma_{(M_0^2)}\Psi_{2^{\sigma_1\sigma_2}}(\mathbf{k}, x), \quad (3.126)$$

where [BE] stands for the term with the kernel K . After rearranging the terms one finds, with all spin indices suppressed,

$$(M^2 - M_0^2)\left[1 + \frac{\alpha}{4\pi^2}W(\Lambda)\right]\Psi = \frac{\alpha}{4\pi^2}[\text{BE}] + \frac{\alpha}{4\pi^2}(M^2 - M_0^2)(\sigma + W(\Lambda))\Psi. \quad (3.127)$$

The r.h.s. is now finite. One must still deal with the divergent piece W on the l.h.s. of the equation. Define

$$\alpha_R = \alpha/(1 + (\alpha/4\pi^2)W(\Lambda)). \quad (3.128)$$

Then one can trade a Λ -dependent bare coupling α in favor of a finite renormalized coupling α_R . One has

$$(M^2 - M_0^2)\Psi = \frac{\alpha_R/4\pi^2}{1 - \alpha_R/4\pi^2(\sigma_{(M^2)} + W(\Lambda))}[\text{BE}]. \quad (3.129)$$

One sees that the form of the equation is identical to what was solved earlier (where all counter terms were ignored) with α replaced by $\alpha_R/[1 - \alpha_R/4\pi^2(\sigma + W)]$. One should note that σ is a function of x and k , and therefore effectively changes the kernel. In lowest-order Tamm–Dancoff the divergent parts of [SE] can hence be absorbed into a renormalized mass and coupling. It is however not clear whether this method will work in higher orders.

Inverting the equation for α_R one has

$$\alpha(\Lambda) = \alpha_R/(1 - (\alpha_R/4\pi^2)W(\Lambda)). \quad (3.130)$$

One sees that for every value of α_R other than $\alpha_R = 0$ there will be a cut-off Λ at which the denominator vanishes and α becomes infinite. This is just a manifestation of “triviality” in this model. The only way the theory can be sensible for arbitrarily large cut-off $\Lambda \rightarrow \infty$, is when $\alpha_R \rightarrow 0$. In practice, this means that for fixed cut-off there will be an upper bound on α_R .

4. Discretized light-cone quantization

Constructing even the lowest state, the “vacuum”, of a quantum field theory has been so notoriously difficult that the conventional Hamiltonian approach was given up altogether long ago in the 1950s, in favor of action-oriented approaches. It was overlooked that Dirac’s “front form of Hamiltonian dynamics” [123] might have less severe problems. Of course, the action and the Hamiltonian forms of dynamics are equivalent to each other. The action is more suitable for deriving cross sections, the Hamiltonian more convenient when considering the structure of bound states in atoms, nuclei, and hadrons. In fact, in the front form with periodic boundary conditions one can combine the aspects of a simple vacuum [448] and a careful treatment of the infrared

degrees of freedom. This method is called “discretized light-cone quantization” (DLCQ) [354] and has three important aspects:

1. the theory is formulated in a Hamiltonian approach;
2. calculations are done in momentum representation;
3. quantization is done at equal light-cone rather than at equal usual time.

As a method, “discretized light-cone quantization” has the ambitious goal to calculate the spectra and wavefunctions of physical hadrons from a covariant gauge field theory. In fact, in $1 + 1$ dimensions this method provides the first total solutions to non-trivial quantum field theories. In $3 + 1$ dimensions, the conversion of this non-perturbative method into a reliable tool for hadronic physics is beset with many difficulties [185]. Their resolution will continue to take time. Since its first formulation [354,355] many problems have been resolved but many remain, as we shall see. Many of these challenges are actually not peculiar to the front form but appear also in conventional Hamiltonian dynamics. For example, the renormalization program for a quantum field theory has been formulated thus far only in order-by-order perturbation theory. Little work has been done on formulating a non-perturbative Hamiltonian renormalization [363,456].

At the beginning, one should emphasize a rather important aspect of periodic boundary conditions: all charges are strictly conserved. Every local Lagrangian field theory has vanishing four-divergences of some “currents” of the form $\partial_\mu J^\mu = 0$. Written out explicitly this reads

$$\partial_+ J^+ + \partial_- J^- = 0. \quad (4.1)$$

The restriction to $1 + 1$ dimensions suffices for the argument. The case of $3 + 1$ dimensions is a simple generalization. The “charge” is defined by

$$Q(x^+) \equiv \int_{-L}^{+L} dx^- J^+(x^+, x^-). \quad (4.2)$$

Conservation is proven by integrating Eq. (4.1),

$$(d/dx^+)Q(x^+) = 0, \quad (4.3)$$

provided that the terms from the boundaries *vanish*, i.e.

$$J^+(x^+, L) - J^+(x^+, -L) = 0. \quad (4.4)$$

This is precisely the condition for periodic boundary conditions. If one does not use periodic boundary conditions, then one has to ensure that all fields tend to vanish “sufficiently fast” at the boundaries. To guarantee the latter is much more difficult than taking the limit $L \rightarrow \infty$ at the end of a calculation. Examples of conserved four-currents are the components of the energy–momentum stress tensor with $\partial_\mu \Theta^{\mu\nu} = 0$, the conserved “charges” being the four components of the energy–momentum four-vector P^ν .

Discretized light-cone quantization applied to abelian and non-abelian quantum field theories faces a number of problems only part of which have been resolved by recent work. Here is a rather incomplete list:

1. Is the front form of Hamiltonian dynamics equivalent to the instant form? Does one get the same results in both approaches? Except for a class of problems involving massless left-handed

fields, it has been established that all explicit calculations with the front form yield the same results as in the instant form, provided the latter are available and reliable.

2. One of the major problems is to find a suitable and appropriate gauge. One has to fix the gauge before one can formulate the Hamiltonian. One faces the problem of quantizing a quantum field theory “under constraints”. Today one knows much better how to cope with these problems, and the Dirac–Bergman method is discussed in detail in Appendix E.
3. Can a Hamiltonian matrix be properly renormalized with a cut-off such that the physical results are independent of the cut-off? Hamiltonian renormalization theory is just starting to be understood.
4. In hadron phenomenology the aspects of chiral symmetry breaking play a central role. In DLCQ applied to QCD they have not been tackled yet.

In this section we shall give a number of concrete examples where the method has been successful.

4.1. Why discretized momenta?

The goal of rigorously diagonalizing a Hamiltonian has not been realized even for a conventional quantum many-body problem. How can one dare to address a field theory, where not even the particle number is conserved?

Let us briefly review the difficulties for a conventional non-relativistic many-body theory. One starts with a many-body Hamiltonian $H = T + U$. The kinetic energy T is usually a one-body operator and thus simple. The potential energy U is at least a two-body operator and thus complicated. One has solved the problem if one has found the eigenvalues and eigenfunctions of the Hamiltonian equation, $H\Psi = E\Psi$. One always can expand the eigenstates in terms of products of single-particle states $\langle \mathbf{x}|m\rangle$, which usually belong to a complete set of orthonormal functions of position \mathbf{x} , labeled by a quantum number m . When antisymmetrized, one refers to them as “Slater determinants”. All Slater determinants with a fixed particle number form a complete set.

One can proceed as follows. In the first step one chooses a complete set of single-particle wavefunctions. These single particle wave functions are solutions of an arbitrary “single-particle Hamiltonian” and its selection is a science of its own. In the second step, one defines one (and only one) reference state, which in field theory finds its analogue as the “Fock-space vacuum”. All Slater determinants can be classified relative to this reference state as 1-particle–1-hole (1-ph) states, 2-particle–2-hole (2-ph) states, and so on. The Hilbert space is truncated at some level. In a third step, one calculates the Hamiltonian matrix within this Hilbert space.

In Fig. 9, the Hamiltonian matrix for a two-body interaction is displayed schematically. Most of the matrix elements vanish, since a two-body Hamiltonian changes the state by upto two particles. Therefore, the structure of the Hamiltonian is a *finite penta-diagonal block matrix*. The dimension within a block, however, is infinite. It is made finite by an *artificial cut-off* on the kinetic energy, i.e. on the single-particle quantum numbers m . A finite matrix, however, can be diagonalized on a computer: the problem becomes “approximately soluble”. Of course, at the end one must verify that the physical results are reasonably insensitive to the cut-off(s) and other formal parameters.

This procedure was actually carried out in one-space dimension [353] with two different sets of single-particle functions,

$$\langle \mathbf{x}|m\rangle = N_m H_m(x/L) \exp\left\{-1/2(x/L)^2\right\}, \quad \langle \mathbf{x}|m\rangle = N_m \exp\{im(x/L)\pi\}. \quad (4.5)$$

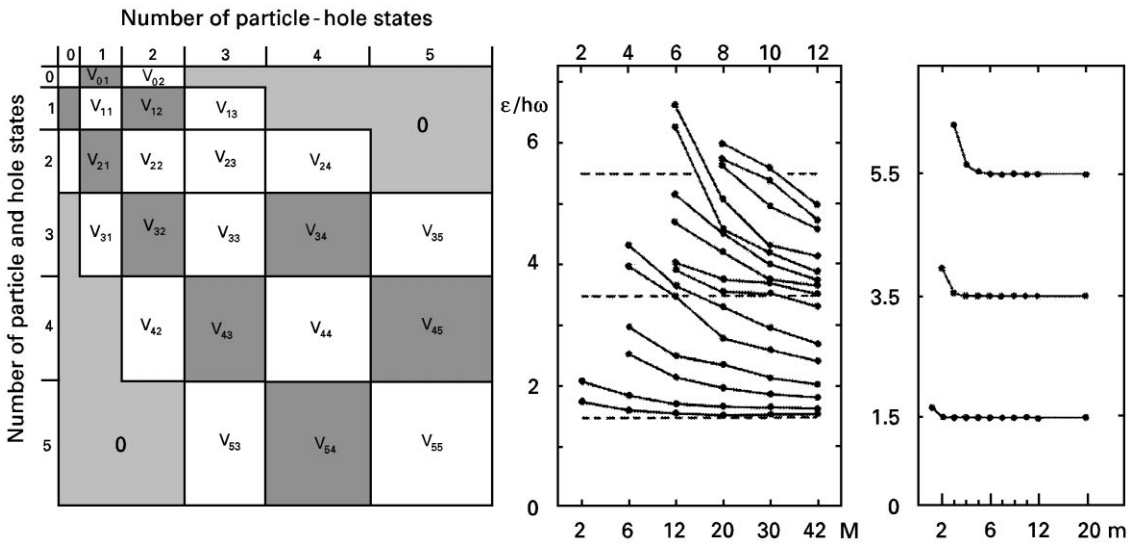


Fig. 9. Non-relativistic many-body theory.

The two sets are the eigenfunctions of the harmonic oscillator ($L \equiv \hbar/m\omega$) with its Hermite polynomials H_m , and the eigenfunctions of the momentum of a free particle with periodic boundary conditions. Both are suitably normalized (N_m), and both depend parametrically on a characteristic length parameter L . The calculations are particularly easy for particle number 2, and for a harmonic two-body interaction. The results are displayed in Fig. 9, and surprisingly different. For the plane waves, the results converge rapidly to the exact eigenvalues $E = \frac{3}{2}, \frac{7}{2}, \frac{11}{2}, \dots$, as shown in the right part of the figure. Opposed to this, the results with the oscillator states converge extremely slowly. Obviously, the larger part of the Slater determinants is wasted on building up the plane-wave states of center of mass motion from the Slater determinants of oscillator wavefunctions. It is obvious, that the plane waves are superior, since they account for the symmetry of the problem, namely Galilean covariance. For completeness one should mention that the approach with discretized plane waves was successful in getting the exact eigenvalues and eigenfunctions for upto 30 particles in one dimension [353] for harmonic and other interactions.

From these calculations, one should conclude:

1. Discretized plane waves are a useful tool for many-body problems.
2. Discretized plane waves and their Slater determinants are denumerable, and thus allow the construction of a Hamiltonian matrix.
3. Periodic boundary conditions generate good wavefunctions even for a “confining” potential like the harmonic oscillator.

A numerical “solution” of the many-body problem is thus possible at least in one-space dimension. Periodic boundary conditions should also be applicable to gauge field theory.

4.2. Quantum chromodynamics in 1 + 1 dimensions (KS)

DLCQ [354] in one-space and one-time dimensions had been applied first to Yukawa theory [354,355] followed by an application to QED [137] and to QCD [227], but the advantages of working with periodic boundary conditions, particularly when discussing the “zero modes” (see Section 7), had been noted first in 1976 by Maskawa and Yamawaki [324]. However, before we go into the technical details, let us first see how much we can say about the theory without doing any calculations. With only one-space dimension there are no rotations – hence no angular momentum. The Dirac equation is only a two-component equation. Chirality can still formally be defined. Second, the gauge field does not contain any dynamical degree of freedom (up to a zero mode which will be discussed in a later section) since there are no transverse dimensions. This can be understood as follows. In four dimensions, the A^μ field has four components. One is eliminated by fixing the gauge. A second component corresponds to the static Coulomb field and only the remaining two transverse components are dynamical (their “equations of motion” contain a time derivative). In contrast, in 1 + 1 dimensions, one starts with only two components of the A^μ -field. Thus, after fixing the gauge and eliminating the Coulomb part, there are no dynamical degrees of freedom left. Furthermore, in an axial gauge the nonlinear term in the only non-vanishing component of $F^{\mu\nu}$ drops out, and there are no gluon–gluon interactions. Nevertheless, the theory confines quarks. One way to see that is to analyze the solution to the Poisson equation in one-space dimension which gives rise to a linearly rising potential. This however is not peculiar to QCD_{1+1} . Most if not all field theories confine in 1 + 1 dimensions.

In 1 + 1 dimensions quantum electrodynamics [137] and quantum chromodynamics [227] show many similarities, both from the technical and from the phenomenological point of view. A plot like that on the left side in Fig. 10 was first given by Eller for periodic boundary conditions on the fermion fields [137], and repeated recently for anti-periodic ones [139]. For a fixed value of the resolution, it shows the full mass spectrum of QED in the charge zero sector for all values of the coupling constant and the fermion mass, parametrized by $\lambda = (1 + \pi(m/g)^2)^{-1/2}$. It includes the free case $\lambda = 0$ ($g = 0$) and the Schwinger model $\lambda = 1$ ($m = 0$). The eigenvalues M_i are plotted in units where the mass of the lowest “positronium” state has the numerical value 1. All states with $M > 2$ are unbound. The lower left part of the figure illustrates the following point. The rich complexity of the spectrum allows for multi-particle Fock states *at the same invariant mass* as the “simple $q\bar{q}$ -states” shown in the figure as the “2 particle sector”. The spectrum includes not only the simple bound-state spectrum, but also the associated discretized continuum of the same particles in relative motion. One can identify the simple bound states as two quarks connected by a confining string as displayed in the figure. The smallest residual interaction mixes the simple configuration with the large number of “continuum states” at the same mass. The few simple states have a much smaller statistical weight, and it looks as if the long string “breaks” into several pieces of smaller strings. Loosely speaking one can interpret such a process as the decay of an excited pion into multi-pion configurations $\pi^* \rightarrow \pi\pi\pi$. In the right part of Fig. 10 some of the results of Hornbostel [227] on the spectrum and the wavefunctions for QCD are displayed. Fock states in non-abelian gauge theory $\text{SU}(N)$ can be made color singlets for any order of the gauge group and thus one can calculate mass spectra for mesons and baryons for almost arbitrary values of N . In the upper right part of the figure the lowest mass eigenvalue of a meson is given for $N = 2, 3, 4$. Lattice gauge calculations to compare with are available only for $N = 2$ and for the lowest two eigenstates; the

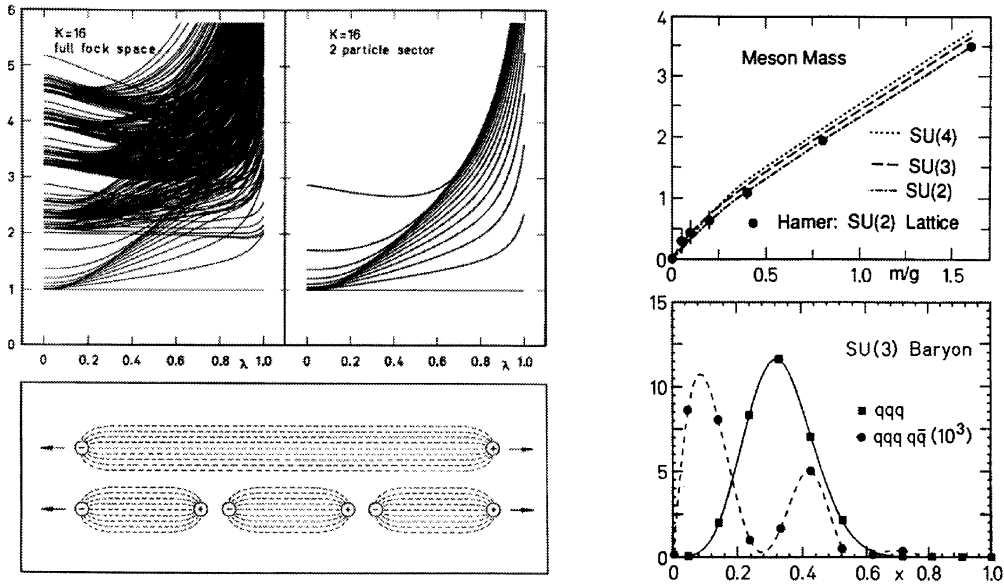


Fig. 10. Spectra and wavefunctions in 1 + 1 dimensions, taken from Refs. [137,227]. Lattice results are from Refs. [195–197].

agreement is very good. In the left lower part of the figure the structure function of a baryon is plotted versus (Björken-) x for $m/g = 1.6$. With DLCQ it is possible to calculate also higher Fock space components. As an example, the figure includes the probability distribution to find a quark in a $qqq q\bar{q}$ -state.

Meanwhile, many calculations have been done for 1 + 1 dimensions, among them those by Eller et al. [137,138], Hornbostel et al. [226–230], Antonuccio et al. [9–11,13], Burkardt et al. [75–79], Dalley et al. [115,116,439], Elser et al. [139,140,219], Fields et al. [143,348,442,443], Fujita et al. [162–167,349,428], Harada et al. [198–202], Harindranath et al., [182,203–205,364,461–463], Hiller et al. [58,4,220–223,315,440,458], Hollenberg et al. [224,225], Itakura et al. [239–241], Pesando et al. [370,371], Kalloniatis et al. [140,219,258–263,358,383], Klebanov et al. [38,115,121], McCartor et al. [325–331], Nardelli et al. [25,27,28], van de Sande et al. [33,116,223,382,435–439], Sugihara et al. [410–412], Tachibana et al. [423], Thies et al. [296,425], Tsujimaru et al. [231,271,344,441], and others [3,253,278,336,391,408]. Aspects of reaction theory can be studied now. Hiller [220], for example, has calculated the total annihilation cross section $R_{e\bar{e}}$ in 1 + 1 dimensions, with success.

We will use the work of Hornbostel et al. [227] as an example to demonstrate how DLCQ works.

Consider the light-cone gauge, $A^+ = 0$, with the gauge group SU(N). In a representation in which γ^5 is diagonal one introduces the chiral components of the fermion spinors:

$$\psi_\alpha = \begin{pmatrix} \psi_L \\ \psi_R \end{pmatrix}, \quad (4.6)$$

The usual group generators for $SU(N)$ are the $T^a = \frac{1}{2}\lambda^a$. In a box with length $2L$ one finds

$$\psi_L(x) = -\frac{im}{4} \int_{-L}^{+L} dy^- \varepsilon(x^- - y^-) \psi_R(x^+, y^-), \quad (4.7)$$

$$A^{-a}(x) = -\frac{g}{2} \int_{-L}^{+L} dy^- |x^- - y^-| \psi_R^\dagger T^a \psi_R(x^+, y^-). \quad (4.8)$$

The light-cone momentum and light-cone energy operators are

$$P^+ = \int_{-L}^{+L} dx^- \psi_R^\dagger \hat{\partial}_- \psi_R, \quad (4.9)$$

$$P^- = -\frac{im^2}{4} \int_{-L}^{+L} dx^- \int_{-L}^{+L} dy^- \psi_R^\dagger(x^-) \varepsilon(x^- - y^-) \psi_R(y^-) \\ - \frac{g^2}{2} \int_{-L}^{+L} dx^- \int_{-L}^{+L} dy^- \psi_R^\dagger T^a \psi_R(x^-) |x^- - y^-| \psi_R^\dagger T^a \psi_R(y^-), \quad (4.10)$$

respectively. Here, ψ is subject to the canonical anti-commutation relations. For example, for anti-periodic boundary conditions one can expand

$$\psi_R(x^-)_c = \frac{1}{\sqrt{2L}} \sum_{n=\frac{1}{2}, \frac{3}{2}, \dots}^{\infty} (b_{n,c} e^{-i n \pi x^- / L} + d_{n,c}^\dagger e^{i n \pi x^- / L}), \quad (4.11)$$

where

$$\{b_{n,c_1}^\dagger, b_{m,c_2}\} = \{d_{n,c_1}^\dagger, d_{m,c_2}\} = \delta_{c_1, c_2} \delta_{n,m}, \quad (4.12)$$

with all other anticommutators vanishing. Inserting this expansion into the expressions for P^+ , Eq. (4.9), one thus finds

$$P^+ = \left(\frac{2\pi}{L}\right) \sum_{n=\frac{1}{2}, \frac{3}{2}, \dots}^{\infty} n (b_{n,c}^\dagger b_{n,c} + d_{n,c}^\dagger d_{n,c}). \quad (4.13)$$

Similarly, one finds for P^- of Eq. (4.10)

$$P^- = \left(\frac{L}{2\pi}\right) (H_0 + V), \quad (4.14)$$

where

$$H_0 = \sum_{n=\frac{1}{2}, \frac{3}{2}, \dots}^{\infty} \frac{m^2}{n} (b_{n,c}^\dagger b_{n,c} + d_{n,c}^\dagger d_{n,c}) \quad (4.15)$$

is the free kinetic term, and the interaction term V is given by

$$V = \frac{g^2}{\pi} \sum_{k=-\infty}^{\infty} j^a(k) \frac{1}{k^2} j^a(-k), \quad (4.16)$$

where

$$j^a(k) = T_{c_1, c_2}^a \sum_{n=-\infty}^{\infty} (\Theta(n)b_{n, c_1}^\dagger + \Theta(-n)d_{n, c_1})(\Theta(n-k)b_{n-k, c_2} + \Theta(k-n)d_{k-n, c_2}^\dagger). \quad (4.17)$$

Since we will restrict ourselves to the color singlet sector, there is no problem from $k = 0$ in Eq. (4.16), since $j^a(0) = 0$ acting on color singlet states. Normal ordering the interaction (4.16) gives a diagonal operator piece

$$V = :V: + \frac{g^2 C_F}{\pi} \sum_{n=\frac{1}{2}, \frac{3}{2}, \dots}^{\infty} \frac{I_n}{n} (b_{n, c}^\dagger b_{n, c} + d_{n, c}^\dagger d_{n, c}), \quad (4.18)$$

with the “self-induced inertia”

$$I_n = -\frac{1}{2n} + \sum_{m=1}^{n+1/2} \frac{1}{m^2}. \quad (4.19)$$

The color factor is $C_F = (N^2 - 1)/2N$. The explicit form of the normal ordered piece $:V:$ can be found in Ref. [227] or in the explicit tables below in this section. It is very important to keep the self-induced inertias from the normal ordering, because they are needed to cancel the infrared singularity in the interaction term in the continuum limit. Already classically, the self energy of one single quark is infrared divergent because its color electric field extends to infinity. The same infrared singularity (with opposite sign) appears in the interaction term. They cancel for color singlet states, because there the color electric field is nonzero only inside the hadron. Since the hadron has a finite size, the resulting total color electric field energy must be infrared finite.

The next step is to actually solve the equations of motions in the discretized space. Typically one proceeds as follows: Since P^+ and P^- commute they can be diagonalized simultaneously. Actually, in the momentum representation, P^+ is already diagonal, with eigenvalues proportional to $2\pi/L$. Therefore, the *harmonic resolution* K [137],

$$K = (L/2\pi)P^+, \quad (4.20)$$

determines the size of the Fock space and thus the dimension of the Hamiltonian matrix, which simplifies the calculations considerably. For a given $K = 1, 2, 3, \dots$, there are only a finite number of Fock states due to the positivity condition on the light-cone momenta. One selects now one value for K and constructs all color singlet states. In the next step one can either diagonalize H in the full space of states with momentum K (DLCQ approximation) or in a subspace of that space (for example with a Tamm–Dancoff approximation). The eigenvalue $E_i(K)$ corresponds to invariant masses

$$M_i^2(K) \equiv 2P_i^+ P_i^- = KE_i(K), \quad (4.21)$$

where we indicated the parametric dependence of the eigenvalues on K .

Notice that the length L drops out in the invariant mass, and that one gets a spectrum for *any value of* K . Most recent developments in string theory, the so-called ‘M(atrix)-theory’ [416], emphasizes this aspect, but for the present one should consider the solutions to be physical only in the continuum limit $K \rightarrow \infty$.

Of course there are limitations on the size of matrices that one can diagonalize (although the Lanczos algorithm allows quite impressive sizes [220]). Therefore what one typically does is to

repeat the calculations for increasing values of K and to extrapolate observables to $K \rightarrow \infty$. The first QCD₂ calculations in that direction were performed in Refs. [227,75]. In these pioneering works it was shown that the numerics actually converged rather quickly (except for very small quark masses, where ground state mesons and ground state baryons become massless) since the lowest Fock component dominates these hadrons (typically less than 1% of the momentum is carried by the sea component). The suppression of the higher particle Fock states is presumably special to super-renormalizable theories where the couplings which change particle number are suppressed as g^2/\mathcal{M}^2 . Due to these fortunate circumstances a variety of phenomena could be investigated. For example, Hornbostel studied hadron masses and structure functions for various N which showed very simple scaling behavior with N . A correspondence with the analytic work of Einhorn [136] for meson form factors in QCD₁₊₁ was also established. Ref. [75] focused more on nuclear phenomena. There it was shown that two nucleons in QCD₁₊₁ with two colors and two flavors form a loosely bound state – the “deuteron”. Since the calculation was based entirely on quark degrees of freedom it was possible to study binding effects on the nuclear structure function (“EMC-effect”). Other applications include a study of “Pauli-blocking” in QCD₁₊₁. Since quarks are fermions, one would expect that sea quarks which have the same flavor as the majority of the valence quarks (the up quarks in a proton) are suppressed compared to those which have the minority flavor (the down quarks in a proton) – at least if isospin breaking effects are small. However, an explicit calculation shows that the opposite is true in QCD₂! This so called “anti Pauli-blocking” has been investigated in Refs. [76,77], where one can also find an intuitive explanation.

4.3. The Hamiltonian operator in 3 + 1 dimensions (BL)

Periodic boundary conditions on \mathcal{L} can be realized by periodic boundary conditions on the vector potentials A_μ and anti-periodic boundary conditions on the spinor fields, since \mathcal{L} is bilinear in the Ψ_α . In momentum representation one expands these fields into plane wave states $e^{-ip_\mu x^\mu}$, and satisfies the boundary conditions by *discretized momenta*

$$p_- = \begin{cases} \frac{\pi}{L}n & \text{with } n = \frac{1}{2}, \frac{3}{2}, \dots, \infty \quad \text{for fermions,} \\ \frac{\pi}{L}n & \text{with } n = 1, 2, \dots, \infty \quad \text{for bosons,} \end{cases} \quad (4.22)$$

$$\mathbf{p}_\perp = \frac{\pi}{L_\perp} \mathbf{n}_\perp \quad \text{with } n_x, n_y = 0, \pm 1, \pm 2, \dots, \pm \infty \quad \text{for both.}$$

As an expense, one has to introduce two artificial length parameters, L and L_\perp . They also define the normalization volume $\Omega \equiv 2L(2L_\perp)^2$.

More explicitly, the free fields are expanded as

$$\tilde{\Psi}_\alpha(x) = \frac{1}{\sqrt{\Omega}} \sum_q \frac{1}{\sqrt{p^+}} (b_q u_\alpha(p, \lambda) e^{-ipx} + d_q^\dagger v_\alpha(p, \lambda) e^{ipx}),$$

$$\tilde{A}_\mu(x) = \frac{1}{\sqrt{\Omega}} \sum_q \frac{1}{\sqrt{p^+}} (a_q \varepsilon_\mu(p, \lambda) e^{-ipx} + a_q^\dagger \varepsilon_\mu^*(p, \lambda) e^{ipx}),$$
(4.23)

particularly for the two transverse vector potentials $\tilde{A}^i \equiv \tilde{A}_\perp^i$ ($i = 1, 2$). The light-cone gauge and the light-cone Gauss equation, i.e. $A^+ = 0$ and $A^- = (2g/(i\partial^+)^2), J^+ - (2/(i\partial^+))i\partial_j A_\perp^j$, respectively, complete the specification of the vector potentials A^μ . The subtlety of the missing *zero-mode* $n = 0$ in the expansion of the \tilde{A}_\perp will be discussed below. Each denumerable single-particle state “ q ” is specified by at least six quantum numbers, i.e.

$$q = \{q \mid k^+, k_{\perp x}, k_{\perp y}, \lambda, c, f\} = \{q \mid n, n_x, n_y, \lambda, c, f\}. \tag{4.24}$$

The quantum numbers denote the three discrete momenta n, n_x, n_y , the two helicities $\lambda = (\uparrow, \downarrow)$, the color index $c = 1, 2, \dots, N_C$, and the flavor index $f = 1, 2, \dots, N_F$. For a gluon state, the color index is replaced by the glue index $a = 1, 2, \dots, N_C^2 - 1$ and the flavor index is absent. Correspondingly, for QED the color- and flavor index are absent. The creation and destruction operators like a_q^\dagger and a_q create and destroy single-particle states q , and obey (anti-) commutation relations like

$$[a_q, a_{q'}^\dagger] = \{b_q, b_{q'}^\dagger\} = \{d_q, d_{q'}^\dagger\} = \delta_{q, q'}. \tag{4.25}$$

The Kronecker symbol is unity only if all six quantum numbers coincide. The spinors u_z and v_z , and the transverse polarization vectors ε_\perp are the usual ones, and can be found in Ref. [66] and in the appendix.

Finally, after inserting all fields in terms of the expansions in Eq. (4.23), one performs the space-like integrations and ends up with the light-cone energy–momenta $P^\nu = P^\nu(a_q, a_q^\dagger, b_q, b_q^\dagger, d_q, d_q^\dagger)$ as operators acting in Fock space. The space-like components of P^ν are simple and diagonal, and its time–time-like component is complicated and off-diagonal. Its Lorentz-invariant contraction

$$H_{\text{LC}} \equiv P^\nu P_\nu = P^+ P^- - \mathbf{P}_\perp^2 \tag{4.26}$$

is then also off-diagonal. For simplicity, it is referred to as the *light-cone Hamiltonian* H_{LC} , and often abbreviated as $H = H_{\text{LC}}$. It carries the dimension of an invariant mass squared. In a frame in which $P_\perp = 0$, it reduces to $H = P^+ P^-$. It is useful to give its general structure in terms of Fock-space operators.

4.3.1. A typical term of the Hamiltonian: Pure gauge theory

As an example consider a typical term in the Hamiltonian, the pure gauge contribution W_1 as defined in Eq. (2.96), i.e.

$$P_{pg}^- = \frac{g^2}{4} \int dx^- d^2 x_\perp \tilde{B}_{\mu\nu}^a \tilde{B}_a^{\mu\nu}.$$

Inserting the free field solutions \tilde{A}_a^μ from Eq. (4.23), one deals with $2^4 = 16$ terms. The various terms can be classified according to their operator structure and belong to one of the six classes.

$$\begin{aligned} a_{q1} a_{q2} a_{q3} a_{q4}, & \quad a_{q4}^\dagger a_{q3}^\dagger a_{q2}^\dagger a_{q1}^\dagger, \\ a_{q1}^\dagger a_{q2} a_{q3} a_{q4}, & \quad a_{q4}^\dagger a_{q3}^\dagger a_{q2}^\dagger a_{q1}, \\ a_{q1}^\dagger a_{q2}^\dagger a_{q3} a_{q4}, & \quad a_{q4}^\dagger a_{q3}^\dagger a_{q2} a_{q1}. \end{aligned}$$

In the first step, we pick out only those terms with one creation and three destruction operators. Integration over the space-like coordinates produces a product of three Kronecker delta functions

$\delta(k_1^+|k_2^+ + k_3^+ + k_4^+)\delta^{(2)}(\mathbf{k}_{\perp 1}|\mathbf{k}_{\perp 2} + \mathbf{k}_{\perp 3} + \mathbf{k}_{\perp 4})$, as opposed to the Dirac delta functions in Section 2.8. The Kronecker delta functions are conveniently defined by

$$\delta(k^+|p^+) = \frac{1}{2L} \int_{-L}^{+L} dx^- e^{+i(k^- - p^-)x^-} = \frac{1}{2L} \int_{-L}^{+L} dx^- e^{+i(n-m)\pi x^-/L} = \delta_{n,m}, \quad (4.27)$$

and similarly for the transverse delta functions. One gets then very explicitly (Tables 1–6)

$$\begin{aligned} P^+ P_{pgf}^- &= \frac{g^2 P^+}{8L(2L_{\perp})^2} \sum_{q_1, q_2} \sum_{q_3, q_4} \frac{1}{\sqrt{k_1^+ k_2^+ k_3^+ k_4^+}} C_{a_1 a_2}^a C_{a_3 a_4}^a \\ &\times (a_{q_1}^\dagger a_{q_2} a_{q_3} a_{q_4} (\varepsilon_1^* \varepsilon_3) (\varepsilon_2 \varepsilon_4) \delta(k_1^+|k_2^+ + k_3^+ + k_4^+) \delta^{(2)}(\mathbf{k}_{\perp 1}|\mathbf{k}_{\perp 2} + \mathbf{k}_{\perp 3} + \mathbf{k}_{\perp 4}) \\ &+ a_{q_1} a_{q_2}^\dagger a_{q_3} a_{q_4} (\varepsilon_1 \varepsilon_3) (\varepsilon_2^* \varepsilon_4) \delta(k_2^+|k_3^+ + k_4^+ + k_1^+) \delta^{(2)}(\mathbf{k}_{\perp 2}|\mathbf{k}_{\perp 3} + \mathbf{k}_{\perp 4} + \mathbf{k}_{\perp 1}) \\ &+ a_{q_1} a_{q_2} a_{q_3}^\dagger a_{q_4} (\varepsilon_1 \varepsilon_3^*) (\varepsilon_2 \varepsilon_4) \delta(k_3^+|k_4^+ + k_1^+ + k_2^+) \delta^{(2)}(\mathbf{k}_{\perp 3}|\mathbf{k}_{\perp 4} + \mathbf{k}_{\perp 1} + \mathbf{k}_{\perp 2}) \\ &+ a_{q_1} a_{q_2} a_{q_3} a_{q_4}^\dagger (\varepsilon_1 \varepsilon_3) (\varepsilon_2 \varepsilon_4^*) \delta(k_4^+|k_1^+ + k_2^+ + k_3^+) \delta^{(2)}(\mathbf{k}_{\perp 4}|\mathbf{k}_{\perp 1} + \mathbf{k}_{\perp 2} + \mathbf{k}_{\perp 3}). \end{aligned}$$

For convenience, introduce the function

$$F_{6,2}(q_1; q_2, q_3, q_4) = \frac{2\Delta}{\sqrt{k_1^+ k_2^+ k_3^+ k_4^+}} (\varepsilon_\mu^*(k_1, \lambda_1) \varepsilon^\mu(k_3, \lambda_3)) (\varepsilon_\nu(k_2, \lambda_2) \varepsilon^\nu(k_4, \lambda_4)) C_{a_1 a_2}^a C_{a_3 a_4}^a, \quad (4.28)$$

with the overall factor Δ containing the Kronecker deltas

$$\Delta(q_1; q_2, q_3, q_4) = \tilde{g}^2 \delta(k_1^+|k_2^+ + k_3^+ + k_4^+) \delta^{(2)}(\mathbf{k}_{\perp 1}|\mathbf{k}_{\perp 2} + \mathbf{k}_{\perp 3} + \mathbf{k}_{\perp 4}) \quad (4.29)$$

Table 1

The vertex interaction in terms of Dirac spinors. The matrix elements V_n are displayed on the right, the corresponding (energy) graphs on the left. All matrix elements are proportional to $\Delta_V = \hat{g} \delta(k_1^+|k_2^+ + k_3^+) \delta^{(2)}(\mathbf{k}_{\perp 1}|\mathbf{k}_{\perp 2} + \mathbf{k}_{\perp 3})$, with $\hat{g} = gP^+/\sqrt{\Omega}$. In the continuum limit, see Section 4.6, $\hat{g} = gP^+/\sqrt{2(2\pi)^3}$

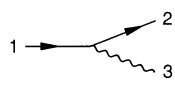
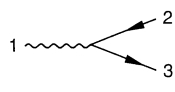
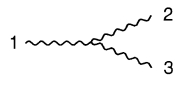
	$V_1 = \frac{\Delta_V}{\sqrt{k_1^+ k_2^+ k_3^+}} (\bar{u}_1 \not{\epsilon}_3 T^{a_3} u_2)$
	$V_2 = \frac{\Delta_V}{\sqrt{k_1^+ k_2^+ k_3^+}} (\bar{v}_2 \not{\epsilon}_1^* T^{a_1} u_3)$
	$\begin{aligned} V_4 &= \frac{iC_{a_2 a_3}^{a_1} \Delta_V}{\sqrt{k_1^+ k_2^+ k_3^+}} (\epsilon_1^* k_3) (\epsilon_2 \epsilon_3) \\ &+ \frac{iC_{a_2 a_3}^{a_1} \Delta_V}{\sqrt{k_1^+ k_2^+ k_3^+}} (\epsilon_3 k_1) (\epsilon_1^* \epsilon_2) \\ &+ \frac{iC_{a_2 a_3}^{a_1} \Delta_V}{\sqrt{k_1^+ k_2^+ k_3^+}} (\epsilon_3 k_2) (\epsilon_1^* \epsilon_2) \end{aligned}$

Table 2

The fork interaction in terms of Dirac spinors. The matrix elements $F_{n,j}$ are displayed on the right, the corresponding (energy) graphs on the left. All matrix elements are proportional to $\Delta = \tilde{g}^2 \delta(k_1^+ |k_2^+ + k_3^+ + k_4^+) \delta^{(2)}(\mathbf{k}_{\perp,1} | \mathbf{k}_{\perp,2} + \mathbf{k}_{\perp,3} + \mathbf{k}_{\perp,4})$, with $\tilde{g}^2 = g^2 P^+ / (2\Omega)$. In the continuum limit, see Section 4.6, one uses $\tilde{g}^2 = g^2 P^+ / (4(2\pi)^3)$

	$F_1 = + \frac{2\Delta}{\sqrt{k_1^+ k_2^+ k_3^+ k_4^+}} \frac{(\bar{u}_1 T^a \gamma^+ u_2) (\bar{v}_3 \gamma^+ T^a u_4)}{(k_1^+ - k_2^+)^2}$
	$F_{3,1} = + \frac{\Delta}{\sqrt{k_1^+ k_2^+ k_3^+ k_4^+}} \frac{(\bar{u}_1 T^{a4} \not{e}_4 \gamma^+ \not{e}_3 T^{a2} u_2)}{(k_1^+ - k_4^+)^2}$
	$F_{3,2} = - \frac{2k_3^+ \Delta}{\sqrt{k_1^+ k_2^+ k_3^+ k_4^+}} \frac{(\bar{u}_1 T^a \gamma^+ u_2) (\epsilon_3 i C^a \epsilon_4)}{(k_1^+ - k_2^+)^2}$
	$F_{5,1} = + \frac{\Delta}{\sqrt{k_1^+ k_2^+ k_3^+ k_4^+}} \frac{(\bar{v}_3 T^{a1} \not{e}_1^* \gamma^+ \not{e}_2 T^{a2} u_4)}{(k_1^+ - k_3^+)^2}$
	$F_{5,2} = - \frac{\Delta}{\sqrt{k_1^+ k_2^+ k_3^+ k_4^+}} \frac{(\bar{v}_3 T^{a2} \not{e}_2 \gamma^+ \not{e}_1^* T^{a1} u_4)}{(k_1^+ - k_4^+)^2}$
	$F_{5,3} = + \frac{2(k_1^+ + k_2^+) \Delta}{\sqrt{k_1^+ k_2^+ k_3^+ k_4^+}} \frac{(\bar{v}_3 T^a \gamma^+ u_4) (\epsilon_1^* i C^a \epsilon_2)}{(k_1^+ - k_2^+)^2}$
	$F_{6,1} = + \frac{2k_3^+ (k_1^+ + k_2^+) \Delta}{\sqrt{k_1^+ k_2^+ k_3^+ k_4^+}} \frac{(\epsilon_1^* C^a \epsilon_2) (\epsilon_3 C^a \epsilon_4)}{(k_1^+ - k_2^+)^2}$
	$F_{6,2} = + \frac{2\Delta}{\sqrt{k_1^+ k_2^+ k_3^+ k_4^+}} (\epsilon_1^* \epsilon_3) (\epsilon_2 \epsilon_4) C_{a_1 a_2}^a C_{a_3 a_4}^a$

Table 3

The coefficient functions $c_{n,j}$ in terms of matrix elements of the seagull interaction are displayed on the right, the corresponding (energy) graphs on the left

	$C_{1,1}(q_1) = \sum_2 (S_{1,1}(1, 2; 2, 1) + S_{3,2}(1, 2; 1, 2))$
	$C_{1,2}(q_1) = \sum_2 (S_{4,1}(1, 2; 1, 2) + S_{4,2}(1, 2; 1, 2)) \left(+ \frac{1}{2} \right)$
	$C_{3,1}(q_1) = \sum_2 (S_{4,1}(1, 2; 1, 2) + S_{4,2}(1, 2; 1, 2)) \left(- \frac{1}{2} \right)$
	$C_{3,2}(q_1) = \sum_2 (S_{7,1}(1, 2; 2, 1) + S_{7,2}(1, 2; 2, 1))$
	$C_{3,3}(q_1) = \sum_2 (S_{7,3}(1, 2; 1, 2) + S_{7,3}(1, 2; 2, 1) + S_{7,4}(1, 2; 1, 2) + S_{7,5}(1, 2; 2, 1))$

Table 4

The seagull interaction in terms of Dirac spinors. The matrix elements $S_{n,j}$ are displayed on the right, the corresponding (energy) graphs on the left. All matrix elements are proportional to $\Delta = \tilde{g}^2 \delta(k_1^+ + k_2^+ | k_3^+ + k_4^+) \delta^{(2)}(\mathbf{k}_{\perp,1} + \mathbf{k}_{\perp,2} | \mathbf{k}_{\perp,3} + \mathbf{k}_{\perp,4})$, with $\tilde{g}^2 = g^2 P^+ / (2\Omega)$. In the continuum limit one, see Section 4.6, uses $\tilde{g}^2 = g^2 P^+ / (4(2\pi)^3)$

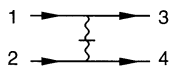
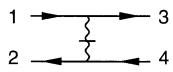
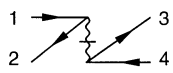
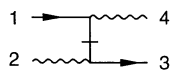
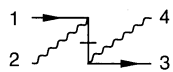
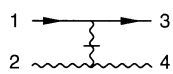
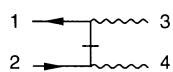

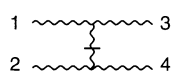
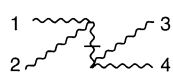



	$S_1 = - \frac{\Delta}{\sqrt{k_1^+ k_2^+ k_3^+ k_4^+}} \frac{(\bar{u}_1 T^a \gamma^+ u_3) (\bar{u}_2 \gamma^+ T^a u_4)}{(k_1^+ - k_3^+)^2}$
	$S_{3,1} = + \frac{2\Delta}{\sqrt{k_1^+ k_2^+ k_3^+ k_4^+}} \frac{(\bar{u}_1 T^a \gamma^+ u_3) (\bar{v}_2 \gamma^+ T^a v_4)}{(k_1^+ - k_3^+)^2}$
	$S_{3,2} = - \frac{2\Delta}{\sqrt{k_1^+ k_2^+ k_3^+ k_4^+}} \frac{(\bar{v}_2 T^a \gamma^+ u_1) (\bar{v}_4 \gamma^+ T^a u_3)}{(k_1^+ + k_2^+)^2}$
	$S_{4,1} = + \frac{\Delta}{\sqrt{k_1^+ k_2^+ k_3^+ k_4^+}} \frac{(\bar{u}_1 T^{a4} \not{e}_4 \gamma^+ \not{e}_2^* T^{a2} u_3)}{(k_1^+ - k_4^+)}$
	$S_{4,2} = + \frac{\Delta}{\sqrt{k_1^+ k_2^+ k_3^+ k_4^+}} \frac{(\bar{u}_1 T^{a2} \not{e}_2^* \gamma^+ \not{e}_4 T^{a4} u_3)}{(k_1^+ + k_2^+)}$
	$S_{4,3} = + \frac{2(k_2^+ + k_4^+) \Delta}{\sqrt{k_1^+ k_2^+ k_3^+ k_4^+}} \frac{(\bar{u}_1 T^a \gamma^+ u_3) (\epsilon_2^* i C^a \epsilon_4)}{(k_1^+ - k_3^+)^2}$
	$S_{6,1} = + \frac{\Delta}{\sqrt{k_1^+ k_2^+ k_3^+ k_4^+}} \frac{(\bar{u}_1 T^{a3} \not{e}_3 \gamma^+ \not{e}_4 T^{a4} v_2)}{(k_1^+ - k_3^+)}$
	$S_{6,2} = - \frac{(k_3^+ - k_4^+) \Delta}{\sqrt{k_1^+ k_2^+ k_3^+ k_4^+}} \frac{(\bar{u}_1 T^a \gamma^+ v_2) (\epsilon_3 i C^a \epsilon_4)}{(k_1^+ + k_2^+)^2}$
	$S_{7,1} = - \frac{(k_1^+ + k_3^+) (k_2^+ + k_4^+) \Delta}{\sqrt{k_1^+ k_2^+ k_3^+ k_4^+}} \frac{(\epsilon_1^* C^a \epsilon_3) (\epsilon_2^* C^a \epsilon_4)}{(k_1^+ - k_3^+)^2}$
	$S_{7,2} = + \frac{2k_3^+ k_4^+ \Delta}{\sqrt{k_1^+ k_2^+ k_3^+ k_4^+}} \frac{(\epsilon_1^* C^a \epsilon_2^*) (\epsilon_3 C^a \epsilon_4)}{(k_1^+ + k_2^+)^2}$
	$S_{7,3} = + \frac{\Delta}{\sqrt{k_1^+ k_2^+ k_3^+ k_4^+}} (\epsilon_1^* \epsilon_3) (\epsilon_2^* \epsilon_4) C_{a_1 a_2}^a C_{a_3 a_4}^a$
	$S_{7,4} = + \frac{\Delta}{\sqrt{k_1^+ k_2^+ k_3^+ k_4^+}} (\epsilon_1^* \epsilon_3) (\epsilon_2^* \epsilon_4) C_{a_1 a_4}^a C_{a_3 a_2}^a$
	$S_{7,5} = + \frac{\Delta}{\sqrt{k_1^+ k_2^+ k_3^+ k_4^+}} (\epsilon_1^* \epsilon_2^*) (\epsilon_3 \epsilon_4) C_{a_1 a_3}^a C_{a_2 a_4}^a$

Table 5
Matrix elements of Dirac spinors $\bar{u}(p)\mathcal{M}u(q)$

\mathcal{M}	$\frac{1}{\sqrt{p^+q^+}}(\bar{u}(p)\mathcal{M}u(q))\delta_{\lambda_p\lambda_q}$	$\frac{1}{\sqrt{p^+q^+}}(\bar{u}(p)\mathcal{M}u(q))\delta_{\lambda_p-\lambda_q}$
γ^+	2	0
γ^-	$\frac{2}{p^+q^+}(\mathbf{p}_\perp \cdot \mathbf{q}_\perp - m^2 + i\lambda_q \mathbf{p}_\perp \wedge \mathbf{q}_\perp)$	$\frac{2m}{p^+q^+}(p_\perp(\lambda_q) - q_\perp(\lambda_q))$
$\boldsymbol{\gamma}_\perp \cdot \mathbf{a}_\perp$	$\mathbf{a}_\perp \cdot \left(\frac{\mathbf{p}_\perp}{p^+} + \frac{\mathbf{q}_\perp}{q^+}\right) - i\lambda_q \mathbf{a}_\perp \wedge \left(\frac{\mathbf{p}_\perp}{p^+} - \frac{\mathbf{q}_\perp}{q^+}\right)$	$-a_\perp(\lambda_q)\left(\frac{m}{p^+} - \frac{m}{q^+}\right)$
1	$\frac{m}{p^+} + \frac{m}{q^+}$	$\frac{p_\perp(\lambda_q)}{q^+} - \frac{q_\perp(\lambda_q)}{p^+}$
$\gamma^-\gamma^+\gamma^-$	$\frac{8}{p^+q^+}(\mathbf{p}_\perp \cdot \mathbf{q}_\perp + m^2 + i\lambda_q \mathbf{p}_\perp \wedge \mathbf{q}_\perp)$	$\frac{8m}{p^+q^+}(p_\perp(\lambda_q) - q_\perp(\lambda_q))$
$\gamma^-\gamma^+\boldsymbol{\gamma}_\perp \cdot \mathbf{a}_\perp$	$\frac{4}{p^+}(\mathbf{a}_\perp \cdot \mathbf{p}_\perp - i\lambda_q \mathbf{a}_\perp \wedge \mathbf{p}_\perp)$	$-\frac{4m}{p^+}a_\perp(\lambda_q)$
$\mathbf{a}_\perp \cdot \boldsymbol{\gamma}_\perp \gamma^+\gamma^-$	$\frac{4}{q^+}(\mathbf{a}_\perp \cdot \mathbf{q}_\perp + i\lambda_q \mathbf{a}_\perp \wedge \mathbf{q}_\perp)$	$\frac{4m}{q^+}a_\perp(\lambda_q)$
$\mathbf{a}_\perp \cdot \boldsymbol{\gamma}_\perp \gamma^+\boldsymbol{\gamma}_\perp \cdot \mathbf{b}_\perp$	$2(\mathbf{a}_\perp \cdot \mathbf{b}_\perp + i\lambda_q \mathbf{a}_\perp \wedge \mathbf{b}_\perp)$	0
Notation	$\lambda = \pm 1, a_\perp(\lambda) = -\lambda a_x - ia_y$	
	$\mathbf{a}_\perp \cdot \mathbf{b}_\perp = a_x b_x + a_y b_y, \mathbf{a}_\perp \wedge \mathbf{b}_\perp = a_x b_y - a_y b_x.$	
Symmetries	$\bar{v}(p)v(q) = -\bar{u}(q)u(p), \bar{v}(p)\gamma^\mu v(q) = \bar{u}(q)\gamma^\mu u(p),$	
	$\bar{v}(p)\gamma^\mu \gamma^\nu \gamma^\rho v(q) = \bar{u}(q)\gamma^\rho \gamma^\nu \gamma^\mu u(p).$	

and the “tilded coupling constant”

$$\tilde{g}^2 = g^2 P^+ / 2\Omega, \tag{4.30}$$

as abbreviations. Recall the normalization volume $\Omega = 2L(2L_\perp)^2$. One can relabel the summation indices in the above equation and get identically

$$P^+ P_{pgf}^- = \frac{1}{4} \sum_{q_1, q_2} \sum_{q_3, q_4} F_{6,2}(q_1; q_2, q_3, q_4) (a_{q_1}^\dagger a_{q_2} a_{q_3} a_{q_4} + a_{q_2} a_{q_1}^\dagger a_{q_4} a_{q_3} + a_{q_3} a_{q_4} a_{q_1}^\dagger a_{q_2} + a_{q_4} a_{q_3} a_{q_2} a_{q_1}^\dagger).$$

We can consider these expressions as the “time-ordered products” in the sense of Wick’s theorem and bring them into normal-ordered form. In the present case all pairwise contractions are either zero identically or vanish by the properties of $F_{6,2}$. The normal ordered contribution to the Hamiltonian becomes then

$$P^+ P_{pgf}^- = \sum_{q_1, q_2, q_3, q_4} F_{6,2}(q_1; q_2, q_3, q_4) a_{q_1}^\dagger a_{q_2} a_{q_3} a_{q_4} \equiv \sum_{1, 2, 3, 4} F_{6,2}(1; 2, 3, 4) a_1^\dagger a_2 a_3 a_4. \tag{4.31}$$

Table 6
Matrix elements of Dirac spinors $\bar{v}(p)\mathcal{M}u(q)$

\mathcal{M}	$\frac{1}{\sqrt{p^+q^+}}(\bar{v}(p)\mathcal{M}u(q))\delta_{\lambda_p\lambda_q}$	$\frac{1}{\sqrt{p^+q^+}}(\bar{v}(p)\mathcal{M}u(q))\delta_{\lambda_p,-\lambda_q}$
γ^+	0	2
γ^-	$\frac{2m}{p^+q^+}(p_\perp(\lambda_q) + q_\perp(\lambda_q))$	$\frac{2}{p^+q^+}(\mathbf{p}_\perp \cdot \mathbf{q}_\perp - m^2 + i\lambda_q \mathbf{p}_\perp \wedge \mathbf{q}_\perp)$
$\boldsymbol{\gamma}_\perp \cdot \mathbf{a}_\perp$	$a_\perp(\lambda_q)\left(\frac{m}{p^+} + \frac{m}{q^+}\right)$	$\mathbf{a}_\perp \cdot \left(\frac{\mathbf{p}_\perp}{p^+} + \frac{\mathbf{q}_\perp}{q^+}\right) - i\lambda_q \mathbf{a}_\perp \wedge \left(\frac{\mathbf{p}_\perp}{p^+} - \frac{\mathbf{q}_\perp}{q^+}\right)$
1	$\frac{p_\perp(\lambda_q)}{p^+} + \frac{q_\perp(\lambda_q)}{q^+}$	$-\frac{m}{p^+} + \frac{m}{q^+}$
$\gamma^-\gamma^+\gamma^-$	$\frac{8m}{p^+q^+}(p_\perp(\lambda_q) + q_\perp(\lambda_q))$	$\frac{8}{p^+q^+}(\mathbf{p}_\perp \cdot \mathbf{q}_\perp - m^2 + i\lambda_q \mathbf{p}_\perp \wedge \mathbf{q}_\perp)$
$\gamma^-\gamma^+\boldsymbol{\gamma}_\perp \cdot \mathbf{a}_\perp$	$\frac{4m}{p^+}a_\perp(\lambda_q)$	$\frac{4}{p^+}(\mathbf{a}_\perp \cdot \mathbf{p}_\perp - i\lambda_q \mathbf{a}_\perp \wedge \mathbf{p}_\perp)$
$\mathbf{a}_\perp \cdot \boldsymbol{\gamma}_\perp \gamma^+\gamma^-$	$\frac{4m}{q^+}a_\perp(\lambda_q)$	$\frac{4}{q^+}(\mathbf{a}_\perp \cdot \mathbf{q}_\perp + i\lambda_q \mathbf{a}_\perp \wedge \mathbf{q}_\perp)$
$\mathbf{a}_\perp \cdot \boldsymbol{\gamma}_\perp \gamma^+\boldsymbol{\gamma}_\perp \cdot \mathbf{b}_\perp$	0	$2(\mathbf{a}_\perp \cdot \mathbf{b}_\perp + i\lambda_q \mathbf{a}_\perp \wedge \mathbf{b}_\perp)$

Notation $\lambda = \pm 1, a_\perp(\lambda) = -\lambda a_x - ia_y$
 $\mathbf{a}_\perp \cdot \mathbf{b}_\perp = a_x b_x + a_y b_y, \mathbf{a}_\perp \wedge \mathbf{b}_\perp = a_x b_y - a_y b_x.$

Symmetries $\bar{v}(p)v(q) = -\bar{u}(q)u(p), \bar{v}(p)\gamma^\mu v(q) = \bar{u}(q)\gamma^\mu u(p),$
 $\bar{v}(p)\gamma^\mu\gamma^\nu\gamma^\rho v(q) = \bar{u}(q)\gamma^\rho\gamma^\nu\gamma^\mu u(p).$

In the second step a self-explaining “compact notation” was introduced which will be used quite often in the sequel. Below, one refers to these contributions as the “fork part”, since their energy diagrams in Table 2 look like the analogous silverware.

Next, consider terms with two creation and two destruction operators. There are six of them,

$$\begin{aligned}
2P^+P_{pgs}^- &= \sum_{1,2,3,4} (a_1^\dagger a_2^\dagger a_3 a_4 S_{7,3}(1, 2; 3, 4) + a_4 a_3 a_2^\dagger a_1^\dagger S_{7,3}(3, 4; 1, 2)) \\
&+ \sum_{1,2,3,4} (a_1^\dagger a_3 a_2^\dagger a_4 S_{7,4}(1, 2; 3, 4) + a_2^\dagger a_4 a_1^\dagger a_3 S_{7,4}(2, 1; 4, 3)) \\
&+ \sum_{1,2,3,4} (a_1^\dagger a_3 a_4 a_2^\dagger S_{7,5}(1, 2; 3, 4) + a_2^\dagger a_4 a_3 a_1^\dagger S_{7,5}(2, 1; 4, 3)), \tag{4.32}
\end{aligned}$$

using compact notation. The functions $S_{7,3}$, $S_{7,4}$ and $S_{7,5}$ can be found in Table 4. According to Wick's theorem, the normal-ordered part is

$$P^+ P_{pgs}^- = \sum_{1,2,3,4} (S_{7,3}(1, 2; 3, 4) + S_{7,4}(1, 2; 3, 4) + S_{7,5}(1, 2; 3, 4)) a_1^\dagger a_2^\dagger a_3 a_4. \quad (4.33)$$

The normal-ordered part of all possible, non-vanishing pairwise contractions is called the contraction term

$$P^+ P_{pgc}^- = \sum_{1,2} a_1^\dagger a_1 (S_{7,3}(1, 2; 1, 2) + S_{7,3}(1, 2; 2, 1) + S_{7,4}(1, 2; 1, 2) + S_{7,5}(1, 2; 2, 1)). \quad (4.34)$$

As a bone fide operator it should not be dropped from the outset. It gives rise to the self-induced inertias as tabulated in Table 3.

Finally, focus on terms with only creation or only destruction operators. Integration over the space-like coordinates leads to a product of three Kronecker delta's

$$\delta(k_1^+ + k_2^+ + k_3^+ + k_4^+ | 0) \delta^{(2)}(\mathbf{k}_{\perp 1} + \mathbf{k}_{\perp 2} + \mathbf{k}_{\perp 3} + \mathbf{k}_{\perp 4} | \mathbf{0}), \quad (4.35)$$

as a consequence of momentum conservation. With $k^+ = n\pi/(2L)$ and n positive one has thus

$$\delta(n_1 + n_2 + n_3 + n_4 | 0) \equiv 0. \quad (4.36)$$

The sum of positive numbers can never add up to zero, and therefore all parts of the light-cone Hamiltonian with *only creation operators or only destruction operators* are *strictly zero*. This is the deeper reason why the vacuum state cannot couple to any Fock state and why the Fock-space vacuum is identical with the physical vacuum. "The vacuum is trivial." This holds in general, as long as one disregards the impact of the so-called zero modes, see, for example, Refs. [258–262,358] and Section 7.

4.3.2. The explicit Hamiltonian for QCD

Unlike in the instant form, the front-form Hamiltonian is additive in the free part T and the interaction U ,

$$H \equiv H_{LC} = P^+ P^- - \mathbf{P}_\perp^2 = T + U. \quad (4.37)$$

The *kinetic energy* T is defined as that part of H which is independent of the coupling constant. It is the sum of the three diagonal operators

$$T = T_1 + T_2 + T_3 = \sum_q (t_1(q) b_q^\dagger b_q + t_2(q) d_q^\dagger d_q + t_3(q) a_q^\dagger a_q), \quad (4.38)$$

with the coefficient functions

$$t_1(q) = t_2(q) = (m^2 + \mathbf{k}_\perp^2/x)_q, \quad t_3(q) = (\mathbf{k}_\perp^2/x)_q. \quad (4.39)$$

The *interaction energy* U breaks up into 20 different operators, grouped into [66]

$$U = V + F + S + C. \quad (4.40)$$

They will be defined one after another.

The *vertex interaction* V is a sum of four operators,

$$\begin{aligned}
 V = V_1 + V_2 + V_3 + V_4 = & \sum_{1,2,3} [b_1^\dagger b_2 a_3 V_1(1; 2, 3) + \text{h.c.}] \\
 & + \sum_{1,2,3} [d_1^\dagger d_2 a_3 V_2(1; 2, 3) + \text{h.c.}] + \sum_{1,2,3} [a_1^\dagger d_2 b_3 V_3(1; 2, 3) + \text{h.c.}] \\
 & + \sum_{1,2,3} [a_1^\dagger a_2 a_3 V_4(1; 2, 3) + \text{h.c.}]. \tag{4.41}
 \end{aligned}$$

It changes the particle number by 1. The matrix elements $V_n(1;2,3)$ are c -numbers with $V_2(1; 2, 3) = -V_1^\dagger(1; 2, 3)$. They are functions of the various single-particle momenta k^+ , \mathbf{k}_\perp , helicities, colors and flavors, as tabulated in Tables 1 and 9. Again, we use the compact notation $b_i = b(q_i)$ and $V_n(1; 2, 3) = V_n(q_1; q_2, q_3)$, and again we emphasize that the graphs in these tables are *energy graphs* but not *Feynman diagrams*. They symbolize *matrix elements* but not *scattering amplitudes*. They conserve three-momentum but not *four-momentum*. One also should emphasize that the present labeling of matrix elements is different from Ref. [66].

The *fork interaction* F is a sum of six operators,

$$\begin{aligned}
 F = F_1 + F_2 + F_3 + F_4 + F_5 + F_6 = & \sum_{1,2,3,4} [b_1^\dagger b_2 d_3 b_4 F_1(1; 2, 3, 4) + \text{h.c.}] \\
 & + [d_1^\dagger d_2 b_3 d_4 F_2(1; 2, 3, 4) + \text{h.c.}] + \sum_{1,2,3,4} [b_1^\dagger b_2 a_3 a_4 F_3(1; 2, 3, 4) + \text{h.c.}] \\
 & + [d_1^\dagger d_2 a_3 a_4 F_4(1; 2, 3, 4) + \text{h.c.}] + \sum_{1,2,3,4} [a_1^\dagger a_2 d_3 b_4 F_5(1; 2, 3, 4) + \text{h.c.}] \\
 & + [a_1^\dagger a_2 a_3 a_4 F_6(1; 2, 3, 4) + \text{h.c.}]. \tag{4.42}
 \end{aligned}$$

It changes the particle number by 2. The matrix elements $F_n(1; 2, 3, 4)$ and their graphs are tabulated in Tables 2 and 10, with $F_2 = F_1$ and $F_4 = F_3$, and for example $F_5 = F_{5,1} + F_{5,2} + F_{5,3}$.

The *seagull interaction* S is a sum of seven operators,

$$\begin{aligned}
 S = S_1 + S_2 + S_3 + S_4 + S_5 + S_6 + S_7 = & \sum_{1,2,3,4} b_1^\dagger b_2^\dagger b_3 b_4 S_1(1, 2; 3, 4) \\
 & + \sum_{1,2,3,4} d_1^\dagger d_2^\dagger d_3 d_4 S_2(1, 2; 3, 4) + \sum_{1,2,3,4} b_1^\dagger d_2^\dagger b_3 d_4 S_3(1, 2; 3, 4) \\
 & + \sum_{1,2,3,4} b_1^\dagger a_2^\dagger b_3 a_4 S_4(1, 2; 3, 4) + \sum_{1,2,3,4} d_1^\dagger a_2^\dagger d_3 a_4 S_5(1, 2; 3, 4) \\
 & + \sum_{1,2,3,4} (b_1^\dagger d_2^\dagger a_3 a_4 S_6(1, 2; 3, 4) + \text{h.c.}) + \sum_{1,2,3,4} a_1^\dagger a_2^\dagger a_3 a_4 S_7(1, 2; 3, 4). \tag{4.43}
 \end{aligned}$$

It does not change particle number. The matrix elements $S_n(1, 2; 3, 4)$ and their energy graphs are tabulated in Tables 4 and 12, with $S_2 = S_1$ and $S_5 = S_4$.

The contraction operator C is a sum of three terms,

$$C = C_1 + C_2 + C_3 = \sum_q (C_1(q)b_q^\dagger b_q + C_2(q)d_q^\dagger d_q + C_3(q)a_q^\dagger a_q), \tag{4.44}$$

using the symbolic labeling of Eq. (4.24). The coefficient functions C_i are

$$C_1(q) = (I_1(q)/x)_q, \quad C_3(q) = (I_3(q)/x)_q. \tag{4.45}$$

For the same flavours one has $C_2(q) = C_1(q)$. The functions I_i are the so-called *self-induced inertias*, in analogy to the mass terms in Eq. (4.38) [354]. They along with their graphs are tabulated in Tables 3 and 11. The contraction operators arise due to bringing P^- into normal ordered form [354,355]. They are part of the operator structure and should not be omitted. But their structure allows to interpret them as mass terms which often can be absorbed into the mass counter terms. Such one are often introduced when regulating the theory, see below. The contraction terms diverge badly. In the continuum limit, i.e.

$$C_{1 \Leftrightarrow} \sum_{\lambda, c, f} \int dk^+ d^2 \mathbf{k}_\perp \frac{I_1(q)}{x} \tilde{b}^\dagger(q) \tilde{b}(q), \tag{4.46}$$

they diverge like $C_i \sim \Lambda^2$, where Λ is the cut-off scale to be introduced below in Section 4.4.1.

Summarizing these considerations, one can state that the light-cone Hamiltonian $H \equiv H_{LC}$ consists of 23 operators with different operator structure. Some of the pieces are diagonal, some conserve the particle number, and some change it. The piece S_6 is special since it make two gluons out of a quark–antiquark pair. It conserves the charge, but it changes the number of gluons. This was displayed already in Fig. 2 and it is emphasized again in Table 7. The block matrix structure of

Table 7

The Fock-space sectors and the Hamiltonian block matrix structure for QCD. Diagonal blocs are marked by D . Off-diagonal blocks are labeled by V , F and S_6 , corresponding to vertex, fork and seagull interactions, respectively. Zero matrices are denoted by dots. Taken from Ref. [361]; see also Fig. 2

Sector	n	1	2	3	4	5	6	7	8	9	10	11	12	13
$q\bar{q}$	1	D	S_6	V	F	.	F
$g g$	2	S_6	D	V	.	V	F	.	.	F
$q\bar{q} g$	3	V	V	D	V	S_6	V	F	.	.	F	.	.	.
$q\bar{q} q\bar{q}$	4	F	.	V	D	.	S_6	V	F	.	.	F	.	.
$g g g$	5	.	V	S_6	.	D	V	.	.	V	F	.	.	.
$q\bar{q} g g$	6	F	F	V	S_6	V	D	V	.	S_6	V	.	.	.
$q\bar{q} q\bar{q} g$	7	.	.	F	V	.	V	D	V	.	S_6	V	F	.
$q\bar{q} q\bar{q} q\bar{q}$	8	.	.	.	F	.	.	V	D	.	.	S_6	V	F
$g g g g$	9	.	F	.	.	V	S_6	.	.	D	V	.	.	.
$q\bar{q} g g g$	10	.	.	F	.	F	V	S_6	.	V	D	V	.	.
$q\bar{q} q\bar{q} g g$	11	.	.	.	F	.	F	V	S_6	.	V	D	V	.
$q\bar{q} q\bar{q} q\bar{q} g$	12	F	V	.	.	V	D	V
$q\bar{q} q\bar{q} q\bar{q} q\bar{q}$	13	F	.	.	.	V	D

this table and the division of the Fock space into sectors will be discussed more thoroughly in Section 4.4. Some of the operators are diagonal (D) and some of them off-diagonal (R) in the sector number, i.e.

$$D = T + C + S - S_6$$

$$= T_1 + T_2 + T_3 + C_1 + C_2 + C_3 + S_1 + S_2 + S_3 + S_4 + S_5 + S_7, \quad (4.47)$$

$$R = V + F + S_6 = V_1 + V_2 + V_3 + V_4 + F_1 + F_2 + F_3 + F_4 + F_5 + F_6 + S_6. \quad (4.48)$$

Most of the blocks are actually plain zero matrices, since the light-cone Hamiltonian

$$H \equiv H_{\text{LC}} = D + R \quad (4.49)$$

has zero matrix element between the corresponding sectors, see Fig. 2 and Table 7. One should make use of that! In DLCQ one aims at diagonalizing the Hamiltonian

$$H|\Psi_i\rangle = E_i|\Psi_i\rangle, \quad E_i = M_i^2. \quad (4.50)$$

In principle, its eigenvalues and eigenfunctions are equivalent to the compactified gauge-field Lagrangian in the light-cone gauge.

4.4. The Hamiltonian matrix and its regularization

The Hilbert space for the single-particle creation and destruction operators is the *Fock space*, i.e. the complete set of all possible *Fock states*

$$|\Phi_i\rangle = \sqrt{N_i} b_{q_1}^\dagger b_{q_2}^\dagger \dots b_{q_N}^\dagger d_{q_1}^\dagger d_{q_2}^\dagger \dots d_{q_{\bar{N}}} a_{q_1}^\dagger a_{q_2}^\dagger \dots a_{q_{\bar{N}}}^\dagger |0\rangle. \quad (4.51)$$

They are the analogues of the Slater determinants of Section 4.1. As a consequence of discretization, the Fock states are orthonormal and enumerable. Only one Fock state, the reference state or *Fock-space vacuum* $|0\rangle$, is annihilated by all destruction operators.

It is natural to decompose the Fock space into sectors, labeled with the number of quarks, antiquarks and gluons, N , \bar{N} and \tilde{N} , respectively. Mesons (or positronium) have total charge $Q = 0$, and thus $N = \bar{N}$. These sectors can be arranged arbitrarily, and can be enumerated differently. A particular example was given in Fig. 2 and Table 7. A second and not unreasonable choice is given in Fig. 11, where the Fock-space sectors are arranged according to total particle number $N + \bar{N} + \tilde{N}$. The resulting block matrix structure is the one of a penta-diagonal block matrix very much in analogy to the block matrix structure of a non-relativistic many-body Hamiltonian, see Fig. 9.

Since all components of the energy momentum commute with each other, and since the space-like momenta are diagonal in momentum representation, all Fock states must have the *same value* of $P^+ = \sum_v p_v^+$ and $\mathbf{P}_\perp = \sum_v (\mathbf{p}_\perp)_v$, with the sums running over all partons $v \in n$ in a particular Fock-space sector. For any fixed P^+ and thus for any fixed resolution K , the number of Fock-space sectors is finite. As a consequence, the DLCQ-Hamiltonian matrix has a *finite number of blocks*, as illustrated in Fig. 11. For the example chosen, the maximum parton number is 5, corresponding to 11 sectors. In 3 + 1 dimensions, the number of Fock states is unlimited within each sector. After regulating the formalism as to be discussed in Section 4.4.1, the number of Fock states in a sector is strictly finite. The light-cone energy operator $P^-(a_q, a_q^\dagger, b_q, b_q^\dagger, d_q, d_q^\dagger)$ is realized [66] as a strictly finite

n Sector	0 g	1 q \bar{q}	2 gg	3 q \bar{q} g	5 ggg	4 q \bar{q} q \bar{q}	6 q \bar{q} gg	9 gggg	7 q \bar{q} q \bar{q} g	10 q \bar{q} ggg	14 ggggg
0 g											
1 q \bar{q}											
2 gg											
3 q \bar{q} g											
5 ggg											
4 q \bar{q} q \bar{q}											
6 q \bar{q} gg											
9 gggg											
7 q \bar{q} q \bar{q} g											
10 q \bar{q} ggg											
14 ggggg											

Fig. 11. The Hamiltonian matrix for a meson. Allowing for a maximum parton number 5, the Fock space can be divided into 11 sectors. Each sector contains enumerably many Fock states. Matrix elements are represented by “energy” diagrams which are characteristic for each block. Blocks with no diagrams are zero matrices. Note that the figure mixes aspects of QCD where the single gluon is absent and of QED which has no three-photon vertices.

Heisenberg matrix with strictly finite matrix elements. From a technical point of view this is simpler than the complicated integral equations discussed in Section 3.

4.4.1. Fock-space regularization

In an arbitrary frame, each particle is on its mass-shell $p^2 = m^2$. Its four-momentum is $p_\mu = (p^+, \mathbf{p}_\perp, p^-)$ with $p^- = (m^2 + \mathbf{p}_\perp^2)/p^+$. For the free theory ($g = 0$), the total four-momentum is $P_{\text{free}}^\mu = \sum_\nu p_\nu^\mu$ where the index ν runs over all particles in a particular Fock-space sector $|\Phi_n\rangle = \langle n|\Phi_n\rangle$. The components of the free four-momentum are

$$P_{\text{free}}^\mu = \sum_{\nu \in n} (p^\mu)_\nu. \tag{4.52}$$

Note that the spatial components are $P^k = P_{\text{free}}^k$. As usual, one introduces *intrinsic* momenta x and \mathbf{k}_\perp by

$$x_\nu = \frac{p_\nu^+}{P^+}, \quad (\mathbf{p}_\perp)_\nu = (\mathbf{k}_\perp)_\nu + x_\nu \mathbf{P}_\perp. \tag{4.53}$$

The spatial components of Eq. (4.52) become then the constraints

$$\sum_{\nu} x_{\nu} = 1, \quad \sum_{\nu} (\mathbf{k}_{\perp})_{\nu} = 0, \quad (4.54)$$

while the free invariant mass of a Fock state becomes

$$M_{\text{free}}^2 = P_{\text{free}}^{\mu} P_{\text{free},\mu} = \left(\sum_{\nu \in n} (p^{\mu})_{\nu} \right) \left(\sum_{\nu \in n} (p_{\mu})_{\nu} \right) \quad (4.55)$$

and, therefore,

$$M_{\text{free}}^2 = \sum_{\nu \in n} \left(\frac{m^2 + \mathbf{k}_{\perp}^2}{x} \right)_{\nu}. \quad (4.56)$$

The free invariant mass squared has a *minimum* with respect to \mathbf{k}_{\perp} and x , at $\mathbf{k}_{\perp} = 0$ and at

$$(x_{\nu})_{\text{min}} = m_{\nu} / \sum_{\nu \in n} m_{\nu}, \quad (4.57)$$

respectively, and has the value

$$\bar{M}_{\text{free}}^2 \equiv \min \left(\sum_{\nu \in n} \left(\frac{m^2 + \mathbf{k}_{\perp}^2}{x} \right)_{\nu} \right) \simeq \left(\sum_{\nu \in n} m_{\nu} \right)^2. \quad (4.58)$$

In the continuum limit the equality is strict. Physically, this corresponds to having all constituents at the same rapidity. The minimal mass-squared is frozen-in and cannot be shared by the particles off-shell. The *available mass-squared* $M_{\text{free}}^2 - \bar{M}_{\text{free}}^2$ is therefore the physically meaningful quantity.

The available mass-squared $M_{\text{free}}^2 - \bar{M}_{\text{free}}^2$ plays the same role in DLCQ as the kinetic energy T in non-relativistic quantum mechanics, see also Section 4.1. The analogy can be used to regulate the Fock space: A Fock state is admitted only when its “off-shell” kinetic energy is below a certain cut-off, i.e.

$$\sum_{\nu \in n} \left(\frac{m^2 + \mathbf{k}_{\perp}^2}{x} \right)_{\nu} - \bar{M}_{\text{free}}^2 \leq \Lambda^2. \quad (4.59)$$

Except for the term \bar{M}_{free}^2 , this *dynamic regularization scheme* is nothing but the Brodsky–Lepage regularization [62,53,299,300]. It also defines a factorization scheme for hard scattering processes in perturbative QCD. Since only Lorentz scalars appear, this regularization is Lorentz but not necessarily gauge-invariant. The constant Λ has the dimension of a $\langle \text{mass} \rangle$ and is at our disposal. Other cut-offs have also been proposed [363,456]. It is self-understood that the cut-off scale can be made sector dependent. DLCQ has an option for having as many “sector-dependent regularization parameters” as might be convenient. As a result of Fock-space regularization the Fock space and therefore the dimension of the Hamiltonian matrix is strictly finite.

4.4.2. Vertex regularization

Fock-space regularization turns out to be insufficient when dealing with *products of operators* like VV . More specifically, sums over intermediate states diverge badly for almost all matrix elements $\langle 1|VV|4 \rangle = \sum_{2,3} \langle 1|V|2,3 \rangle \langle 2,3|V|4 \rangle$. One must introduce additional regularization

schemes, which is not always easy. One possible choice is to *regulate the interaction* on the operator level, for example by multiplying each matrix element in Eq. (4.41) with a cut-off function Θ . For the vertex interaction one can thus define

$$V_n(q_1; q_2, q_3) \Rightarrow \bar{V}_n(q_1; q_2, q_3) = V_n(q_1; q_2, q_3) \Theta_V(q_1; q_2, q_3),$$

with

$$\Theta_V(q_1; q_2, q_3) = \Theta_Q(q_1; q_2) \Theta_M(q_2, q_3). \quad (4.60)$$

The two-step functions are

$$\Theta_Q(q_1; q_2) = \begin{cases} 1 & \text{if } [(p_1 - p_2)^2 - (m_1 - m_2)^2] \leq \Lambda^2, \\ 0 & \text{otherwise,} \end{cases} \quad (4.61)$$

$$\Theta_M(q_1; q_2) = \begin{cases} 1 & \text{if } [(p_1 + p_2)^2 - (m_1 + m_2)^2] \leq \Lambda^2, \\ 0 & \text{otherwise.} \end{cases} \quad (4.62)$$

The single-particle momenta p_i are those associated with the state q_i , see above. Θ_Q is a measure for the momentum transfer and Θ_M a measure for the off-shell mass induced across the vertex. The scale parameter Λ may be (or may not be) the same as in Section 4.4.1. This *vertex regularization* realizes what has been referred to by Lepage as a local regulator as opposed to the *global* Fock-space regulator in Eq. (4.59). It is generalizable to forks and seagulls and reads there

$$F_n(q_1; q_2, q_3, q_4) \Rightarrow \bar{F}_n(q_1; q_2, q_3) = F_n(q_1; q_2, q_3, q_4) \Theta_F(q_1; q_2, q_3, q_4),$$

with

$$\begin{aligned} \Theta_F(q_1; q_2, q_3, q_4) &= \Theta_Q(q_1; q_2) \Theta_M(q_3, q_4), \\ S_n(q_1, q_2; q_3, q_4) &\Rightarrow \bar{S}_n(q_1, q_2; q_3, q_4) = S_n(q_1, q_2; q_3, q_4) \Theta_S(q_1, q_2; q_3, q_4), \end{aligned} \quad (4.63)$$

with

$$\Theta_S(q_1, q_2; q_3, q_4) = \Theta_Q(q_1; q_2) \Theta_Q(q_3, q_4) \Theta_M(q_3, q_4). \quad (4.64)$$

It regulates automatically the contractions, i.e. the regulated expressions in Eq. (4.34) become finite

$$P^+ P_{pgc}^- = \sum_{1,2} a_1^\dagger a_1 (\bar{S}_{7,3}(1, 2; 1, 2) + \bar{S}_{7,3}(1, 2; 2, 1) + \bar{S}_{7,4}(1, 2; 1, 2) + \bar{S}_{7,5}(1, 2; 2, 1)). \quad (4.65)$$

Note that vertex regularization is *frame-independent*.

4.4.3. Renormalization

Renormalization is simple in principle: The eigenvalues may not depend on the regulator scale(s) Λ . Thus, if the eigenvalue equation is

$$H(\Lambda)|\Psi_i\rangle = E_i(\Lambda)|\Psi_i\rangle, \quad E_i = M_i^2 \quad (4.66)$$

one must require that

$$dE_i(\Lambda)/d\Lambda = 0 \quad \text{for all } i, \quad (4.67)$$

up to terms of order $1/\Lambda$. To require this is easier than to find a practical realization. As a matter of fact, it has not been found yet, irrespective of whether one deals with the compactified or the continuum theory, see Section 8.

4.4.4. The key challenge in DLCQ

In principle, one can proceed for $3 + 1$ dimensions like in Section 4.2 for $1 + 1$ dimensions: One selects a particular value of the harmonic resolution K and the cut-off Λ , and diagonalizes the finite-dimensional Hamiltonian matrix by numerical methods.

If this is all so simple, why has the problem not been solved a long time ago? What is the key problem?

The bottle neck of any field theoretic Hamiltonian approach in physical space–time is that the dimension of the Hamiltonian matrix increases exponentially fast with Λ , and that one may not simply truncate the Fock-space at pleasure, because of gauge invariance. Let us consider the concrete example of harmonic resolution $K = 5$, as illustrated in Fig. 2 and Table 7. Suppose, the regularization procedure allows for 10 discrete momentum states in each direction. A single particle has about 10^3 degrees of freedom. A Fock-space sector with n particles has then roughly 10^{n-1} different Fock states. The $q\bar{q}$ -sector has thus about 10^3 Fock states. Sector 13 in Fig. 2 with its 8 particles has thus about 10^{21} Fock states. Chemists are able to handle matrices with some 10^7 dimensions, but 10^{21} dimensions exceed the calculational capacity of any computer in the foreseeable future. The problem is a grave one, in particular since one has to diagonalize the Hamiltonian for $K \rightarrow \infty$.

For physical space–time one is thus thrown back to the same (insoluble?) problem as in conventional many-body physics as displayed in Fig. 9. One has to diagonalize finite matrices with exponentially large dimensions (typically $> 10^6$). In fact, in quantum field theory the problem is worse since particle number is not conserved. Even advanced numerical methods or the methods of modern quantum chemistry are apparently insufficient for the task. One needs to develop effective interactions which act in smaller matrix spaces and still are related to the full interaction. In a way, deriving an effective interaction can be understood as the aim to reduce the dimension of a matrix in a diagonalization problem from 10^{21} to 10^3 !

In the present we shall mention three perhaps promising developments, namely the Tamm–Dancoff approach, the similarity scheme and the Hamiltonian flow equations, but for physical space–time, the final break-through has not been achieved, yet.

1. The effective interaction à la Tamm [421] and Dancoff [117] can be generalized by *the method of iterated resolvents* [188,357,361,362] to avoid the most brutal violations of gauge invariance. Because of this, Wolfgang Pauli is reported to have called the Tamm–Dancoff approach “the most stupid idea I have ever seen”. This approach will be presented more thoroughly in Section 4.7.
2. The similarity scheme of Głazek and Wilson [184,185,456] will be discussed in Section 8.
3. The Hamiltonian flow equations have been proposed recently by Wegner [188,447]. In view of recent work by Lenz and Wegner on the particle–phonon model in solid state theory [294] they seem to be rather promising. Wegner has found and applied a unitary transformation $U(l)$ to an arbitrary matrix as given for example in Table 8, such that $U(l)$ depends on a continuous parameter l . It has the property that

$$d/dl \operatorname{Tr}(R(l)R(l)) < 0, \quad (4.68)$$

Table 8

A typical Hamiltonian matrix with diagonal (D) and off-diagonal (R) block matrices, corresponding to $H = D + R$. Zero matrices are symbolized by dots

n	1	2	3	4	5	6	7	8	9	10	11	12	13
1	D	R	R	R	.	R
2	R	D	R	.	R	R	.	.	R
3	R	R	D	R	R	R	R	.	.	R	.	.	.
4	R	.	R	D	.	R	R	R	.	.	R	.	.
5	.	R	R	.	D	R	.	.	R	R	.	.	.
6	R	R	R	R	R	D	R	.	R	R	R	.	.
7	.	.	R	R	.	R	D	R	.	R	R	R	.
8	.	.	.	R	.	.	R	D	.	.	R	R	R
9	.	R	.	.	R	R	.	.	D	R	.	.	.
10	.	.	R	.	R	R	R	.	R	D	R	.	.
11	.	.	.	R	.	R	R	R	.	R	D	R	.
12	R	R	.	.	R	D	R
13	R	.	.	.	R	D

for all l . In the limit $l \rightarrow \infty$, the off-diagonal blocks tend therefore to zero and can be neglected. Only the diagonal blocks survive and can be diagonalized blockwise. Except for some rather preliminary work [194], the flow equations have not yet been applied to gauge theory.

4.5. Further evaluation of the Hamiltonian matrix elements

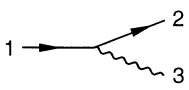
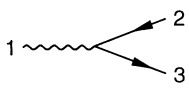
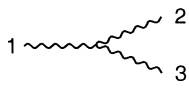
The light-cone Hamiltonian matrix elements in Figs. 1–4 are expressed in terms of the Dirac spinors and polarization vectors, $u_x(k, \lambda)$, $v_x(k, \lambda)$ and $\varepsilon_\mu(k, \lambda)$, respectively, which can be found in Appendices A and B. This representation is particularly useful for perturbative calculations as we have seen in Section 3. However, the practitioner needs these matrix elements often as explicit functions of the single-particle momenta k^+ and \mathbf{k}_\perp . The calculation is straightforward but cumbersome. To facilitate the calculation, the tables of Lepage and Brodsky [299] on the spinor contractions $\bar{u}_\alpha \Gamma_{\alpha\beta} u_\beta$ and $\bar{v}_\alpha \Gamma_{\alpha\beta} v_\beta$ are included here in Tables 5 and 6, respectively, adapted to the present notation. The general symmetry relations between spinor matrix elements are given in Appendix A. Inserting them into the matrix elements of Tables 1–4, one obtains those in Tables 9–12, respectively. One should emphasize like in Section 2.7 that all of these tables hold for QED as well as for non-abelian gauge theory SU(N) including QCD. Essentially, they hold for arbitrary n -space and 1-time dimensions as well. Using the translation keys in Section 4.6, the matrix elements in all of these tables can be translated easily into the continuum formulation.

4.6. Retrieving the continuum formulation

As argued in Section 3, the continuum formulation of the Hamiltonian problem in gauge field theory with its endless multiple integrals is usually cumbersome and untransparent. In DLCQ, the

Table 9

The explicit matrix elements of the vertex interaction. The vertex interaction in terms of Dirac spinors. The matrix elements V_n are displayed on the right, the corresponding (energy) graphs on the left. All matrix elements are proportional to $A_V = \hat{g}\delta(k_1^+|k_2^+ + 3)\delta^{(2)}(\mathbf{k}_{\perp,1}|\mathbf{k}_{\perp,2} + \mathbf{k}_{\perp,3})$, with $\hat{g} = gP^+/\sqrt{\Omega}$. In the continuum limit, see Section 4.6, one uses $\hat{g} = gP^+/\sqrt{2(2\pi)^3}$

	$ \begin{aligned} V_1 = & +\Delta_V \sqrt{\frac{1}{x_3}} m_F \left[\frac{1}{x_1} - \frac{1}{x_2} \right] \delta_{-\lambda_1}^{\lambda_2} \delta_{\lambda_1}^{\lambda_3} \delta_{f_1}^{f_2} T_{c_1 c_2}^{a_3} \\ & +\Delta_V \sqrt{\frac{2}{x_3}} \vec{\epsilon}_{\perp,3} \cdot \left[\left(\frac{\vec{k}_{\perp}}{x} \right)_3 - \left(\frac{\vec{k}_{\perp}}{x} \right)_2 \right] \delta_{+\lambda_1}^{\lambda_2} \delta_{\lambda_1}^{\lambda_3} \delta_{f_1}^{f_2} T_{c_1 c_2}^{a_3} \\ & +\Delta_V \sqrt{\frac{2}{x_3}} \vec{\epsilon}_{\perp,3} \cdot \left[\left(\frac{\vec{k}_{\perp}}{x} \right)_3 - \left(\frac{\vec{k}_{\perp}}{x} \right)_1 \right] \delta_{+\lambda_1}^{\lambda_2} \delta_{-\lambda_1}^{\lambda_3} \delta_{f_1}^{f_2} T_{c_1 c_2}^{a_3} \end{aligned} $
	$ \begin{aligned} V_3 = & +\Delta_V \sqrt{\frac{1}{x_1}} m_F \left[\frac{1}{x_2} + \frac{1}{x_3} \right] \delta_{+\lambda_2}^{\lambda_3} \delta_{+\lambda_1}^{\lambda_3} \delta_{f_2}^{f_3} T_{c_2 c_3}^{a_1} \\ & +\Delta_V \sqrt{\frac{2}{x_1}} \vec{\epsilon}_{\perp,1} \cdot \left[\left(\frac{\vec{k}_{\perp}}{x} \right)_1 - \left(\frac{\vec{k}_{\perp}}{x} \right)_3 \right] \delta_{-\lambda_2}^{\lambda_3} \delta_{-\lambda_1}^{\lambda_3} \delta_{f_2}^{f_3} T_{c_2 c_3}^{a_1} \\ & +\Delta_V \sqrt{\frac{2}{x_1}} \vec{\epsilon}_{\perp,1} \cdot \left[\left(\frac{\vec{k}_{\perp}}{x} \right)_1 - \left(\frac{\vec{k}_{\perp}}{x} \right)_2 \right] \delta_{-\lambda_2}^{\lambda_3} \delta_{+\lambda_1}^{\lambda_3} \delta_{f_2}^{f_3} T_{c_2 c_3}^{a_1} \end{aligned} $
	$ \begin{aligned} V_4 = & -\Delta_V \sqrt{\frac{x_3}{2x_1 x_2}} \vec{\epsilon}_{\perp,1}^* \cdot \left[\left(\frac{\vec{k}_{\perp}}{x} \right)_1 - \left(\frac{\vec{k}_{\perp}}{x} \right)_3 \right] \delta_{-\lambda_2}^{\lambda_3} & iC_{a_2 a_3}^{a_1} \\ & -\Delta_V \sqrt{\frac{x_1}{2x_2 x_3}} \vec{\epsilon}_{\perp,3} \cdot \left[\left(\frac{\vec{k}_{\perp}}{x} \right)_3 - \left(\frac{\vec{k}_{\perp}}{x} \right)_2 \right] \delta_{\lambda_1}^{\lambda_2} & iC_{a_2 a_3}^{a_1} \\ & -\Delta_V \sqrt{\frac{x_2}{2x_3 x_1}} \vec{\epsilon}_{\perp,3} \cdot \left[\left(\frac{\vec{k}_{\perp}}{x} \right)_3 - \left(\frac{\vec{k}_{\perp}}{x} \right)_1 \right] \delta_{\lambda_1}^{\lambda_2} & iC_{a_2 a_3}^{a_1} \end{aligned} $

continuum limit corresponds to harmonic resolution $K \rightarrow \infty$. The compactified formulation with its simple multiple sums is straightforward. The key relation is the connection between sums and integrals

$$\int dk^+ f(k^+, \mathbf{k}_{\perp}) \Leftrightarrow (\pi/2L) \sum_n f(k^+, \mathbf{k}_{\perp}),$$

$$\int d^2 \mathbf{k}_{\perp} f(k^+, \mathbf{k}_{\perp}) \Leftrightarrow (\pi/L_{\perp}) \sum_{n_{\perp}} f(k^+, \mathbf{k}_{\perp}). \quad (4.69)$$

Combined they yield

$$\int dk^+ d^2 \mathbf{k}_{\perp} f(k^+, \mathbf{k}_{\perp}) \Leftrightarrow (2(2\pi)^3/\Omega) \sum_{n, n_{\perp}} f(k^+, \mathbf{k}_{\perp}). \quad (4.70)$$

Table 10

The matrix elements of the fork interaction. The matrix elements $F_{n,j}$ are displayed on the right, the corresponding (energy) graphs on the left. All matrix elements are proportional to $\Delta = \tilde{g}^2 \delta(k_1^+ | k_2^+ + k_3^+ + k_4^+) \delta^{(2)}(\mathbf{k}_{\perp,1} | \mathbf{k}_{\perp,2} + \mathbf{k}_{\perp,3} + \mathbf{k}_{\perp,4})$, with $\tilde{g}^2 = g^2 P^+ / (2\Omega)$. In the continuum limit, see Section 4.6, one uses $\tilde{g}^2 = g^2 P^+ / (4(2\pi)^3)$

	$F_{1,1} = \frac{2\Delta}{(x_1 - x_2)^2}$	$\delta_{\lambda_1}^{\lambda_2} \delta_{-\lambda_3}^{\lambda_4}$	$\delta_{f_1}^{f_2} \delta_{f_3}^{f_4} T_{c_1 c_2}^a T_{c_3 c_4}^a$
	$F_{3,1} = \frac{\Delta}{(x_1 - x_4)^2} \frac{1}{\sqrt{x_3 x_4}}$	$\delta_{\lambda_1}^{\lambda_2} \delta_{-\lambda_3}^{\lambda_4} \delta_{+\lambda_1}^{\lambda_4}$	$\delta_{f_1}^{f_2} T_{c_1 c}^a T_{cc_2}^{a_4}$
	$F_{3,2} = \frac{\Delta}{(x_1 - x_2)^2} \sqrt{\frac{x_3}{x_4}}$	$\delta_{\lambda_1}^{\lambda_2} \delta_{-\lambda_3}^{\lambda_4}$	$\delta_{f_1}^{f_2} iT_{c_1 c_2}^a C_{a_3 a_4}^a$
	$F_{5,1} = \frac{\Delta}{(x_1 - x_3)^2} \frac{1}{\sqrt{x_1 x_2}}$	$\delta_{\lambda_1}^{\lambda_2} \delta_{-\lambda_3}^{\lambda_4} \delta_{-\lambda_1}^{\lambda_4}$	$\delta_{f_3}^{f_4} T_{c_3 c}^a T_{cc_4}^{a_2}$
	$F_{5,2} = \frac{-\Delta}{(x_1 - x_4)^2} \frac{1}{\sqrt{x_1 x_2}}$	$\delta_{\lambda_1}^{\lambda_2} \delta_{-\lambda_3}^{\lambda_4} \delta_{+\lambda_1}^{\lambda_4}$	$\delta_{f_3}^{f_4} T_{c_3 c}^a T_{cc_4}^{a_1}$
	$F_{5,3} = \frac{\Delta}{(x_1 - x_2)^2} \frac{(x_1 + x_2)}{\sqrt{x_1 x_2}}$	$\delta_{\lambda_1}^{\lambda_2} \delta_{-\lambda_3}^{\lambda_4}$	$\delta_{f_3}^{f_4} iC_{a_1 a_2}^a T_{c_3 c_4}^a$
	$F_{6,1} = \frac{\Delta}{2(x_1 - x_2)^2} \frac{(x_1 + x_2)x_3}{\sqrt{x_1 x_2 x_3 x_4}}$	$\delta_{\lambda_1}^{\lambda_2} \delta_{-\lambda_3}^{\lambda_4}$	$C_{a_1 a_2}^a C_{a_3 a_4}^a$
	$F_{6,2} = \frac{\Delta}{2\sqrt{x_1 x_2 x_3 x_4}}$	$\delta_{\lambda_1}^{\lambda_3} \delta_{\lambda_2}^{\lambda_4}$	$C_{a_1 a_2}^a C_{a_3 a_4}^a$

Table 11

The matrix elements of the contractions. The self-induced inertias $I_{n,j}$ are displayed on the right, the corresponding (energy) graphs on the left. The number of colors and flavors is denoted by N_c and N_f , respectively. In the discrete case, one uses $\bar{g}^2 = 2g^2 / (\Omega P^+)$. In the continuum limit, see Section 4.6, one uses $\bar{g}^2 = g^2 / (2\pi)^3$

	$I_{1,1}(q_1) = \bar{g}^2 \frac{(N_c^2 - 1)}{2N_c} \sum_{x, \vec{k}_1} \left[\frac{x_1}{(x_1 - x)^2} - \frac{x_1}{(x_1 + x)^2} \right]$
	$I_{1,2}(q_1) = \bar{g}^2 \frac{(N_c^2 - 1)}{4N_c} \sum_{x, \vec{k}_1} \left[\frac{x_1}{x_1 - x} + \frac{x_1}{x_1 + x} \right] \frac{1}{x}$
	$I_{3,1}(q_1) = \bar{g}^2 \frac{N_f}{2} \sum_{x, \vec{k}_1} \left[\frac{1}{(x_1 - x)} - \frac{1}{(x_1 + x)} \right]$
	$I_{3,2}(q_1) = \bar{g}^2 \frac{N_c}{4} \sum_{x, \vec{k}_1} \left[\frac{(x_1 + x)^2}{(x_1 - x)^2} + \frac{(x_1 - x)^2}{(x_1 + x)^2} \right] \frac{1}{x}$
	$I_{3,3}(q_1) = \bar{g}^2 \frac{N_c}{2} \sum_{x, \vec{k}_1} \frac{1}{x}$

Table 12

The matrix elements of the seagull interaction. The matrix elements $S_{n,j}$ are displayed on the right, the corresponding (energy) graphs on the left. All matrix elements are proportional to $\Delta = \tilde{g}^2 \delta(k_1^+ k_2^+ |k_3^+ + k_4^+) \delta^{(2)}(\mathbf{k}_{\perp,1} + \mathbf{k}_{\perp,2} | \mathbf{k}_{\perp,3} + \mathbf{k}_{\perp,4})$, with $\tilde{g}^2 = g^2 P^+ / (2\Omega)$. In the continuum limit, see Section 4.6, one uses $\tilde{g}^2 = g^2 P^+ / (4(2\pi)^3)$

	$S_1 = \frac{-\Delta}{(x_1 - x_3)^2}$	$\delta_{\lambda_1}^{\lambda_3} \delta_{\lambda_2}^{\lambda_4}$	$\delta_{f_1}^{f_3} \delta_{f_2}^{f_4} T_{c_1 c_3}^a T_{c_2 c_4}^a$
	$S_{3,1} = \frac{2\Delta}{(x_1 - x_3)^2}$	$\delta_{\lambda_1}^{\lambda_3} \delta_{\lambda_2}^{\lambda_4}$	$\delta_{f_1}^{f_3} \delta_{f_2}^{f_4} T_{c_1 c_3}^a T_{c_4 c_2}^a$
	$S_{3,2} = \frac{-2\Delta}{(x_1 + x_2)^2}$	$\delta_{-\lambda_1}^{\lambda_2} \delta_{-\lambda_3}^{\lambda_4}$	$\delta_{f_1}^{f_2} \delta_{f_3}^{f_4} T_{c_1 c_2}^a T_{c_4 c_3}^a$
	$S_{4,1} = \frac{\Delta}{x_1 - x_4} \frac{1}{\sqrt{x_2 x_4}}$	$\delta_{\lambda_1}^{\lambda_3} \delta_{\lambda_2}^{\lambda_4} \delta_{\lambda_1}^{\lambda_2}$	$\delta_{f_1}^{f_3} T_{c_1 c}^a T_{cc_3}^{a_2}$
	$S_{4,2} = \frac{\Delta}{x_1 + x_2} \frac{1}{\sqrt{x_2 x_4}}$	$\delta_{\lambda_1}^{\lambda_3} \delta_{\lambda_2}^{\lambda_4} \delta_{-\lambda_1}^{\lambda_2}$	$\delta_{f_1}^{f_3} T_{c_1 c}^{a_2} T_{cc_3}^{a_4}$
	$S_{4,3} = \frac{\Delta}{(x_1 - x_3)^2} \frac{(x_2 + x_4)}{\sqrt{x_2 x_4}}$	$\delta_{\lambda_1}^{\lambda_3} \delta_{\lambda_2}^{\lambda_4}$	$\delta_{f_1}^{f_3} iT_{c_1 c_3}^a C_{a_2 a_4}^a$
	$S_{6,1} = \frac{\Delta}{x_1 - x_3} \frac{1}{\sqrt{x_3 x_4}}$	$\delta_{-\lambda_1}^{\lambda_2} \delta_{-\lambda_3}^{\lambda_4} \delta_{\lambda_1}^{\lambda_3}$	$\delta_{f_1}^{f_2} T_{c_1 c}^{a_3} T_{cc_2}^{a_4}$
	$S_{6,2} = \frac{\Delta}{(x_1 + x_2)^2} \frac{(x_3 - x_4)}{\sqrt{x_3 x_4}}$	$\delta_{-\lambda_1}^{\lambda_2} \delta_{-\lambda_3}^{\lambda_4}$	$\delta_{f_1}^{f_2} iT_{c_1 c_2}^a C_{a_3 a_4}^a$
	$S_{7,1} = \frac{-\Delta(x_1 + x_3)}{4(x_1 - x_3)^2} \frac{(x_2 + x_4)}{\sqrt{x_1 x_2 x_3 x_4}}$	$\delta_{\lambda_1}^{\lambda_3} \delta_{\lambda_2}^{\lambda_4}$	$C_{a_1 a_3}^a C_{a_2 a_4}^a$
	$S_{7,2} = \frac{\Delta}{2(x_1 + x_2)^2} \sqrt{\frac{x_1 x_3}{x_2 x_4}}$	$\delta_{-\lambda_1}^{\lambda_2} \delta_{-\lambda_3}^{\lambda_4}$	$C_{a_1 a_2}^a C_{a_3 a_4}^a$
	$S_{7,3} = \frac{\Delta}{4\sqrt{x_1 x_2 x_3 x_4}}$	$\delta_{\lambda_1}^{\lambda_3} \delta_{\lambda_2}^{\lambda_4}$	$C_{a_1 a_2}^a C_{a_3 a_4}^a$
	$S_{7,4} = \frac{\Delta}{4\sqrt{x_1 x_2 x_3 x_4}}$	$\delta_{-\lambda_1}^{\lambda_2} \delta_{-\lambda_3}^{\lambda_4}$	$C_{a_1 a_3}^a C_{a_2 a_4}^a$
	$S_{7,5} = \frac{\Delta}{4\sqrt{x_1 x_2 x_3 x_4}}$	$\delta_{\lambda_1}^{\lambda_3} \delta_{\lambda_2}^{\lambda_4}$	$C_{a_1 a_4}^a C_{a_3 a_2}^a$

Similarly, Dirac delta and Kronecker delta functions are related by

$$\delta(k^+) \delta^{(2)}(\mathbf{k}_\perp) \Leftrightarrow \frac{\Omega}{2(2\pi)^3} \delta(k^+ | 0) \delta^{(2)}(\mathbf{k}_\perp | \mathbf{0}). \tag{4.71}$$

Because of that, in order to satisfy the respective commutation relations, the boson operators \tilde{a} and a must be related by

$$\tilde{a}(q) \Leftrightarrow \sqrt{(\Omega/2(2\pi)^3)} a_q, \tag{4.72}$$

and correspondingly for fermion operators. The commutation relations, Eq. (4.25), become then, for example,

$$[a_q, a_q^\dagger] \Leftrightarrow [\tilde{a}(q_1), \tilde{a}^\dagger(q_2)] = \delta_{a_1, a_2} \delta_{\lambda_1, \lambda_2} \delta(k_1^+ - k_2^+) \delta^{(2)}(\mathbf{k}_{\perp 1} - \mathbf{k}_{\perp 2}). \quad (4.73)$$

Substituting Eqs. (4.70), (4.71) and (4.72) into Eq. (4.31), for example, one gets straightforwardly

$$P^+ P_{pg}^- = \int dk_1^+ d^2 \mathbf{k}_{\perp 1} \int dk_2^+ d^2 \mathbf{k}_{\perp 2} \int dk_3^+ d^2 \mathbf{k}_{\perp 3} \int dk_4^+ d^2 \mathbf{k}_{\perp 4} \\ \times \sum_{a_1, a_2, a_3, a_4} \sum_{\lambda_1, \lambda_2, \lambda_3, \lambda_4} F_{6,2}(q_1; q_2, q_3, q_4) \tilde{a}(q_1)^\dagger \tilde{a}(q_2) \tilde{a}(q_3) \tilde{a}(q_4). \quad (4.74)$$

This appears to be a clumsy expression as compared to Eq. (4.31). The physics is the same in both of them. The matrix element $F_{6,2}$ is defined formally like in Eq. (4.28), except for the Dirac delta functions, i.e.

$$\Delta(q_1; q_2, q_3, q_4) = (g^2 P^+ / 4(2\pi)^3) \delta(k_1^+ - k_2^+ - k_3^+ - k_4^+) \delta^{(2)}(\mathbf{k}_{\perp 1} - \mathbf{k}_{\perp 2} - \mathbf{k}_{\perp 3} - \mathbf{k}_{\perp 4}). \quad (4.75)$$

Of course, one has formally to replace sums by integrals, Kronecker delta by Dirac delta functions, and single-particle operators by their tilded versions. But as a net effect and in practice, one replaces

$$\tilde{g}^2 = g^2 P^+ / 2\Omega \quad \text{by} \quad \tilde{g}^2 = g^2 P^+ / 4(2\pi)^3 \quad (4.76)$$

in order to convert the discretized expressions in Tables 1–4 and Tables 9–12 to the continuum limit. See also the captions to the tables.

The DLCQ method can be considered a general framework for solving problems such as relativistic many-body theories or approximate models. The general procedure is:

1. Phrase your physics problem in a compactified version like DLCQ.
2. Apply your approximation and simplifications.
3. Derive your final result.
4. At the end of calculation convert expressions back to the continuum formulation.

This procedure was applied in Section 4.8.

4.7. Effective interactions in 3 + 1 dimensions

Instead of an infinite set of coupled integral equations like in Eq. (3.14), the eigenvalue equation $H_{\text{LC}}|\Psi\rangle = M^2|\Psi\rangle$ leads in DLCQ to a strictly finite set of coupled matrix equations

$$\sum_{j=1}^N \langle i|H|j\rangle \langle j|\Psi\rangle = E \langle i|\Psi\rangle \quad \text{for all } i = 1, 2, \dots, N. \quad (4.77)$$

The rows and columns of the block matrices $\langle i|H|j\rangle$ are denumerated by the sector numbers $i, j = 1, 2, \dots, N$, in accord with the Fock-space sectors in Fig. 2 or Fig. 11. Each sector contains many individual Fock states with different values of x, \mathbf{p}_\perp and λ , but due to Fock-space regularization (Λ), their number is finite.

Effective interactions are a well known tool in many-body physics [337]. In field theory the method is known as the Tamm–Dancoff approach. It was applied first by Tamm [421] and by Dancoff [117] to Yukawa theory for describing the nucleon–nucleon interaction. For the front form, a considerable amount of work has been done thus far, for instance by Tang et al. [422], Burkardt et al. [80–84], Fuda et al. [155–161], Głazek et al. [182,456], Gubankova et al. [194], Hamer et al. [420], Heinzl et al. [211–215], Hiller et al. [458], Hollenberg et al. [224], Jones et al. [255,256], Kaluza et al. [264], Kalloniatis et al. [260,386], Krautgärtner et al. [279], Prokhatilov et al. [14], Trittmann et al. [429–431], Wort [459], Zhang et al. [461–466], and others [49,134,191,233,251,252,270,285], but the subject continues to be a challenge for QCD. In particular one faces the problem of non-perturbative renormalization but with recent progress in Refs. [8,2,85,464], particularly see the work of Bakker et al. [306,310,399], Bassetto et al. [5,23–26], Brisudova et al. [48–50], as will be discussed in Section 8.

Let us review in short the general procedure [337] on which the Tamm–Dancoff approach [117,421] is based. The rows and columns of any Hamiltonian matrix can always be split into two parts. One speaks of the P -space and of the rest, the Q -space $Q \equiv 1 - P$. The division is arbitrary, but for being specific let us identify first the P -space with the $q\bar{q}$ -space:

$$P = |1\rangle\langle 1|, \quad Q = \sum_{j=2}^N |j\rangle\langle j|. \quad (4.78)$$

Eq. (4.77) can then be rewritten conveniently as a 2×2 block matrix

$$\begin{pmatrix} \langle P|H|P\rangle & \langle P|H|Q\rangle \\ \langle Q|H|P\rangle & \langle Q|H|Q\rangle \end{pmatrix} \begin{pmatrix} \langle P|\Psi\rangle \\ \langle Q|\Psi\rangle \end{pmatrix} = E \begin{pmatrix} \langle P|\Psi\rangle \\ \langle Q|\Psi\rangle \end{pmatrix}, \quad (4.79)$$

or explicitly

$$\langle P|H|P\rangle \langle P|\Psi\rangle + \langle P|H|Q\rangle \langle Q|\Psi\rangle = E \langle P|\Psi\rangle, \quad (4.80)$$

$$\langle Q|H|P\rangle \langle P|\Psi\rangle + \langle Q|H|Q\rangle \langle Q|\Psi\rangle = E \langle Q|\Psi\rangle. \quad (4.81)$$

Rewriting the second equation as

$$\langle Q|E - H|Q\rangle \langle Q|\Psi\rangle = \langle Q|H|P\rangle \langle P|\Psi\rangle, \quad (4.82)$$

one observes that the quadratic matrix $\langle Q|E - H|Q\rangle$ could be inverted to express the Q -space wavefunction $\langle Q|\Psi\rangle$ in terms of the P -space wavefunction $\langle P|\Psi\rangle$. But the eigenvalue E is unknown at this point. To avoid this, one solves first another problem: One introduces *the starting point energy* ω as a redundant parameter at disposal, and *defines the Q -space resolvent* as the inverse of the block matrix $\langle Q|\omega - H|Q\rangle$,

$$G_Q(\omega) = 1/\langle Q|\omega - H|Q\rangle. \quad (4.83)$$

In line with Eq. (4.82) one thus defines

$$\langle Q|\Psi\rangle \equiv \langle Q|\Psi(\omega)\rangle = G_Q(\omega)\langle Q|H|P\rangle\langle P|\Psi\rangle, \quad (4.84)$$

and inserts it into Eq. (4.81). This yields an eigenvalue equation

$$H_{\text{eff}}(\omega)|P\rangle\langle P|\Psi_k(\omega)\rangle = E_k(\omega)|\Psi_k(\omega)\rangle, \quad (4.85)$$

which defines unambiguously the effective interaction

$$\langle P|H_{\text{eff}}(\omega)|P\rangle = \langle P|H|P\rangle + \langle P|H|Q\rangle G_Q(\omega)\langle Q|H|P\rangle. \quad (4.86)$$

Both of them act only in the usually much smaller model space, the P -space. The effective interaction is thus well defined: It is the original block matrix $\langle P|H|P\rangle$ plus a part where the system is scattered virtually into the Q -space, propagating there by impact of the true interaction, and finally is scattered back into the P -space: $\langle P|H|Q\rangle G_Q(\omega)\langle Q|H|P\rangle$. Every numerical value of ω defines a different Hamiltonian and a different spectrum. Varying ω one generates a set of *energy functions* $E_k(\omega)$. Whenever one finds a solution to the *fixed-point equation* [352,467]

$$E_k(\omega) = \omega, \quad (4.87)$$

one has found one of the true eigenvalues and eigenfunctions of H , by construction.

It looks therefore as if one has mapped a difficult problem, the diagonalization of a large matrix (10^{21}) onto a simpler problem, the diagonalization of a much smaller matrix in the model space (10^3). But this is only true in a restricted sense. One has to invert a matrix. The numerical inversion of a matrix takes about the same effort as its diagonalization. In addition, one has to vary ω and solve the fixed-point equation (4.87). The numerical work is thus rather larger than smaller as compared to a direct diagonalization. But the procedure is exact in principle. In particular, one can find all eigenvalues of the full Hamiltonian H , irrespective of how small one chooses the P -space. Explicit examples for that can be found in Refs. [352,361,467].

The key problem is how to get $(\langle Q|\omega - H|Q\rangle)^{-1}$, the inversion of the Hamiltonian matrix in the Q -sector, as required by Eq. (4.83). Once this is achieved, for example by an approximation (see below), the sparseness of the Hamiltonian matrix can be made use of rather effectively: Only comparatively few block matrices $\langle P|H|Q\rangle$ differ from being strict zero matrices, see Fig. 2 or Fig. 11.

In fact, the sparseness of the Hamiltonian matrix can be made use of even more effectively by introducing more than two projectors, as done in the method of iterated resolvents [357,361,362]. One easily recognizes that Eqs. (4.79), (4.80), (4.81), (4.82), (4.83), (4.84), (4.85) and (4.86) can be interpreted as the reduction of the block matrix dimension from 2 to 1. But there is no need to identify the P -space with the lowest sector. One can also choose the Q -space identical to the last sector and identify the P -space with the rest, $P = 1 - Q$:

$$P = \sum_{j=1}^n |j\rangle\langle j| \quad \text{with } 1 \leq n \leq N, \quad Q \equiv 1 - P. \quad (4.88)$$

The same steps as above then reduce the block matrix dimension from N to $N - 1$. The effective interaction acts in the now smaller space of $N - 1$ sectors. This procedure can be repeated until one arrives at a block matrix dimension 1 where the procedure stops: The effective interaction in the Fock-space sector with only one quark and one antiquark is defined again unambiguously. More explicitly, suppose that in the course of this reduction one has arrived at block matrix dimension n . Denote the corresponding effective interaction $H_n(\omega)$. The eigenvalue problem corresponding to Eq. (4.77) then reads

$$\sum_{j=1}^n \langle i|H_n(\omega)|j\rangle\langle j|\Psi(\omega)\rangle = E(\omega)\langle i|\Psi(\omega)\rangle \quad \text{for } i = 1, 2, \dots, n. \quad (4.89)$$

Observe that i and j refer here to sector numbers. Since one has started from the full Hamiltonian in the last sector, one has to convene that $H_N = H$. Now, in analogy with Eqs. (4.83) and (4.84), define the resolvent of the effective sector Hamiltonian $H_n(\omega)$ by

$$G_n(\omega) = \frac{1}{\langle n|\omega - H_n(\omega)|n\rangle}, \quad (4.90)$$

$$\langle n|\Psi(\omega) = G_n(\omega) \sum_{j=1}^{n-1} \langle n|H_n(\omega)|j\rangle \langle j|\Psi(\omega)\rangle, \quad (4.91)$$

respectively. The effective interaction in the $(n - 1)$ -space then becomes [357]

$$H_{n-1}(\omega) = H_n(\omega) + H_n(\omega)G_n(\omega)H_n(\omega) \quad (4.92)$$

for every block matrix element $\langle i|H_{n-1}(\omega)|j\rangle$. To obtain the corresponding eigenvalue equation one substitutes n by $n - 1$ everywhere in Eq. (4.89). Everything proceeds as above, including the fixed point equation $E(\omega) = \omega$. But one has achieved much more: Eq. (4.92) is a *recursion relation* which holds for all $1 < n < N!$ Notice that this so-called *method of iterated resolvents* requires only the inversion of the effective sector Hamiltonians $\langle n|H_n|n\rangle$. On a computer, this is an easier problem than the inversion of the full Q -space matrix as in Eq. (4.83). Moreover, one can now make use of all zero block matrices in the Hamiltonian, as worked out in Ref. [361].

The Tamm–Dancoff approach (TDA) as used in the literature, however, does not follow literally the outline given in Eqs. (4.78), (4.79), (4.80), (4.81), (4.82), (4.83), (4.84), (4.85) and (4.86), rather one substitutes the “energy denominator” in Eq. (4.83) according to

$$\frac{1}{\langle Q|\omega - T - U|Q\rangle} = \frac{1}{\langle Q|T^* - T - \delta U(\omega)|Q\rangle} \Rightarrow \frac{1}{\langle Q|T^* - T|Q\rangle}, \quad (4.93)$$

with

$$\delta U(\omega) = \omega - T^* - U.$$

Here, T^* is not an operator but a c -number, denoting the mean kinetic energy in the P -space [117,421]. In fact, the two resolvents

$$G_Q(\omega) = \frac{1}{\langle Q|T^* - T - \delta U(\omega)|Q\rangle}, \quad G_0 = \frac{1}{\langle Q|T^* - T|Q\rangle} \quad (4.94)$$

are identically related by

$$G_Q(\omega) = G_0 + G_0 \delta U(\omega) G_Q(\omega) \quad (4.95)$$

or by the infinite series of perturbation theory

$$G_Q(\omega) = G_0 + G_0 \delta U(\omega) G_0 + G_0 \delta U(\omega) G_0 \delta U(\omega) G_0 + \dots \quad (4.96)$$

The idea is that the operator $\delta U(\omega)$ in some sense is small, or at least that its mean value in the Q -space is close to zero, $\langle \delta U(\omega) \rangle \approx 0$. In such a case it is justified to restrict to the very first term in the expansion, $G_Q(\omega) = G_0$, as usually done in TDA. Notice that the diagonal kinetic energy $T^* - T$ can be inverted trivially to get the resolvent G_0 .

4.8. Quantum electrodynamics in $3 + 1$ dimensions

Tang et al. [422] gave the first application to DLCQ to QED_{3+1} at strong coupling, followed later by Kaluza et al. [264]. Both works addressed the positronium eigenvalue spectrum as a test of the method. In either case the Fock space was truncated to include only the $q\bar{q}$ and $q\bar{q}g$ states. The so-truncated DLCQ-matrix was diagonalized numerically, with rather slow convergence of the results. Omitting the one-photon state g , they have excluded the impact of annihilation. Therefore, rather than “positronium”, one should call such models “muonium with equal masses”. Langnau and Burkardt have calculated the anomalous magnetic moment of the electron for very strong coupling [76,77,291,292]. Krautgärtner et al. [279,265] proceeded in a more general way by using the effective interaction of the Tamm–Dancoff approach. A detailed analysis of the Coulomb singularity and its impact on numerical calculations in momentum representation has led them to develop a Coulomb counter-term technology, which did improve the rate of numerical convergence significantly. It was then possible to reproduce quantitatively the Bohr aspects of the spectrum, as well as the fine and hyperfine structure.

One should emphasize that the aim of calculating the positronium spectrum by a Hamiltonian eigenvalue equation is by no means a trivial problem. In the instant form, for example, the hyperfine interaction is so singular, that thus far the Hamiltonian eigenvalue equation has not been solved. The hyperfine corrections have only been calculated in the lowest non-trivial orders of perturbation theory, see Ref. [44]. One also should note that the usual problems in configuration space associated with recoil and reduced mass, are simply absent in momentum representation.

Although the Tamm–Dancoff approach was originally applied in the instant form [117,421], one can translate it easily into the front form, as we have discussed above. The approximation of Eqs. (4.93) and (4.86) give $G_Q(\omega) \approx G_0$, and thus the virtual scattering into the Q -space produces an additional P -space interaction, the one-photon exchange interaction VG_0V . Its two time orderings are given diagrammatically in Fig. 12. The original P -space interaction is the kinetic energy, of course, plus the seagull interaction. Of the latter, we keep here only the instantaneous-photon exchange and denote it as W , which is represented by the first graph in Fig. 12. Without the annihilation terms, the effective Hamiltonian is thus

$$H_{\text{eff}} = T + W + VG_0V = T + U_{\text{eff}}. \quad (4.97)$$

The only difference is that the unperturbed energy has to be replaced by the mean kinetic energy T^* as introduced in Eq. (4.93), which in light-cone quantization is given by

$$T^* = \frac{1}{2} \left(\frac{m_q^2 + \mathbf{k}_\perp^2}{x} + \frac{m_{\bar{q}}^2 + \mathbf{k}_\perp^2}{1-x} + \frac{m_q^2 + \mathbf{k}'_\perp^2}{x'} + \frac{m_{\bar{q}}^2 + \mathbf{k}'_\perp^2}{1-x'} \right). \quad (4.98)$$

The same “trick” was applied by Tamm and by Dancoff in their original work [117,421]. In correspondence to Eq. (3.34), the energy denominator in the intermediate state of the Q -space

$$T^* - T = -Q^2/|x - x'| \quad (4.99)$$

can now be expressed in terms of Q , of the average four-momentum transfer along the electron and the positron line, i.e.

$$Q^2 = -\frac{1}{2}((k_q - k'_q)^2 + (k_{\bar{q}} - k'_{\bar{q}})^2). \quad (4.100)$$

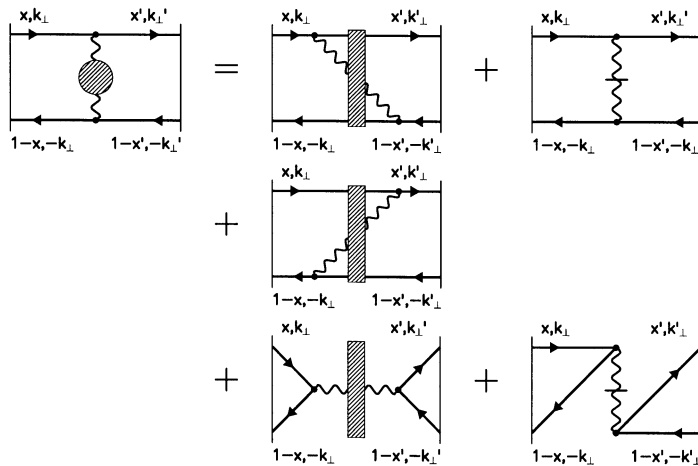


Fig. 12. The graphs of the effective one-photon exchange interaction. The effective interaction is a sum of the dynamic one-photon exchange with both time orderings, the instantaneous one-photon exchange, the dynamic and the instantaneous annihilation interactions, all represented by energy graphs. The hashed rectangles represent the effective photon or the effective propagator G_0 . Taken from Ref. [431].

As illustrated in Fig. 12, the effective interaction U_{eff} scatters an electron with on-shell four-momentum k_q and helicity λ_q into a state with k'_q and λ'_q , and correspondingly the positron from $k_{\bar{q}}$ and $\lambda_{\bar{q}}$ to $k'_{\bar{q}}$ and $\lambda'_{\bar{q}}$. The evaluation of the so-defined effective interaction has been done explicitly in Section 3.4.

In the sequel, we follow the more recent work of Trittmann et al. [429–431], where the Coulomb counter-term technology was improved further to the extent that a calculation of all spin-parity multiplets of positronium was meaningful. In particular, it was possible to investigate the important question to which extent the members of the multiplets are numerically degenerate with J_z . One recalls that the operator for the projection of total angular momentum J_z is kinematic in the front form, whereas total angular momentum J^2 is not, see Section 2.6.

Up to this point it was convenient to work with DLCQ, and coupled matrix equations. All spatial momenta k^+ and \mathbf{k}_\perp are still discrete. But now that all the approximations have been done, one goes over conveniently to the *continuum limit* according to Section 4.6. The DLCQ-matrix equation is converted into an integral equation in momentum space,

$$M^2 \langle x, \mathbf{k}_\perp; \lambda_q, \lambda_{\bar{q}} | \Psi \rangle = \left[\frac{m_q + \mathbf{k}_\perp^2}{x} + \frac{m_{\bar{q}} + \mathbf{k}_\perp^2}{1-x} \right] \langle x, \mathbf{k}_\perp; \lambda_q, \lambda_{\bar{q}} | \Psi \rangle + \sum_{\lambda'_q, \lambda'_{\bar{q}}} \int_D dx' d^2 \mathbf{k}'_\perp \langle x, \mathbf{k}_\perp; \lambda_q, \lambda_{\bar{q}} | U_{\text{eff}} | x', \mathbf{k}'_\perp; \lambda'_q, \lambda'_{\bar{q}} \rangle \langle x', \mathbf{k}'_\perp; \lambda'_q, \lambda'_{\bar{q}} | \Psi \rangle. \tag{4.101}$$

The domain D restricts integration in line with Fock-space regularization

$$\frac{m_q^2 + \mathbf{k}_\perp^2}{x} + \frac{m_{\bar{q}}^2 + \mathbf{k}_\perp^2}{1-x} \leq (m_q + m_{\bar{q}})^2 + \Lambda^2. \tag{4.102}$$

The bras and kets refer to $q\bar{q}$ Fock states, $|x, \mathbf{k}_\perp; \lambda_q, \lambda_{\bar{q}}\rangle = b^\dagger(k_q, \lambda_q)d^\dagger(k_{\bar{q}}, \lambda_{\bar{q}})|0\rangle$. The goal of the calculation is to obtain the momentum-space wavefunctions $\langle x, \mathbf{k}_\perp; \lambda_q, \lambda_{\bar{q}}|\psi\rangle$ and the eigenvalues M^2 . The former are the probability amplitudes for finding the quark with helicity projection λ_q , longitudinal momentum fraction $x \equiv k_q^+/P^+$ and transverse momentum \mathbf{k}_\perp , and simultaneously the antiquark with $\lambda_{\bar{q}}$, $1 - x$ and $-\mathbf{k}_\perp$. According to Eq. (3.43), the effective interaction U_{eff} becomes

$$U_{\text{eff}} = -\frac{1}{4\pi^2} \frac{\alpha}{Q^2} \frac{[\bar{u}(k_q, \lambda_q)\gamma^\mu u(k'_q, \lambda'_q)][\bar{u}(k_{\bar{q}}, \lambda_{\bar{q}})\gamma_\mu u(k'_{\bar{q}}, \lambda'_{\bar{q}})]}{\sqrt{x(1-x)x'(1-x')}} \quad (4.103)$$

with $\alpha \equiv g^2/4\pi$. Notice that both the dynamic and the instantaneous one-photon exchange interaction in Eqs. (3.41) and (3.42), respectively, contain a non-integrable singularity $\sim (x - x')^{-2}$, which cancel each other in the final expressions, Eq. (3.43) or Eq. (4.103). Only the square integrable ‘‘Coulomb singularity’’ $1/Q^2$ remains, see also Ref. [299].

In the numerical work [279,429] it is favorable to replace the two transverse momenta $k_{\perp x}$ and $k_{\perp y}$ by the absolute value of k_\perp and the angles θ, φ . The integral equation is approximated by Gaussian quadratures, and the results are studied as a function of the number of integration points N , as displayed in Fig. 13. One sees there that the results stabilize themselves quickly. All eigenvalues displayed have the same eigenvalue of total angular momentum projection, i.e. $J_z = 0$. Since one calculates the values of an invariant mass squared, a comparative large value of the fine structure constant $\alpha = 0.3$ has been chosen. One recognizes the ionization threshold at $M^2 \sim 4m^2$, the Bohr spectrum, and even more important, the fine structure. The two lowest eigenvalues correspond to the singlet and triplet state of positronium, respectively. The agreement is quantitative, particularly for the physical value of the fine structure constant $\alpha = \frac{1}{137}$. In order to verify this agreement, one needs a relative numerical accuracy of roughly 10^{-11} . The numerical stability and precision is remarkable, indeed. The stability with respect to the cut-off Λ has been also studied (Fig. 14).

An inspection of the numerical wavefunctions $\psi(x, \mathbf{k}_\perp)$, as displayed for example in Fig. 15, reveals that they are strongly peaked around $\mathbf{k}_\perp \sim 0$ and $x \sim \frac{1}{2}$. Outside the region

$$\mathbf{k}_\perp^2 \ll m^2, \quad (x - \frac{1}{2})^2 \ll 1, \quad (4.104)$$

they are smaller than the peak value by many orders of magnitude. Also, the singlet wave function with anti-parallel helicities is dominant with more than a factor 20 over the component with parallel helicities. The latter would be zero in a non-relativistic calculation. Relativistic effects are responsible also for the fact that the singlet-($\uparrow\downarrow$) wavefunction is not rotationally symmetric. To see this, the wavefunction is plotted in Fig. 14 versus the off-shell momentum variable μ , defined by [268,392,393]

$$x = \frac{1}{2}(1 + \mu \cos \theta / (\sqrt{m^2 + \mu^2})), \quad (4.105)$$

$$\mathbf{k}_\perp = (\mu \sin \theta \cos \varphi, \mu \sin \theta \sin \varphi), \quad (4.106)$$

for different values of θ . A numerically significant deviation, however, occurs only for very relativistic momenta $\mu \geq 10m$, as displayed in Fig. 14.

Trittmann et al. [429–431] have also included the annihilation interaction as illustrated in Fig. 12 and calculated numerically the spectrum for various values of J_z . The results are compiled

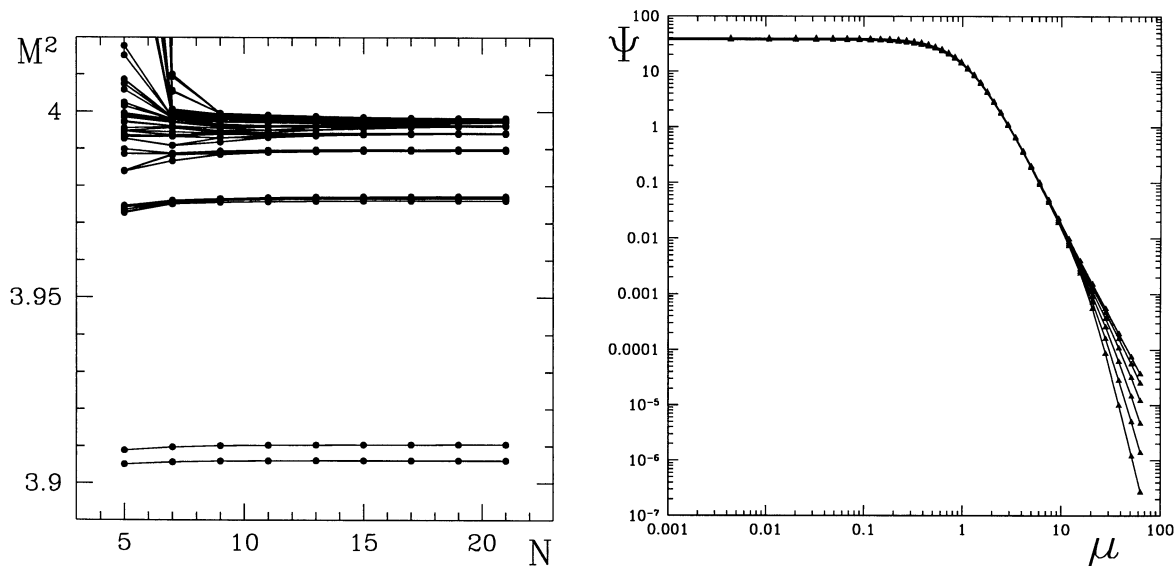


Fig. 13. Stability of positronium spectrum for $J_z = 0$, without the annihilation interaction. Eigenvalues M_i^2 for $\alpha = 0.3$ and $A = 1$ are plotted versus N , the number of integration Gaussian points. Masses are in units of the electron mass. Taken from Ref. [430].

Fig. 14. The decrease of the $J_z = 0$ singlet ground-state wavefunction with antiparallel helicities as a function of the momentum variable μ for $\alpha = 0.3$ and $A = 1.0$. The six different curves correspond to six values of θ , see Eq. (4.106). Taken from Ref. [429].

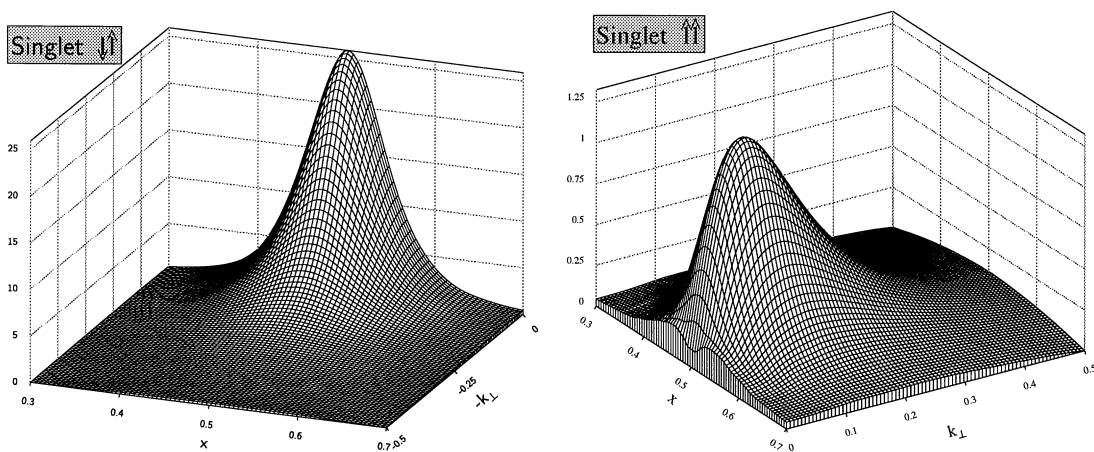


Fig. 15. Singlet wavefunctions of positronium [430].

in Fig. 16. As one can see, certain mass eigenvalues at $J_z = 0$ are degenerate with certain eigenvalues at other J_z to a very high degree of numerical precision. As an example, consider the second lowest eigenvalue for $J_z = 0$. It is degenerate with the lowest eigenvalue for $J_z = \pm 1$, and can thus be classified as a member of the triplet with $J = 1$. Correspondingly, the lowest eigenvalue for $J_z = 0$ having no companion can be classified as the singlet state with $J = 0$. Quite in general one can interpret degenerate multiplets as members of a state with total angular momentum $J = 2J_{z,\max} + 1$. An inspection of the wavefunctions allows to conclude whether the component with parallel or anti-parallel helicity is the leading one. In a pragmatismal sense, one thus can conclude on the “total spin” S , and on “total orbital angular momentum” L , although in the front form neither J nor S nor L make sense as operator eigenvalues. In fact they are not, as discussed in Section 2.6. Nevertheless, one can make contact with the conventional classification scheme $^{3S+1}L_{J_z}^J$, as indicated in Fig. 16. It is remarkable, that one finds *all the expected states* [431], that is all members of the multiplets are found without a single exception.

4.9. The Coulomb interaction in the front form

The $j^\mu j_\mu$ -term in Eq. (4.103) represents retardation and mediates the fine and hyperfine interactions. One can switch them off by substituting the momenta by the equilibrium values,

$$\bar{k}_\perp = 0, \quad \bar{x} = m_q/(m_q + m_{\bar{q}}), \tag{4.107}$$

which gives by means of Table 5:

$$[\bar{u}(k_q, \lambda_q)\gamma^\mu u(k'_q, \lambda'_q)][\bar{u}(k_{\bar{q}}, \lambda_{\bar{q}})\gamma_\mu u(k'_{\bar{q}}, \lambda'_{\bar{q}})] \Rightarrow (m_q + m_{\bar{q}})^2 \delta_{\lambda_q, \lambda'_q} \delta_{\lambda_{\bar{q}}, \lambda'_{\bar{q}}}. \tag{4.108}$$

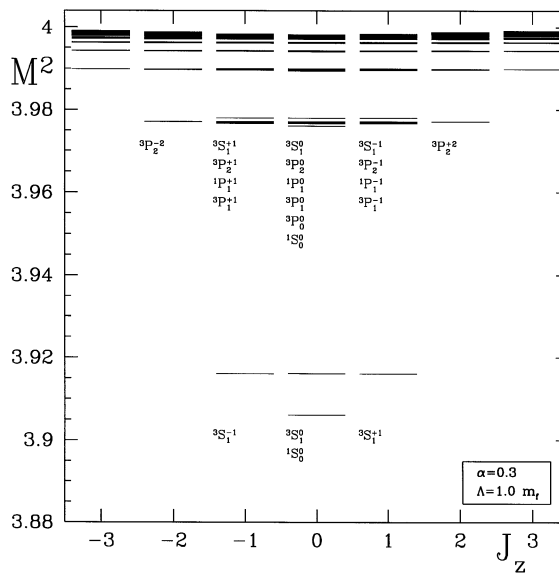


Fig. 16. Positronium spectrum for $-3 \leq J_z \leq 3$, $\alpha = 0.3$ and $\Lambda = 1$ including the annihilation interaction. For an easier identification of the spin-parity multiplets, the corresponding non-relativistic notation $^{3S+1}L_{J_z}^J$ is inserted. Masses are given in units of the electron mass. Taken from Ref. [431].

The effective interaction in Eq. (4.103) simplifies correspondingly and becomes the front form Coulomb interaction:

$$U_{\text{eff}} = - \frac{1}{4\pi^2} \frac{\alpha}{Q^2} \frac{(m_q + m_{\bar{q}})^2}{\sqrt{x(1-x)x'(1-x')}}. \quad (4.109)$$

To see that one performs a variable transformation from x to $k_z(x)$, the inverse transformation [359]

$$x = x(k_z) = \frac{k_z + E_1}{E_1 + E_2} \quad \text{with } E_i = \sqrt{m_i^2 + \mathbf{k}_\perp^2 + k_z^2}, \quad i = 1, 2, \quad (4.110)$$

maps the domain of integration $-\infty \leq k_z \leq \infty$ into the domain $0 \leq x \leq 1$, and produces the equilibrium value for $k_z = 0$, Eq. (4.107). One can combine k_z and \mathbf{k}_\perp into a three-vector $\mathbf{k} = (\mathbf{k}_\perp, k_z)$. By means of the identity

$$x(1-x) = (E_1 + k_z)(E_2 - k_z)/(E_1 + E_2)^2, \quad (4.111)$$

the Jacobian of the transformation becomes straightforwardly

$$\frac{dx'}{\sqrt{x(1-x)x'(1-x')}} = dk_z \left(\frac{1}{E_1} + \frac{1}{E_2} \right) \sqrt{\frac{(E_1 + k'_z)(E_2 - k'_z)}{(E_1 + k_z)(E_2 - k_z)}}. \quad (4.112)$$

For equal masses $m_1 = m_2 = m$ (positronium), the kinetic energy is

$$(m^2 + \mathbf{k}_\perp^2)/x(1-x) = 4m^2 + 4\mathbf{k}^2, \quad (4.113)$$

and the domain of integration Eq. (4.102) reduces to $4\mathbf{k}^2 \leq \Lambda^2$. The momentum scale μ [268,392,393], as introduced in Eq. (4.106), identifies itself as $\mu = 2|\mathbf{k}|$. As shown by Ref. [359], the four-momentum transfer Eq. (4.100) can exactly be rewritten as

$$Q^2 = (\mathbf{k} - \mathbf{k}')^2. \quad (4.114)$$

Finally, after substituting the invariant mass squared eigenvalue M^2 by an energy eigenvalue E ,

$$M^2 = 4m^2 + 4mE, \quad (4.115)$$

and introducing a new wavefunction ϕ ,

$$\phi(\mathbf{k}) = \langle x(k_z), \mathbf{k}_\perp; \lambda_q, \lambda_{\bar{q}} | \psi \rangle (1/m) \sqrt{m^2 + \mathbf{k}_\perp^2}, \quad (4.116)$$

one rewrites Eq. (4.101) with Eq. (4.109) identically as

$$\left(E - \frac{\mathbf{k}^2}{2m_r} \right) \phi(\mathbf{k}) = - \frac{\alpha}{2\pi^2} \frac{m}{\sqrt{m^2 + \mathbf{k}^2}} \int_D d^3\mathbf{k}' \frac{1}{(\mathbf{k} - \mathbf{k}')^2} \phi(\mathbf{k}'). \quad (4.117)$$

Since $m_r = m/2$ is the reduced mass, this is the non-relativistic Schrödinger equation in momentum representation for $k^2 \ll m^2$ (see also Ref. [359]).

Notice that only retardation was suppressed to get this result. The impact of the relativistic light-cone treatment resides in the factor $(1 + k^2/m^2)^{-1/2}$. It induces a weak non-locality in the

effective Coulomb potential. Notice also that the solution of Eq. (4.117) is rotationally symmetric for the lowest state. Therefore, the original front form wavefunction $\langle x(k_z), \mathbf{k}_\perp | \psi \rangle$ in Eq. (4.116) cannot be rotationally symmetric. The deviations from rotational symmetry, however, are small and can occur only for $k^2 \gg m^2$, as can be observed in Fig. 14.

5. The impact on hadronic physics

In this section we discuss a number of novel applications of quantum chromodynamics to nuclear structure and dynamics, such as the reduced amplitude formalism for exclusive nuclear amplitudes. We particularly emphasize the importance of light-cone Hamiltonian and Fock state methods as a tool for describing the wavefunctions of composite relativistic many-body systems and their interactions. We also show that the use of covariant kinematics leads to non-trivial corrections to the standard formulae for the axial, magnetic, and quadrupole moments of nucleons and nuclei.

In principle, quantum chromodynamics can provide a fundamental description of hadron and nuclei structure and dynamics in terms of elementary quark and gluon degrees of freedom. In practice, the direct application of QCD to hadron and nuclear phenomena is extremely complex because of the interplay of non-perturbative effects such as color confinement and multi-quark coherence. Despite these challenging theoretical difficulties, there has been substantial progress in identifying specific QCD effects in nuclear physics. A crucial tool in these analyses is the use of relativistic light-cone quantum mechanics and Fock state methods in order to provide a tractable and consistent treatment of relativistic many-body effects. In some applications, such as exclusive processes at large momentum transfer, one can make first-principle predictions using factorization theorems which separate hard perturbative dynamics from the non-perturbative physics associated with hadron or nuclear binding. In other applications, such as the passage of hadrons through nuclear matter and the calculation of the axial, magnetic, and quadrupole moments of light nuclei, the QCD description provides new insights which go well beyond the usual assumptions of traditional nuclear physics.

5.1. Light-cone methods in QCD

In recent years quantization of quantum chromodynamics at fixed light-cone time $\tau = t - z/c$ has emerged as a promising method for solving relativistic bound-state problems in the strong coupling regime including nuclear systems. Light-cone quantization has a number of unique features that make it appealing, most notably, the ground state of the free theory is also a ground state of the full theory, and the Fock expansion constructed on this vacuum state provides a complete relativistic many-particle basis for diagonalizing the full theory. The light-cone wavefunctions $\psi_n(x_i, k_{\perp i}, \lambda_i)$, which describe the hadrons and nuclei in terms of their fundamental quark and gluon degrees of freedom, are frame-independent. The essential variables are the boost-invariant light-cone momentum fractions $x_i = p_i^+ / P^+$, where P^μ and p_i^μ are the hadron and quark or gluon momenta, respectively, with $P^\pm = P^0 \pm P^z$. The internal transverse momentum variables $\mathbf{k}_{\perp i}$ are given by $\mathbf{k}_{\perp i} = \mathbf{p}_{\perp i} - x_i \mathbf{P}_\perp$ with the constraints $\sum \mathbf{k}_{\perp i} = 0$ and $\sum x_i = 1$, i.e., the light-cone momentum fractions x_i and $\mathbf{k}_{\perp i}$ are relative coordinates, and they describe the hadronic

system independent of its total four momentum p^μ . The entire spectrum of hadrons and nuclei and their scattering states is given by the set of eigenstates of the light-cone Hamiltonian H_{LC} of QCD. The Heisenberg problem takes the form

$$H_{\text{LC}}|\Psi\rangle = M^2|\Psi\rangle. \quad (5.1)$$

For example, each hadron has the eigenfunction $|\Psi_H\rangle$ of $H_{\text{LC}}^{\text{QCD}}$ with eigenvalue $M^2 = M_H^2$. If we could solve the light-cone Heisenberg problem for the proton in QCD, we could then expand its eigenstate on the complete set of quark and gluon eigensolutions $|n\rangle = |uud\rangle, |uudg\rangle, \dots$ of the free Hamiltonian H_{LC}^0 with the same global quantum numbers:

$$|\Psi_p\rangle = \sum_n |n\rangle \psi_n(x_i, k_{\perp i}, \lambda_i). \quad (5.2)$$

The ψ_n ($n = 3, 4, \dots$) are first-quantized amplitudes analogous to the Schrödinger wave function, but it is Lorentz-frame-independent. Particle number is generally not conserved in a relativistic quantum field theory. Thus, each eigenstate is represented as a sum over Fock states of arbitrary particle number and in QCD each hadron is expanded as second-quantized sums over fluctuations of color-singlet quark and gluon states of different momenta and number. The coefficients of these fluctuations are the light-cone wavefunctions $\psi_n(x_i, k_{\perp i}, \lambda_i)$. The invariant mass \mathcal{M} of the partons in a given Fock state can be written in the elegant form $\mathcal{M}^2 = \sum_{i=1}^3 (\mathbf{k}_{\perp i}^2 + m_i^2)/x_i$. The dominant configurations in the wavefunction are generally those with minimum values of \mathcal{M}^2 . Note that except for the case $m_i = 0$ and $\mathbf{k}_{\perp i} = \mathbf{0}$, the limit $x_i \rightarrow 0$ is an ultraviolet limit; i.e. it corresponds to particles moving with infinite momentum in the negative z direction: $k_i^z \rightarrow -k_i^0 \rightarrow -\infty$.

In the case of QCD in one-space and one-time dimensions, the application of discretized light-cone quantization [66], see Section 4, provides complete solutions of the theory, including the entire spectrum of mesons, baryons, and nuclei, and their wavefunctions [227]. In the DLCQ method, one simply diagonalizes the light-cone Hamiltonian for QCD on a discretized Fock state basis. The DLCQ solutions can be obtained for arbitrary parameters including the number of flavors and colors and quark masses. More recently, DLCQ has been applied to new variants of QCD(1 + 1) with quarks in the adjoint representation, thus obtaining color-singlet eigenstates analogous to gluonium states [115].

The DLCQ method becomes much more numerically intense when applied to physical theories in 3 + 1 dimensions; however, progress is being made. An analysis of the spectrum and light-cone wavefunctions of positronium in QED(3 + 1) is given in Ref. [279]. Currently, Hiller et al. [222] are pursuing a non-perturbative calculation of the lepton anomalous moment in QED using this method. Burkardt has recently solved scalar theories with transverse dimensions by combining a Monte Carlo lattice method with DLCQ [79].

Given the light-cone wavefunctions, $\psi_{n/H}(x_i, \mathbf{k}_{\perp i}, \lambda_i)$, one can compute virtually any hadronic quantity by convolution with the appropriate quark and gluon matrix elements. For example, the leading-twist structure functions measured in deep inelastic lepton scattering are immediately related to the light-cone probability distributions:

$$2MF_1(x, Q) = \frac{F_2(x, Q)}{x} \approx \sum_a e_a^2 G_{a/p}(x, Q), \quad (5.3)$$

where

$$G_{a/p}(x, Q) = \sum_{n, \lambda_i} \int \prod_i \frac{dx_i d^2 \mathbf{k}_{\perp i}}{16\pi^3} |\psi_n^{(Q)}(x_i, \mathbf{k}_{\perp i}, \lambda_i)|^2 \sum_{b=a} \delta(x_b - x) \quad (5.4)$$

is the number density of partons of type a with longitudinal momentum fraction x in the proton. This follows from the observation that deep-inelastic lepton scattering in the Bjorken-scaling limit occurs if x_{bj} matches the light-cone fraction of the struck quark. (The \sum_b is over all partons of type a in state n .) However, the light cone wavefunctions contain much more information for the final state of deep-inelastic scattering, such as the multi-parton distributions, spin and flavor correlations, and the spectator jet composition.

As was first shown by Drell and Yan [133], it is advantageous to choose a coordinate frame where $q^+ = 0$ to compute form factors $F_i(q^2)$, structure functions, and other current matrix elements at space-like photon momentum. With such a choice the quark current cannot create or annihilate pairs, and $\langle p' | j^+ | p \rangle$ can be computed as a simple overlap of Fock space wavefunctions; all off-diagonal terms involving pair production or annihilation by the current or vacuum vanish. In the interaction picture, one can equate the full Heisenberg current to the quark current described by the free Hamiltonian at $\tau = 0$. Accordingly, the form factor is easily expressed in terms of the pion's light cone wavefunctions by examining the $\mu = +$ component of this equation in a frame where the photon's momentum is transverse to the incident pion momentum, with $q_{\perp}^2 = Q^2 = -q^2$. The space-like form factor is then just a sum of overlap integrals analogous to the corresponding non-relativistic formula [133] (See Fig. 17)

$$F(q^2) = \sum_{n, \lambda_i} \sum_a e_a \int \prod_i \frac{dx_i d^2 \mathbf{k}_{\perp i}}{16\pi^3} \psi_n^{(A)*}(x_i, \ell_{\perp i}, \lambda_i) \psi_n^{(A)}(x_i, \mathbf{k}_{\perp i}, \lambda_i). \quad (5.5)$$

Here e_a is the charge of the struck quark, $A^2 \gg q_{\perp}^2$, and

$$\ell_{\perp i} \equiv \begin{cases} \mathbf{k}_{\perp i} - x_i \mathbf{q}_{\perp} + \mathbf{q}_{\perp} & \text{for the struck quark,} \\ \mathbf{k}_{\perp i} - x_i \mathbf{q}_{\perp} & \text{for all other partons.} \end{cases} \quad (5.6)$$

Notice that the transverse momenta appearing as arguments of the first wavefunctions correspond not to the actual momenta carried by the partons but to the actual momenta minus $x_i \mathbf{q}_{\perp}$, to account for the motion of the final hadron. Notice also that ℓ_{\perp} and \mathbf{k}_{\perp} become equal as $\mathbf{q}_{\perp} \rightarrow 0$, and that $F_{\pi} \rightarrow 1$ in this limit due to wavefunctions normalization. All of the various form factors of hadrons with spin can be obtained by computing the matrix element of the plus current between states of different initial and final hadron helicities [39].

As we have emphasized above, in principle, the light-cone wavefunctions determine all properties of a hadron. The general rule for calculating an amplitude involving the wavefunctions $\psi_n^{(A)}$, describing Fock state n in a hadron with $\underline{P} = (P^+, \mathbf{P}_{\perp})$, has the form [62] (see Fig. 18)

$$\sum_{\lambda_i} \int \prod_i \frac{dx_i d^2 \mathbf{k}_{\perp i}}{\sqrt{x_i} 16\pi^3} \psi_n^{(A)}(x_i, \mathbf{k}_{\perp i}, \lambda_i) T_n^{(A)}(x_i P^+, x_i \mathbf{P}_{\perp} + \mathbf{k}_{\perp i}, \lambda_i), \quad (5.7)$$

where $T_n^{(A)}$ is the irreducible scattering amplitude in LCPT with the hadron replaced by Fock state n . If only the valence wavefunction is to be used, $T_n^{(A)}$ is irreducible with respect to the valence

Fock state only, e.g. $T_n^{(A)}$ for a pion has no $q\bar{q}$ intermediate states. Otherwise, contributions from all

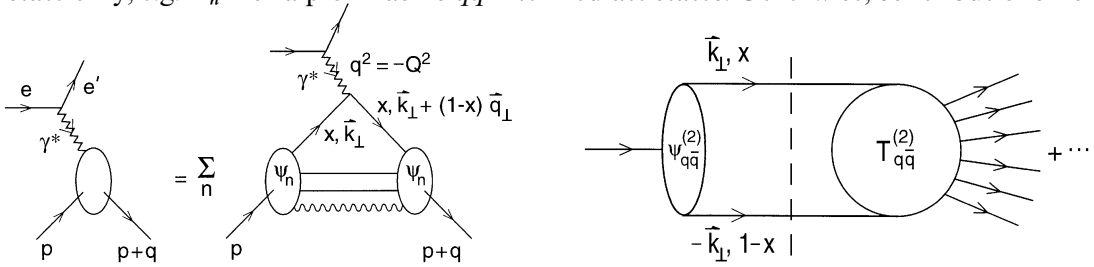


Fig. 17. Calculation of the form factor of a bound state from the convolution of light-cone Fock amplitudes. The result is exact if one sums over all ψ_n .

Fig. 18. Calculation of hadronic amplitudes in the light-cone Fock formalism.

Fock states must be summed, and $T_n^{(A)}$ is completely irreducible.

The leptonic decay of the π^\pm is one of the simplest processes to compute since it involves only the $q\bar{q}$ Fock state. The sole contribution to π^- decay is from

$$\begin{aligned} \langle 0 | \bar{\psi}_u \gamma^+ (1 - \gamma_5) \psi_d | \pi^- \rangle &= -\sqrt{2} P^+ f_\pi \\ &= \int \frac{dx d^2 \mathbf{k}_\perp}{16\pi^3} \psi_{d\bar{u}}^{(A)}(x, \mathbf{k}_\perp) \frac{\sqrt{n_c}}{\sqrt{2}} \left\{ \frac{\bar{v}_\downarrow}{\sqrt{1-x}} \gamma^+ (1 - \gamma_5) \frac{u_\uparrow}{\sqrt{x}} + (\uparrow \leftrightarrow \downarrow) \right\}, \end{aligned} \tag{5.8}$$

where $n_c = 3$ is the number of colors, $f_\pi \approx 93$ MeV, and where only the $L_z = S_z = 0$ component of the general $q\bar{q}$ wavefunction contributes. Thus, we have

$$\int \frac{dx d^2 \mathbf{k}_\perp}{16\pi^3} \psi_{d\bar{u}}^{(A)}(x, \mathbf{k}_\perp) = \frac{f_\pi}{2\sqrt{3}}. \tag{5.9}$$

This result must be independent of the ultraviolet cutoff Λ of the theory provided Λ is large compared with typical hadronic scales. This equation is an important constraint upon the normalization of the $d\bar{u}$ wavefunction. It also shows that there is a finite probability for finding a π^- in a pure $d\bar{u}$ Fock state.

The fact that a hadron can have a non-zero projection on a Fock state of fixed particle number seems to conflict with the notion that bound states in QCD have an infinitely recurring parton substructure, both from the infrared region (from soft gluons) and the ultraviolet regime (from QCD evolution to high momentum). In fact, there is no conflict. Because of coherent color-screening in the color-singlet hadrons, the infrared gluons with wavelength longer than the hadron size decouple from the hadron wavefunction.

The question of parton substructure is related to the resolution scale or ultraviolet cut-off of the theory. Any renormalizable theory must be defined by imposing an ultraviolet cutoff Λ on the momenta occurring in theory. The scale Λ is usually chosen to be much larger than the physical scales μ of interest; however it is usually more useful to choose a smaller value for Λ , but at the

expense of introducing new higher-twist terms in an effective Lagrangian: [301]

$$\mathcal{L}^{(A)} = \mathcal{L}_0^{(A)}(\alpha_s(A), m(A)) + \sum_{n=1}^N (1/A)^n \delta \mathcal{L}_n^{(A)}(\alpha_s(A), m(A)) + \mathcal{O}(1/A)^{N+1}, \quad (5.10)$$

where

$$\mathcal{L}_0^{(A)} = -\frac{1}{4} F_{a\mu\nu}^{(A)} F_n^{(A)a\mu\nu} + \bar{\psi}^{(A)} [i\not{D}^{(A)} - m(A)] \psi^{(A)}. \quad (5.11)$$

The neglected physics of parton momenta and substructure beyond the cutoff scale has the effect of renormalizing the values of the input coupling constant $g(A^2)$ and the input mass parameter $m(A^2)$ of the quark partons in the Lagrangian.

One clearly should choose A large enough to avoid large contributions from the higher-twist terms in the effective Lagrangian, but small enough so that the Fock space domain is minimized. Thus, if A is chosen of order 5–10 times the typical QCD momentum scale, then it is reasonable to hope that the mass, magnetic moment and other low momentum properties of the hadron could be well-described on a Fock basis of limited size. Furthermore, by iterating the equations of motion, one can construct a relativistic Schrödinger equation with an effective potential acting on the valence lowest-particle number state wavefunction [297,298]. Such a picture would explain the apparent success of constituent quark models for explaining the hadronic spectrum and low-energy properties of hadron.

It should be emphasized that infinitely growing parton content of hadrons due to the evolution of the deep inelastic structure functions at increasing momentum transfer, is associated with the renormalization group substructure of the quarks themselves, rather than the “intrinsic” structure of the bound state wavefunction [63,65]. The fact that the light-cone kinetic energy $\langle (\mathbf{k}_\perp^2 + m^2)/x \rangle$ of the constituents in the bound state is bounded by A^2 excludes singular behavior of the Fock wavefunctions at $x \rightarrow 0$. There are several examples where the light-cone Fock structure of the bound-state solutions is known. In the case of the super-renormalizable gauge theory, QED(1 + 1), the probability of having non-valence states in the light-cone expansion of the lowest lying meson and baryon eigenstates to be less than 10^{-3} , even at very strong coupling [227]. In the case of QED(3 + 1), the lowest state of positronium can be well described on a light-cone basis with two to four particles, $|e^+e^- \rangle$, $|e^+e^-\gamma \rangle$, $|e^+e^-\gamma\gamma \rangle$, and $|e^+e^-e^+e^- \rangle$; in particular, the description of the Lambshift in positronium requires the coupling of the system to light-cone Fock states with two photons “in flight” in light-cone gauge. The ultraviolet cut-off scale A only needs to be taken large compared to the electron mass. On the other hand, a charged particle such as the electron does not have a finite Fock decomposition, unless one imposes an artificial infrared cut-off.

We thus expect that a limited light-cone Fock basis should be sufficient to represent bound color-singlet states of heavy quarks in QCD(3 + 1) because of the coherent color cancelations and the suppressed amplitude for transversely polarized gluon emission by heavy quarks. However, the description of light hadrons is undoubtedly much more complex due to the likely influence of chiral symmetry breaking and zero-mode gluons in the light-cone vacuum. We return to this problem later.

Even without solving the QCD light-cone equations of motion, we can anticipate some general features of the behavior of the light-cone wavefunctions. Each Fock component describes a system of free particles with kinematic invariant mass squared:

$$\mathcal{M}^2 = \sum_i^n (\mathbf{k}_{\perp i}^2 + m_i^2)/x_i. \quad (5.12)$$

On general dynamical grounds, we can expect that states with very high \mathcal{M}^2 are suppressed in physical hadrons, with the highest mass configurations computable from perturbative considerations. We also note that $\ln x_i = \ln(k^0 + k^z)_i / (P^0 + P^z) = y_i - y_P$ is the rapidity difference between the constituent with light-cone fraction x_i and the rapidity of the hadron itself. Since correlations between particles rarely extend over two units of rapidity in hadron physics, this argues that constituents which are correlated with the hadron's quantum numbers are primarily found with $x > 0.2$.

The limit $x \rightarrow 0$ is normally an ultraviolet limit in a light-cone wavefunction. Recall, that in any Lorentz frame, the light-cone fraction is $x = k^+ / p^+ = (k^0 + k^z) / (P^0 + P^z)$. Thus in a frame where the bound state is moving infinitely fast in the positive z direction (“the infinite momentum frame”), the light-cone fraction becomes the momentum fraction $x \rightarrow k^z / p^z$. However, in the rest frame $\mathbf{P} = \mathbf{0}$, $x = (k^0 + k^z) / M$. Thus, $x \rightarrow 0$ generally implies very large constituent momentum $k^z \rightarrow -k^0 \rightarrow -\infty$ in the rest frame; it is excluded by the ultraviolet regulation of the theory – unless the particle has strictly zero mass and transverse momentum.

If a particle has non-relativistic momentum in the bound state, then we can identify $k^z \sim xM - m$. This correspondence is useful when one matches physics at the relativistic/non-relativistic interface. In fact, any non-relativistic solution to the Schrödinger equation can be immediately written in light-cone form by identifying the two forms of coordinates. For example, the Schrödinger solution for particles bound in a harmonic oscillator potential can be taken as a model for the light-cone wavefunction for quarks in a confining linear potential [299]:

$$\psi(x_i, \mathbf{k}_{\perp i}) = A \exp(-b\mathcal{M}^2) = \exp\left(-b \sum_i^n \frac{k_{\perp i}^2 + m_i^2}{x_i}\right). \quad (5.13)$$

This form exhibits the strong fall-off at large relative transverse momentum and at the $x \rightarrow 0$ and $x \rightarrow 1$ endpoints expected for soft non-perturbative solutions in QCD. The perturbative corrections due to hard gluon exchange give amplitudes suppressed only by power laws and thus will eventually dominate wave function behavior over the soft contributions in these regions. This ansatz is the central assumption required to derive dimensional counting perturbative QCD predictions for exclusive processes at large momentum transfer and the $x \rightarrow 1$ behavior of deep-inelastic structure functions. A review is given in Ref. [62]. A model for the polarized and unpolarized gluon distributions in the proton which takes into account both perturbative QCD constraints at large x and coherent cancelations at low x and small transverse momentum is given in Refs. [63,65].

The light-cone approach to QCD has immediate application to nuclear systems: The formalism provides a covariant many-body description of nuclear systems formally similar to non-relativistic many-body theory.

One can derive rigorous predictions for the leading power-law fall-off of nuclear amplitudes, including the nucleon–nucleon potential, the deuteron form factor, and the distributions of nucleons within nuclei at large momentum fraction. For example, the leading electro-magnetic form factor of the deuteron falls as $F_d(Q^2) = f(\alpha_s(Q^2)) / (Q^2)^5$, where, asymptotically, $f(\alpha_s(Q^2)) \propto \alpha_s(Q^2)^{5+\gamma}$. The leading anomalous dimension γ is computed in Ref. [59].

In general, the six-quark Fock state of the deuteron is a mixture of five different color-singlet states. The dominant color configuration of the six quarks corresponds to the usual proton–neutron bound state. However, as Q^2 increases, the deuteron form factor becomes sensitive to

deuteron wavefunction configurations where all six quarks overlap within an impact separation $b^{\perp i} < \mathcal{O}(1/Q)$. In the asymptotic domain, all five Fock color-singlet components acquire equal weight; i.e., the deuteron wavefunction becomes 80% “hidden color” at short distances. The derivation of the evolution equation for the deuteron distribution amplitude is given in Refs. [59,249].

QCD predicts that Fock components of a hadron with a small color dipole moment can pass through nuclear matter without interactions [36,60]; see also [334]. Thus, in the case of large momentum transfer reactions where only small-size valence Fock state configurations enter the hard scattering amplitude, both the initial and final state interactions of the hadron states become negligible. There is now evidence for QCD “color transparency” in exclusive virtual photon ρ production for both nuclear coherent and incoherent reactions in the E665 experiment at Fermilab [141], as well as the original measurement at BNL in quasi-elastic pp scattering in nuclei [216]. The recent NE18 measurement of quasielastic electron–proton scattering at SLAC finds results which do not clearly distinguish between conventional Glauber theory predictions and PQCD color transparency [320].

In contrast to color transparency, Fock states with large-scale color configurations strongly interact with high particle number production [42].

The traditional nuclear physics assumption that the nuclear form factor factorizes in the form $F_A(Q^2) = \sum_N F_N(Q^2) F_{N/A}^{\text{body}}(Q^2)$, where $F_N(Q^2)$ is the on-shell nucleon form factor is in general incorrect. The struck nucleon is necessarily off-shell, since it must transmit momentum to align the spectator nucleons along the direction of the recoiling nucleus.

Nuclear form factors and scattering amplitudes can be factored in the form given by the reduced amplitude formalism [55], which follows from the cluster decomposition of the nucleus in the limit of zero nuclear binding. The reduced form factor formalism takes into account the fact that each nucleon in an exclusive nuclear transition typically absorbs momentum $Q_N \simeq Q/N$. Tests of this formalism are discussed in a later section.

The use of covariant kinematics leads to a number of striking conclusions for the electromagnetic and weak moments of nucleons and nuclei. For example, magnetic moments cannot be written as the naive sum $\mu = \sum \mu_i$ of the magnetic moments of the constituents, except in the non-relativistic limit where the radius of the bound state is much larger than its Compton scale: $R_A M_A \gg 1$. The deuteron quadrupole moment is in general non-zero even if the nucleon–nucleon bound state has no D-wave component [58]. Such effects are due to the fact that even “static” moments have to be computed as transitions between states of different momentum p^μ and $p^\mu + q^\mu$ with $q^\mu \rightarrow 0$. Thus, one must construct current matrix elements between boosted states. The Wigner boost generates non-trivial corrections to the current interactions of bound systems [51].

One can also use light-cone methods to show that the proton’s magnetic moment μ_p and its axial-vector coupling g_A have a relationship independent of the assumed form of the light-cone wave function [71]. At the physical value of the proton radius computed from the slope of the Dirac form factor, $R_1 = 0.76$ fm, one obtains the experimental values for both μ_p and g_A ; the helicity carried by the valence u and d quarks are each reduced by a factor $\simeq 0.75$ relative to their non-relativistic values. At infinitely small radius $R_p M_p \rightarrow 0$, μ_p becomes equal to the Dirac moment, as demanded by the Drell–Hearn–Gerasimov sum rule [174,129]. Another surprising fact is that as $R_1 \rightarrow 0$, the constituent quark helicities become completely disoriented and $g_A \rightarrow 0$. We discuss these features in more detail in the following section.

In the case of the deuteron, both the quadrupole and magnetic moments become equal to that of an elementary vector boson in the Standard Model in the limit $M_a R_a \rightarrow 0$. The three form factors of the deuteron have the same ratio as that of the W boson in the Standard Model [58].

The basic amplitude controlling the nuclear force, the nucleon–nucleon scattering amplitude can be systematically analyzed in QCD in terms of basic quark and gluon scattering subprocesses. The high momentum transfer behavior of the amplitude from dimensional counting is $\mathcal{M}_{pp \rightarrow pp} \simeq \int_{pp \rightarrow pp} (t/s)/t^4$ at fixed center of mass angle. A review is given in Ref. [62]. The fundamental subprocesses, including pinch contributions [289], can be classified as arising from both quark interchange and gluon exchange contributions. In the case of meson–nucleon scattering, the quark exchange graphs [43] can explain virtually all of the observed features of large momentum transfer fixed CM angle scattering distributions and ratios [90]. The connection between Regge behavior and fixed angle scattering in perturbative QCD for quark exchange reactions is discussed in Ref. [69]. Sotiropoulos and Sterman [407] have shown how one can consistently interpolate from fixed angle scaling behavior to the $1/t^8$ scaling behavior of the elastic cross section in the $s \gg -t$, large $-t$ regime.

One of the most striking anomalies in elastic proton–proton scattering is the large spin correlation A_{NN} observed at large angles [280]. At $\sqrt{s} \simeq 5$ GeV, the rate for scattering with incident proton spins parallel and normal to the scattering plane is four times larger than scattering with anti-parallel polarization. This phenomena in elastic pp scattering can be explained as the effect due to the onset of charm production in the intermediate state at this energy [61]. The intermediate state $|uud\bar{u}dc\bar{c}\rangle$ has odd intrinsic parity and couples to the $J = S = 1$ initial state, thus strongly enhancing scattering when the incident projectile and target protons have their spins parallel and normal to the scattering plane.

The simplest form of the nuclear force is the interaction between two heavy quarkonium states, such as the $\Upsilon(b\bar{b})$ and the $J/\psi(c\bar{c})$. Since there are no valence quarks in common, the dominant color-singlet interaction arises simply from the exchange of two or more gluons, the analog of the van der Waals molecular force in QED. In principle, one could measure the interactions of such systems by producing pairs of quarkonia in high energy hadron collisions. The same fundamental QCD van der Waals potential also dominates the interactions of heavy quarkonia with ordinary hadrons and nuclei. As shown in Ref. [313], the small size of the $Q\bar{Q}$ bound state relative to the much larger hadron sizes allows a systematic expansion of the gluonic potential using the operator product potential. The matrix elements of multigluon exchange in the quarkonium state can be computed from non-relativistic heavy quark theory. The coupling of the scalar part of the interaction to large-size hadrons is rigorously normalized to the mass of the state via the trace anomaly. This attractive potential dominates the interactions at low relative velocity. In this way, one establishes that the nuclear force between heavy quarkonia and ordinary nuclei is attractive and sufficiently strong to produce nuclear-bound quarkonium [64].

5.2. Moments of nucleons and nuclei in the light-cone formalism

Let us consider an effective three-quark light-cone Fock description of the nucleon in which additional degrees of freedom (including zero modes) are parameterized in an effective potential. After truncation, one could in principle obtain the mass M and light-cone wavefunction of the

three-quark bound states by solving the Hamiltonian eigenvalue problem. It is reasonable to assume that adding more quark and gluonic excitations will only refine this initial approximation [363]. In such a theory the constituent quarks will also acquire effective masses and form factors. However, even without explicit solutions, one knows that the helicity and flavor structure of the baryon eigenfunctions will reflect the assumed global SU(6) symmetry and Lorentz invariance of the theory. Since we do not have an explicit representation for the effective potential in the light-cone Hamiltonian $H_{\text{LC}}^{\text{effective}}$ for three-quarks, we shall proceed by making an ansatz for the momentum space structure of the wavefunction Ψ . As we will show below, for a given size of the proton, the predictions and interrelations between observables at $Q^2 = 0$, such as the proton magnetic moment μ_p and its axial coupling g_A , turn out to be essentially independent of the shape of the wavefunction [71].

The light-cone model given in Refs. [395–397] provides a framework for representing the general structure of the effective three-quark wavefunctions for baryons. The wavefunction Ψ is constructed as the product of a momentum wavefunction, which is spherically symmetric and invariant under permutations, and a spin–isospin wavefunction, which is uniquely determined by SU(6)-symmetry requirements. A Wigner–Melosh [450,332] rotation is applied to the spinors, so that the wavefunction of the proton is an eigenfunction of J and J_z in its rest frame [105,68]. To represent the range of uncertainty in the possible form of the momentum wave function, we shall choose two simple functions of the invariant mass \mathcal{M} of the quarks:

$$\psi_{\text{HO}}(\mathcal{M}^2) = N_{\text{HO}} \exp(-\mathcal{M}^2/2\beta^2), \quad \psi_{\text{Power}}(\mathcal{M}^2) = N_{\text{Power}}(1 + \mathcal{M}^2/\beta^2)^{-p}, \quad (5.14)$$

where β sets the characteristic internal momentum scale. Perturbative QCD predicts a nominal power-law fall off at large k_{\perp} corresponding to $p = 3.5$ [299,395–398]. The Melosh rotation insures that the nucleon has $j = \frac{1}{2}$ in its rest system. It has the matrix representation [332]

$$R_M(x_i, k_{\perp i}, m) = \frac{m + x_i \mathcal{M} - \mathbf{i}\sigma \cdot (\mathbf{n} \times \mathbf{k}_i)}{\sqrt{(m + x_i \mathcal{M})^2 + \mathbf{k}_{\perp i}^2}} \quad (5.15)$$

with $\mathbf{n} = (0, 0, 1)$, and it becomes the unit matrix if the quarks are collinear $R_M(x_i, 0, m) = 1$. Thus, the internal transverse momentum dependence of the light-cone wavefunctions also affects its helicity structure [51].

The Dirac and Pauli form factors $F_1(Q^2)$ and $F_2(Q^2)$ of the nucleons are given by the spin-conserving and the spin-flip vector current J_V^+ matrix elements ($Q^2 = -q^2$) [61]

$$F_1(Q^2) = \langle p + q, \uparrow | J_V^+ | p, \uparrow \rangle, \quad (5.16)$$

$$(Q_1 - iQ_2)F_2(Q^2) = -2M \langle p + q, \uparrow | J_V^+ | p, \downarrow \rangle. \quad (5.17)$$

We can then calculate the anomalous magnetic moment $a = \lim_{Q^2 \rightarrow 0} F_2(Q^2)$. [The total proton magnetic moment is $\mu_p = (e/2M)(1 + a_p)$.] The same parameters as in Ref. [396] are chosen; namely $m = 0.263$ GeV (0.26 GeV) for the up- and down-quark masses, and $\beta = 0.607$ GeV (0.55 GeV) for $\psi_{\text{Power}}(\psi_{\text{HO}})$ and $p = 3.5$. The quark currents are taken as elementary currents with Dirac moments $e_q/2m_q$. All of the baryon moments are well-fit if one takes the strange quark mass as 0.38 GeV. With the above values, the proton magnetic moment is 2.81 nuclear magnetons, the neutron magnetic moment is -1.66 nuclear magnetons. (The neutron value can be improved by

relaxing the assumption of isospin symmetry.) The radius of the proton is 0.76 fm, i.e., $M_p R_1 = 3.63$.

In Fig. 19 we show the functional relationship between the anomalous moment a_p and its Dirac radius predicted by the three-quark light-cone model. The value of $R_1^2 = -6dF_1(Q^2)/dQ^2|_{Q^2=0}$ is varied by changing β in the light-cone wave function while keeping the quark mass m fixed. The prediction for the power-law wavefunction ψ_{Power} is given by the broken line; the continuous line represents ψ_{HO} . Fig. 19 shows that when one plots the dimensionless observable a_p against the dimensionless observable MR_1 the prediction is essentially independent of the assumed power-law or Gaussian form of the three-quark light-cone wavefunction. Different values of $p > 2$ also do not affect the functional dependence of $a_p(M_p R_1)$ shown in Fig. 19. In this sense the predictions of the three-quark light-cone model relating the $Q^2 \rightarrow 0$ observables are essentially model-independent. The only parameter controlling the relation between the dimensionless observables in the light-cone three-quark model is m/M_p which is set to 0.28. For the physical proton radius $M_p R_1 = 3.63$ one obtains the empirical value for $a_p = 1.79$ (indicated by the dotted lines in Fig. 19).

The prediction for the anomalous moment a can be written analytically as $a = \langle \gamma_V \rangle a^{\text{NR}}$, where $a^{\text{NR}} = 2M_p/3m$ is the non-relativistic ($R \rightarrow \infty$) value and γ_V is given as [103]

$$\gamma_V(x_i, k_{\perp i}, m) = \frac{3m}{\mathcal{M}} \left[\frac{(1-x_3)\mathcal{M}(m+x_3\mathcal{M}) - \mathbf{k}_{\perp 3}^2/2}{(m+x_3\mathcal{M})^2 + \mathbf{k}_{\perp 3}^2} \right]. \quad (5.18)$$

The expectation value $\langle \gamma_V \rangle$ is evaluated as

$$\langle \gamma_V \rangle = \frac{\int [d^3k] \gamma_V |\psi|^2}{\int [d^3k] |\psi|^2}, \quad (5.19)$$

where $[d^3k] = d\mathbf{k}_1 d\mathbf{k}_2 d\mathbf{k}_3 \delta(\mathbf{k}_1 + \mathbf{k}_2 + \mathbf{k}_3)$. The third component of \mathbf{k} is defined as $k_{3i} = \frac{1}{2}(x_i \mathcal{M} - (m^2 + \mathbf{k}_{\perp i}^2)/x_i \mathcal{M})$. This measure differs from the usual one used in Ref. [299] by the Jacobian $[[dk_{3i}/dx_i]$ which can be absorbed into the wavefunction.

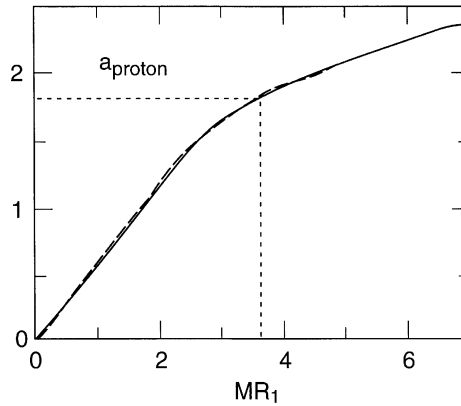


Fig. 19. The anomalous magnetic moment $a = F_2(0)$ of the proton as a function of $M_p R_1$: broken line, pole type wavefunction; continuous line, Gaussian wavefunction. The experimental value is given by the dotted lines. The prediction of the model is independent of the wavefunction for $Q^2 = 0$.

Let us take a closer look at the two limits $R \rightarrow \infty$ and $R \rightarrow 0$. In the non-relativistic limit we let $\beta \rightarrow 0$ and keep the quark mass m and the proton mass M_p fixed. In this limit the proton radius $R_1 \rightarrow \infty$ and $a_p \rightarrow 2M_p/3m = 2.38$ since $\langle \gamma_V \rangle \rightarrow 1$. (This differs slightly from the usual non-relativistic formula $1 + a = \sum_q (e_q/e) M_p/m_q$ due to the non-vanishing binding energy which results in $M_p \neq 3m_q$.) Thus, the physical value of the anomalous magnetic moment at the empirical proton radius $M_p R_1 = 3.63$ is reduced by 25% from its non-relativistic value due to relativistic recoil and nonzero k_\perp (The non-relativistic value of the neutron magnetic moment is reduced by 31%.)

To obtain the ultra-relativistic limit, we let $\beta \rightarrow \infty$ while keeping m fixed. In this limit the proton becomes pointlike ($M_p R_1 \rightarrow 0$) and the internal transverse momenta $k_\perp \rightarrow \infty$. The anomalous magnetic momentum of the proton goes linearly to zero as $a = 0.43 M_p R_1$ since $\langle \gamma_V \rangle \rightarrow 0$. Indeed, the Drell–Hearn–Gerasimov sum rule [174,129] demands that the proton magnetic moment becomes equal to the Dirac moment at small radius. For a spin- $\frac{1}{2}$ system

$$a^2 = \frac{M^2}{2\pi^2\alpha} \int_{s_{\text{th}}}^{\infty} \frac{ds}{s} [\sigma_P(s) - \sigma_A(s)], \quad (5.20)$$

where $\sigma_{P(A)}$ is the total photo-absorption cross section with parallel (anti-parallel) photon and target spins. If we take the point-like limit, such that the threshold for inelastic excitation becomes infinite while the mass of the system is kept finite, the integral over the photo-absorption cross section vanishes and $a = 0$ [61]. In contrast, the anomalous magnetic moment of the proton does not vanish in the non-relativistic quark model as $R \rightarrow 0$. The non-relativistic quark model does not take into account the fact that the magnetic moment of a baryon is derived from lepton scattering at non-zero momentum transfer, i.e. the calculation of a magnetic moment requires knowledge of the boosted wave function. The Melosh transformation is also essential for deriving the DHG sum rule and low energy theorems of composite systems [51].

A similar analysis can be performed for the axial-vector coupling measured in neutron decay. The coupling g_A is given by the spin-conserving axial current J_A^+ matrix element $g_A(0) = \langle p, \uparrow | J_A^+ | p, \uparrow \rangle$. The value for g_A can be written as $g_A = \langle \gamma_A \rangle g_A^{\text{NR}}$ with g_A^{NR} being the non-relativistic value of g_A and with γ_A as [103,316]

$$\gamma_A(x_i, k_{\perp i}, m) = \frac{(m + x_3 \mathcal{M})^2 - \mathbf{k}_{\perp 3}^2}{(m + x_3 \mathcal{M})^2 + \mathbf{k}_{\perp 3}^2}. \quad (5.21)$$

In Fig. 20a since $\langle \gamma_A \rangle = 0.75$, the measured value is $g_A = 1.2573 \pm 0.0028$ [351]. This is a 25% reduction compared to the non-relativistic SU(6) value $g_A = 5/3$, which is only valid for a proton with large radius $R_1 \gg 1/M_p$. As shown in Ref. [316], the Melosh rotation generated by the internal transverse momentum spoils the usual identification of the $\gamma^+ \gamma_5$ quark current matrix element with the total rest-frame spin projection s_z , thus resulting in a reduction of g_A .

Thus, given the empirical values for the proton's anomalous moment a_p and radius $M_p R_1$, its axial-vector coupling is automatically fixed at the value $g_A = 1.25$. This prediction is an essentially model-independent prediction of the three-quark structure of the proton in QCD. The Melosh rotation of the light-cone wavefunction is crucial for reducing the value of the axial coupling from its non-relativistic value $5/3$ to its empirical value. In Fig. 20b we plot $g_A/g_A(R_1 \rightarrow \infty)$ versus $a_p/a_p(R_1 \rightarrow \infty)$ by varying the proton radius R_1 . The near equality of these ratios reflects the relativistic spinor structure of the nucleon bound state, which is essentially independent of the

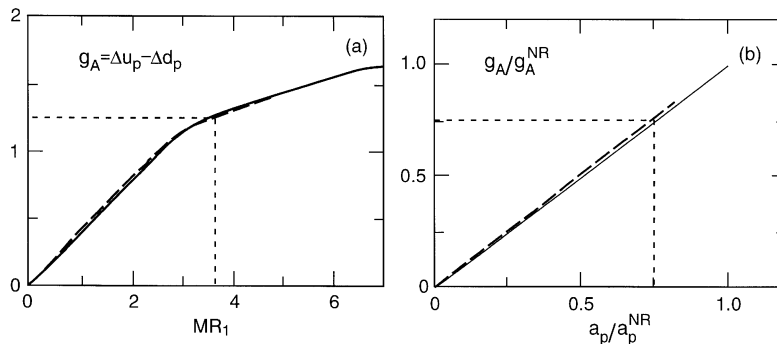


Fig. 20. (a) The axial vector coupling g_A of the neutron to proton decay as a function of $M_p R_1$. The experimental value is given by the dotted lines. (b) The ratio $g_A/g_A(R_1 \rightarrow \infty)$ versus $a_p/a_p(R_1 \rightarrow \infty)$ as a function of the proton radius R_1 .

detailed shape of the momentum-space dependence of the light-cone wave function. We emphasize that at small proton radius the light-cone model predicts not only a vanishing anomalous moment but also $\lim_{R_1 \rightarrow 0} g_A(M_p R_1) = 0$. One can understand this physically: in the zero radius limit the internal transverse momenta become infinite and the quark helicities become completely dis-oriented. This is in contradiction with chiral models which suggest that for a zero radius composite baryon one should obtain the chiral symmetry result $g_A = 1$.

The helicity measures Δu and Δd of the nucleon each experience the same reduction as g_A due to the Melosh effect. Indeed, the quantity Δq is defined by the axial current matrix element

$$\Delta q = \langle p, \uparrow | \bar{q} \gamma^+ \gamma_5 q | p, \uparrow \rangle, \quad (5.22)$$

and the value for Δq can be written analytically as $\Delta q = \langle \gamma_A \rangle \Delta q^{\text{NR}}$ with Δq^{NR} being the non-relativistic or naive value of Δq and with γ_A .

The light-cone model also predicts that the quark helicity sum $\Delta \Sigma = \Delta u + \Delta d$ vanishes as a function of the proton radius R_1 . Since the helicity sum $\Delta \Sigma$ depends on the proton size, and thus it cannot be identified as the vector sum of the rest-frame constituent spins. As emphasized in Refs. [316,52], the rest-frame spin sum is not a Lorentz invariant for a composite system. Empirically, one measures Δq from the first moment of the leading twist polarized structure function $g_1(x, Q)$. In the light-cone and parton model descriptions, $\Delta q = \int_0^1 dx [q^\uparrow(x) - q^\downarrow(x)]$, where $q^\uparrow(x)$ and $q^\downarrow(x)$ can be interpreted as the probability for finding a quark or antiquark with longitudinal momentum fraction x and polarization parallel or anti-parallel to the proton helicity in the proton's infinite momentum frame [299]. (In the infinite momentum there is no distinction between the quark helicity and its spin-projection s_z .) Thus, Δq refers to the difference of helicities at fixed light-cone time or at infinite momentum; it cannot be identified with $q(s_z = +\frac{1}{2}) - q(s_z = -\frac{1}{2})$, the spin carried by each quark flavor in the proton rest frame in the equal time formalism.

Thus, the usual SU(6) values $\Delta u^{\text{NR}} = 4/3$ and $\Delta d^{\text{NR}} = -1/3$ are only valid predictions for the proton at large $M_p R_1$. At the physical radius the quark helicities are reduced by the same ratio 0.75 as g_A/g_A^{NR} due to the Melosh rotation. Qualitative arguments for such a reduction have been given in Refs. [266,151]. For $M_p R_1 = 3.63$, the three-quark model predicts $\Delta u = 1$, $\Delta d = -1/4$, and

$\Delta\Sigma = \Delta u + \Delta d = 0.75$. Although the gluon contribution $\Delta G = 0$ in our model, the general sum rule

$$\frac{1}{2}\Delta\Sigma + \Delta G + L_z = \frac{1}{2} \quad (5.23)$$

is still satisfied, since the Melosh transformation effectively contributes to L_z .

Suppose one adds polarized gluons to the three-quark light-cone model. Then the flavor-singlet quark-loop radiative corrections to the gluon propagator will give an anomalous contribution $\delta(\Delta q) = -(\alpha_s/2\pi)\Delta G$ to each light quark helicity. The predicted value of $g_A = \Delta u - \Delta d$ is of course unchanged. For illustration we shall choose $(\alpha_s/2\pi)\Delta G = 0.15$. The gluon-enhanced quark model then gives the values in Table 13, which agree well with the present experimental values. Note that the gluon anomaly contribution to Δs has probably been overestimated here due to the large strange quark mass. One could also envision other sources for this shift of Δq such as intrinsic flavor [151]. A specific model for the gluon helicity distribution in the nucleon bound state is given in Ref. [70].

In summary, we have shown that relativistic effects are crucial for understanding the spin structure of the nucleons. By plotting dimensionless observables against dimensionless observables we obtain model-independent relations independent of the momentum-space form of the three-quark light-cone wavefunctions. For example, the value of $g_A \simeq 1.25$ is correctly predicted from the empirical value of the proton's anomalous moment. For the physical proton radius $M_p R_1 = 3.63$ the inclusion of the Wigner (Melosh) rotation due to the finite relative transverse momenta of the three quarks results in a $\simeq 25\%$ reduction of the non-relativistic predictions for the anomalous magnetic moment, the axial vector coupling, and the quark helicity content of the proton. At zero radius, the quark helicities become completely disoriented because of the large internal momenta, resulting in the vanishing of g_A and the total quark helicity $\Delta\Sigma$.

5.3. Applications to nuclear systems

We can analyze a nuclear system in the same way as we did the nucleon in the preceding section. The triton, for instance, is modeled as a bound state of a proton and two neutrons. The same formulae as in the preceding section are valid (for spin- $\frac{1}{2}$ nuclei); we only have to use the appropriate parameters for the constituents.

The light-cone analysis yields non-trivial corrections to the moments of nuclei. For example, consider the anomalous magnetic moment a_d and anomalous quadrupole moment

Table 13

Comparison of the quark content of the proton in the non-relativistic quark model (NR), in the three-quark model (3q), in a gluon-enhanced three-quark model (3q + g), and with experiment

Quantity	NR	3q	3q + g	Experiment
Δu	$\frac{4}{3}$	1	0.85	0.83 ± 0.03
Δd	$-\frac{1}{3}$	$-\frac{1}{4}$	-0.40	-0.43 ± 0.03
Δs	0	0	-0.15	-0.10 ± 0.03
$\Delta\Sigma$	1	$\frac{3}{4}$	0.30	0.31 ± 0.07

$Q_d^a = Q_d + e/M_d^2$ of the deuteron. As shown in Ref. [432], these moments satisfy the sum rule

$$a_d^2 + \frac{2t}{M_d^2} \left(a_d + \frac{M_d Q_d^a}{2} \right)^2 = \frac{1}{4\pi} \int_{v_{th}^2}^{\infty} \frac{dv^2}{(v - t/4)^3} (\text{Im} f_P(v, t) - \text{Im} f_A(v, t)). \quad (5.24)$$

Here $f_{P(A)}(v, t)$ is the non-forward Compton amplitude for incident parallel (anti-parallel) photon–deuteron helicities. Thus, in the point-like limit where the threshold for particle excitation $v_{th} \rightarrow \infty$, the deuteron acquires the same electro-magnetic moments $Q_d^a \rightarrow 0, a_d \rightarrow 0$ as that of the W in the Standard Model [58]. The approach to zero anomalous magnetic and quadrupole moments for $R_d \rightarrow 0$ is shown in Figs. 21 and 22. Thus, even if the deuteron has no D-wave component, a non-zero quadrupole moment arises from the relativistic recoil correction. This correction, which is mandated by relativity, could cure a long-standing discrepancy between experiment and the traditional nuclear physics predictions for the deuteron quadrupole. Conventional nuclear theory predicts a quadrupole moment of 7.233 GeV^{-2} which is smaller than the experimental value $(7.369 \pm 0.039) \text{ GeV}^{-2}$. The light-cone calculation for a pure S-wave gives a positive contribution of 0.08 GeV^{-2} which accounts for most of the previous discrepancy.

In the case of the tritium nucleus, the value of the Gamow–Teller matrix element can be calculated in the same way as we calculated the axial vector coupling g_A of the nucleon in the previous section. The correction to the non-relativistic limit for the S-wave contribution is

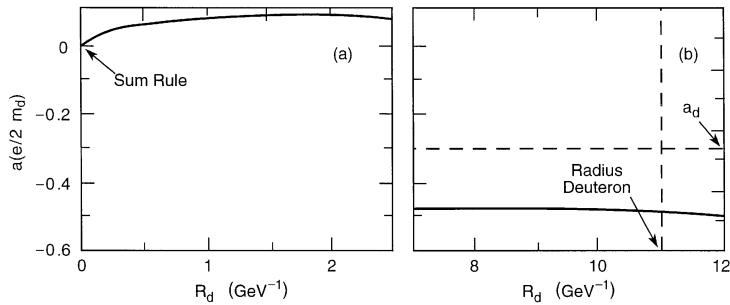


Fig. 21. The anomalous moment a_d of the deuteron as a function of the deuteron radius R_d . In the limit of zero radius, the anomalous moment vanishes.

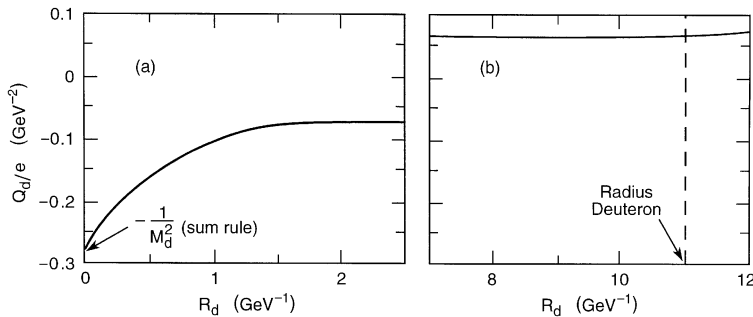


Fig. 22. The quadrupole moment Q_d of the deuteron as a function of the deuteron radius R_d . In the limit of zero radius, the quadrupole moment approaches its canonical value $Q_d = -e/M_d^2$.

$g_A = \langle \gamma_A \rangle g_A^{\text{NR}}$. For the physical quantities of the triton we get $\langle \gamma_A \rangle = 0.99$. This means that even at the physical radius, we find a non-trivial non-zero correction of order -0.01 to $g_A^{\text{triton}}/g_A^{\text{nucleon}}$ due to the relativistic recoil correction implicit in the light-cone formalism. The Gamow–Teller matrix element is measured to be 0.961 ± 0.003 . The wavefunction of the tritium (${}^3\text{H}$) is a superposition of a dominant S-state and small D- and S'-state components $\phi = \phi_S + \phi_{S'} + \phi_D$. The Gamow–Teller matrix element in the non-relativistic theory is then given by $g_A^{\text{triton}}/g_A^{\text{nucleon}} = (|\phi_S|^2 - \frac{1}{3}|\phi_{S'}|^2 + \frac{1}{3}|\phi_D|^2)(1 + 0.0589) = 0.974$, where the last term is a correction due to meson exchange currents. Fig. 23 shows that the Gamow–Teller matrix element of tritium must approach zero in the limit of small nuclear radius, just as in the case of the nucleon as a bound state of three quarks. This phenomenon is confirmed in the light-cone analysis.

5.4. Exclusive nuclear processes

One of the most elegant areas of application of QCD to nuclear physics is the domain of large momentum transfer exclusive nuclear processes [102]. Rigorous results for the asymptotic properties of the deuteron form factor at large momentum transfer are given in Ref. [59]. In the asymptotic limit $Q^2 \rightarrow \infty$ the deuteron distribution amplitude, which controls large momentum transfer deuteron reactions, becomes fully symmetric among the five possible color-singlet combinations of the six quarks. One can also study the evolution of the “hidden color” components (orthogonal to the np and $\Delta\Delta$ degrees of freedom) from intermediate to large momentum transfer scales; the results also give constraints on the nature of the nuclear force at short distances in QCD. The existence of hidden color degrees of freedom further illustrates the complexity of nuclear systems in QCD. It is conceivable that six-quark d^* resonances corresponding to these new degrees of freedom may be found by careful searches of the $\gamma^*d \rightarrow \gamma d$ and $\gamma^*d \rightarrow \pi d$ channels.

The basic scaling law for the helicity-conserving deuteron form factor, $F_d(Q^2) \sim 1/Q^{10}$, comes from simple quark counting rules, as well as perturbative QCD. One cannot expect this asymptotic prediction to become accurate until very large Q^2 since the momentum transfer has to be shared by at least six constituents. However, one can identify the QCD physics due to the compositeness of the nucleus, with respect to its nucleon degrees of freedom by using the reduced amplitude

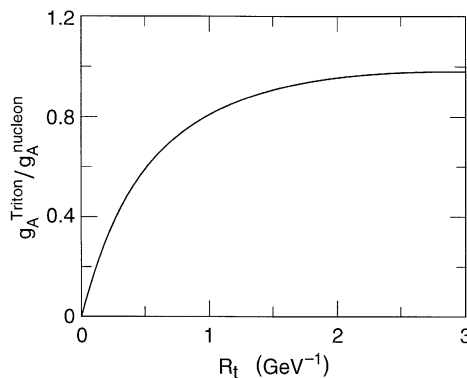


Fig. 23. The reduced Gamow–Teller matrix element for tritium decay as a function of the tritium radius.

formalism [68]. For example, consider the deuteron form factor in QCD. By definition this quantity is the probability amplitude for the deuteron to scatter from p to $p + q$ but remain intact.

Note that for vanishing nuclear binding energy $\varepsilon_d \rightarrow 0$, the deuteron can be regarded as two nucleons sharing the deuteron four-momentum (see Fig. 24a). In the zero-binding limit, one can show that the nuclear light-cone wavefunction properly decomposes into a product of uncorrelated nucleon wavefunctions [249,308]. The momentum ℓ is limited by the binding and can thus be neglected, and to first approximation, the proton and neutron share the deuteron's momentum equally. Since the deuteron form factor contains the probability amplitudes for the proton and neutron to scatter from $p/2$ to $p/2 + q/2$, it is natural to define the reduced deuteron form factor [68,59,249]:

$$f_d(Q^2) \equiv \frac{F_d(Q^2)}{F_{1N}(\frac{1}{4}Q^2)F_{1N}(\frac{1}{4}Q^2)}. \quad (5.25)$$

The effect of nucleon compositeness is removed from the reduced form factor. QCD then predicts the scaling

$$f_d(Q^2) \sim 1/Q^2, \quad (5.26)$$

i.e. the same scaling law as a meson form factor. Diagrammatically, the extra power of $1/Q^2$ comes from the propagator of the struck quark line, the one propagator not contained in the nucleon form factors. Because of hadron helicity conservation, the prediction is for the leading helicity-conserving deuteron form factor ($\lambda = \lambda' = 0$). As shown in Fig. 25, this scaling is consistent with experiment for $Q = p_T \sim 1$ GeV.

The data are summarized in Ref. [58]. The distinction between the QCD and other treatments of nuclear amplitudes is particularly clear in the reaction $\gamma d \rightarrow np$, i.e. photo-disintegration of the deuteron at fixed center of mass angle. Using dimensional counting [54], the leading power-law prediction from QCD is simply $(d\sigma/dt)(\gamma d \rightarrow np) \sim F(\theta_{cm})/s^{11}$. A comparison of the QCD prediction with the recent experiment of Ref. [31] is shown in Fig. 26, confirming the validity of the QCD scaling prediction up to $E_\gamma \simeq 3$ GeV. One can take into account much of the finite-mass, higher-twist corrections by using the reduced amplitude formalism [58]. The photo-disintegration

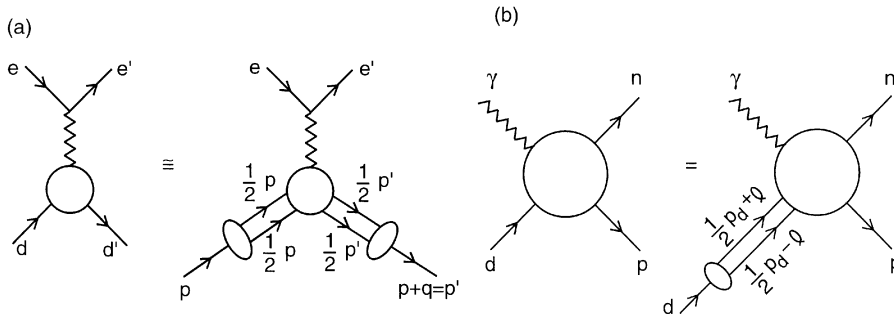


Fig. 24. (a) Application of the reduced amplitude formalism to the deuteron form factor at large momentum transfer. (b) Construction of the reduced nuclear amplitude for two-body inelastic deuteron reactions.

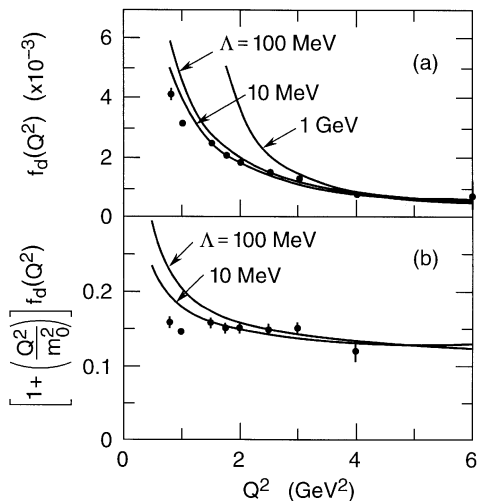
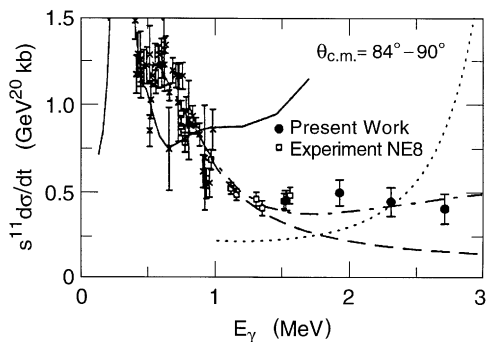


Fig. 25. Scaling of the deuteron reduced form factor.

Fig. 26. Comparison of deuteron photo-disintegration data with the scaling prediction which requires $s^{11}d\sigma/dt(s, \theta_{cm})$ to be at most logarithmically dependent on energy at large momentum transfer.

amplitude contains the probability amplitude (i.e. nucleon form factors) for the proton and neutron to each remain intact after absorbing momentum transfers $p_p - 1/2p_d$ and $p_n - 1/2p_d$, respectively (see Fig. 24b). After the form factors are removed, the remaining “reduced” amplitude should scale as $F(\theta_{cm})/p_T$. The single inverse power of transverse momentum p_T is the slowest conceivable in any theory, but it is the unique power predicted by PQCD.

The data and predictions from conventional nuclear theory are summarized in Ref. [133]. There are a number of related tests of QCD and reduced amplitudes which require \bar{p} beams [249], such as $\bar{p}d \rightarrow \gamma n$ and $\bar{p}d \rightarrow \pi p$ in the fixed θ_{cm} region. These reactions are particularly interesting tests of QCD in nuclei. Dimensional counting rules predict the asymptotic behavior $(d\sigma/dt)(\bar{p}d \rightarrow \pi p) \sim (1/(p_T^2)^{12})f(\theta_{cm})$ since there are 14 initial and final quanta involved. Again one notes that the $\bar{p}d \rightarrow \pi p$ amplitude contains a factor representing the probability amplitude (i.e. form factor) for the proton to remain intact after absorbing momentum transfer squared $\hat{t} = (p - 1/2p_d)^2$ and the $\bar{N}N$ time-like form factor at $\hat{s} = (\bar{p} + 1/2p_d)^2$. Thus, $\mathcal{M}_{\bar{p}d \rightarrow \pi p} \sim F_{1N}(\hat{t})F_{1N}(\hat{s})\mathcal{M}_r$, where \mathcal{M}_r has the same QCD scaling properties as quark meson scattering. One thus predicts

$$(d\sigma/d\Omega)(\bar{p}d \rightarrow \pi p)/F_{1N}^2(\hat{t})F_{1N}^2(\hat{s}) \sim f(\Omega)/p_T^2. \quad (5.27)$$

Other work has been done by Cardarelli et al. [86].

5.5. Conclusions

As we have emphasized in this section, QCD and relativistic light-cone Fock methods provide a new perspective on nuclear dynamics and properties. In many some cases the covariant approach fundamentally contradicts standard nuclear assumptions. More generally, the synthesis of QCD with the standard non-relativistic approach can be used to constrain the analytic form and

unknown parameters in the conventional theory, as in Bohr's correspondence principle. For example, the reduced amplitude formalism and PQCD scaling laws provide analytic constraints on the nuclear amplitudes and potentials at short distances and large momentum transfers.

6. Exclusive processes and light-cone wavefunctions

One of the major advantages of the light-cone formalism is that many properties of large momentum transfer exclusive reactions can be calculated without explicit knowledge of the form of the non-perturbative light-cone wavefunctions. The main ingredients of this analysis are asymptotic freedom, and the power-law scaling relations and quark helicity conservation rules of perturbative QCD. For example, consider the light-cone expression (5.5) for a meson form factor at high momentum transfer Q^2 . If the internal momentum transfer is large then one can iterate the gluon-exchange term in the effective potential for the light-cone wavefunctions. The result is that the hadron form factors can be written in a factorized form as a convolution of quark "distribution amplitudes" $\phi(x_i, Q)$, one for each hadron involved in the amplitude, with a hard-scattering amplitude T_H [297–299]. The pion's electro-magnetic form factor, for example, can be written as

$$F_\pi(Q^2) = \int_0^1 dx \int_0^1 dy \phi_\pi^*(y, Q) T_H(x, y, Q) \phi_\pi(x, Q) (1 + \mathcal{O}(1/Q)). \quad (6.1)$$

Here T_H is the scattering amplitude for the form factor but with the pions replaced by collinear $q\bar{q}$ pairs, i.e. the pions are replaced by their valence partons. We can also regard T_H as the free particle matrix element of the order $1/q^2$ term in the effective Lagrangian for $\gamma^* q\bar{q} \rightarrow q\bar{q}$.

The process-independent distribution amplitude [297–299] $\phi_\pi(x, Q)$ is the probability amplitude for finding the $q\bar{q}$ pair in the pion with $x_q = x$ and $x_{\bar{q}} = 1 - x$. It is directly related to the light-cone valence wavefunction:

$$\phi_\pi(x, Q) = \int \frac{d^2 k_\perp}{16\pi^3} \psi_{q\bar{q}/\pi}^{(Q)}(x, \mathbf{k}_\perp) \quad (6.2)$$

$$= P_\pi^+ \int \frac{dz^-}{4\pi} e^{ixP^+ + \pi z^-/2} \langle 0 | \bar{\psi}(0) \frac{\gamma^+ \gamma_5}{2\sqrt{2}n_c} \psi(z) | \pi \rangle_{z^+ = z_\perp = 0}^{(Q)}. \quad (6.3)$$

The \mathbf{k}_\perp integration in Eq. (6.2) is cut off by the ultraviolet cutoff $\Lambda = Q$ implicit in the wave function; thus only Fock states with invariant mass squared $\mathcal{M}^2 < Q^2$ contribute. We will return later to the discussion of ultraviolet regularization in the light-cone formalism.

It is important to note that the distribution amplitude is gauge-invariant. In gauges other than light-cone gauge, a path-ordered "string operator" $P \exp(\int_0^1 ds ig A(sz) \cdot z)$ must be included between the $\bar{\psi}$ and ψ . The line integral vanishes in light-cone gauge because $A \cdot z = A^+ z^-/2 = 0$ and so the factor can be omitted in that gauge. This (non-perturbative) definition of ϕ uniquely fixes the definition of T_H which must itself then be gauge-invariant.

The above result is in the form of a factorization theorem; all of the non-perturbative dynamics is factorized into the non-perturbative distribution amplitudes, which sums all internal momentum transfers up to the scale Q^2 . On the other hand, all momentum transfers higher than Q^2 appear in T_H , which, because of asymptotic freedom, can be computed perturbatively in powers of the QCD running coupling constant $\alpha_s(Q^2)$.

Given the factorized structure, one can read off a number of general features of the PQCD predictions, e.g. the dimensional counting rules, hadron helicity conservation, color transparency, etc. [62]. In addition, the scaling behavior of the exclusive amplitude is modified by the logarithmic dependence of the distribution amplitudes in $\ln Q^2$ which is in turn determined by QCD evolution equations [297–299].

An important application of the PQCD analysis is exclusive Compton scattering and the related cross process $\gamma\gamma \rightarrow \bar{p}p$. Each helicity amplitude for $\gamma p \rightarrow \gamma p$ can be computed at high momentum transfer from the convolution of the proton distribution amplitude with the $\mathcal{O}(\alpha_s^2)$ amplitudes for $qqq\gamma \rightarrow qq\gamma$. The result is a cross section which scales as

$$(d\sigma/dt)(\gamma p \rightarrow \gamma p) = F(\theta_{\text{CM}}, \ln s)/s^6 \quad (6.4)$$

if the proton helicity is conserved. The helicity-flip amplitude and contributions involving more quarks or gluons in the proton wavefunction are power-law suppressed. The nominal s^{-6} fixed angle scaling follows from dimensional counting rules [54]. It is modified logarithmically due to the evolution of the proton distribution amplitude and the running of the QCD coupling constant [297–299]. The normalization, angular dependence, and phase structure are highly sensitive to the detailed shape of the non-perturbative form of $\phi_p(x_i, Q^2)$. Recently, Kronfeld and Nizic [284] have calculated the leading Compton amplitudes using model forms for ϕ_p predicted in the QCD sum rule analyses [100]; the calculation is complicated by the presence of integrable poles in the hard-scattering subprocess T_H . The results for the unpolarized cross section are shown in Fig. 27.

There also has been important progress testing PQCD experimentally using measurements of the $p \rightarrow N^*$ form factors. In an analysis of existing SLAC data, Stoler [409] has obtained measurements of several transition form factors of the proton to resonances at $W = 1232, 1535,$ and 1680 MeV. As is the case of the elastic proton form factor, the observed behavior of the transition form factors to the $N^*(1535)$ and $N^*(1680)$ are each consistent with the Q^{-4} fall-off and dipole scaling predicted by PQCD and hadron helicity conservation over the measured range $1 < Q^2 < 21$ GeV². In contrast, the $p \rightarrow \Delta(1232)$ form factor decreases faster than $1/Q^4$ suggesting that non-leading processes are dominant in this case. Remarkably, this pattern of scaling behavior

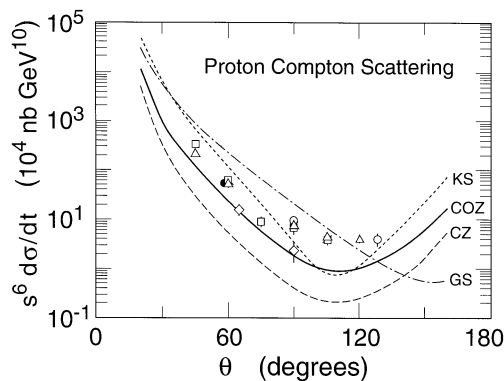


Fig. 27. Comparison of the order α_s^4/s^6 PQCD prediction for proton Compton scattering with the available data. The calculation assumes PQCD factorization and distribution amplitudes computed from QCD sum rule moments.

is what is expected from PQCD and the QCD sum rule analyses [100], since, unlike the case of the proton and its other resonances, the distribution amplitude $\phi_{N^*}(x_1, x_2, x_3, Q)$ of the Δ resonance is predicted to be nearly symmetric in the x_i , and a symmetric distribution leads to a strong cancelation [89] of the leading helicity-conserving terms in the matrix elements of the hard scattering amplitude for $qqq \rightarrow \gamma^*qqq$.

These comparisons of the proton form factor and Compton scattering predictions with experiment are very encouraging, showing agreement in both the fixed-angle scaling behavior predicted by PQCD and the normalization predicted by QCD sum rule forms for the proton distribution amplitude. Assuming one can trust the validity of the leading order analysis, a systematic series of polarized target and beam Compton scattering measurements on proton and neutron targets and the corresponding two-photon reactions $\gamma\gamma \rightarrow p\bar{p}$ will strongly constrain a fundamental quantity in QCD, the nucleon distribution amplitude $\phi(x_i, Q^2)$. It is thus imperative for theorists to develop methods to calculate the shape and normalization of the non-perturbative distribution amplitudes from first principles in QCD.

6.1. Is PQCD factorization applicable to exclusive processes?

One of the concerns in the derivation of the PQCD results for exclusive amplitudes is whether the momentum transfer carried by the exchanged gluons in the hard scattering amplitude T_H is sufficiently large to allow a safe application of perturbation theory [238]. The problem appears to be especially serious if one assumes a form for the hadron distribution amplitudes $\phi_H(x_i, Q^2)$ which has strong support at the endpoints, as in the QCD sum rule model forms suggested by Chernyak and Zhitnitskii and others [100,468].

This problem has now been clarified by two groups: Gari et al. [170] in the case of baryon form factors, and Mankiewicz and Szczepaniak [419], for the case of meson form factors. Each of these authors has pointed out that the assumed non-perturbative input for the distribution amplitudes must vanish strongly in the endpoint region; otherwise, there is a double-counting problem for momentum transfers occurring in the hard scattering amplitude and the distribution amplitudes. Once one enforces this constraint, (e.g. by using exponentially suppressed wavefunctions [299]) on the basis functions used to represent the QCD moments, or uses a sufficiently large number of polynomial basis functions, the resulting distribution amplitudes do not allow significant contribution to the high Q^2 form factors to come from soft gluon exchange region. The comparison of the PQCD predictions with experiment thus becomes phenomenologically and analytically consistent. An analysis of exclusive reactions on the effective Lagrangian method is also consistent with this approach. In addition, as discussed by Botts [47], potentially soft contributions to large angle hadron-hadron scattering reactions from Landshoff pinch contributions [289] are strongly suppressed by Sudakov form factor effects.

The empirical successes of the PQCD approach, together with the evidence for color transparency in quasi-elastic pp scattering [62] gives strong support for the validity of PQCD factorization for exclusive processes at moderate momentum transfer. It seems difficult to understand this pattern of form factor behavior if it is due to simple convolutions of soft wavefunctions. Thus, it should be possible to use these processes to empirically constrain the form of the hadron distribution amplitudes, and thus confront non-perturbative QCD in detail. For recent work, see Refs. [7,122,254,334].

6.2. Light-cone quantization and heavy particle decays

One of the most interesting applications of the light-cone PQCD formalism is to large momentum transfer exclusive processes to heavy quark decays. For example, consider the decay $\eta_c \rightarrow \gamma\gamma$. If we can choose the Lagrangian cutoff $\Lambda^2 \sim m_c^2$, then to leading order in $1/m_c$, all of the bound state physics and virtual loop corrections are contained in the $c\bar{c}$ Fock wavefunction $\psi_{\eta_c}(x_i, k_{\perp i})$. The hard scattering matrix element of the effective Lagrangian coupling $c\bar{c} \rightarrow \gamma\gamma$ contains all of the higher corrections in $\alpha_s(\Lambda^2)$ from virtual momenta $|k^2| > \Lambda^2$. Thus,

$$\begin{aligned} \mathcal{M}(\eta_c \rightarrow \gamma\gamma) &= \int d^2k_{\perp} \int_0^1 dx \psi_{\eta_c}^{(\Lambda)}(x, k_{\perp}) T_H^{(\Lambda)}(c\bar{c} \rightarrow \gamma\gamma) \\ &\Rightarrow \int_0^1 dx \phi(x, \Lambda) T_H^{(\Lambda)}(c\bar{c} \rightarrow \gamma\gamma), \end{aligned} \tag{6.5}$$

where $\phi(x, \Lambda^2)$ is the η_c distribution amplitude. This factorization and separation of scales is shown in Fig. 28. Since η_c is quite non-relativistic, its distribution amplitude is peaked at $x = 1/2$, and its integral over x is essentially equivalent to the wavefunction at the origin, $\psi(\mathbf{r} = \mathbf{0})$.

Another interesting calculational example of quarkonium decay in PQCD is the annihilation of the J/ψ into baryon pairs. The calculation requires the convolution of the hard annihilation amplitude $T_H(c\bar{c} \rightarrow ggg \rightarrow uud\bar{u}\bar{d})$ with the J/ψ , baryon, and anti-baryon distribution amplitudes [297–299] (see Fig. 29). The magnitude of the computed decay amplitude for $\psi \rightarrow \bar{p}p$ is consistent with experiment assuming the proton distribution amplitude computed from QCD sum rules [100], see also Keister [269]. The angular distribution of the proton in $e^+e^- \rightarrow J/\psi \rightarrow \bar{p}p$ is also consistent with the hadron helicity conservation rule predicted by PQCD, i.e. opposite proton and anti-proton helicity. The spin structure of hadrons has been investigated by Ma [318,319], using light-cone methods.

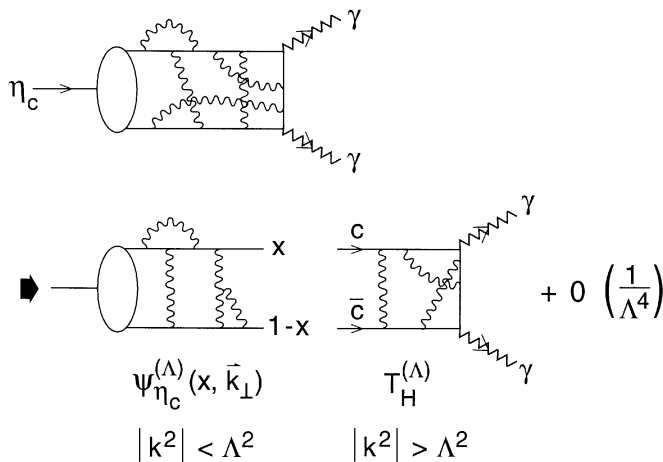


Fig. 28. Factorization of perturbative and non-perturbative contributions to the decay $\eta_c \rightarrow \gamma\gamma$.

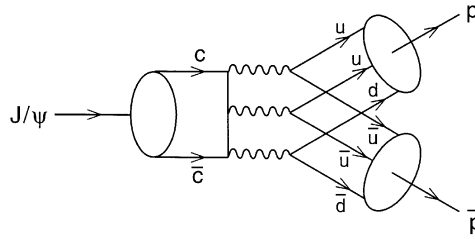


Fig. 29. Calculation of $J/\psi \rightarrow p\bar{p}$ in PQCD.

The effective Lagrangian method was used by Lepage et al. [301] to systematically compute the order $\alpha_s(\hat{Q})$ corrections to the hadronic and photon decays of quarkonium. The scale \hat{Q} can then be set by incorporating vacuum polarization corrections into the running coupling constant [57]. A summary of the results can be found in Ref. [286].

6.3. Exclusive weak decays of heavy hadrons

An important application of the PQCD effective Lagrangian formalism is to the exclusive decays of heavy hadrons to light hadrons, such as $B^0 \rightarrow \pi^+\pi^-$, K^+ , K^- [418]. To a good approximation, the decay amplitude $\mathcal{M} = \langle B | H_{wk} | \pi^+\pi^- \rangle$ is caused by the transition $\bar{b} \rightarrow W^+\bar{u}$; thus $\mathcal{M} = f_\pi p_\pi^\mu (G_F/\sqrt{2}) \langle \pi^- | J_\mu | B^0 \rangle$ where J_μ is the $\bar{b} \rightarrow \bar{u}$ weak current. The problem is then to recouple the spectator d quark and the other gluon and possible quark pairs in each B^0 Fock state to the corresponding Fock state of the final state π^- (see Fig. 30). The kinematic constraint that $(p_B - p_\pi)^2 = m_\pi^2$ then demands that at least one quark line is far off shell: $p_{\bar{u}}^2 = (yp_B - p_\pi)^2 \sim -\mu m_B \sim -1.5 \text{ GeV}^2$, where we have noted that the light quark takes only a fraction $(1-y) \sim \sqrt{(k_\perp^2 + m_d^2)}/m_B$ of the heavy meson's momentum since all of the valence quarks must have nearly equal velocity in a bound state. In view of the successful applications [409] of PQCD factorization to form factors at momentum transfers in the few GeV^2 range, it is reasonable to assume that $\langle |p_{\bar{u}}^2| \rangle$ is sufficiently large that we can begin to apply perturbative QCD methods.

The analysis of the exclusive weak decay amplitude can be carried out in parallel to the PQCD analysis of electro-weak form factors [57] at large Q^2 . The first step is to iterate the wavefunction equations of motion so that the large momentum transfer through the gluon exchange potential is exposed. The heavy quark decay amplitude can then be written as a convolution of the hard scattering amplitude for $Q\bar{q} \rightarrow W^+q\bar{q}$ convoluted with the B and π distribution amplitudes. The minimum number valence Fock state of each hadron gives the leading power law contribution. Equivalently, we can choose the ultraviolet cut-off scale in the Lagrangian at $(\Lambda^2 < \mu m_B)$ so that the hard scattering amplitude $T_H(Q\bar{q} \rightarrow W^+q\bar{q})$ must be computed from the matrix elements of the order $1/\Lambda^2$ terms in $\delta\mathcal{L}$. Thus, T_H contains all perturbative virtual loop corrections of order $\alpha_s(\Lambda^2)$. The result is the factorized form

$$\mathcal{M}(B \rightarrow \pi\pi) = \int_0^1 dx \int_0^1 dy \phi_B(y, \Lambda) T_H \phi_\pi(x, \Lambda) \quad (6.6)$$

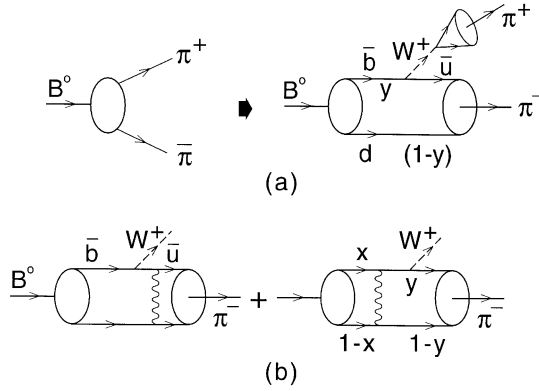


Fig. 30. Calculation of the weak decay $B \rightarrow \pi\pi$ in the PQCD formalism of Ref. [418]. The gluon exchange kernel of the hadron wavefunction is exposed where hard momentum transfer is required.

be correct up to terms of order $1/\Lambda^4$. All of the non-perturbative corrections with momenta $|k^2| < \Lambda^2$ are summed in the distribution amplitudes.

In order to make an estimate of the size of the $B \rightarrow \pi\pi$ amplitude, in Ref. [418], we have taken the simplest possible forms for the required wavefunctions

$$\phi_\pi(y) \propto \gamma_5 \not{p}_\pi y(1-y) \tag{6.7}$$

for the pion and

$$\phi_B(x) \propto \frac{\gamma_5 [\not{p}_B + m_B g(x)]}{[1 - (1/x) - \varepsilon^2/(1-x)]^2} \tag{6.8}$$

for the B, each normalized to its meson decay constant. The above form for the heavy quark distribution amplitude is chosen so that the wavefunction peaks at equal velocity; this is consistent with the phenomenological forms used to describe heavy quark fragmentation into heavy hadrons. We estimate $\varepsilon \sim 0.05$ to 0.10 . The functional dependence of the mass term $g(x)$ is unknown; however, it should be reasonable to take $g(x) \sim 1$ which is correct in the weak binding approximation.

One now can compute the leading order PQCD decay amplitude

$$\mathcal{M}(B^0 \rightarrow \pi^- \pi^+) = (G_F/\sqrt{2}) V_{ud}^* V_{ub} P_{\pi^+}^\mu \langle \pi^- | V^\mu | B^0 \rangle \tag{6.9}$$

where

$$\begin{aligned} \langle \pi^- | V^\mu | B^0 \rangle = & \frac{8\pi\alpha_s(Q^2)}{3} \int_0^1 dx \int_0^{1-\varepsilon} dy \phi_B(x) \phi_\pi(y) \frac{\text{Tr}[\not{P}_\pi \gamma_5 \gamma^\nu \not{k}_1 \gamma^\mu (\not{P}_B + M_B g(x)) \gamma_5 \gamma_\nu]}{k_1^2 q^2} \\ & + \frac{\text{Tr}[\not{P}_\pi - \gamma_5 \gamma^\nu (\not{k}_2 + M_B) \gamma^\nu (\not{P}_B + M_B g(x)) \gamma_5 \gamma_\nu]}{(k_2^2 - M_B^2) Q^2}. \end{aligned} \tag{6.10}$$

Numerically, this gives the branching ratio

$$\text{BR}(B^0 \rightarrow \pi^+ \pi^-) \sim 10^{-8} \xi^2 N, \tag{6.11}$$

where $\xi = 10|V_{ub}/V_{cb}|$ is probably less than unity, and N has strong dependence on the value of g : $N = 180$ for $g = 1$ and $N = 5.8$ for $g = 1/2$. The present experimental limit [21] is

$$\text{BR}(B^0 \rightarrow \pi^+ \pi^-) < 3 \times 10^{-4}. \quad (6.12)$$

A similar PQCD analysis can be applied to other two-body decays of the B ; the ratios of the widths will not be so sensitive to the form of the distribution amplitude, allowing tests of the flavor symmetries of the weak interaction. Semi-leptonic decay rates can be calculated [99,128,187,246,404], and the construction of the heavy quark wavefunctions [101,465], can be helpful for that.

6.4. Can light-cone wavefunctions be measured?

Essential information on the shape and form of the valence light-cone wavefunctions can be obtained empirically through measurements of exclusive processes at large momentum transfer. In the case of the pion, data for the scaling and magnitude of the photon transition form factor $F_{\gamma\pi^0}(q^2)$ suggest that the distribution amplitude of the pion $\phi_\pi(x, Q)$ is close in form to the asymptotic form $\phi_\pi^{\text{as}}(x) = \sqrt{3}f_\pi(1-x)$, the solution to the evolution equation for the pion at infinite resolution $Q \rightarrow \infty$, [299]. Note that the pion distribution amplitude is constrained by $\pi \rightarrow \mu\nu$ decay,

$$\int_0^1 dx \phi_\pi(x, Q) = f_\pi/2\sqrt{3}. \quad (6.13)$$

The proton distribution amplitude as determined by the proton form factor at large momentum transfer, and Compton scattering is apparently highly asymmetric as suggested by QCD sum rules and SU(6) flavor-spin symmetry.

The most direct way to measure the hadron distribution wavefunction is through the diffractive dissociation of a high energy hadron to jets or nuclei, e.g. $\pi A \rightarrow \text{Jet} + \text{Jet} + A'$, where the final-state nucleus remains intact [36,149]. The incoming hadron is a sum over all of its H_{LC}^0 fluctuations. When the pion fluctuates into a $q\bar{q}$ state with small impact separation $b_\perp^0(1/Q)$, its color interactions are minimal the “color transparency” property of QCD [60]. Thus, this fluctuation will interact coherently throughout the nucleus without initial or final state absorption corrections. The result is that the pion is coherently materialized into two jets of mass \mathcal{M}^ϵ with minimal momentum transfer to the nucleus

$$\Delta Q_L = \frac{\mathcal{M}^\epsilon - \hat{p}_\pi^\epsilon}{2E_L}. \quad (6.14)$$

Thus, the jets carry nearly all of the momentum of the pion. The forward amplitude at $Q_\perp, Q_L \ll R_\pi^{-1}$ is linear in the number of nucleons. The total rate integrated over the forward diffraction peak is thus proportional to $A^2/R_\pi^2 \propto A^{1/3}$.

The most remarkable feature of the diffractive $\pi A \rightarrow \text{Jet} + \text{Jet} + X$ reactions is its potential to measure the shape of the pion wavefunction. The partition of jet longitudinal momentum gives the x -distribution; the relative transverse momentum distribution provides the \mathbf{k}_\perp -distribution of $\psi_{q\bar{q}/\pi}(x, \mathbf{k}_\perp)$. Such measurements are now being carried out by the E791 collaboration at Fermilab.

In principle, such experiments can be carried out with a photon beam, which should confirm the $x^2 + (1-x)\gamma \rightarrow q\bar{q}$ distribution of the basic photon wavefunction. Measurements of $pA \rightarrow \text{Jet } p + \text{Jet } A$ could, in principle, provide a direct measurement of the proton distribution amplitude $\phi_p(x_i; Q)$.

7. The light-cone vacuum

The unique features of “front form” or light-cone quantized field theory [123] provide a powerful tool for the study of QCD. Of primary importance in this approach is the existence of a vacuum state that is the ground state of the full theory. The existence of this state gives a firm basis for the investigation of many of the complexities that must exist in QCD. In this picture the rich structure of vacuum is transferred to the zero modes of the theory. Within this context the long-range physical phenomena of spontaneous symmetry breaking [206–208] [33,382,223,389,375,376] as well as the topological structure of the theory [259,377,378,383,384,261] can be associated with the zero mode(s) of the fields in a quantum field theory defined in a finite spatial volume and quantized at equal light-cone time [299].

7.1. Constrained zero modes

As mentioned previously, the light-front vacuum state is simple; it contains no particles in a massive theory. In other words, the Fock space vacuum is the physical vacuum. However, one commonly associates important long-range properties of a field theory with the vacuum: spontaneous symmetry breaking, the Goldstone pion, and color confinement. How do these complicated phenomena manifest themselves in light-front field theory?

If one cannot associate long-range phenomena with the vacuum state itself, then the only alternative is the zero momentum components or “zero modes” of the field (long range \leftrightarrow zero momentum). In some cases, the zero mode operator is not an independent degree of freedom but obeys a constraint equation. Consequently, it is a complicated operator-valued function of all the other modes of the field. Zero modes of this type have been investigated first by Maskawa and Yamawaki as early as in 1976 [324].

This problem has recently been attacked from several directions. The question of whether boundary conditions can be consistently defined in light-front quantization has been discussed by McCartor and Robertson [325–331,388], and by Lenz [295,296]. They have shown that for massive theories the energy and momentum derived from light-front quantization are conserved and are equivalent to the energy and momentum one would normally write down in an equal-time theory. In the analyses of Lenz et al. [295,296] and Hornbostel [230] one traces the fate of the equal-time vacuum in the limit $P^3 \rightarrow \infty$ and equivalently in the limit $\theta \rightarrow \pi/2$ when rotating the evolution parameter $\tau = x^0 \cos \theta + x^3 \sin \theta$ from the instant parametrization to the front parametrization. Heinzl and Werner et al. [206–210,214] considered ϕ^4 theory in (1 + 1) dimensions and attempted to solve the zero mode constraint equation by truncating the equation to one particle. Other authors [203,204,389] find that, for theories allowing spontaneous symmetry breaking, there is a degeneracy of light-front vacua and the true vacuum state can differ from the perturbative vacuum through the addition of zero mode quanta. In addition to these approaches there

are many others, like Refs. [78,356,262], Refs. [73,112,232,257], or Refs. [107,214,276]. Grangé et al. [45,46] have dealt with a broken phase in such scalar models, see also Refs. [97,175,283].

An analysis of the zero mode constraint equation for $(1+1)$ -dimensional ϕ^4 field theory $[(\phi^4)_{1+1}]$ with symmetric boundary conditions shows how spontaneous symmetry breaking occurs within the context of this model. This theory has a Z_2 symmetry $\phi \rightarrow -\phi$ which is spontaneously broken for some values of the mass and coupling. The approach of Pinsky et al. [33,382,223] is to apply a Tamm–Dancoff truncation to the Fock space. Thus, operators are finite matrices and the operator-valued constraint equation can be solved numerically. The truncation assumes that states with a large number of particles or large momentum do not have an important contribution to the zero mode.

Since this represents a completely new paradigm for spontaneous symmetry breaking we will present this calculation in some detail. One finds the following general behavior: for small coupling (large g , where $g \propto 1/\text{coupling}$) the constraint equation has a single solution and the field has no vacuum expectation value (VEV). As one increases the coupling (decreases g) to the “critical coupling” g_{critical} , two additional solutions which give the field a non-zero VEV appear. These solutions differ only infinitesimally from the first solution near the critical coupling, indicating the presence of a second-order phase transition. Above the critical coupling ($g < g_{\text{critical}}$), there are three solutions: one with zero VEV, the “unbroken phase”, and two with non-zero VEV, the “broken phase”. The “critical curves”, shown in Fig. 31, is a plot of the VEV as a function of g .

Since the vacuum in this theory is trivial, all of the long-range properties must occur in the operator structure of the Hamiltonian. Above the critical coupling ($g < g_{\text{critical}}$) quantum oscillations spontaneously break the Z_2 symmetry of the theory. In a loose analogy with a symmetric double-well potential, one has two new Hamiltonians for the broken phase, each producing states localized in one of the wells. The structure of the two Hamiltonians is determined from the broken phase solutions of the zero mode constraint equation. One finds that the two Hamiltonians have equivalent spectra. In a discrete theory without zero modes it is well known that, if one increases

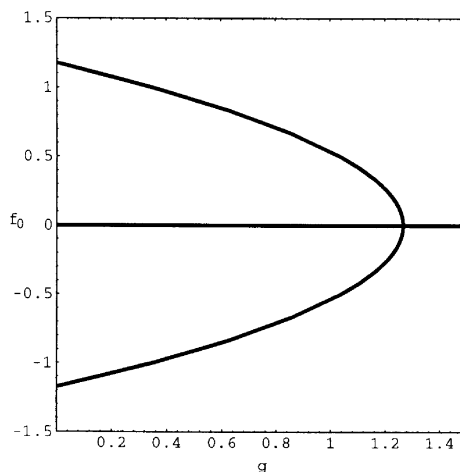


Fig. 31. $f_0 = \sqrt{4\pi}\langle 0|\phi|0\rangle$ vs. $g = 24\pi\mu^2/\lambda$ in the one mode case with $N = 10$.

the coupling sufficiently, quantum correction will generate tachyons causing the theory to break down near the critical coupling. Here the zero mode generates new interactions that prevent tachyons from developing. In effect what happens is that, while quantum corrections attempt to drive the mass negative, they also change the vacuum energy through the zero mode and the mass eigenvalue can never catch the vacuum eigenvalue. Thus, tachyons never appear in the spectra.

In the weak coupling limit (g large) the solution to the constraint equation can be obtained in perturbation theory. This solution does not break the Z_2 symmetry and is believed to simply insert the missing zero momentum contributions into internal propagators. This must happen if light-front perturbation theory is to agree with equal-time perturbation theory [94–96].

Another way to investigate the zero mode is to study the spectrum of the field operator ϕ . Here one finds a picture that agrees with the symmetric double-well potential analogy. In the broken phase, the field is localized in one of the minima of the potential and there is tunneling to the other minimum.

7.1.1. Canonical quantization

For a classical field the $(\phi^4)_{1+1}$ Lagrange density is

$$L = \partial_+ \phi \partial_- \phi - \frac{1}{2} \mu^2 \phi^2 - (\lambda/4!) \phi^4. \quad (7.1)$$

One puts the system in a box of length d and imposes periodic boundary conditions. Then

$$\phi(x) = (1/\sqrt{d}) \sum_n q_n(x^+) e^{ik_n^- x^-}, \quad (7.2)$$

where $k_n^+ = 2\pi n/d$ and summations run over all integers unless otherwise noted.

It is convenient to define the integral $\int dx^- \phi(x)^n - (\text{zero modes}) = \Sigma_n$. In terms of the modes of the field it has the form,

$$\Sigma_n = \frac{1}{n!} \sum_{i_1, i_2, \dots, i_n \neq 0} q_{i_1} q_{i_2} \dots q_{i_n} \delta_{i_1 + i_2 + \dots + i_n, 0}. \quad (7.3)$$

Then the canonical Hamiltonian is

$$P^- = \frac{\mu^2 q_0^2}{2} + \mu^2 \Sigma_2 + \frac{\lambda q_0^4}{4!d} + \frac{\lambda q_0^2 \Sigma_2}{2!d} + \frac{\lambda q_0 \Sigma_3}{d} + \frac{\lambda \Sigma_4}{d}. \quad (7.4)$$

Following the Dirac–Bergman prescription, described in Appendix E, one identifies firstclass constraints which define the conjugate momenta

$$0 = p_n - ik_n^+ q_{-n}, \quad (7.5)$$

where

$$[q_m, p_n] = \frac{1}{2} \delta_{n,m}, \quad m, n \neq 0. \quad (7.6)$$

The secondary constraint is [457],

$$0 = \mu^2 q_0 + \frac{\lambda q_0^3}{3!d} + \frac{\lambda q_0 \Sigma_2}{d} + \frac{\lambda \Sigma_3}{d}, \quad (7.7)$$

which determines the zero mode q_0 . This result can also be obtained by integrating the equations of motion.

To quantize the system one replaces the classical fields with the corresponding field operators, and the Dirac bracket by i times a commutator. One must choose a regularization and an operator-ordering prescription in order to make the system well-defined.

One begins by defining creation and annihilation operators a_k^\dagger and a_k ,

$$q_k = \sqrt{\frac{d}{4\pi|k|}} a_k, \quad a_k = a_{-k}^\dagger, \quad k \neq 0, \quad (7.8)$$

which satisfy the usual commutation relations

$$[a_k, a_l] = 0, \quad [a_k^\dagger, a_l^\dagger] = 0, \quad [a_k, a_l^\dagger] = \delta_{k,l}, \quad k, l > 0. \quad (7.9)$$

Likewise, one defines the zero mode operator

$$q_0 = \sqrt{(d/4\pi)} a_0. \quad (7.10)$$

In the quantum case, one normal orders the operator Σ_n .

General arguments suggest that the Hamiltonian should be symmetric ordered [32]. However, it is not clear how one should treat the zero mode since it is not a dynamical field. As an ansatz one treats a_0 as an ordinary field operator when symmetric ordering the Hamiltonian. The tadpoles are removed from the symmetric ordered Hamiltonian by normal ordering the terms having no zero mode factors and by subtracting

$$\frac{3}{2} a_0^2 \sum_{n \neq 0} \frac{1}{|n|}. \quad (7.11)$$

In addition, one subtracts a constant so that the VEV of H is zero. Note that this renormalization prescription is equivalent to a conventional mass renormalization and does not introduce any new operators into the Hamiltonian. The constraint equation for the zero mode can be obtained by taking a derivative of P^- with respect to a_0 . One finds

$$0 = g a_0 + a_0^3 + \sum_{n \neq 0} \frac{1}{|n|} \left(a_0 a_n a_{-n} + a_n a_{-n} a_0 + a_n a_0 a_{-n} - \frac{3a_0}{2} \right) + 6\Sigma_3, \quad (7.12)$$

where $g = 24\pi\mu^2/\lambda$. It is clear from the general structure of Eq. (7.12) that a_0 as a function of the other modes is not necessarily odd under the transform $a_k \rightarrow -a_k$, ($k \neq 0$) associated with the Z_2 symmetry of the system. Consequently, the zero mode can induce Z_2 symmetry breaking in the Hamiltonian.

In order to render the problem tractable, we impose a Tamm–Dancoff truncation on the Fock space. One defines M to be the number of non-zero modes and N to be the maximum number of allowed particles. Thus, each state in the truncated Fock space can be represented by a vector of length $S = (M + N)/(M!N!)$ and operators can be represented by $S \times S$ matrices. One can define the usual Fock space basis, $|n_1, n_2, \dots, n_M\rangle$ where $n_1 + n_2 + \dots + n_M \leq N$. In matrix form, a_0 is real and symmetric. Moreover, it is block diagonal in states of equal P^+ eigenvalue.

7.1.2. Perturbative solution of the constraints

In the limit of large g , one can solve the constraint equation perturbatively. Then one substitutes the solution back into the Hamiltonian and calculates various amplitudes to arbitrary order in $1/g$ using Hamiltonian perturbation theory.

It can be shown that the solutions of the constraint equation and the resulting Hamiltonian are divergence free to all orders in perturbation theory for both the broken and unbroken phases. To do this one starts with the perturbative solution for the zero mode in the unbroken phase,

$$a_0 = -\frac{6}{g}\Sigma_3 + \frac{6}{g^2}\left(2\Sigma_2\Sigma_3 + 2\Sigma_3\Sigma_2 + \sum_{k=1}^M \frac{a_k\Sigma_3 a_k^\dagger + a_k^\dagger\Sigma_3 a_k - \Sigma_3}{k}\right) + \mathcal{O}(1/g^3), \quad (7.13)$$

and substitutes this into the Hamiltonian to obtain a complicated but well-defined expression for the Hamiltonian in terms of the dynamical operators.

The finite volume box acts as an infra-red regulator and the only possible divergences are ultraviolet. Using diagrammatic language, any loop of momentum k with ℓ internal lines has asymptotic form $k^{-\ell}$. Only the case of tadpoles $\ell = 1$ is divergent. If there are multiple loops, the effect is to put factors of $\ln(k)$ in the numerator and the divergence structure is unchanged. Looking at Eq. (7.13), the only possible tadpole is from the contraction in the term

$$a_k\Sigma_3 a_{-k}/k \quad (7.14)$$

which is canceled by the Σ_3/k term. This happens to all orders in perturbation theory: each tadpole has an associated term which cancels it. Likewise, in the Hamiltonian one has similar cancelations to all orders in perturbation theory.

For the unbroken phase, the effect of the zero mode should vanish in the infinite volume limit, giving a “measure zero” contribution to the continuum Hamiltonian. However, for finite box volume the zero mode does contribute, compensating for the fact that the longest wavelength mode has been removed from the system. Thus, inclusion of the zero mode improves convergence to the infinite volume limit. In addition, one can use the perturbative expansion of the zero mode to study the operator ordering problem. One can directly compare our operator ordering ansatz with a truly Weyl ordered Hamiltonian and with Maeno’s operator ordering ansatz [320].

As an example, let us examine $\mathcal{O}(\lambda^2)$ contributions to the processes $1 \rightarrow 1$. As shown in Fig. 32, including the zero mode greatly improves convergence to the large volume limit. The zero mode compensates for the fact that one has removed the longest wavelength mode from the system.

7.1.3. Non-perturbative solution: One mode, many particles

Consider the case of one mode $M = 1$ and many particles. In this case, the zero mode is diagonal and can be written as

$$a_0 = f_0|0\rangle\langle 0| + \sum_{k=1}^N f_k|k\rangle\langle k|. \quad (7.15)$$

Note that a_0 in Eq. (7.15) is even under $a_k \rightarrow -a_k$, $k \neq 0$ and any non-zero solution breaks the Z_2 symmetry of the original Hamiltonian. The VEV is given by

$$\langle 0|\phi|0\rangle = (1/\sqrt{4\pi})\langle 0|a_0|0\rangle = (1/\sqrt{4\pi})f_0. \quad (7.16)$$

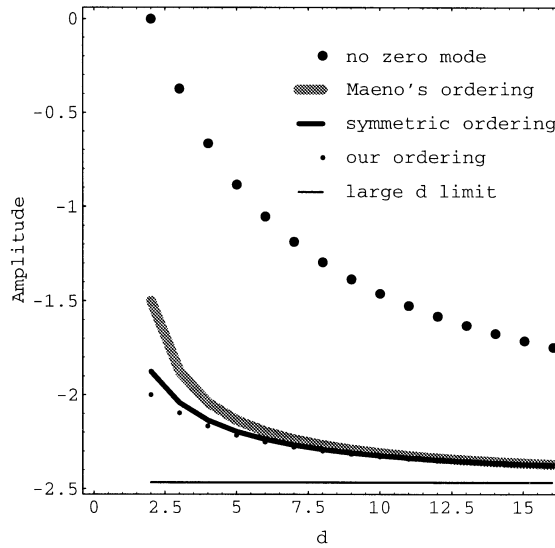


Fig. 32. Convergence to the large d limit of $1 \rightarrow 1$ setting $E = g/p$ and dropping any constant terms.

Substituting Eq. (7.15) into the constraint Eq. (7.12) and sandwiching the constraint equation between Fock states, one get a recursion relation for $\{f_n\}$:

$$0 = g f_n + f_n^3 + (4n - 1)f_n + (n + 1)f_{n+1} + n f_{n-1}, \quad (7.17)$$

where $n \leq N$, and one defines f_{N+1} to be unknown. Thus, $\{f_1, f_2, \dots, f_{N+1}\}$ is uniquely determined by a given choice of g and f_0 . In particular, if $f_0 = 0$ all the f_k 's are zero independent of g . This is the unbroken phase.

Consider the asymptotic behavior for large n . If $f_n \gg 1$, the f_n^3 term will dominate and

$$f_{n+1} \sim f_n^3/n, \quad (7.18)$$

thus,

$$\lim_{n \rightarrow \infty} f_n \sim (-1)^n \exp(3^n \text{constant}). \quad (7.19)$$

One must reject this rapidly growing solution. One only seeks solutions where f_n is small for large n . For large n , the terms linear in n dominate and Eq. (7.17) becomes

$$f_{n+1} + 4f_n + f_{n-1} = 0. \quad (7.20)$$

There are two solutions to this equation:

$$f_n \propto (\sqrt{3} \pm 2)^n. \quad (7.21)$$

One must reject the plus solution because it grows with n . This gives the condition

$$-\frac{\sqrt{3}-3+g}{2\sqrt{3}}=K, \quad K=0, 1, 2, \dots \quad (7.22)$$

Concentrating on the $K=0$ case, one finds a critical coupling

$$g_{\text{critical}}=3-\sqrt{3} \quad (7.23)$$

or

$$\lambda_{\text{critical}}=4\pi(3+\sqrt{3})\mu^2 \approx 60\mu^2. \quad (7.24)$$

In comparison, values of $\lambda_{\text{critical}}$ from $22\mu^2$ to $55\mu^2$ have been reported for equal-time quantized calculations [93,1,168,282]. The solution to the linearized equation is an approximate solution to the full Eq. (7.17) for f_0 sufficiently small. Next, one needs to determine solutions of the full non-linear equation which converge for large n .

One can study the critical curves by looking for numerical solutions to Eq. (7.17). The method used here is to find values of f_0 and g such that $f_{N+1}=0$. Since one seeks a solution where f_n is decreasing with n , this is a good approximation. One finds that for $g > 3 - \sqrt{3}$ the only real solution is $f_n=0$ for all n . For g less than $3 - \sqrt{3}$ there are two additional solutions. Near the critical point $|f_0|$ is small and

$$f_n \approx f_0(2 - \sqrt{3})^n. \quad (7.25)$$

The critical curves are shown in Fig. 31. These solutions converge quite rapidly with N . The critical curve for the broken phase is approximately parabolic in shape:

$$g \approx 3 - \sqrt{3} - 0.9177f_0^2. \quad (7.26)$$

One can also study the eigenvalues of the Hamiltonian for the one-mode case. The Hamiltonian is diagonal for this Fock space truncation and

$$\langle n|H|n\rangle = \frac{3}{2}n(n-1) + ng - \frac{f_n^4}{4} - \frac{2n+1}{4}f_n^2 + \frac{n+1}{4}f_{n+1}^2 + \frac{n}{4}f_{n-1}^2 - C. \quad (7.27)$$

The invariant mass eigenvalues are given by

$$P^2|n\rangle = 2P^+P^-|n\rangle = \frac{n\lambda\langle n|H|n\rangle}{24\pi}|n\rangle. \quad (7.28)$$

In Fig. 33 the dashed lines show the first few eigenvalues as a function of g without the zero mode. When one includes the broken phase of the zero mode, the energy levels shift as shown by the solid curves. For $g < g_{\text{critical}}$ the energy levels increase above the value they had without the zero mode. The higher levels change very little because f_n is small for large n .

In the more general case of many modes and many particles many of the features that were seen in the one-mode and one-particle cases remain. In order to calculate the zero mode for a given value of g one converts the constraint Eq. (7.12) into an $S \times S$ matrix equation in the truncated Fock space. This becomes a set of S^2 coupled cubic equations and one can solve for the matrix

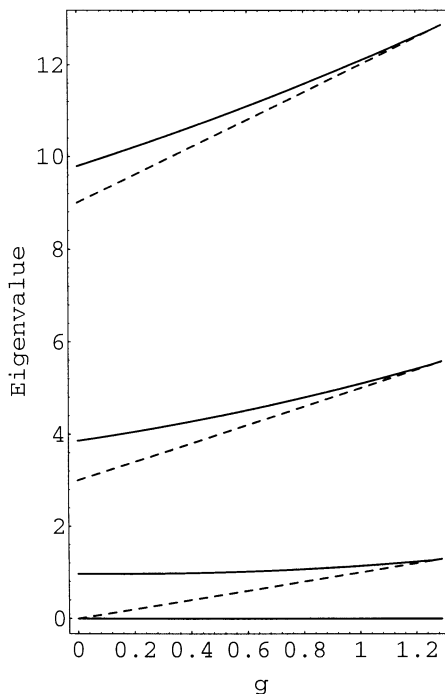


Fig. 33. The lowest three energy eigenvalues for the one-mode case as a function of g from the numerical solution of Eq. (7.27) with $N = 10$. The dashed lines are for the unbroken phase $f_0 = 0$ and the solid lines are for the broken phase $f_0 \neq 0$.

elements of a_0 numerically. Considerable simplification occurs because a_0 is symmetric and is block diagonal in states of equal momentum. For example, in the case $M = 3$, $N = 3$, the number of coupled equations is 34 instead of $S^2 = 400$. In order to find the critical coupling, one takes $\langle 0|a_0|0\rangle$ as given and g as unknown and solves the constraint equation for g and the other matrix elements of a_0 in the limit of small but non-zero $\langle 0|a_0|0\rangle$. One sees that the solution converges quickly as N increases, and that there is a logarithmic divergence as M increases. The logarithmic divergence of g_{critical} is the major remaining missing part of this calculation and requires a careful non-perturbative renormalization [281].

When one substitutes the solutions for the broken phase of a_0 into the Hamiltonian, one gets two Hamiltonians H^+ and H^- corresponding to the two signs of $\langle 0|a_0|0\rangle$ and the two branches of the curve in Fig. 31. This is the new paradigm for spontaneous symmetry breaking: multiple vacua are replaced by multiple Hamiltonians. Picking the Hamiltonian defines the theory in the same sense that picking the vacuum defines the theory in the equal-time paradigm. The two solutions for a_0 are related to each other in a very specific way. Let Π be the unitary operator associated with the Z_2 symmetry of the system; $\Pi a_k \Pi^\dagger = -a_k$, $k \neq 0$. One breaks up a_0 into an even part $\Pi a_0^E \Pi^\dagger = a_0^E$ and an odd part $\Pi a_0^O \Pi^\dagger = -a_0^O$. The even part a_0^E breaks the Z_2 symmetry of the theory. For $g < g_{\text{critical}}$, the three solutions of the constraint equation are: a_0^O corresponding to the unbroken phase, $a_0^O + a_0^E$ corresponding to the $\langle 0|a_0|0\rangle > 0$ solution, and $a_0^O - a_0^E$ for the $\langle 0|a_0|0\rangle < 0$

solution. Thus, the two Hamiltonians are

$$H^+ = H(a_k, a_0^O + a_0^E) \tag{7.29}$$

and

$$H^- = H(a_k, a_0^O - a_0^E), \tag{7.30}$$

where H has the property

$$H(a_k, a_0) = H(-a_k, -a_0) \tag{7.31}$$

and a_k represents the non-zero modes. Since Π is a unitary operator, if $|\Psi\rangle$ is an eigenvector of H with eigenvalue E then $\Pi|\Psi\rangle$ is an eigenvalue of $\Pi H \Pi^\dagger$ with eigenvalue E . Since,

$$\Pi H^- \Pi^\dagger = \Pi H(a_k, a_0^O - a_0^E) \Pi^\dagger = H(-a_k, -a_0^O - a_0^E) = H(a_k, a_0^O + a_0^E) = H^+, \tag{7.32}$$

H^+ and H^- have the same eigenvalues.

Consider the $M = 3, N = 3$ case as an example and let us examine the spectrum of H . For large g the eigenvalues are obviously $0, g, g/2, 2g, g/3, 3g/2$ and $3g$. However, as one decreases g one of the last three eigenvalues will be driven negative. This signals the breakdown of the theory near the critical coupling when the zero mode is not included.

Including the zero mode fixes this problem. Fig. 34 shows the spectrum for the three lowest nonzero momentum sectors. This spectrum illustrates several characteristics which seem to hold generally (at least for truncations that have been examined, $N + M \leq 6$). For the broken phase, the vacuum is the lowest energy state, there are no level crossings as a function of g , and the theory does

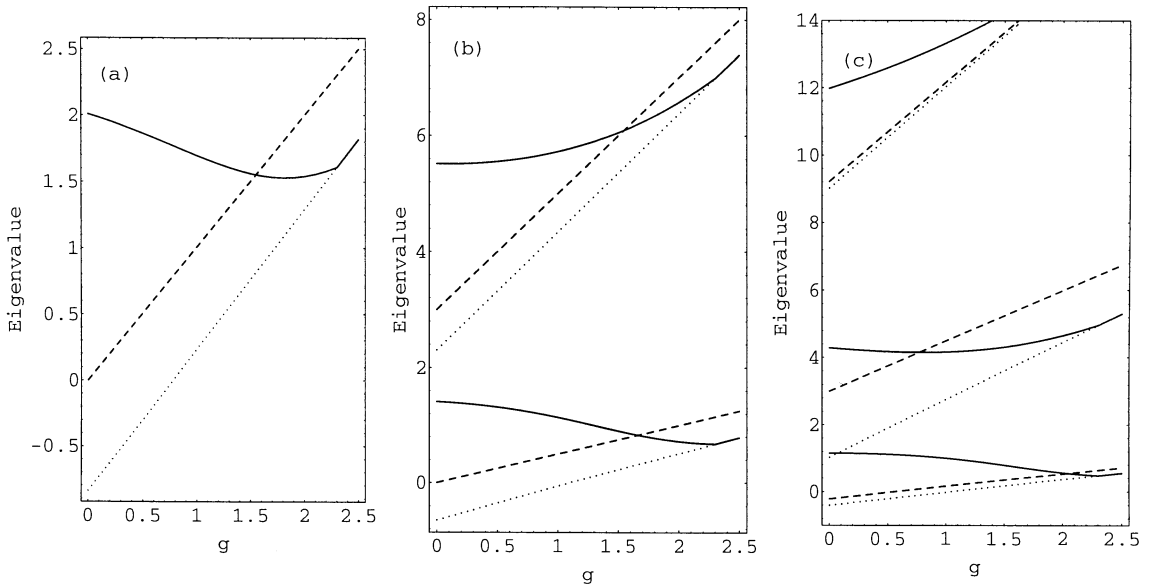


Fig. 34. The spectrum for (a) $P^+ = 2\pi/d$, (b) $P^+ = 4\pi/d$, and (c) $P^+ = 6\pi/d$, all with $M = 3, N = 3$. The dashed line shows the spectrum with no zero mode. The dotted line is the unbroken phase and the solid line is the broken phase.

not break down in the vicinity of the critical point. None of these are true for the spectrum with the zero mode removed or for the unbroken phase below the critical coupling.

One can also investigate the shape of the critical curve near the critical coupling as a function of the cutoff K . In scalar field theory, $\langle 0|\phi|0\rangle$ acts as the order parameter of the theory. Near the critical coupling, one can fit the VEV to some power of $g - g_{\text{critical}}$; this will give us the associated critical exponent β ,

$$\langle 0|a_0|0\rangle \propto (g_{\text{critical}} - g)^\beta. \quad (7.33)$$

Pinsky et al. [223] have calculated this as a function of cutoff and found a result consistent with $\beta = 1/2$, independent of cutoff K . The theory $(\phi^4)_{1+1}$ is in the same universality class as the Ising model in 2 dimensions and the correct critical exponent for this universality class is $\beta = 1/8$. If one were to use the mean field approximation to calculate the critical exponent, the result would be $\beta = 1/2$. This is what was obtained in this calculation. Usually, the presence of a mean field result indicates that one is not probing all length scales properly. If one had a cutoff K large enough to include many length scales, then the critical exponent should approach the correct value. However, one cannot be certain that this is the correct explanation of our result since no evidence that β decreases with increase K is seen.

7.1.4. Spectrum of the field operator

How does the zero mode affect the field itself? Since ϕ is a Hermitian operator it is an observable of the system and one can measure ϕ for a given state $|\alpha\rangle$. $\tilde{\phi}_i$ and $|\chi_i\rangle$ are the eigenvalue and eigenvector, respectively, of $\sqrt{4\pi}\phi$:

$$\sqrt{4\pi}\phi|\chi_i\rangle = \tilde{\phi}_i|\chi_i\rangle, \quad \langle \chi_i|\chi_j\rangle = \delta_{i,j}. \quad (7.34)$$

The expectation value of $\sqrt{4\pi}\phi$ in the state $|\alpha\rangle$ is $|\langle \chi_i|\alpha\rangle|^2$.

In the limit of large N , the probability distribution becomes continuous. If one ignores the zero mode, the probability of obtaining $\tilde{\phi}$ as the result of a measurement of $\sqrt{4\pi}\phi$ for the vacuum state is

$$P(\tilde{\phi}) = \frac{1}{\sqrt{2\pi\tau}} \exp\left(-\frac{\tilde{\phi}^2}{2\tau}\right) d\tilde{\phi}, \quad (7.35)$$

where $\tau = \sum_{k=1}^M 1/k$. The probability distribution comes from the ground-state wavefunction of the harmonic oscillator where one identifies ϕ with the position operator. This is just the Gaussian fluctuation of a free field. Note that the width of the Gaussian diverges logarithmically in M . When N is finite, the distribution becomes discrete as shown in Fig. 35.

In general, there are $N + 1$ eigenvalues such that $\langle \chi_i|0\rangle \neq 0$, independent of M . Thus, if one wants to examine the spectrum of the field operator for the vacuum state, it is better to choose Fock space truncations where N is large. With this in mind, one examines the $N = 50$ and $M = 1$ case as a function of g in Fig. 36. Note that near the critical point, Fig. 36a, the distribution is approximately equal to the free field case shown in Fig. 35. As one moves away from the critical point, Fig. 36b–Fig. 36d, the distribution becomes increasingly narrow with a peak located at the VEV of what would be the minimum of the symmetric double-well potential in the equal-time paradigm. In addition, there is a small peak corresponding to minus the VEV. In the language of the equal-time

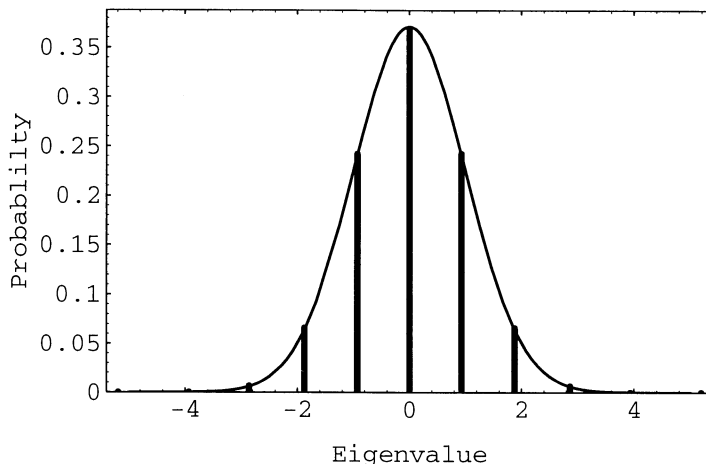


Fig. 35. Probability distribution of eigenvalues of $\sqrt{4\pi}\phi$ for the vacuum with $M = 1$, $N = 10$, and no zero mode. Also shown is the infinite N limit from Eq. (7.35).

paradigm, there is tunneling between the two minima of the potential. The spectrum of ϕ has been examined for other values of M and N ; the results are consistent with the example discussed here.

7.2. Physical picture and classification of zero modes

When considering a gauge theory, there is a “zero-mode” problem associated with the choice of gauge in the compactified case. This subtlety, however, is not particular to the light cone; indeed, its occurrence is quite familiar in equal-time quantization on a torus [321,335,290]. In the present context, the difficulty is that the zero mode in A^+ is in fact gauge-invariant, so that the light-cone gauge $A^+ = 0$ cannot be reached. Thus we have a pair of interconnected problems: first, a practical choice of gauge; and second, the presence of constrained zero modes of the gauge field. In two recent papers [258,259] these problems were separated and consistent gauge fixing conditions were introduced to allow isolation of the dynamical and constrained fields. In Ref. [259] the generalize gauge fixing is described, and the Poincaré generators are constructed in perturbation theory.

One observes that in the traditional treatment, choosing the light-cone gauge $A^+ = 0$ enables Gauss’s law to be solved for A^- . In any case the spinor projection ψ_- is constrained and determined from the equations of motion.

Discretization is achieved by putting the theory in a light-cone “box”, with $-L_\perp \leq x^i \leq L_\perp$ and $-L \leq x^- \leq L$, and imposing boundary conditions on the fields. A_μ must be taken to be periodic in both x^- and x_\perp . It is most convenient to choose the Fermion fields to be periodic in x_\perp and anti-periodic in x^- . This eliminates the zero longitudinal momentum mode while still allowing an expansion of the field in a complete set of basis functions.

The functions used to expand the fields may be taken to be plane waves, and for periodic fields these will of course include zero-momentum modes. Let us define, for a periodic quantity f , its

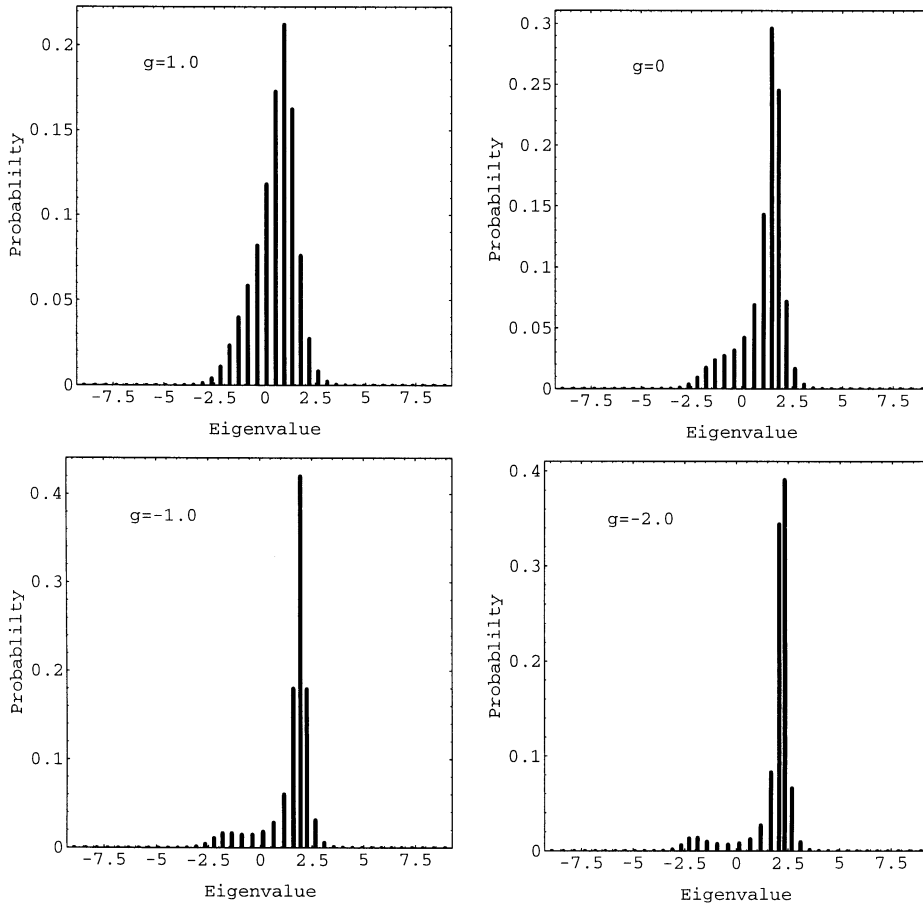


Fig. 36. Probability distribution of eigenvalues of $\sqrt{4\pi}\phi$ for the vacuum with couplings $g = 1$, $g = 0$, $g = -1$, and $g = -2$, all for $M = 1$ and $N = 50$. The positive VEV solution to the constraint equation is used.

longitudinal zero mode

$$\langle f \rangle_0 \equiv \frac{1}{2L} \int_{-L}^L dx^- f(x^-, x_\perp) \quad (7.36)$$

and the corresponding normal mode part

$$\langle f \rangle_n \equiv f - \langle f \rangle_0. \quad (7.37)$$

We shall further denote the “global zero mode” – the mode independent of all the spatial coordinates – by $\langle f \rangle$:

$$\langle f \rangle \equiv \frac{1}{\Omega} \int_{-L}^L dx^- \int_{-L_\perp}^{L_\perp} d^2x_\perp f(x^-, x_\perp). \quad (7.38)$$

Finally, the quantity which will be of most interest to us is the “proper zero mode”, defined by

$$f_0 \equiv \langle f \rangle_0 - \langle f \rangle. \quad (7.39)$$

By integrating over the appropriate direction(s) of space, we can project the equations of motion onto the various sectors. The global zero mode sector requires some special treatment, and will not be discussed here.

We concentrate our attention on the proper zero mode sector, in which the equations of motion become

$$-\partial_{\perp}^2 A_0^+ = gJ_0^+, \quad (7.40)$$

$$-2(\partial_+)^2 A_0^+ - \partial_{\perp}^2 A_0^- - 2\partial_i \partial_+ A_0^i = gJ_0^-, \quad (7.41)$$

$$-\partial_{\perp}^2 A_0^i + \partial_i \partial_+ A_0^+ + \partial_i \partial_j A_0^j = gJ_0^i. \quad (7.42)$$

We first observe that Eq. (7.40), the projection of Gauss’ law, is a constraint which determines the proper zero mode of A^+ in terms of the current J^+ :

$$A_0^+ = -g(1/\partial_{\perp}^2)J_0^+. \quad (7.43)$$

Eqs. (7.41) and (7.42) then determine the zero modes A_0^- and A_0^i .

Eq. (7.43) is clearly incompatible with the strict light-cone gauge $A^+ = 0$, which is most natural in light-cone analyses of gauge theories. Here we encounter a common problem in treating axial gauges on compact spaces, which has nothing to do with light-cone quantization per se. The point is that any x^- -independent part of A^+ is in fact gauge invariant, since under a gauge transformation

$$A^+ \rightarrow A^+ + 2\partial_- A, \quad (7.44)$$

where A is a function periodic in all coordinates. Thus, it is not possible to bring an arbitrary gauge field configuration to one satisfying $A^+ = 0$ via a gauge transformation, and the light-cone gauge is incompatible with the chosen boundary conditions. The closest we can come is to set the normal mode part of A^+ to zero, which is equivalent to

$$\partial_- A^+ = 0. \quad (7.45)$$

This condition does not, however, completely fix the gauge – we are free to make arbitrary x^- -independent gauge transformations without undoing Eq. (7.45). We may therefore impose further conditions on A_{μ} in the zero-mode sector of the theory.

To see what might be useful in this regard, let us consider solving Eq. (7.42). We begin by acting on Eq. (7.42) with ∂_i . The transverse field A_0^i then drops out and we obtain an expression for the time derivative of A_0^+ :

$$\partial_+ A_0^+ = g(1/\partial_{\perp}^2)\partial_i J_0^i. \quad (7.46)$$

[This can also be obtained by taking a time derivative of Eq. (7.43), and using current conservation to re-express the right-hand side in terms of J^i]. Inserting this back into Eq. (7.42) we then find, after some rearrangement,

$$-\partial_{\perp}^2(\delta_j^i - \partial_i \partial_j / \partial_{\perp}^2)A_0^i = g(\delta_j^i - \partial_i \partial_j / \partial_{\perp}^2)J_0^j. \quad (7.47)$$

Now the operator $(\delta_j^i - \partial_i \partial_j / \partial_\perp^2)$ is nothing more than the projector of the two-dimensional transverse part of the vector fields A_0^i and J_0^i . No trace remains of the longitudinal projection of the field $(\partial_i \partial_j / \partial_\perp^2) A_0^j$ in Eq. (7.47). This reflects precisely the residual gauge freedom with respect to x^- -independent transformations. To determine the longitudinal part, an additional condition is required.

More concretely, the general solution to Eq. (7.47) is

$$A_0^i = -g(1/\partial_\perp^2) J_0^i + \partial_i \varphi(x^+, x_\perp), \quad (7.48)$$

where φ must be independent of x^- but is otherwise arbitrary. Imposing a condition on, say, $\partial_i A_0^i$ will uniquely determine φ .

In Ref. [259], for example, the condition

$$\partial_i A_0^i = 0 \quad (7.49)$$

was proposed as being particularly natural. This choice, taken with the other gauge conditions we have imposed, has been called the “compactification gauge”. In this case

$$\varphi = g(1/(\partial_\perp^2)^2) \partial_i J_0^i. \quad (7.50)$$

Of course, other choices are also possible. For example, we might generalize Eq. (7.50) to

$$\varphi = \alpha g(1/(\partial_\perp^2)^2) \partial_i J_0^i, \quad (7.51)$$

with α a real parameter. The gauge condition corresponding to this solution is

$$\partial_i A_0^i = -g(1 - \alpha)(1/\partial_\perp^2) \partial_i J_0^i. \quad (7.52)$$

We shall refer to this as the “generalized compactification gauge”. An arbitrary gauge field configuration B^μ can be brought to one satisfying Eq. (7.52) via the gauge function

$$A(x_\perp) = -(1/\partial_\perp^2) [g(1 - \alpha)(1/\partial_\perp^2) \partial_i J_0^i + \partial_i B_0^i]. \quad (7.53)$$

This is somewhat unusual in that $A(x_\perp)$ involves the sources as well as the initial field configuration, but this is perfectly acceptable. More generally, φ can be any (dimensionless) function of gauge invariants constructed from the fields in the theory, including the currents J^\pm . For our purposes Eq. (7.52) suffices.

We now have relations defining the proper zero modes of A^i ,

$$A_0^i = -g(1/\partial_\perp^2) (\delta_j^i - \alpha \partial_i \partial_j / \partial_\perp^2) J_0^j, \quad (7.54)$$

as well as A_0^+ [Eq. (7.43)]. All that remains is to use the final constraint, Eq. (7.41), to determine A_0^- . Using Eqs. (7.46) and (7.52), we find that Eq. (7.41) can be written as

$$\partial_\perp^2 A_0^- = -g J_0^- - 2\alpha g(1/\partial_\perp^2) \partial_+ \partial_i J_0^i. \quad (7.55)$$

After using the equations of motion to express $\partial_+ J_0^i$ in terms of the dynamical fields at $x^+ = 0$, this may be straightforwardly solved for A_0^- by inverting the ∂_\perp^2 . In what follows, however, we shall have no need of A_0^- . It does not enter the Hamiltonian, for example; as usual, it plays the role of a multiplier to Gauss’ law, Eq. (7.42), which we are able to implement as an operator identity.

We have shown how to perform a general gauge fixing of Abelian gauge theory in DLCQ and cleanly separate the dynamical from the constrained zero-longitudinal momentum fields. The

various zero-mode fields *must* be retained in the theory if the equations of motion are to be realized as the Heisenberg equations. We have further seen that taking the constrained fields properly into account renders the ultraviolet behavior of the theory more benign, in that it results in the automatic generation of a counter term for a non-covariant divergence in the fermion self-energy in lowest-order perturbation theory.

The solutions to the constraint relations for the A_0^i are all physically equivalent, being related by different choices of gauge in the zero mode sector of the theory. There is a gauge which is particularly simple, however, in that the fields may be taken to satisfy the usual canonical anti-commutation relations. This is most easily exposed by examining the kinematical Poincaré generators and finding the solution for which these retain their free-field forms. The unique solution that achieves this is $\varphi = 0$ in Eq. (7.48). For solutions other than this one, complicated commutation relations between the fields will be necessary to correctly translate them in the initial-value surface.

It would be interesting to study the structure of the operators induced by the zero modes from the point of view of the light-cone power-counting analysis of Wilson [456]. As noted in the Introduction, to the extent that DLCQ coincides with reality, effects which we would normally associate with the vacuum must be incorporated into the formalism through the new, non-canonical interactions arising from the zero modes. Particularly interesting is the appearance of operators that are non-local in the transverse directions. These are interesting because the strong infrared effects they presumably mediate could give rise to transverse confinement in the effective Hamiltonian for QCD. There is longitudinal confinement already at the level of the canonical Hamiltonian; that is, the effective potential between charges separated only in x^- grows linearly with the separation. This comes about essentially from the non-locality in x^- (i.e. the small- k^+ divergences) of the light-cone formalism.

It is clearly of interest to develop non-perturbative methods for solving the constraints, since we are ultimately interested in non-perturbative diagonalization of P^- . Several approaches to this problem have recently appeared in the literature [209,210,33,382], in the context of scalar field theories in $1 + 1$ dimensions. For QED with a realistic value of the electric charge, however, it might be that a perturbative treatment of the constraints could suffice; that is, that we could use a perturbative solution of the constraint to construct the Hamiltonian, which would then be diagonalized non-perturbatively. An approach similar in spirit has been proposed in Ref. [456], where the idea is to use a perturbative realization of the renormalization group to construct an effective Hamiltonian for QCD, which is then solved non-perturbatively. There is some evidence that this kind of approach might be useful. Wivoda and Hiller have recently used DLCQ to study a theory of neutral and interacting charged scalar fields in $3 + 1$ dimensions [458]. They discovered that including four-fermion operators precisely analogous to the perturbative ones appearing in P^- significantly improved the numerical behavior of the simulation.

The extension of the present work to the case of QCD is complicated by the fact that the constraint relations for the gluonic zero modes are non-linear, as in the ϕ^4 theory. A perturbative solution of the constraints is of course still possible, but in this case, since the effective coupling at the relevant (hadronic) scale is large, it is clearly desirable to go beyond perturbation theory. In addition, because of the central role played by gauge fixing in the present work, we may expect complications due to the Gribov ambiguity [189], which prevents the selection of unique representatives on gauge orbits in non-perturbative treatments of Yang–Mills theory. As a step in this

direction, work is in progress on the pure glue theory in 2 + 1 dimensions [259]. There it is expected that some of the non-perturbative techniques used recently in 1 + 1 dimensions [33,382,379–381,331] can be applied.

7.3. Dynamical zero modes

Our concern in this section is with zero modes that are true dynamical independent fields. They can arise due to the boundary conditions in gauge theory one cannot fully implement the traditional light-cone gauge $A^+ = 0$. The development of the understanding of this problem in DLCQ can be traced in Refs. [206–209,325,326]. The field A^+ turns out to have a zero mode which cannot be gauged away [258,259,261,379–381,331]. This mode is indeed dynamical, and is the object we study in this paper. It has its analogue in instant form approaches to gauge theory. For example, there exists a large body of work on Abelian and non-Abelian gauge theories in 1 + 1 dimensions quantized on a cylinder geometry [321,217]. There indeed this dynamical zero mode plays an important role. We too shall concern ourselves in the present section with non-Abelian gauge theory in 1 + 1 dimensions, revisiting the model introduced by 't Hooft [424].

The specific task we undertake here is to understand the zero-mode *subsector* of the pure glue theory, namely where only zero-mode external sources excite only zero-mode gluons. We shall see that this is not an approximation but rather a consistent solution, a sub-regime within the complete theory. A similar framing of the problem lies behind the work of Lüscher [314] and van Baal [434] using the instant form Hamiltonian approach to pure glue gauge theory in 3 + 1 dimensions. The beauty of this reduction in the (1 + 1)-dimensional theory is twofold. First, it yields a theory which is exactly soluble. This is useful given the dearth of soluble models in field theory. Secondly, the zero-mode theory represents a paring down to the point where the front and instant forms are manifestly *identical*, which is nice to know indeed. We solve the theory in this specific dynamical regime and find a discrete spectrum of states whose wavefunctions can be completely determined. These states have the quantum numbers of the vacuum.

We consider an SU(2) non-Abelian gauge theory in 1 + 1 dimensions with classical sources coupled to the gluons. The Lagrangian density is

$$\mathcal{L} = \frac{1}{2}\text{Tr}(F_{\mu\nu}F^{\mu\nu}) + 2 \text{Tr}(J_\mu A^\mu) \quad (7.56)$$

where $F_{\mu\nu} = \partial_\nu A_\mu - \partial_\mu A_\nu - g[A_\mu, A_\nu]$. With a finite interval in x^- from $-L$ to L , we impose periodic boundary conditions on all gauge potentials A_μ .

We cannot eliminate the zero mode of the gauge potential. The reason is evident: it is *invariant* under periodic gauge transformations. But, of course, we can always perform a rotation in color space. In line with other authors [14,385,146–148], we choose this so that A_3^+ is the only non-zero element, since in our representation only σ^3 is diagonal. In addition, we can impose the subsidiary gauge condition $A_3^- = 0$. The reason is that there still remains freedom to perform gauge transformations that depend only on light-cone time x^+ and the color matrix σ^3 .

The above procedure would appear to have enabled complete fixing of the gauge. This is still not so. Gauge transformations

$$V = \exp\{ix^-(n\pi/2L)\sigma^3\} \quad (7.57)$$

generate shifts, according to Eq. (7.53), in the zero-mode component

$$\overset{o}{A}_3^+ \rightarrow \overset{o}{A}_3^+ + n\pi/gL. \quad (7.58)$$

All of these possibilities, labelled by the integer n , of course still satisfy $\partial_- A^+ = 0$, but as one sees $n = 0$ should not really be included. One can verify that the transformations V also preserve the subsidiary condition. One notes that the transformation is x^- -dependent and Z_2 periodic. It is thus a simple example of a Gribov copy [189] in $1 + 1$ dimensions. We follow the conventional procedure by demanding

$$\overset{o}{A}_3^+ \neq n\pi/gL, \quad n = \pm 1, \pm 2, \dots. \quad (7.59)$$

This eliminates singularity points at the Gribov “horizons” which in turn correspond to a vanishing Faddeev–Popov determinant [434].

For convenience, we henceforth use the notation

$$\overset{o}{A}_3^+ = v, \quad x^+ = t, \quad w^2 = J_+^+ J_+^- / g^2 \quad \text{and} \quad J_3^- = \frac{1}{2}B. \quad (7.60)$$

We pursue a Hamiltonian formulation. The only conjugate momentum is

$$p \equiv \overset{o}{\Pi}_3^- = \partial^- \overset{o}{A}_3^+ = \partial^- v. \quad (7.61)$$

The Hamiltonian density $T^{+-} = \partial^- \overset{o}{A}_3^+ \overset{o}{\Pi}_3^- - \mathcal{L}$ leads to the Hamiltonian

$$H = \frac{1}{2}[p^2 + (w^2/v^2) + Bv](2L). \quad (7.62)$$

Quantization is achieved by imposing a commutation relation at equal light-cone time on the dynamical degree of freedom. Introducing the variable $q = 2Lv$, the appropriate commutation relation is $[q(x^+), p(x^+)] = i$. The field theoretic problem reduces to quantum mechanics of a single particle as in Manton’s treatment of the Schwinger model in Refs. [321]. One thus has to solve the Schrödinger equation

$$\frac{1}{2} \left(-\frac{d^2}{dq^2} + \frac{(2Lw)^2}{q^2} + \frac{Bq}{2L} \right) \psi = \mathcal{E} \psi, \quad (7.63)$$

with the eigenvalue $\mathcal{E} = E/(2L)$ actually being an energy density.

All eigenstates ψ have the quantum numbers of the naive vacuum adopted in standard front form field theory: all of them are eigenstates of the light-cone momentum operator P^+ with zero eigenvalue. The true vacuum is now that state with lowest P^- eigenvalue. In order to get an exactly soluble system we eliminate the source $2B = J_3^-$.

The boundary condition that is to be imposed comes from the treatment of the Gribov problem. Since the wavefunction vanishes at $q = 0$ we must demand that the wavefunctions vanish at the first Gribov horizon $q = \pm 2\pi/g$. The overall constant R is then fixed by normalization. This leads

to the energy density only assuming the discrete values

$$\mathcal{E}_m^{(\nu)} = (g^2/8\pi^2)(X_m^{(\nu)})^2, \quad m = 1, 2, \dots, \quad (7.64)$$

where $X_m^{(\nu)}$ denotes the m th zero of the ν th Bessel function J_ν . In general, these zeroes can only be obtained numerically. Thus

$$\psi_m(q) = R\sqrt{q}J_\nu(\sqrt{2\mathcal{E}_m^{(\nu)}}q) \quad (7.65)$$

is the complete solution. The true vacuum is the state of lowest energy namely with $m = 1$.

The exact solution we obtained is genuinely non-perturbative in character. It describes vacuum-like states since for all of these states $P^+ = 0$. Consequently, they all have zero invariant mass $M^2 = P^+P^-$. The states are labelled by the eigenvalues of the operator P^- . The linear dependence on L in the result for the discrete energy levels is also consistent with what one would expect from a loop of color flux running around the cylinder.

In the source-free equal time case Hetrick [217,218] uses a wavefunction that is symmetric about $q = 0$. For our problem this corresponds to

$$\psi_m(q) = N \cos(\sqrt{2\varepsilon_m}q), \quad (7.66)$$

where N is fixed by normalization. At the boundary of the fundamental modular region $q = 2\pi/g$ and $\psi_m = (-1)^m N$, thus $\sqrt{2\varepsilon_m}2\pi/g = m\pi$ and

$$\varepsilon = \frac{1}{8}g^2(m^2 - 1). \quad (7.67)$$

Note that $m = 1$ is the lowest-energy state and has as expected one node in the allowed region $0 \leq q \leq 2\pi/g$. Hetrick [217] discusses the connection to the results of Rajeev [387] but it amounts to a shift in ε and a redefining of $m \rightarrow m/2$. It has been argued by van Baal that the correct boundary condition at $q = 0$ is $\psi(0) = 0$. This would give a sine which matches smoothly with the Bessel function solution. This calculation offers the lesson that even in a front-form approach, the vacuum might not be just the simple Fock vacuum. Dynamical zero modes do imbue the vacuum with a rich structure.

8. Non-perturbative regularization and renormalization

The subject of renormalization is a large one and high-energy theorists have developed a standard set of renormalization techniques based on perturbation theory (see, for example, Ref. [111]). However, many of these techniques are poorly suited for light-front field theory. Researchers in light-front field theory must either borrow techniques from condensed matter physics [374,435,453] or nuclear physics or come up with entirely new approaches. Some progress in this direction has already been made, see, for example, Refs. [294,444–447,456]. A considerable amount of work is focusing on these questions [8,2,85,134,194,233,464]; particularly see the work of Bassetto et al. [5,23–26], Bakker et al. [309,310,399], Brisudova et al. [48–50], and Zhang et al. [461–466]. It should be noted, however, that the work of Perry and collaborators [48–50,461–466] has strange aspects beyond all the effort. Front-form QCD is a theory with many useful symmetries like gauge invariance, Lorentz invariance, thus boost, rotational and chiral invariance. But these

authors, particularly in Refs. [49,50,466], somehow manage to admittedly give up each and every one of them, including rotational invariance (thus no degeneracies of multiplets). This shows how difficult the problem is. But it is not really what one aims at.

The biggest challenge to renormalization of light-front field theory is the infrared divergences that arise. Recall that the Hamiltonian for a free particle is

$$P^- = (\mathbf{P}_\perp^2 + m^2)/2P^+. \quad (8.1)$$

Small longitudinal momentum P^+ is associated with large energies. Thus, light-front field theory is subject to infrared longitudinal divergences. These divergences are quite different in nature from the infrared divergences found in equal-time quantized field theory. In order to remove small P^+ states, one must introduce non-local counter terms into the Hamiltonian. Power counting arguments allow arbitrary *functions* of transverse momenta to be associated with these counter terms. This is in contrast to more conventional approaches where demanding locality strongly constrains the number of allowed operators.

One hopes to use light-front field theory to perform bound state calculations. In this case one represents a bound state by a finite number of particles (a Tamm–Dancoff truncation) whose momenta are restricted to some finite interval. This has a number of implications. In particular, momentum cutoffs and Tamm–Dancoff truncations both tend to break various symmetries of a theory. Proper renormalization must restore these symmetries. In contrast, conventional calculations choose regulators (like dimensional regularization) that do not break many symmetries.

In conventional approaches, one is often concerned simply whether the system is renormalizable, that is, whether the large cutoff limit is well defined. In bound-state calculations, one is also interested in how quickly the results converge as one increases the cutoffs since numerical calculations must be performed with a finite cutoff. Thus, one is potentially interested in the effects of irrelevant operators along with the usual marginal and relevant operators.

Conventional renormalization is inherently perturbative in nature. However, we are interested in many phenomena that are essentially non-perturbative: bound states, confinement, and spontaneous symmetry breaking. The bulk of renormalization studies in light-front field theory to date have used perturbative techniques [456,182]. Non-perturbative techniques must be developed.

Generally, one expects that renormalization will produce a large number of operators in the light-front Hamiltonian. A successful approach to renormalization must be able to produce these operators automatically (say, as part of a numerical algorithm). In addition, there should be only a few free parameters which must be fixed phenomenologically. Otherwise, the predictive power of a theory will be lost.

8.1. Tamm–Dancoff integral equations

Let us start by looking at a simple toy model that has been studied by a number of authors [435,182,374,426,427,244]. In fact, it is the famous Kondo problem truncated to one-particle states [277]. Consider the homogeneous integral equation

$$(p - E)\phi(p) + g \int_0^A dp' \phi(p') = 0 \quad (8.2)$$

with eigenvalue E and eigenvector $\phi(p)$. This is a model for Tamm–Dancoff equation of a single particle of momentum p with Hamiltonian $H(p,p') = p\delta(p - p') + g$. We will focus on the $E < 0$ bound state solution:

$$\phi(p) = \text{constant}/(p - E), \quad E = \Lambda/(1 - e^{-1/g}). \quad (8.3)$$

Note that the eigenvalue diverges in the limit $\Lambda \rightarrow \infty$. Proper renormalization involves modifying the system to make E and $\phi(p)$ independent of Λ in the limit $\Lambda \rightarrow \infty$. Towards this end, we add a counterterm C_Λ to the Hamiltonian. Invoking the high-low analysis [454], we divide the interval $0 < p < \Lambda$ into two subintervals: $0 < p < L$, a “low-momentum region”, and $L < p < \Lambda$, a “high-momentum region”, where the momentum scales characterized by E , L , and Λ are assumed to be widely separated. The idea is that the eigenvalue and eigenvector should be independent of the behavior of the system in the high momentum region. The eigenvalue equation can be written as two coupled equations

$$p \in [0, L], \quad (p - E)\phi(p) + (g + C_\Lambda) \int_0^L dp' \phi(p') + (g + C_\Lambda) \int_L^\Lambda dp' \phi(p') = 0, \quad (8.4)$$

$$p \in [L, \Lambda], \quad (p - E)\phi(p) + (g + C_\Lambda) \int_L^\Lambda dp' \phi(p') + (g + C_\Lambda) \int_0^L dp' \phi(p') = 0. \quad (8.5)$$

Integrating Eq. (8.5) in the limit $L, \Lambda \gg E$,

$$\int_L^\Lambda dp \phi(p) = - \frac{(g + C_\Lambda) \log(\Lambda/L)}{1 + (g + C_\Lambda) \log(\Lambda/L)} \int_0^L dp' \phi(p'), \quad (8.6)$$

and substituting this expression into Eq. (8.4), we obtain an eigenvalue equation with the high-momentum region integrated out

$$p \in [0, L], \quad (p - E)\phi(p) + \frac{(g + C_\Lambda)}{1 + (g + C_\Lambda) \log(\Lambda/L)} \int_0^L dp' \phi(p') = 0. \quad (8.7)$$

If we demand this expression to be independent of Λ ,

$$\frac{d}{d\Lambda} \left(\frac{(g + C_\Lambda)}{1 + (g + C_\Lambda) \log(\Lambda/L)} \right) = 0, \quad (8.8)$$

we obtain a differential equation for C_Λ ,

$$dC_\Lambda/d\Lambda = (g + C_\Lambda)^2/\Lambda. \quad (8.9)$$

Solving this equation, we are free to insert an arbitrary constant $-1/A_\mu - \log \mu$

$$g + C_\Lambda = \frac{A_\mu}{1 - A_\mu \log(\Lambda/\mu)}. \quad (8.10)$$

Substituting this result back into Eq. (8.7),

$$p \in [0, L], \quad (p - E)\phi(p) + \frac{A_\mu}{1 - A_\mu \log(L/\mu)} \int_0^L dp' \phi(p') = 0, \quad (8.11)$$

we see that Λ has been removed from the equation entirely. Using Eq. (8.10) in the original eigenvalue equation

$$(p - E)\phi(p) + \frac{A_\mu}{1 - A_\mu \log(\Lambda/\mu)} \int_0^\Lambda dp' \phi(p') = 0 \quad (8.12)$$

gives the same equation as Eq. (8.11) with L replaced by Λ . The eigenvalue is now,

$$E = \Lambda / (1 - (\Lambda/\mu)e^{-1/A_\mu}), \quad \lim_{\Lambda \rightarrow \infty} E = -\mu e^{1/A_\mu}. \quad (8.13)$$

Although the eigenvalue is still a function of the cutoff for finite Λ , the eigenvalue does become independent of the cutoff in the limit $\Lambda \rightarrow \infty$, and the system is properly renormalized.

One can think of A_μ as the renormalized coupling constant and μ as the renormalization scale. In that case, the eigenvalue should depend on the choice of A_μ for a given μ but be independent of μ itself. Suppose, for Eq. (8.13), we want to change μ to a new value, say μ' . In order that the eigenvalue remains the same, we must also change the coupling constant from A_μ to $A_{\mu'}$,

$$\mu e^{1/A_\mu} = \mu' e^{1/A_{\mu'}}. \quad (8.14)$$

In the same manner, one can write down a β -function for A_μ [436],

$$\mu(d/d\mu)A_\mu = A_\mu^2. \quad (8.15)$$

Using these ideas one can examine the general case. Throughout, we will be working with operators projected onto some Tamm–Dancoff subspace (finite particle number) of the full Fock space. In addition, we will regulate the system by demanding that each component of momentum of each particle lies within some finite interval. One defines the “cutoff” Λ to be an operator which projects onto this subspace of finite particle number and finite momenta. Thus, for any operator O , $O \equiv \Lambda O \Lambda$. Consider the Hamiltonian

$$H = H_0 + V + C_\Lambda, \quad (8.16)$$

where, in the standard momentum space basis, H_0 is the diagonal part of the Hamiltonian, V is the interaction term, and C_Λ is the counter term which is to be determined and is a function of the cutoff. Each term of the Hamiltonian is hermitian and compact. Schrödinger’s equation can be written

$$(H_0 - E)|\phi\rangle + (V + C_\Lambda)|\phi\rangle = 0 \quad (8.17)$$

with energy eigenvalue E and eigenvector $|\phi\rangle$. The goal is to choose C_Λ such that E and $|\phi\rangle$ are independent of Λ in the limit of large cutoff.

One now makes an important assumption: the physics of interest is characterized by energy scale E and is independent of physics near the boundary of the space spanned by Λ . Following the approach of the previous section, one defines two projection operators, \mathcal{Q} and \mathcal{P} , where $\Lambda = \mathcal{Q} + \mathcal{P}$, $\mathcal{Q}\mathcal{P} = \mathcal{P}\mathcal{Q} = 0$, and \mathcal{Q} and \mathcal{P} commute with H_0 . \mathcal{Q} projects onto a “high-momentum region” which contains energy scales one does not care about, and \mathcal{P} projects onto a “low-momentum region” which contains energy scales characterized by E . Schrödinger’s equation (8.17)

can be rewritten as two coupled equations:

$$(H_0 - E)\mathcal{P}|\phi\rangle + \mathcal{P}(V + C_A)\mathcal{P}|\phi\rangle + \mathcal{P}(V + C_A)\mathcal{Q}|\phi\rangle = 0, \quad (8.18)$$

and

$$(H_0 - E)\mathcal{Q}|\phi\rangle + \mathcal{Q}(V + C_A)\mathcal{Q}|\phi\rangle + \mathcal{Q}(V + C_A)\mathcal{P}|\phi\rangle = 0. \quad (8.19)$$

Using Eq. (8.19), one can formally solve for $\mathcal{Q}|\phi\rangle$ in terms of $\mathcal{P}|\phi\rangle$,

$$\mathcal{Q}|\phi\rangle = (1/2(E - H)\mathcal{Q})(V + C_A)\mathcal{P}|\phi\rangle. \quad (8.20)$$

The term with the denominator is understood to be defined in terms of its series expansion in V . One can substitute this result back into Eq. (8.18),

$$(H_0 - E)\mathcal{P}|\phi\rangle + \mathcal{P}(V + C_A)\mathcal{P}|\phi\rangle + \mathcal{P}(V + C_A)(1/2(E - H)\mathcal{Q})(V + C_A)\mathcal{P}|\phi\rangle = 0. \quad (8.21)$$

In order to properly renormalize the system, we could choose C_A such that Eq. (8.21) is independent of one's choice of A for a fixed \mathcal{P} in the limit of large cutoffs. However, we will make a stronger demand: that Eq. (8.21) should be equal to Eq. (8.17) with the cutoff A replaced by \mathcal{P} .

One can express C_A as the solution of an operator equation, the “counter term equation”,

$$V_A = V - VFV_A. \quad (8.22)$$

where $V_A = V + C_A$, and provided that we can make the approximation

$$V(\mathcal{Q}/(E - H_0))V \approx V\mathcal{Q}FV. \quad (8.23)$$

This is what we will call the “renormalizability condition”. A system is properly renormalized if, as we increase the cutoffs A and \mathcal{P} , Eq. (8.23) becomes an increasingly good approximation. In the standard momentum space basis, this becomes a set of coupled inhomogeneous integral equations. Such equations generally have a unique solution, allowing us to renormalize systems without having to resort to perturbation theory. This includes cases where the perturbative expansion diverges or converges slowly.

There are many possible choices for F that satisfy the renormalizability condition. For instance, one might argue that we want F to resemble $1/(E - H_0)$ as much as possible and choose

$$F = 1/(\mu - H_0), \quad (8.24)$$

where the arbitrary constant μ is chosen to be reasonably close to E . In this case, one might be able to use a smaller cutoff in numerical calculations.

One might argue that physics above some energy scale μ is simpler and that it is numerically too difficult to include the complications of the physics at energy scale E in the solution of the counter term equation. Thus, one could choose

$$F = -\theta(H_0 - \mu)/H_0, \quad (8.25)$$

where the arbitrary constant μ is chosen to be somewhat larger than E but smaller than the energy scale associated with the cutoff. The θ -function is assumed to act on each diagonal element in the standard momentum space basis. The difficulty with this renormalization scheme is that it involves three different energy scales, E , μ and the cutoff which might make the numerical problem more

difficult. One can relate our approach to conventional renormalization group concepts. In renormalization group language, V_A is the bare interaction term and V is the renormalized interaction term. In both of the renormalization schemes introduced above, we introduced an arbitrary energy scale μ ; this is the renormalization scale. Now, physics (the energy eigenvalues and eigenvectors) should not depend on this parameter or on the renormalization scheme itself, for that matter. How does one move from one renormalization scheme to another? Consider a particular choice of renormalized interaction term V associated with a renormalization scheme which uses F in the counter term equation. We can use the counter term equation to find the bare coupling V_A in terms of V . Now, to find the renormalized interaction term V' associated with a different renormalization scheme using a different operator F' in the counter term equation, we simply use the counter term equation with V_A as given and solve for V'

$$V' = V_A + V_A F' V' . \quad (8.26)$$

Expanding this procedure order by order in V and summing the result, we can obtain an operator equation relating the two renormalized interaction terms directly

$$V' = V + V(F' - F)V' . \quad (8.27)$$

The renormalizability condition ensures that this expression will be independent of the cutoff in the limit of large cutoff.

For the two particular renormalization schemes mentioned above, Eqs. (8.24) and (8.25), we can regard the renormalized interaction term V as an implicit function of μ . We can see how the renormalized interaction term changes with μ in the case (8.24):

$$\mu dV/d\mu = -V(\mu/(H_0 - \mu)^2)V \quad (8.28)$$

and in the case of Eq. (8.25),

$$\mu dV/d\mu = V\delta(H_0 - \mu)V . \quad (8.29)$$

This is a generalization of the β -function. The basic idea of asymptotic and box counter term renormalization in the 3 + 1 Yukawa model calculation in an earlier section can be illustrated with a simple example. Consider an eigenvalue equation of the form [426,427],

$$k\phi(k) - g \int_0^A dq V(k, q)\phi(q) = E\phi(k) . \quad (8.30)$$

Making a high–low analysis of this equation as above and assuming that

$$V_{\text{LH}}(k, q) = V_{\text{HL}}(k, q) = V_{\text{HH}}(k, q) = f . \quad (8.31)$$

Then one finds the following renormalized equation:

$$k\phi(k) - g \int_0^A dq [V(k, q) - f]\phi(q) - \frac{A_\mu}{1 + A_\mu \ln(A/\mu)} \int_0^A dq \phi(q) = E\phi(k) . \quad (8.32)$$

One has renormalized the original equation in the sense that the low-energy eigenvalue E is independent of the high-energy cutoff and we have an arbitrary parameter C which can be adjusted to fit the ground-state energy level.

One can motivate both the asymptotic counter term and one-box counter term in the Yukawa calculation as different choices in our analysis. For a fixed μ we are free to choose A_μ at will. The simple asymptotic counter term corresponds to $A_\mu = 0$. However, subtracting the asymptotic behavior of the kernel with the term gf causes the wavefunction to fall off more rapidly than it would otherwise at large q . As a result the $(A_\mu/(1 + A_\mu \ln \Lambda/\mu)) \int \phi dq$ is finite, and this term can be retained as an arbitrary adjustable finite counter term.

The perturbative counter terms correspond to $A_\mu = gf$ then expanding in $g \ln \Lambda/\mu$. Then one finds

$$k\phi(k) - g \int_0^\Lambda dq [V(k, q) - f]\phi(q) - gf \sum_{n=0}^{\infty} (-gf \ln \Lambda/\mu)^n \int_0^\Lambda dq \phi(q) = E. \quad (8.33)$$

Keeping the first two terms in the expansion one gets the so-called “Box counter term”

$$k\phi(k) - g \int_0^\Lambda dq V(k, q)\phi(q) + g^2 f^2 \ln \Lambda/\mu \int_0^\Lambda dq \phi(q) = E. \quad (8.34)$$

Note that the box counter term contains f^2 indicating that it involves the kernel at high momentum twice. Ideally, one would like to carry out the non-perturbative renormalization program rigorously in the sense that the cutoff independence is achieved for any value of the coupling constant and any value of the cutoff. In practical cases, either one may not have the luxury to go to very large cutoff or the analysis itself may get too complicated. For example, the assumption of a uniform high-energy limit was essential for summing up the series. In reality, V_{HH} may differ from V_{LH} .

The following is a simplified two-variable problems that are more closely related to the equations and approximations used in the Yukawa calculation. The form of the asymptotic counter term that was used can be understood by considering the following equation:

$$\frac{k}{x(1-x)}\phi(k, x) - g \int_0^\Lambda dq \int_0^1 dy K(k, q)\phi(q, y) = E\phi(k, x). \quad (8.35)$$

This problem contains only x dependence associated with the free energy, and no x dependence in the kernel. It is easily solved using the high–low analysis used above and one finds

$$k\phi(kx) - g \int_0^\Lambda dq \int_0^1 dy (K(k, q) - f)\phi(q, y) \quad (8.36)$$

$$- \frac{A_\mu}{1 + \frac{1}{6}A_\mu \ln \Lambda/\mu} \int_0^\Lambda dq \int_0^1 dy \phi(q, y) = E\phi(kx). \quad (8.37)$$

The factor of $1/6$ comes from the integral $\int_0^1 dx x(1-x)$. This result motivates our choice for G_A in the Yukawa calculation.

8.2. Wilson renormalization and confinement

QCD was a step backwards in the sense that it forced upon us a complex and mysterious vacuum. In QCD, because the effective coupling grows at long distances, there is always copious production of low-momentum gluons, which immediately invalidates any picture based on a few

constituents. Of course, this step was necessary to understand the nature of confinement and of chiral symmetry breaking, both of which imply a nontrivial vacuum structure. But for 20 years we have avoided the question: Why did the CQM work so well that no one saw any need for a complicated vacuum before QCD came along?

A bridge between equal-time quantized QCD and the equal-time CQM would clearly be extremely complicated, because in the equal-time formalism there is no easy non-perturbative way to make the vacuum simple. Thus, a sensible description of constituent quarks and gluons would be in terms of quasiparticle states, i.e., complicated collective excitations above a complicated ground state. Understanding the relation between the bare states and the collective states would involve understanding the full solution to the theory. Wilson and collaborators argue that on the light front, however, simply implementing a cutoff on small longitudinal momenta suffices to make the vacuum completely trivial. Thus, one immediately obtains a constituent-type picture, in which all partons in a hadronic state are connected directly to the hadron. The price one pays to achieve this constituent framework is that the renormalization problem becomes considerably more complicated on the light front [178–183].

Wilson and collaborators also included a mass term for the gluons as well as the quarks (they include only transverse polarization states for the gluons) in H_{free} . They have in mind here that all masses that occur in H_{free} should roughly correspond to constituent rather than current masses. There are two points that should be emphasized in this regard.

First, cutoff-dependent masses for both the quarks and gluons will be needed anyway as counter terms. This occurs because all the cutoffs one has for a non-perturbative Hamiltonian calculations violate both equal-time chiral symmetry and gauge invariance. These symmetries, if present, would have protected the quarks and gluons from acquiring this kind of mass correction. Instead, in the calculations discussed here both the fermion and gluon self-masses are quadratically divergent in a transverse momentum cutoff Λ .

The second point is more physical. When setting up perturbation theory (more on this below) one should always keep the zeroth order problem as close to the observed physics as possible. Furthermore, the division of a Hamiltonian into free and interacting parts is always completely arbitrary, though the convergence of the perturbative expansion may hinge crucially on how this division is made. Non-zero constituent masses for both quarks and gluons clearly come closer to the phenomenological reality (for hadrons) than do massless gluons and nearly massless light quarks.

Now, the presence of a non-zero gluon mass has important consequences. First, it automatically stops the running of the coupling below a scale comparable to the mass itself. This allows one to (arbitrarily) start from a small coupling at the gluon mass scale so that perturbation theory is everywhere valid, and only extrapolate back to the physical value of the coupling at the end. The quark and gluon masses also provide a kinematic barrier to parton production; the minimum free energy that a massive parton can carry is m^2/p^+ , so that as more partons are added to a state and the typical p^+ of each parton becomes small, the added partons are forced to have high energies. Finally, the gluon mass eliminates any infrared problems of the conventional equal-time type.

In their initial work they use a simple cutoff on constituent energies, that is, requiring

$$(p_{\perp}^2 + m^2)/p^+ < \Lambda^2/P^+ \quad (8.38)$$

for each constituent in a given Fock state. Imposing Eq. (8.38) does not completely regulate the theory, however; there are additional small- p^+ divergences coming from the instantaneous terms in

the Hamiltonian. They regulate these by treating them as if the instantaneously exchanged gluons and quarks were actually constituents.

Having stopped the running of the coupling below the constituent mass scale, one arbitrarily take it to be small at this scale, so that perturbation theory is valid at all energy scales. Now one can use power counting to identify all relevant and marginal operators (relevant or marginal in the renormalization group sense). Because of the cutoffs one must use, these operators are not restricted by Lorentz or gauge invariance. Because we have forced the vacuum to be trivial, the effects of spontaneous chiral symmetry breaking must be manifested in explicit chiral symmetry-breaking effective interactions. This means the operators are not restricted by chiral invariance either. There are thus a large number of allowed operators. Furthermore, since transverse divergences occur for any longitudinal momentum, the operators that remove transverse cutoff dependence contain functions of dimensionless ratios of all available longitudinal momenta. That is, many counter terms are not parameterized by single coupling constants, but rather by entire functions of longitudinal momenta. A precisely analogous result obtains for the counter terms for light-front infrared divergences; these will involve entire functions of transverse momenta. The counter term functions can in principle be determined by requiring that Lorentz and gauge invariance will be restored in the full theory.

The cutoff Hamiltonian, with renormalization counter terms, will thus be given as a power series in g_A :

$$H(\Lambda) = H^{(0)} + g_A H^{(1)} + g_A^2 H^{(2)} + \dots, \quad (8.39)$$

where all dependence on the cutoff Λ occurs through the running coupling g_A , and cutoff-dependent masses.

The next stage in building a bridge from the CQM to QCD is to establish a connection between the ad hoc $q\bar{q}$ potentials of the CQM and the complex many-body Hamiltonian of QCD.

In lowest order the canonical QCD Hamiltonian contains gluon emission and absorption terms, including emission and absorption of high-energy gluons. Since a gluon has energy $(k_\perp^2 + \mu^2)/k^+$ for momentum k , a high-energy gluon can result either if k_\perp is large or k^+ is small. But in the CQM, gluon emission is ignored and only low-energy states matter. How can one overcome this double disparity? The answer is that we can change the initial cutoff Hamiltonian $H(\Lambda)$ by applying a unitary transformation to it. We imagine constructing a transformation U that generates a new effective Hamiltonian H_{eff} :

$$H_{\text{eff}} = U^\dagger H(\Lambda) U. \quad (8.40)$$

We then choose U to cause H_{eff} to look as much like a CQM as we can [35,444–446].

The essential idea is to start out as though we were going to diagonalize the Hamiltonian $H(\Lambda)$, except that we stop short of computing actual bound states. A complete diagonalization would generate an effective Hamiltonian H_{eff} in diagonal form; all its off-diagonal matrix elements would be zero. Furthermore, in the presence of bound states the fully diagonalized Hamiltonian would act in a Hilbert space with discrete bound states as well as continuum quark–gluon states. In a confined theory there would only be bound states. What we seek is a compromise: an effective Hamiltonian in which some of the off-diagonal elements can be nonzero, but in return the Hilbert space for H_{eff} remains the quark–gluon continuum that is the basis for $H(\Lambda)$. No bound states

should arise. All bound states are to occur through the diagonalization of H_{eff} , rather than being part of the basis in which H_{eff} acts.

To obtain a CQM-like effective Hamiltonian, we would ideally eliminate all off-diagonal elements that involve emission and absorption of gluons or of $q\bar{q}$ pairs. It is the emission and absorption processes that are absent from the CQM, so we should remove them by the unitary transformation. However, we would allow off-diagonal terms to remain within any given Fock sector, such as $q\bar{q} \rightarrow q\bar{q}$ off-diagonal terms or $qqq \rightarrow qqq$ terms. This means we allow off-diagonal potentials to remain, and trust that bound states appear only when the potentials are diagonalized.

Actually, as discussed in Ref. [456], we cannot remove all the off-diagonal emission and absorption terms. This is because the transformation U is sufficiently complex that we only know how to compute it in perturbation theory. Thus, we can reliably remove in this way only matrix elements that connect states with a large energy difference; perturbation theory breaks down if we try to remove, for example, the coupling of low-energy quark to a low-energy quark–gluon pair. They therefore introduce a second cutoff parameter λ^2/P^+ , and design the similarity transformation to remove off-diagonal matrix elements between sectors where the energy *difference* between the initial and final states is greater than this cutoff. For example, in second order the effective Hamiltonian has a one-gluon exchange contribution in which the intermediate gluon state has an energy above the running cutoff. Since the gluon energy is $(k_{\perp}^2 + \mu^2)/k^+$, where k is the exchanged gluon momentum, the cutoff requirement is

$$(k_{\perp}^2 + \mu^2)/k^+ > \lambda^2/P^+. \quad (8.41)$$

This procedure is known as the “similarity renormalization group” method. For a more detailed discussion and for connections to renormalization group concepts see Ref. [456].

The result of the similarity transformation is to generate an effective light-front Hamiltonian H_{eff} , which must be solved non-perturbatively. Guided by the assumption that a constituent picture emerges, in which the physics is dominated by potentials in the various Fock space sectors, we can proceed as follows.

We first split H_{eff} anew into an unperturbed part H_0 and a perturbation V . The principle guiding this new division is that H_0 should contain the most physically relevant operators, e.g., constituent-scale masses and the potentials that are most important for determining the bound-state structure. All operators that change particle number should be put into V , as we anticipate that transitions between sectors should be a small effect. This is consistent with our expectation that a constituent picture results, but this must be verified by explicit calculations. Next we solve H_0 non-perturbatively in the various Fock space sectors, using techniques from many-body physics. Finally, we use bound-state perturbation theory to compute corrections due to V .

We thus introduce a second perturbation theory as part of building the bridge. The first perturbation theory is that used in the computation of the unitary transformation U for the incomplete diagonalization. The second perturbation theory is used in the diagonalization of H_{eff} to yield bound-state properties. Perry in particular has emphasized the importance of distinguishing these two different perturbative treatments [367]. The first is a normal field-theoretic perturbation theory based on an unperturbed free field theory. In the second perturbation theory a different unperturbed Hamiltonian is chosen, one that includes the dominant potentials that establish the bound-state structure of the theory. Our working assumption is that the dominant potentials come from the lowest-order potential terms generated in the perturbation

expansion for H_{eff} itself. Higher-order terms in H_{eff} would be treated as perturbations relative to these dominant potentials.

It is only in the second perturbative analysis that constituent masses are employed for the free quark and gluon masses. In the first perturbation theory, where we remove transitions to high-mass intermediate states, it is assumed that the expected field theoretic masses can be used, i.e., near-zero up- and down-quark masses and a gluon mass of zero. Because of renormalization effects, however, there are divergent mass counter terms in second order in $H(\Lambda)$. H_{eff} also has second-order mass terms, but they must be finite – all divergent renormalizations are accomplished through the transformation U . When we split H_{eff} into H_0 and V , we include in H_0 both constituent quark and gluon masses and the dominant potential terms necessary to give a reasonable qualitative description of hadronic bound states. Whatever is left in H_{eff} after subtracting H_0 is defined to be V .

In both perturbation computations the same expansion parameter is used, namely the coupling constant g . In the second perturbation theory the running value of g measured at the hadronic mass scale is used. In relativistic field theory g at the hadronic scale has a fixed value g_s of order one; but in the computations an expansion for arbitrarily small g is used. It is important to realize that covariance and gauge invariance are violated when g differs from g_s ; the QCD coupling at any given scale is not a free parameter. These symmetries can only be fully restored when the coupling at the hadronic scale takes its physical value g_s .

The conventional wisdom is that any weak-coupling Hamiltonian derived from QCD will have only Coulomb-like potentials, and certainly will not contain confining potentials. Only a strong-coupling theory can exhibit confinement. This wisdom is wrong [456]. When H_{eff} is constructed by the unitary transformation of Eq. (8.40), with U determined by the “similarity renormalization group” method, H_{eff} has an explicit confining potential already in second order! We shall explain this result below. However, first we should give the bad news. If quantum electrodynamics (QED) is solved by the same process as we propose for QCD, then the effective Hamiltonian for QED has a confining potential too. In the electro-dynamic case, the confining potential is purely an artifact of the construction of H_{eff} , an artifact which disappears when the bound states of H_{eff} are computed. Thus the key issues, discussed below, are to understand how the confining potential is cancelled in the case of electrodynamics, and then to establish what circumstances would prevent a similar cancelation in QCD.

9. Chiral symmetry breaking

In the mid-70s QCD emerged from current algebra and the Parton model. In current algebra one makes use of the partially conserved axial-current hypothesis (PCAC), which states that light hadrons would be subjected to a fermionic symmetry called “chiral symmetry” if only the pion mass was zero. If this were the case, the symmetry would be spontaneously broken, and the pions and kaons would be the corresponding Goldstone bosons. The real world slightly misses this state of affairs by effects quantifiable in terms of the pion mass and decay constant. This violation can be expressed in terms of explicit symmetry breaking due to the nonzero masses of the fundamental fermion fields, quarks of three light flavors, and typically one assigns values of 4 MeV for the up-quark, 7 MeV for the down-quark and 130 MeV for the strange-quark [171,403]. Light-front

field theory is particularly well suited to study these symmetries [152]. This section follows closely the review of Daniel Mustaki [341].

9.1. Current algebra

To any given transformation of the fermion field we associate a current

$$\frac{\delta \mathcal{L}}{\delta(\partial_\mu \psi)} \frac{\delta \psi}{\theta} = i \bar{\psi} \gamma^\mu \frac{\delta \psi}{\theta}, \quad (9.1)$$

where $\delta \psi$ is the infinitesimal variation parameterized by θ . Consider first the free Dirac theory in space–time and light-front frames. For example, the vector transformation is defined in space–time by

$$\psi \mapsto e^{-i\theta} \psi, \quad \delta \psi = -i\theta \psi, \quad (9.2)$$

whence the current

$$j^\mu = \bar{\psi} \gamma^\mu \psi. \quad (9.3)$$

In a light-front frame the vector transformation will be defined as

$$\psi \mapsto e^{-i\theta} \psi_+, \quad \delta \psi_+ = -i\theta \psi_+, \quad \delta \psi = \delta \psi_+ + \delta \psi_-, \quad (9.4)$$

where $\delta \psi_-$ is calculated in Section 2. The distinction in the case of the vector is of course academic:

$$\delta \psi_- = -i\theta \psi_- \Rightarrow \delta \psi = -i\theta \psi. \quad (9.5)$$

Therefore, for the free Dirac theory the light-front current \tilde{j}^μ is

$$\tilde{j}^\mu = j^\mu. \quad (9.6)$$

One checks easily that the vector current is conserved:

$$\partial_\mu j^\mu = 0. \quad (9.7)$$

therefore the space–time and light-front vector charges, which measure fermion number

$$Q \equiv \int d^3 \mathbf{x} j^0(x), \quad \tilde{Q} \equiv \int d^3 \tilde{\mathbf{x}} j^+(x), \quad (9.8)$$

are equal [325].

The space–time chiral transformation is defined by

$$\psi \mapsto e^{-i\theta \gamma_5} \psi, \quad \delta \psi = -i\theta \gamma_5 \psi, \quad (9.9)$$

where $\gamma_5 \equiv i\gamma^0 \gamma^1 \gamma^2 \gamma^3$. From the Hamiltonian, one sees that the space–time theory with nonzero fermion masses is not chirally symmetric. The space–time axial-vector current associated to the transformation is

$$j_5^\mu = \bar{\psi} \gamma^\mu \gamma_5 \psi \quad (9.10)$$

and

$$\partial_\mu j_5^\mu = 2im \bar{\psi} \gamma_5 \psi. \quad (9.11)$$

As expected, this current is not conserved for non-zero fermion mass. The associated charge is

$$Q_5 \equiv \int d^3\mathbf{x} j_5^0 = \int d^3\mathbf{x} \bar{\psi} \gamma^0 \gamma_5 \psi. \quad (9.12)$$

The light-front chiral transformation is

$$\psi_{+} \mapsto e^{-i\theta\gamma_5} \psi_{+}, \quad \delta\psi_{+} = -i\theta\gamma_5\psi_{+}. \quad (9.13)$$

This is a symmetry of the light-front theory without requiring zero bare masses. Using $\{\gamma^\mu, \gamma_5\} = 0$, one finds

$$\delta\psi_{-}(x) = -\theta\gamma_5 \int dy^{-} \frac{\varepsilon(x^{-} - y^{-})}{4} (i\gamma_{\perp} \cdot \partial_{\perp} - m) \gamma^{+} \psi_{+}(y). \quad (9.14)$$

This expression differs from

$$-i\theta\gamma_5\psi_{-} = -\theta\gamma_5 \int dy^{-} \frac{\varepsilon(x^{-} - y^{-})}{4} (i\gamma_{\perp} \cdot \partial_{\perp} + m) \gamma^{+} \psi_{+}(y), \quad (9.15)$$

therefore $\tilde{j}_5^\mu \neq j_5^\mu$ (except for the plus component, due to $(\gamma^+)^2 = 0$). To be precise,

$$\tilde{j}_5^\mu = j_5^\mu + im\bar{\psi}\gamma^\mu\gamma_5 \int dy^{-} \frac{\varepsilon(x^{-} - y^{-})}{2} \gamma^{+} \psi_{+}(y). \quad (9.16)$$

A straightforward calculation shows that

$$\partial_\mu \tilde{j}_5^\mu = 0, \quad (9.17)$$

as expected. Finally, the light-front chiral charge is

$$\tilde{Q}_5 \equiv \int d^3\tilde{\mathbf{x}} \tilde{j}_5^+ = \int d^3\tilde{\mathbf{x}} \bar{\psi} \gamma^+ \gamma_5 \psi \quad (9.18)$$

From the canonical anti-commutator

$$\{\psi(x), \psi^\dagger(y)\}_{x^0=y^0} = \delta^3(\mathbf{x} - \mathbf{y}), \quad (9.19)$$

one derives

$$[\psi, Q_5] = \gamma_5\psi \Rightarrow [Q, Q_5] = 0, \quad (9.20)$$

so that fermion number, viz., the number of quarks minus the number of anti-quarks is conserved by the chiral charge. However, the latter are not conserved *separately*. This can be seen by using the momentum expansion of the field one finds

$$Q_5 = \int \frac{d^3\mathbf{p}}{2p^0} \sum_{s=\pm 1} s \left[\frac{|\mathbf{p}|}{p^0} (b^\dagger(\mathbf{p}, s)b(\mathbf{p}, s) + d^\dagger(\mathbf{p}, s)d(\mathbf{p}, s) + \frac{m}{p^0} (d^\dagger(-\mathbf{p}, s)b^\dagger(\mathbf{p}, s)e^{2ip^0t} + b(\mathbf{p}, s)d(-\mathbf{p}, s)e^{-2ip^0t}) \right]. \quad (9.21)$$

This implies that when Q_5 acts on a hadronic state, it will add or absorb a continuum of quark–antiquark pairs (the well-known pion pole) with a probability amplitude proportional to the fermion mass and inversely proportional to the energy of the pair. Thus, Q_5 is most unsuited for classification purposes.

In contrast, the light-front chiral charge conserves not only fermion number, but also the number of quarks and anti-quarks separately. In effect, the canonical anti-commutator is

$$\{\psi_+(x), \psi_+^\dagger(y)\}_{x^+=y^+} = (\Lambda_+/\sqrt{2}) \delta^3(\vec{x} - \vec{y}), \quad (9.22)$$

hence the momentum expansion of the field reads

$$\psi_+(x) = \int \frac{d^3\tilde{p}}{(2\pi)^{3/2} 2^{3/4} \sqrt{p^+}} \sum_{h=\pm 1/2} [w(h)e^{-ipx}b(\tilde{p}, h) + w(-h)e^{ipx}d^\dagger(\tilde{p}, h)] \quad (9.23)$$

and

$$\{b(\tilde{p}, h), b^\dagger(\tilde{q}, h')\} = 2p^+ \delta^3(\tilde{p} - \tilde{q})\delta_{hh'} = \{d(\tilde{p}, h), d^\dagger(\tilde{q}, h')\}, \quad (9.24)$$

$$\sum_{h=\pm 1/2} w(h)w^\dagger(h) = \Lambda_+. \quad (9.25)$$

In the rest frame of a system, its total angular momentum along the z -axis is called “light-front helicity”; the helicity of an elementary particle is just the usual spin projection; we label the eigenvalues of helicity with the letter “ h ”. It is easiest to work in the so-called “chiral representation” of Dirac matrices, where

$$\gamma_5 = \begin{bmatrix} 1 & 0 & 0 & 0 \\ 0 & 1 & 0 & 0 \\ 0 & 0 & -1 & 0 \\ 0 & 0 & 0 & -1 \end{bmatrix}, \quad w\left(+\frac{1}{2}\right) = \begin{bmatrix} 1 \\ 0 \\ 0 \\ 0 \end{bmatrix}, \quad w\left(-\frac{1}{2}\right) = \begin{bmatrix} 0 \\ 0 \\ 0 \\ 1 \end{bmatrix} \quad (9.26)$$

$$\Rightarrow w^\dagger(h)\gamma_5 w(h') = 2h\delta_{hh'}. \quad (9.27)$$

Inserting Eq. (9.23) into Eq. (9.18), one finds

$$\tilde{Q}_5 = \int \frac{d^3\tilde{p}}{2p^+} \sum_h 2h [b^\dagger(\tilde{p}, h)b(\tilde{p}, h) + d^\dagger(\tilde{p}, h)d(\tilde{p}, h)]. \quad (9.28)$$

This is just a superposition of fermion and anti-fermion number operators, and thus our claim is proved. This expression also shows that \tilde{Q}_5 annihilates the vacuum, and that it simply measures (twice) the sum of the helicities of all the quarks and anti-quarks of a given state. Indeed, in a light-front frame, the handedness of an individual fermion is automatically determined by its helicity. To show this, note that

$$\gamma_5 w(\pm \frac{1}{2}) = \pm w(\pm \frac{1}{2}) \Rightarrow \frac{1}{2}(1 \pm \gamma_5)w(\pm \frac{1}{2}) = w(\pm \frac{1}{2}), \quad \frac{1}{2}(1 \pm \gamma_5)w(\mp \frac{1}{2}) = 0. \quad (9.29)$$

Defining as usual

$$\psi_{+R} \equiv \frac{1}{2}(1 + \gamma_5)\psi_+, \quad \psi_{+L} \equiv \frac{1}{2}(1 - \gamma_5)\psi_+, \quad (9.30)$$

it follows from Eq. (9.23) that ψ_{+R} contains only fermions of helicity $+\frac{1}{2}$ and anti-fermions of helicity $-\frac{1}{2}$, while ψ_{+L} contains only fermions of helicity $-\frac{1}{2}$ and anti-fermions of helicity $+\frac{1}{2}$. Also, we see that when acted upon by the right- and left-hand charges

$$\tilde{Q}_R \equiv \frac{1}{2}(\tilde{Q} + \tilde{Q}_5), \quad \tilde{Q}_L \equiv \frac{1}{2}(\tilde{Q} - \tilde{Q}_5), \quad (9.31)$$

a chiral fermion (or anti-fermion) state may have eigenvalues $+1$ (resp. -1) or zero.

In a space–time frame, this identification between helicity and chirality applies only to massless fermions.

9.2. Flavor symmetries

We proceed now to the theory of three flavors of free fermions ψ_f , where $f = u, d, s$, and

$$\psi \equiv \begin{bmatrix} \psi_u \\ \psi_d \\ \psi_s \end{bmatrix} \quad \text{and} \quad M \equiv \begin{bmatrix} m_u & 0 & 0 \\ 0 & m_d & 0 \\ 0 & 0 & m_s \end{bmatrix}. \quad (9.32)$$

The vector, and axial-vector, flavor non-singlet transformations are defined, respectively, as

$$\psi \mapsto e^{-i\lambda^\alpha \theta^\alpha / 2} \psi, \quad \psi \mapsto e^{-i\lambda^\alpha \theta^\alpha \gamma_5 / 2} \psi, \quad (9.33)$$

where the summation index α runs from 1 to 8. The space–time Hamiltonian P^0 is invariant under vector transformations if the quarks have equal masses (“SU(3) limit”), and invariant under chiral transformations if all masses are zero (“chiral limit”).

The light-front Hamiltonian is

$$\begin{aligned} P^- &= \sum_f \frac{i\sqrt{2}}{4} \int d^3\tilde{x} \int dy^- \varepsilon(x^- - y^-) \psi_{f+}^\dagger(y) (m_f^2 - \Delta_\perp) \psi_{f+}(x) \\ &= \frac{i\sqrt{2}}{4} \int d^3\tilde{x} \int dy^- \varepsilon(x^- - y^-) \psi_+^\dagger(y) (M^2 - \Delta_\perp) \psi_+(x). \end{aligned} \quad (9.34)$$

Naturally, P^- is not invariant under the vector transformations

$$\psi_{+} \mapsto e^{-i\lambda^2 \theta^2 / 2} \psi_+ \quad (9.35)$$

unless the quarks have equal masses. But if they do, then P^- is also invariant under the chiral transformations

$$\psi_{+} \mapsto e^{-i\lambda^2 \theta^2 \gamma_5 / 2} \psi_+, \quad (9.36)$$

whether this common mass is zero or not.

One finds that the space–time currents

$$j^{\mu\alpha} = \frac{1}{2} \bar{\psi} \gamma^\mu \lambda^\alpha \psi, \quad j_5^{\mu\alpha} = \frac{1}{2} \bar{\psi} \gamma^\mu \gamma_5 \lambda^\alpha \psi, \quad (9.37)$$

have the following divergences:

$$\partial_\mu j^{\mu\alpha} = i\bar{\psi} [M, \frac{1}{2}\lambda^\alpha]\psi, \quad \partial_\mu j_5^{\mu\alpha} = i\bar{\psi}\gamma_5\{M, \frac{1}{2}\lambda^\alpha\}\psi. \quad (9.38)$$

These currents have obviously the expected conservation properties.

Turning to the light-front frame we find

$$\tilde{j}^{\mu\alpha} = j^{\mu\alpha} - i\bar{\psi} \left[M, \frac{\lambda^\alpha}{2} \right] \gamma^\mu \int dy^- \frac{\varepsilon(x^- - y^-)}{4} \gamma^+ \psi_+(y). \quad (9.39)$$

So $\tilde{j}^{\mu\alpha}$ and $j^{\mu\alpha}$ may be equal for all μ only if the quarks have equal masses. The *vector*, flavor non-singlet charges in each frame are two different octets of operators, except in the SU(3) limit.

For the light-front current associated with axial transformations, we get

$$\tilde{j}_5^{\mu\alpha} = j_5^{\mu\alpha} - i\bar{\psi} \left\{ M, \frac{\lambda^\alpha}{2} \right\} \gamma_5 \gamma^\mu \int dy^- \frac{\varepsilon(x^- - y^-)}{4} \gamma^+ \psi_+(y). \quad (9.40)$$

Hence, $\tilde{j}_5^{\mu\alpha}$ and $j_5^{\mu\alpha}$ are not equal (except for $\mu = +$), even in the SU(3) limit, unless all quark masses are zero. Finally, one obtains the following divergences:

$$\partial_\mu \tilde{j}^{\mu\alpha} = \bar{\psi} \left[M^2, \frac{\lambda^\alpha}{2} \right] \int dy^- \frac{\varepsilon(x^- - y^-)}{4} \gamma^+ \psi_+(y), \quad (9.41)$$

$$\partial_\mu \tilde{j}_5^{\mu\alpha} = -\bar{\psi} \left[M^2, \frac{\lambda^\alpha}{2} \right] \gamma_5 \int dy^- \frac{\varepsilon(x^- - y^-)}{4} \gamma^+ \psi_+(y).$$

As expected, both light-front currents are conserved in the SU(3) limit, without requiring zero masses. Also note how light-front relations often seem to involve the masses *squared*, while the corresponding space–time relations are *linear* in the masses. The integral operator

$$\int dy^- \frac{\varepsilon(x^- - y^-)}{2} \equiv \frac{1}{\partial^{\tilde{x}}} \quad (9.42)$$

compensates for the extra power of mass.

The associated light-front charges are

$$\tilde{Q}^\alpha \equiv \int d^3\tilde{x} \bar{\psi} \gamma^+ \frac{\lambda^\alpha}{2} \psi, \quad \tilde{Q}_5^\alpha \equiv \int d^3\tilde{x} \bar{\psi} \gamma^+ \gamma_5 \frac{\lambda^\alpha}{2} \psi. \quad (9.43)$$

Using the momentum expansion of the fermion triplet, Eq. (9.23), where now

$$b(\tilde{p}, h) \equiv [b_u(\tilde{p}, h), b_d(\tilde{p}, h), b_s(\tilde{p}, h)] \quad \text{and} \quad d(\tilde{p}, h) \equiv [d_u(\tilde{p}, h), d_d(\tilde{p}, h), d_s(\tilde{p}, h)], \quad (9.44)$$

one can express the charges as

$$\tilde{Q}^\alpha = \int \frac{d^3\tilde{p}}{2p^+} \sum_h \left[b^\dagger(\tilde{p}, h) \frac{\lambda^\alpha}{2} b(\tilde{p}, h) - d^\dagger(\tilde{p}, h) \frac{\lambda^{\alpha T}}{2} d(\tilde{p}, h) \right], \quad (9.45)$$

$$\tilde{Q}_5^\alpha = \int \frac{d^3\tilde{p}}{2p^+} \sum_h 2h \left[b^\dagger(\tilde{p}, h) \frac{\lambda^\alpha}{2} b(\tilde{p}, h) - d^\dagger(\tilde{p}, h) \frac{\lambda^{\alpha T}}{2} d(\tilde{p}, h) \right], \quad (9.46)$$

where the superscript T denotes matrix transposition. Clearly, all 16 charges annihilate the vacuum [235,247,248,302,303,394]. As \tilde{Q}^α and \tilde{Q}_5^α conserve the number of quarks and anti-quarks separately, these charges are well-suited for classifying hadrons in terms of their valence constituents, *whether the quark masses are equal or not* [120]. Since the charges commute with P^+ and P_\perp , all hadrons belonging to the same multiplet have the same momentum. But this common value of momentum is arbitrary, because in a light-front frame one can boost between any two values of momentum, using only kinematic operators.

One finds that these charges generate an $SU(3) \otimes SU(3)$ algebra:

$$[\tilde{Q}^\alpha, \tilde{Q}^\beta] = if_{\alpha\beta\gamma} \tilde{Q}^\gamma, \quad [\tilde{Q}^\alpha, \tilde{Q}_5^\beta] = if_{\alpha\beta\gamma} \tilde{Q}_5^\gamma, \quad [\tilde{Q}_5^\alpha, \tilde{Q}_5^\beta] = if_{\alpha\beta\gamma} \tilde{Q}^\gamma, \quad (9.47)$$

and the corresponding right- and left-hand charges generate two commuting algebras denoted $SU(3)_R$ and $SU(3)_L$ [247,248,302,303,305,306,307,411–120,135,142,234–237,332,350,87,88,394]. Most of these papers in fact study a larger algebra of light-like charges, namely $SU(6)$, but the sub-algebra $SU(3)_R \otimes SU(3)_L$ suffices for our purposes.

Since

$$[\psi_+, \tilde{Q}_5^\alpha] = \frac{1}{2} \gamma_5 \lambda^\alpha \psi_+, \quad (9.48)$$

the quarks form an irreducible representation of this algebra. To be precise, the quarks (resp. anti-quarks) with helicity $+\frac{1}{2}$ (resp. $-\frac{1}{2}$) transform as a triplet of $SU(3)_R$ and a singlet of $SU(3)_L$, the quarks (resp. anti-quarks) with helicity $-\frac{1}{2}$ (resp. $+\frac{1}{2}$) transform as a triplet of $SU(3)_L$ and a singlet of $SU(3)_R$. Then, for example, the ordinary vector $SU(3)$ decuplet of $J = \frac{3}{2}$ baryons with $h = +\frac{3}{2}$ is a pure right-handed (10,1) under $SU(3)_R \otimes SU(3)_L$. The octet ($J = \frac{1}{2}$) and decuplet ($J = \frac{3}{2}$) with $h = +\frac{1}{2}$ transform together as a (6,3). For bosonic states we expect both chiralities to contribute with equal probability. For example, the octet of pseudo-scalar mesons arises from a superposition of irreducible representations of $SU(3)_R \otimes SU(3)_L$:

$$|J^{PC} = 0^{-+}\rangle = (1/\sqrt{2})|(8,1) - (1,8)\rangle, \quad (9.49)$$

while the octet of vector mesons with zero helicity corresponds to

$$|J^{PC} = 1^{-+}\rangle = (1/\sqrt{2})|(8,1) + (1,8)\rangle, \quad (9.50)$$

and so on. These low-lying states have $L_z = 0$, where

$$L_z = -i \int d^3\tilde{x} \bar{\psi} \gamma^+ (x^1 \partial_2 - x^2 \partial_1) \psi \quad (9.51)$$

is the orbital angular momentum along z .

In the realistic case of unequal masses, the chiral charges are not conserved. Hence, they generate multiplets which are not mass-degenerate – a welcome feature. The fact that the invariance of the vacuum does not enforce the “invariance of the world” (viz., of energy), in sharp contrast with the order of things in space–time (Coleman’s theorem), is yet another remarkable property of the light-front frame.

In contrast with the space–time picture, free light-front *current* quarks are also *constituent* quarks because

- They can be massive without preventing chiral symmetry, which we know is (approximately) obeyed by hadrons,
- They form a basis for a classification of hadrons under the light-like chiral algebra.

9.3. Quantum chromodynamics

In the quark–quark–gluon vertex $gj^\mu A_\mu$, the transverse component of the vector current is

$$j_\perp(x) = \dots + \frac{im}{4} \int dy^- \varepsilon(x^- - y^-) [\bar{\psi}_+(y)\gamma^+\gamma_\perp\psi_+(x) + \bar{\psi}_+(x)\gamma^+\gamma_\perp\psi_+(y)], \quad (9.52)$$

where the dots represent chirally symmetric terms, and where color, as well as flavor, factors and indices have been omitted for clarity. The term explicitly written out breaks chiral symmetry for non-zero quark mass. Not surprisingly, it generates vertices in which the two quark lines have opposite helicity.

The canonical anti commutator for the bare fermion fields still holds in the interactive theory (for each flavor). The momentum expansion of $\psi_+(x)$ remains the same except that now the x^+ dependence in b and d and

$$\{b(\vec{p}, h, x^+), b^\dagger(\vec{q}, h', y^+)\}_{x^+=y^+} = 2p^+ \delta^3(\vec{p} - \vec{q})\delta_{hh'} = \{d(\vec{p}, h, x^+), d^\dagger(\vec{q}, h', y^+)\}_{x^+=y^+} \quad (9.53)$$

The momentum expansions of the light-like charges remain the same (keeping in mind that the creation and annihilation operators are now unknown functions of “time”). Hence, the charges still annihilate the Fock vacuum, and are suitable for classification purposes.

We do not require annihilation of the physical vacuum (QCD ground state). The successes of CQMs suggest that to understand the properties of the hadronic spectrum, it may not be necessary to take the physical vacuum into account. This is also the point of view taken by the authors of a recent paper on the renormalization of QCD [182]. Their approach consists in imposing an “infrared” cutoff in longitudinal momentum, and in compensating for this suppression by means of Hamiltonian counter terms. Now, only terms that annihilate the *Fock vacuum* are allowed in their Hamiltonian P^- . Since all states in the truncated Hilbert space have strictly positive longitudinal momentum except for the Fock vacuum (which has $p^+ = 0$), the authors hope to be able to adjust the renormalizations in order to fit the observed spectrum, without having to solve first for the physical vacuum.

Making the standard choice of gauge: $A_- = 0$, one finds that the properties of vector and axial-vector currents are also unaffected by the inclusion of QCD interactions, except for the replacement of the derivative by the covariant derivative. The divergence of the renormalized, space–time, non-singlet axial current is anomaly-free [111]. As $j_5^{\mu z}$ and $\tilde{j}_5^{\mu z}$ become equal in the chiral limit, the divergence of the light-front current is also anomaly-free (and goes to zero in the chiral limit). The corresponding charges, however, *do not* become equal in the chiral limit. This can only be due to contributions at x^- -infinity coming from the Goldstone boson fields, which presumably cancel the pion pole of the space–time axial charges. Equivalently, if one chooses

periodic boundary conditions, one can say that this effect comes from the longitudinal zero modes of the fundamental fields.

From soft pion physics we know that the chiral limit of $SU(2) \otimes SU(2)$ is well-described by PCAC. Now, using PCAC one can show that in the chiral limit Q_5^α ($\alpha = 1, 2, 3$) is conserved, but Q_5^z is not [87,234]. In other words, the renormalized light-front charges are sensitive to spontaneous symmetry breaking, although they do annihilate the vacuum. It is likely that this behavior generalizes to $SU(3) \otimes SU(3)$, viz., to the other five light-like axial charges. Its origin, again, must lie in zero modes.

In view of this “time”-dependence, one might wonder whether the light-front axial charges are observables. From PCAC, we know that it is indeed the case: their matrix elements between hadron states are directly related to off-shell pion emission [142,87]. For a hadron A decaying into a hadron B and a pion, one finds

$$\langle B | \tilde{Q}_5^z(0) | A \rangle = - \frac{2i(2\pi)^3 p_A^+}{m_A^2 - m_B^2} \langle B, \pi^z | A \rangle \delta^3(\tilde{p}_A - \tilde{p}_B). \quad (9.54)$$

Note that in this reaction, the mass of hadron A must be larger than the mass of B due to the pion momentum.

9.4. Physical multiplets

Naturally, we shall assume that real hadrons fall into representations of an $SU(3) \otimes SU(3)$ algebra. We have identified the generators of this algebra with the light-like chiral charges. But this was done in the artificial case of the free quark model. It remains to check whether this identification works in the real world.

Of course, we already know that the predictions based on isospin ($\alpha = 1, 2, 3$) and hyper-charge ($\alpha = 8$) are true. Also, the nucleon-octet ratio D/F is correctly predicted to be $3/2$, and several relations between magnetic moments match well with experimental data.

Unfortunately, several other predictions are in disagreement with observations [104]. For example, G_A/G_V for the nucleon is expected to be equal to $5/3$, while the experimental value is about 1.25. Dominant decay channels such as $N^* \rightarrow N\pi$, or $b_1 \rightarrow \omega\pi$, are forbidden by the light-like current algebra. The anomalous magnetic moments of nucleons, and all form factors of the rho-meson would have to vanish. De Alwis and Stern [120] point out that the matrix element of $\tilde{j}^{\mu\alpha}$ between two given hadrons would be equal to the matrix element of $\tilde{j}_5^{\mu\alpha}$ between the same two hadrons, up to a ratio of Clebsch-Gordan coefficients. This is excluded though because vector and axial-vector form factors have very different analytic properties as functions of momentum transfer.

In addition there is, in general, disagreement between the values of L_z assigned to any given hadron. This comes about because in the classification scheme, the value of L_z is essentially an afterthought, when group-theoretical considerations based on flavor and helicity have been taken care of. On the other hand, at the level of the current quarks, this value is determined by covariance and external symmetries. Consider, for example, the L_z assignments in the case of the pion, and of the rho-meson with zero helicity. As we mentioned earlier, the classification assigns to these states a pure value of L_z , namely zero. However, at the fundamental level, one expects these mesons to contain a wave-function ϕ_1 attached to $L_z = 0$ (anti-parallel $q\bar{q}$ helicities), and also a wavefunction

ϕ_2 attached to $L_z = \pm 1$ (parallel helicities). Actually, the distinction between the pion and the zero-helicity rho is only based on the different momentum dependence of ϕ_1 and ϕ_2 [305,306]. If the interactions were turned off, ϕ_2 would vanish and the masses of the two mesons would be degenerate (and equal to $(m_u + m_d)$).

We conclude from this comparison with experimental data, that if indeed real hadrons are representations of some $SU(3) \otimes SU(3)$ algebra, then the generators G^α and G_3^α of this classifying algebra must be different from the current light-like charges \tilde{Q}^α and \tilde{Q}_3^α (except however for $\alpha = 1, 2, 3, 8$). Furthermore, in order to avoid the phenomenological discrepancies discussed above, one must forego kinematical invariance for these generators; that is, $G^\alpha(\tilde{k})$ and $G_3^\alpha(\tilde{k})$ must depend on the momentum \tilde{k} of the hadrons in a particular irreducible multiplet.

Does that mean that our efforts to relate the physical properties of hadrons to the underlying field theory turn out to be fruitless? Fortunately no, as argued by De Alwis and Stern [120]. The fact that these two sets of generators (the \tilde{Q} 's and the G 's) act in the same Hilbert space, in addition to satisfying the same commutation relations, implies that they must actually be unitary equivalent (this equivalence was originally suggested by Dashen, and by Gell-Mann [173]). There exists a set of momentum-dependent unitary operators $U(\tilde{k})$ such that

$$G^\alpha(\tilde{k}) = U(\tilde{k})\tilde{Q}^\alpha U^\dagger(\tilde{k}), \quad G_3^\alpha(\tilde{k}) = U(\tilde{k})\tilde{Q}_3^\alpha U^\dagger(\tilde{k}). \tag{9.55}$$

Current quarks, and the real-world hadrons built out of them, fall into representations of this algebra. Equivalently (e.g., when calculating electro-weak matrix elements), one may consider the original current algebra, and define its representations as “constituent” quarks and “constituent” hadrons. These quarks (and antiquarks) within a hadron of momentum \tilde{k} are represented by a “constituent fermion field”,

$$\chi_{\pm}^{\tilde{k}}(x)|_{x^+=0} \equiv U(\tilde{k})\psi_{\pm}(x)|_{x^+=0}U^\dagger(\tilde{k}), \tag{9.56}$$

on the basis of which the physical generators can be written in canonical form:

$$\tilde{G}^\alpha \equiv \int d^3\tilde{x} \tilde{\chi}\gamma^+\frac{\lambda^\alpha}{2}\chi, \quad \tilde{G}_3^\alpha \equiv \int d^3\tilde{x} \tilde{\chi}\gamma^+\gamma_5\frac{\lambda^\alpha}{2}\chi. \tag{9.57}$$

it follows that the constituent annihilation/creation operators are derived from the current operators via

$$a^{\tilde{k}}(\tilde{p}, h) \equiv U(\tilde{k})b(\tilde{p}, h)U^\dagger(\tilde{k}), \quad c^{\tilde{k}}(\tilde{p}, h) \equiv U(\tilde{k})d^\dagger(\tilde{p}, h)U^\dagger(\tilde{k}). \tag{9.58}$$

Due to isospin invariance, this unitary transformation cannot mix flavors, it only mixes helicities. It can therefore be represented by three unitary 2×2 matrices $T^f(\tilde{k}, \tilde{p})$ such that

$$a^{\tilde{k}}_f(\tilde{p}, h) = \sum_{h'=\pm 1/2} T^f_{hh'}(\tilde{k}, \tilde{p}) b_f(\tilde{p}, h'), \quad c^{\tilde{k}}_f(\tilde{p}, h) = \sum_{h'=\pm 1/2} T^f_{hh'}(\tilde{k}, \tilde{p}) d_f(\tilde{p}, h'), \tag{9.59}$$

one for each flavor $f = u, d, s$. Since we need the transformation to be unaffected when \tilde{k} and \tilde{p} are boosted along z or rotated around z together, the matrix T must actually be a function of only kinematical invariants. These are

$$\xi \equiv \frac{p^+}{k^+} \quad \text{and} \quad \kappa_\perp \equiv \mathbf{p}_\perp - \xi \mathbf{k}_\perp \quad \text{where} \quad \sum_{\text{constituents}} \xi = 1, \quad \sum_{\text{constituents}} \kappa_\perp = \mathbf{0}. \tag{9.60}$$

Invariance under time reversal ($x^+ \mapsto -x^+$) and parity ($x^1 \mapsto -x^1$) further constrains its functional form, so that finally [305,306]

$$T^J(\tilde{\mathbf{k}}, \tilde{\mathbf{p}}) = \exp[-i(\kappa_\perp/|\kappa_\perp|) \cdot \sigma_\perp \beta_f(\xi, \kappa_\perp^2)]. \quad (9.61)$$

Thus, the relationship between current and constituent quarks is embodied in the three functions $\beta_f(\xi, \kappa_\perp^2)$, which we must try to extract from comparison with experiment. (In first approximation it is legitimate to take β_u and β_d equal since SU(2) is such a good symmetry.)

Based on some assumptions abstracted from the free-quark model [150,304–306] has derived a set of sum rules obeyed by mesonic wavefunctions. Implementing then the transformation described above, Leutwyler finds various relations involving form factors and scaling functions of mesons, and computes the current quark masses. For example, he obtains

$$F_\pi < F_\rho, \quad F_\rho = 3F_\omega, \quad F_\rho < (3/\sqrt{2})|F_\phi|, \quad (9.62)$$

and the ω/ϕ mixing angle is estimated to be about 0.07 rad. Ref. [304] also shows that the average transverse momentum of a quark inside a meson is substantial ($\langle \mathbf{p}_\perp \rangle_{\text{rms}} > 400$ MeV), thus justifying a posteriori the basic assumptions of the relativistic CQM (e.g., Fock space truncation and relativistic energies). This large value also provides an explanation for the above-mentioned failures of the SU(3) \otimes SU(3) classification scheme [104]. On the negative side, it appears that the functional dependence of the β_f 's cannot be easily determined with satisfactory precision.

10. The prospects and challenges

Future work on light-cone physics can be discussed in terms of developments along two distinct lines. One direction focuses on solving phenomenological problems while the other will focus on the use of light-cone methods to understand various properties of quantum field theory. Ultimately both point towards understanding the physical world.

An essential feature of relativistic quantum field theories such as QCD is that particle number is not conserved, i.e. if we examine the wavefunction of a hadron at fixed-time t or light-cone time x^+ , any number of particles can be in flight. The expansion of a hadronic eigenstate of the full Hamiltonian has to be represented as a sum of amplitudes representing the fluctuations over particle number, momentum, coordinate configurations, color partitions, and helicities. The advantage of the light-cone Hamiltonian formalism is that one can conceivably predict the individual amplitudes for each of these configurations. As we have discussed in this review, the basic procedure is to diagonalize the full light-cone Hamiltonian in the free light-cone Hamiltonian basis. The eigenvalues are the invariant mass squared of the discrete and continuum eigenstates of the spectrum. The projection of the eigenstate on the free Fock basis are the light-cone wavefunctions and provide a rigorous relativistic many-body representation in terms of its degrees of freedom. Given the light-cone wavefunction one can compute the structure functions and distribution amplitudes. More generally, the light-cone wavefunctions provide the interpolation between hadron scattering amplitudes and the underlying parton subprocesses.

The unique property of light-cone quantization that makes the calculations of light cone wavefunctions particularly useful is that they are independent of the reference frame. Thus, when

one does a non-perturbative bound-state calculation of a light-cone wavefunction, that same wavefunction can be used in many different problems.

Light-cone methods have been quite successful in understanding recent experimental results, as we discussed in Sections 5 and 6. We have seen that light-cone methods are very useful for understanding a number of properties of nucleons as well as many exclusive processes. We also saw that these methods can be applied in conjunction with perturbative QCD calculations. Future phenomenological application will continue to address specific experimental results that have a distinct non-perturbative character and which are therefore difficult to address by other methods.

The simple structure of the light-cone Hamiltonian can be used as a basis to infer information on the non-perturbative and perturbative structure of QCD. For example, factorization theories separating hard and soft physics in large momentum transfer exclusive and inclusive reactions [299]. Mueller et al. [67,98] have pioneered the investigation of structure functions at $x \rightarrow 0$ in the light-cone Hamiltonian formalism. Mueller's approach is to consider the light-cone wavefunctions of heavy quarkonium in the large N_c limit. The resulting structure functions display energy dependence related to the Pomeron.

One can also consider the hard structure of the light-cone wavefunction. The wavefunctions of a hadron contain fluctuations which are arbitrarily far off the energy shell. In the case of light-wave quantization, the hadron wavefunction contains partonic states of arbitrarily high invariant mass. If the light-cone wavefunction is known in the domain of low invariant mass, then one can use the projection operators formalism to construct the wavefunction for large invariant mass by integration of the hard interactions. Two types of hard fluctuations emerge: “extrinsic” components associated with gluon splitting $g \rightarrow q\bar{q}$ and the $q \rightarrow qq$ bremsstrahlung process and “intrinsic” components associated with multi-parton interactions within the hadrons, $gg \rightarrow Q\bar{Q}$, etc.

One can use the probability of the intrinsic contribution to compute the $x \rightarrow 1$ power-law behavior of structure functions, the high relative transverse momentum fall-off of the light-cone wavefunctions, and the probability for high mass or high mass $Q\bar{Q}$ pairs in the sea quark distribution of the hadrons [67]. The full analysis of the hard components of hadron wavefunction can be carried out systematically using an effective Hamiltonian operator approach.

If we contrast the light-cone approach with lattice calculations we see the potential power of the light-cone method. In the lattice approach one calculates a set of numbers, for example a set of operator product coefficients [322], and then one uses them to calculate a physical observable where the expansion is valid. This should be contrasted with the calculation of a light-cone wavefunction which gives predictions for all physical observables independent of the reference frame. There is a further advantage in that the shape of the light-cone wavefunction can provide a deeper understanding of the physics that underlies a particular experiment.

The focus is then on how to find reasonable approximations to light-cone wavefunctions that make non-perturbative calculations tractable. For many problems it is not necessary to know everything about the wavefunction to make physically interesting predictions. Thus, one attempts to isolate and calculate the important aspects of the light-cone wavefunction. We saw in the discussion of the properties of nuclei in this review, that spectacular results can be obtained this way with a minimal input. Simply incorporating the angular momentum properties lead to very successful results almost independent of the rest of the structure of the light-cone wavefunction.

Thus far there has been remarkable success in applying the light-cone method to theories in one-space and one-time dimension. Virtually, any $1 + 1$ quantum field theory can be solved using

light-cone methods. For calculation in $3 + 1$ dimensions the essential problem is that the number of degrees of freedom needed to specify each Fock state even in a discrete basis quickly grows since each particles' color, helicity, transverse momenta and light-cone longitudinal momenta have to be specified. Conceivably advanced computational algorithms for matrix diagonalization, such as the Lanczos method could allow the diagonalization of sufficiently large matrix representations to give physically meaningful results. A test of this procedure in QED is now being carried out by J. Hiller et al. [222] for the diagonalization of the physical electron in QED. The goal is to compute the electron's anomalous moment at large α_{QED} non-perturbatively.

Much of the current work in this area attempts to find approximate solution to problems in $3 + 1$ dimensions by starting from a $(1 + 1)$ -dimensionally-reduced version of that theory. In some calculations this reduction is very explicit while in others it is hidden.

An interesting approach has been proposed by Klebanov and coworkers [38,121,115]. One decomposes the Hamiltonian into two classes of terms. Those which have the matrix elements that are at least linear in the transverse momentum (non-collinear) and those that are independent of the transverse momentum (collinear). In the collinear models one discards the non-linear interactions and calculates distribution functions which do not explicitly depend on transverse dimensions. These can then be directly compared with data. In this approximation QCD $(3 + 1)$ reduces to a $1 + 1$ theory in which all the partons move along $\mathbf{k}_{\perp i} = 0$. However, the transverse polarization of the dynamical gluons is retained. In effect the physical gluons are replaced by two scalar fields representing left- and right-handed polarized quanta.

Collinear QCD has been solved in detail by Antonuccio et al. [9–11,13]. The results are hadronic eigenstates such as mesons with a full complement of $q\bar{q}$ and g light-cone Fock states. Antonuccio and Dalley also obtain a glueball spectrum which closely resembles the gluonium states predicted by lattice gauge theory in $3 + 1$ QCD. They have also computed the wavefunction and structure functions of the mesons, including the quark and gluon helicity structure functions. One interesting result, shows that the gluon helicity is strongly correlated with the helicity of the parent hadron, a result also expected in $3 + 1$ QCD [70]. While collinear QCD is a drastic approximation to physical QCD, it provides a solvable basis as a first step to actually theory.

More recently, Antonuccio et al. [9–11,13] have noted that Fock states differing by 1 or 2 gluons are coupled in the form of ladder relations which constrain the light-cone wavefunctions at the edge of phase space. These relations in turn allow one to construct the leading behavior of the polarized and unpolarized structure function at $x \rightarrow 0$, see in particular Ref. [12].

The transverse lattice method includes the transverse behavior approximately through a lattice that only operates in the transverse directions. In this method which was proposed by Bardeen et al. [17,18], the transverse degrees of freedom of the gauge theory are represented by lattice variables and the longitudinal degrees of freedom are treated with light-cone variables. Considerable progress has been made in recent years on the integrated method by Burkardt [78,79], Griffin [190] and van de Sande et al. [116,437–439]; see also Gaete et al. [169]. This method is particularly promising for analyzing confinement in QCD.

The importance of renormalization is seen in the Tamm–Dancoff solution of the Yukawa model. We present some simple examples of non-perturbative renormalization in the context of integral equations which seems to have all the ingredients one would want. However, the method has not been successfully transported to a $(3 + 1)$ -dimensional field theory. We also discussed the Wilson approach which focuses on this issue as a guide to developing their light-cone method. They use

a unique unitary transformation to band-diagonalize the theory on the way to renormalization. The method, however, is perturbative at its core which calls into question its applicability as a true non-perturbative renormalization. They essentially start from the confining potential one gets from the longitudinal confinement that is fundamental to lower dimensional theories and then builds the three-dimensional structure on that. The methods has been successfully applied to solving for the low-lying levels of positronium and their light-cone wavefunctions. Jones and Perry [255,256] have also shown how the Lamb shift and its associated non-perturbative Bethe-logarithm arises in the light cone Hamiltonian formulation of QED.

There are now many examples, some of which were reviewed here, that show that DLCQ as a numerical method provides excellent solutions to almost all two-dimensional theories with a minimal effort. For models in $3 + 1$ dimensions, the method is also applicable, while much more complicated. To date only QED has been solved with a high degree of precision and some of those results are presented in this review [279,264,429–431]. Of course, there one has high-order perturbative results to check against. This has proven to be an important laboratory for developing light-cone methods. Among the most interesting results of these calculations is the fact, that rotational symmetry of the result appears in spite of the fact that the approximation must break that symmetry.

One can use light-cone quantization to study the structure of quantum field theory. The theories considered are often not physical, but are selected to help in the understanding of a particular non-perturbative phenomenon. The relatively simple vacuum properties of light-front field theories underly many of these “analytical” approaches. The relative simplicity of the light-cone vacuum provides a firm starting point to attack many non perturbative issues. As we saw in this review in two dimensions not only are the problems tractable from the outset, but in many cases, like the Schwinger model, the solution gives a unique insight and understanding. In the Schwinger model we saw that the Schwinger particle indeed has the simple parton structure that one hopes to see QCD.

It has been known for some time that light-cone field theory is uniquely suited for to address problems in string theory. In addition, recently new developments in formal field theory associated with string theory, matrix models and M-theory have appeared which also seem particularly well suited to the light-cone approach [416]. Some issues in formal field theory which have proven to be intractable analytically, such as the density of the states at high energy, have been successfully addressed with numerical light-cone methods.

In the future one hopes to address a number of outstanding issues, and one of the most interesting is spontaneous symmetry breaking. We have already seen in this review that the light cone provides a new paradigm for spontaneous symmetry breaking in ϕ^4 in 2 dimensions. Since the vacuum is simple in the light-cone approach the physics of spontaneous symmetry breaking must reside in the zero-mode operators. It has been known for some time that these operators satisfy a constraint equation. We reviewed here the now well-known fact that the solution of this constraint equation can spontaneously break a symmetry. In fact, in the simple ϕ^4 -model the numerical results for the critical coupling constant and the critical exponent are quite good.

The light cone has a number of unique properties with respect to chiral symmetry. It has been known for a long time, for example, that the free theory of a fermion with a mass still has a chiral symmetry in a light-cone theory. In Section 9 we reviewed chiral symmetry on the light cone. There

has recently been a few applications of light-cone methods to solve supersymmetry but as yet no one has addressed the issue of dynamical supersymmetry breaking.

Finally, let us highlight the intrinsic advantages of light-cone field theory:

- The light-cone wavefunctions are independent of the momentum of the bound state – only relative momentum coordinates appear.
- The vacuum state is simple and in many cases trivial.
- Fermions and fermion derivatives are treated exactly; there is no fermion doubling problem.
- The minimum number of physical degrees of freedom are used because of the light-cone gauge. No Gupta–Bleuler or Faddeev–Popov ghosts occur and unitarity is explicit.
- The output is the full color-singlet spectrum of the theory, both bound states and continuum, together with their respective wavefunctions.

Appendix A. General conventions

For completeness notational conventions are collected in line with the textbooks [39,242].

Lorentz vectors. We write contravariant four-vectors of position x^μ in the instant form as

$$x^\mu = (x^0, x^1, x^2, x^3) = (t, x, y, z) = (x^0, \mathbf{x}_\perp, x^3) = (x^0, \mathbf{x}). \quad (\text{A.1})$$

The covariant four-vector x_μ is given by

$$x_\mu = (x_0, x_1, x_2, x_3) = (t, -x, -y, -z) = g_{\mu\nu}x^\nu, \quad (\text{A.2})$$

and obtained from the contravariant vector by the metric tensor

$$g_{\mu\nu} = \begin{pmatrix} +1 & 0 & 0 & 0 \\ 0 & -1 & 0 & 0 \\ 0 & 0 & -1 & 0 \\ 0 & 0 & 0 & -1 \end{pmatrix}. \quad (\text{A.3})$$

Implicit summation over repeated Lorentz (μ, ν, κ) or space (i, j, k) indices is understood. Scalar products are

$$x \cdot p = x^\mu p_\mu = x^0 p_0 + x^1 p_1 + x^2 p_2 + x^3 p_3 = tE - \mathbf{x} \cdot \mathbf{p}, \quad (\text{A.4})$$

with four-momentum $p^\mu = (p^0, p^1, p^2, p^3) = (E, \mathbf{p})$. The metric tensor $g^{\mu\nu}$ raises the indices.

Dirac matrices. Up to unitary transformations, the 4×4 Dirac matrices γ^μ are defined by

$$\gamma^\mu \gamma^\nu + \gamma^\nu \gamma^\mu = 2g^{\mu\nu}. \quad (\text{A.5})$$

γ^0 is hermitean and γ^k anti-hermitean. Useful combinations are $\beta = \gamma^0$ and $\alpha^k = \gamma^0 \gamma^k$, as well as

$$\sigma^{\mu\nu} = \frac{1}{2}i(\gamma^\mu \gamma^\nu - \gamma^\nu \gamma^\mu), \quad \gamma_5 = \gamma^5 = i\gamma^0 \gamma^1 \gamma^2 \gamma^3. \quad (\text{A.6})$$

They usually are expressed in terms of the 2×2 Pauli matrices

$$I = \begin{bmatrix} 1 & 0 \\ 0 & 1 \end{bmatrix}, \quad \sigma^1 = \begin{bmatrix} 0 & 1 \\ 1 & 0 \end{bmatrix}, \quad \sigma^2 = \begin{bmatrix} 0 & -i \\ i & 0 \end{bmatrix}, \quad \sigma^3 = \begin{bmatrix} 1 & 0 \\ 0 & -1 \end{bmatrix}. \quad (\text{A.7})$$

In Dirac representation [39,242] the matrices are

$$\gamma^0 = \begin{pmatrix} I & 0 \\ 0 & -I \end{pmatrix}, \quad \gamma_k = \begin{pmatrix} 0 & \sigma^k \\ -\sigma^k & 0 \end{pmatrix}, \quad (\text{A.8})$$

$$\gamma_5 = \begin{pmatrix} 0 & +I \\ I & 0 \end{pmatrix}, \quad \alpha^k = \begin{pmatrix} 0 & \sigma^k \\ +\sigma^k & 0 \end{pmatrix}, \quad \sigma^{ij} = \begin{pmatrix} \sigma^k & 0 \\ 0 & \sigma^k \end{pmatrix}. \quad (\text{A.9})$$

In chiral representation [242] γ_0 and γ_5 are interchanged:

$$\gamma^0 = \begin{pmatrix} 0 & +I \\ I & 0 \end{pmatrix}, \quad \gamma^k = \begin{pmatrix} 0 & \sigma^k \\ -\sigma^k & 0 \end{pmatrix}, \quad (\text{A.10})$$

$$\gamma_5 = \begin{pmatrix} I & 0 \\ 0 & -I \end{pmatrix}, \quad \alpha^k = \begin{pmatrix} \sigma^k & 0 \\ 0 & -\sigma^k \end{pmatrix}, \quad \sigma^{ij} = \begin{pmatrix} \sigma^k & 0 \\ 0 & \sigma^k \end{pmatrix}. \quad (\text{A.11})$$

$(i, j, k) = 1, 2, 3$ are used cyclically.

Projection operators. Combinations of Dirac matrices like the hermitean matrices

$$A_+ = \frac{1}{2}(1 + \alpha^3) = \frac{1}{2}\gamma^0(\gamma^0 + \gamma^3) \quad \text{and} \quad A_- = \frac{1}{2}(1 - \alpha^3) = \frac{1}{2}\gamma^0(\gamma^0 - \gamma^3) \quad (\text{A.12})$$

often have projector properties, particularly

$$A_+ + A_- = \mathbf{1}, \quad A_+ A_- = 0, \quad A_+^2 = A_+, \quad A_-^2 = A_-. \quad (\text{A.13})$$

They are diagonal in the chiral and maximally off-diagonal in the Dirac representation:

$$(A_+)_{\text{chiral}} = \begin{pmatrix} 1 & 0 & 0 & 0 \\ 0 & 0 & 0 & 0 \\ 0 & 0 & 0 & 0 \\ 0 & 0 & 0 & 1 \end{pmatrix}, \quad (A_+)_{\text{Dirac}} = \frac{1}{2} \begin{pmatrix} 1 & 0 & 1 & 0 \\ 0 & 1 & 0 & -1 \\ 1 & 0 & 1 & 0 \\ 0 & -1 & 0 & 1 \end{pmatrix}. \quad (\text{A.14})$$

Dirac spinors. The spinors $u_\alpha(p, \lambda)$ and $v_\alpha(p, \lambda)$ are solutions of the Dirac equation

$$(\not{p} - m)u(p, \lambda) = 0, \quad (\not{p} + m)v(p, \lambda) = 0. \quad (\text{A.15})$$

They are orthonormal and complete:

$$\bar{u}(p, \lambda)u(p, \lambda') = -\bar{v}(p, \lambda')v(p, \lambda) = 2m\delta_{\lambda\lambda'}, \quad (\text{A.16})$$

$$\sum_{\lambda} u(p, \lambda)\bar{u}(p, \lambda) = \not{p} + m, \quad \sum_{\lambda} v(p, \lambda)\bar{v}(p, \lambda) = \not{p} - m. \quad (\text{A.17})$$

Note the different normalization as compared to the textbooks [39,242]. The “Feynman slash” is $\not{p} = p_\mu \gamma^\mu$. The Gordon decomposition of the currents is useful:

$$\bar{u}(p, \lambda) \gamma^\mu u(q, \lambda') = \bar{v}(q, \lambda') \gamma^\mu v(p, \lambda) = (1/2m) \bar{u}(p, \lambda) ((p+q)^\mu + i\sigma^{\mu\nu}(p-q)_\nu) u(q, \lambda'). \quad (\text{A.18})$$

With $\lambda = \pm 1$, the spin projection is $s = \lambda/2$. The relations

$$\gamma^\mu \not{a} \gamma_\mu = -2a, \quad (\text{A.19})$$

$$\gamma^\mu \not{a} \not{b} \gamma_\mu = 4ab, \quad (\text{A.20})$$

$$\gamma^\mu \not{a} \not{b} \not{c} \gamma_\mu = \not{c} \not{b} \not{a} \quad (\text{A.21})$$

are useful.

Polarization vectors. The two polarization four-vectors $\varepsilon_\mu(p, \lambda)$ are labeled by the spin projections $\lambda = \pm 1$. As solutions of the free Maxwell equations they are orthonormal and complete:

$$\varepsilon^\mu(p, \lambda) \varepsilon_\mu^*(p, \lambda') = -\delta_{\lambda\lambda'}, \quad p^\mu \varepsilon_\mu(p, \lambda) = 0. \quad (\text{A.22})$$

The star (*) refers to complex conjugation. The polarization sum is

$$d_{\mu\nu}(p) = \sum_\lambda \varepsilon_\mu(p, \lambda) \varepsilon_\nu^*(p, \lambda) = -g_{\mu\nu} + \frac{\eta_\mu p_\nu + \eta_\nu p_\mu}{p^\kappa \eta_\kappa}, \quad (\text{A.23})$$

with the null vector $\eta^\mu \eta_\mu = 0$ given below.

Appendix B. The Lepage–Brodsky convention (LB)

This section summarizes the conventions which have been used by Lepage, Brodsky and others [66,300,299].

Lorentz vectors. The contravariant four-vectors of position x^μ are written as

$$x^\mu = (x^+, x^-, x^1, x^2) = (x^+, x^-, \mathbf{x}_\perp). \quad (\text{B.1})$$

Its time-like and space-like components are related to the instant form by [66,300,299]

$$x^+ = x^0 + x^3 \quad \text{and} \quad x^- = x^0 - x^3, \quad (\text{B.2})$$

respectively, and referred to as the “light-cone time” and “light-cone position”. The covariant vectors are obtained by $x_\mu = g_{\mu\nu} x^\nu$, with the metric tensor(s)

$$g^{\mu\nu} = \begin{pmatrix} 0 & 2 & 0 & 0 \\ 2 & 0 & 0 & 0 \\ 0 & 0 & -1 & 0 \\ 0 & 0 & 0 & -1 \end{pmatrix} \quad \text{and} \quad g_{\mu\nu} = \begin{pmatrix} 0 & \frac{1}{2} & 0 & 0 \\ \frac{1}{2} & 0 & 0 & 0 \\ 0 & 0 & -1 & 0 \\ 0 & 0 & 0 & -1 \end{pmatrix}. \quad (\text{B.3})$$

Scalar products are

$$x \cdot p = x^\mu p_\mu = x^+ p_- + x^- p_+ + x^1 p_1 + x^2 p_2 = \frac{1}{2}(x^+ p^- + x^- p^+) - \mathbf{x}_\perp \cdot \mathbf{p}_\perp. \quad (\text{B.4})$$

All other four-vectors including γ^μ are treated correspondingly.

Dirac matrices. The Dirac representation of the γ -matrices is used, particularly

$$\gamma^+ \gamma^+ = \gamma^- \gamma^- = 0. \quad (\text{B.5})$$

Alternating products are, for example,

$$\gamma^+ \gamma^- \gamma^+ = 4\gamma^+ \quad \text{and} \quad \gamma^- \gamma^+ \gamma^- = 4\gamma^-. \quad (\text{B.6})$$

Projection operators. The projection matrices become

$$A_+ = \frac{1}{2}\gamma^0 \gamma^+ = \frac{1}{4}\gamma^- \gamma^+ \quad \text{and} \quad A_- = \frac{1}{2}\gamma^0 \gamma^- = \frac{1}{4}\gamma^+ \gamma^-. \quad (\text{B.7})$$

Dirac spinors. Lepage and Brodsky [66,300,299] use a particularly simple spinor representation

$$u(p, \lambda) = \frac{1}{\sqrt{p^+}} (p^+ + \beta m + \boldsymbol{\alpha}_\perp \mathbf{p}_\perp) \times \begin{cases} \chi(\uparrow) & \text{for } \lambda = +1, \\ \chi(\downarrow) & \text{for } \lambda = -1, \end{cases} \quad (\text{B.8})$$

$$v(p, \lambda) = \frac{1}{\sqrt{p^+}} (p^+ - \beta m + \boldsymbol{\alpha}_\perp \mathbf{p}_\perp) \times \begin{cases} \chi(\downarrow) & \text{for } \lambda = +1, \\ \chi(\uparrow) & \text{for } \lambda = -1. \end{cases} \quad (\text{B.9})$$

The two χ -spinors are

$$\chi(\uparrow) = \frac{1}{\sqrt{2}} \begin{pmatrix} 1 \\ 0 \\ 1 \\ 0 \end{pmatrix} \quad \text{and} \quad \chi(\downarrow) = \frac{1}{\sqrt{2}} \begin{pmatrix} 0 \\ 1 \\ 0 \\ -1 \end{pmatrix}. \quad (\text{B.10})$$

Polarization vectors: The null vector is

$$\eta^\mu = (0, 2, \mathbf{0}). \quad (\text{B.11})$$

In Björken–Drell convention [39], one works with circular polarization, with spin projections $\lambda = \pm 1 = \uparrow\downarrow$. The transversal polarization vectors are $\boldsymbol{\varepsilon}_\perp(\uparrow) = -1/\sqrt{2}(1, i)$ and $\boldsymbol{\varepsilon}_\perp(\downarrow) = 1/\sqrt{2}(1, -i)$, or collectively

$$\boldsymbol{\varepsilon}_\perp(\lambda) = (-1/\sqrt{2})(\lambda \mathbf{e}_x + i \mathbf{e}_y), \quad (\text{B.12})$$

with \mathbf{e}_x and \mathbf{e}_y as unit vectors in p_x - and p_y -direction, respectively. With $\varepsilon^+(p, \lambda) = 0$, induced by the light-cone gauge, the polarization vector is

$$\varepsilon^\mu(p, \lambda) = \left(0, \frac{2\boldsymbol{\varepsilon}_\perp(\lambda)\mathbf{p}_\perp}{p^+}, \boldsymbol{\varepsilon}_\perp(\lambda) \right), \quad (\text{B.13})$$

which satisfies $p_\mu \varepsilon^\mu(p, \lambda)$.

Appendix C. The Kogut–Soper convention (KS)

Lorentz vectors. Kogut and Soper [274,406,41,275] have used

$$x^+ = (1/\sqrt{2})(x^0 + x^3) \quad \text{and} \quad x^- = (1/\sqrt{2})(x^0 - x^3), \quad (\text{C.1})$$

respectively, referred to as the “light-cone time” and “light-cone position”. The covariant vectors are obtained by $x_\mu = g_{\mu\nu}x^\nu$, with the metric tensor

$$g^{\mu\nu} = g_{\mu\nu} = \begin{pmatrix} 0 & 1 & 0 & 0 \\ 1 & 0 & 0 & 0 \\ 0 & 0 & -1 & 0 \\ 0 & 0 & 0 & -1 \end{pmatrix}. \quad (\text{C.2})$$

Scalar products are

$$x \cdot p = x^\mu p_\mu = x^+ p_- + x^- p_+ + x^1 p_1 + x^2 p_2 + = x^+ p^- + x^- p^+ - \mathbf{x}_\perp \mathbf{p}_\perp. \quad (\text{C.3})$$

All other four-vectors including γ^μ are treated correspondingly.

Dirac matrices. The chiral representation of the γ -matrices is used, particularly

$$\gamma^+ \gamma^+ = \gamma^- \gamma^- = 0. \quad (\text{C.4})$$

Alternating products are, for example,

$$\gamma^+ \gamma^- \gamma^+ = 2\gamma^+ \quad \text{and} \quad \gamma^- \gamma^+ \gamma^- = 2\gamma^-. \quad (\text{C.5})$$

Projection operators. The projection matrices become

$$A_+ = (1/\sqrt{2})\gamma^0\gamma^+ = \frac{1}{2}\gamma^- \gamma^+ \quad \text{and} \quad A_- = (1/\sqrt{2})\gamma^0\gamma^- = \frac{1}{2}\gamma^+ \gamma^-. \quad (\text{C.6})$$

In the chiral representation the projection matrices have a particularly simple structure, see Eq. (A.14).

Dirac spinors. Kogut and Soper [274] use as Dirac spinors

$$u(k, \uparrow) = \frac{1}{2^{1/4}\sqrt{k^+}} \begin{pmatrix} \sqrt{2}k^+ \\ k_x + ik_y \\ m \\ 0 \end{pmatrix}, \quad u(k, \downarrow) = \frac{1}{2^{1/4}\sqrt{k^+}} \begin{pmatrix} 0 \\ m \\ -k_x + ik_y \\ \sqrt{2}k^+ \end{pmatrix}, \quad (\text{C.7})$$

$$v(k, \uparrow) = \frac{1}{2^{1/4}\sqrt{k^+}} \begin{pmatrix} 0 \\ -m \\ -k_x + ik_y \\ \sqrt{2}k^+ \end{pmatrix}, \quad v(k, \downarrow) = \frac{1}{2^{1/4}\sqrt{k^+}} \begin{pmatrix} \sqrt{2}k^+ \\ k_x + ik_y \\ -m \\ 0 \end{pmatrix}.$$

Polarization vectors. The null vector is

$$\eta^\mu = (0, 1, \mathbf{0}). \quad (\text{C.8})$$

The polarization vectors of Kogut and Soper [274] correspond to linear polarization $\lambda = 1$ and $\lambda = 2$:

$$\begin{aligned} \varepsilon^\mu(p, \lambda = 1) &= (0, p_x/p^+, 1, 0), \\ \varepsilon^\mu(p, \lambda = 2) &= (0, p_y/p^+, 0, 1). \end{aligned} \quad (\text{C.9})$$

The following are useful relations:

$$\begin{aligned}
 \gamma^\alpha \gamma^\beta d_{\alpha\beta}(p) &= -2, \\
 \gamma^\alpha \gamma^\nu \gamma^\beta d_{\alpha\beta}(p) &= (2/p^+) (\gamma^+ p^\nu + g^{+\nu} \not{p}), \\
 \gamma^\alpha \gamma^\mu \gamma^\nu \gamma^\beta d_{\alpha\beta}(p) &= -4g^{\mu\nu} + 2(p_\alpha/p^+) \{g^{\mu\alpha} \gamma^\nu \gamma^+ - g^{\alpha\nu} \gamma^\mu \gamma^+ + g^{\alpha+} \gamma^\mu \gamma^\nu \\
 &\quad - g^{+\nu} \gamma^\mu \gamma^\alpha + g^{+\mu} \gamma^\nu \gamma^\alpha\}.
 \end{aligned}
 \tag{C.10}$$

The remainder is the same as in Appendix A.

Appendix D. Comparing BD- with LB-spinors

The Dirac spinors $u_\alpha(p, \lambda)$ and $v_\alpha(p, \lambda)$ (with $\lambda = \pm 1$) are the four linearly independent solutions of the free Dirac equations $(\not{p} - m) u(p, \lambda) = 0$ and $(\not{p} + m) v(p, \lambda) = 0$. Instead of $u(p, \lambda)$ and $v(p, \lambda)$, it is sometimes convenient [39] to use spinors $w^r(p)$ defined by

$$w_\alpha^1(p) = u_\alpha(p, \uparrow), \quad w_\alpha^2(p) = u_\alpha(p, \downarrow), \quad w_\alpha^3(p) = v_\alpha(p, \uparrow), \quad w_\alpha^4(p) = v_\alpha(p, \downarrow).
 \tag{D.1}$$

With $p^0 = E = \sqrt{m^2 + \mathbf{p}^2}$ holds quite in general

$$u(p, \lambda) = (1/\sqrt{N}) (E + \boldsymbol{\alpha} \cdot \mathbf{p} + \beta m) \chi^r \quad \text{for } r = 1, 2,
 \tag{D.2}$$

$$v(p, \lambda) = (1/\sqrt{N}) (E + \boldsymbol{\alpha} \cdot \mathbf{p} - \beta m) \chi^r \quad \text{for } r = 3, 4.
 \tag{D.3}$$

Björken–Drell (BD) [39] choose $\chi_\alpha^r = \delta_{\alpha r}$. With $N = 2m(E + m)$, the four spinors are then explicitly

$$w_\alpha^r(p) = \frac{1}{\sqrt{N}} \begin{pmatrix} E + m & 0 & p_z & p_x - ip_y \\ 0 & E + m & p_x + ip_y & -p_z \\ p_z & p_x - ip_y & E + m & 0 \\ p_x + ip_y & -p_z & 0 & E + m \end{pmatrix}.
 \tag{D.4}$$

Alternatively (A), one can choose

$$\chi_\alpha^1 = \chi(\uparrow), \quad \chi_\alpha^2 = \chi(\downarrow), \quad \chi_\alpha^3 = \chi(\uparrow), \quad \chi_\alpha^4 = \chi(\downarrow),
 \tag{D.5}$$

with given in Eq. (B.10). With $N = 2m(E + p_z)$, the spinors become explicitly

$$w_\alpha^r(p) = \frac{1}{\sqrt{2N}} \begin{pmatrix} E + p_z + m & -p_x + ip_y & E + p_z - m & -p_x + ip_y \\ p_x + ip_y & E + p_z + m & p_x + ip_y & E + p_z - m \\ E + p_z - m & p_x - ip_y & E + p_z + m & p_x - ip_y \\ p_x + ip_y & -E - p_z + m & p_x + ip_y & -E - p_z - m \end{pmatrix}.
 \tag{D.6}$$

One verifies that both spinor conventions (BD) and (A) satisfy orthogonality and completeness

$$\sum_{\alpha=1}^4 \bar{w}_\alpha^r w_\alpha^{r'} = \gamma_{rr'}^0, \quad \sum_{r=1}^4 \gamma_{rr'}^0 w_\alpha^r \bar{w}_\beta^{r'} = \delta_{\alpha\beta},
 \tag{D.7}$$

respectively, with $\bar{w} = w^\dagger \gamma^0$. But the two *do not have* the same form for a particle at rest, $\mathbf{p} = 0$, namely

$$w_\alpha^r(m)_{\text{BD}} = \begin{pmatrix} 1 & 0 & 0 & 0 \\ 0 & 1 & 0 & 0 \\ 0 & 0 & 1 & 0 \\ 0 & 0 & 0 & 1 \end{pmatrix} \quad \text{and} \quad w_\alpha^r(m)_{\text{A}} = \begin{pmatrix} 1 & 0 & 0 & 0 \\ 0 & 1 & 0 & 0 \\ 0 & 0 & 1 & 0 \\ 0 & 0 & 0 & -1 \end{pmatrix}, \quad (\text{D.8})$$

respectively, but they have the same spin projection:

$$\sigma^{12}u(m, \lambda) = \lambda u(m, \lambda) \quad \text{and} \quad \sigma^{12}v(m, \lambda) = \lambda v(m, \lambda). \quad (\text{D.9})$$

Actually, Lepage and Brodsky [299] have *not* used Eq. (4.5), but rather

$$\chi_\alpha^1 = \chi(\uparrow), \quad \chi_\alpha^2 = \chi(\downarrow), \quad \chi_\alpha^3 = \chi(\downarrow), \quad \chi_\alpha^4 = \chi(\uparrow). \quad (\text{D.10})$$

by which reason Eq. (4.9) becomes

$$\sigma^{12}u(0, \lambda) = \lambda u(0, \lambda) \quad \text{and} \quad \sigma^{12}v(0, \lambda) = -\lambda v(0, \lambda). \quad (\text{D.11})$$

In the LC formulation the $\sigma/2$ operator is a helicity operator which has a different spin for fermions and anti-fermions.

Appendix E. The Dirac–Bergmann method

The dynamics of a classical, non-relativistic system with N degrees of freedom can be derived from the blockian. Obtained from an action principle, this Lagrangian is a function of the velocity phase space variables:

$$L = L(q_n, \dot{q}_n), \quad n = 1, \dots, N, \quad (\text{E.1})$$

where the q 's and \dot{q} 's are the generalized coordinates and velocities respectively. For simplicity we consider only Lagrangians without explicit time dependence. The momenta conjugate to the generalized coordinates are defined by

$$p_n = \partial L / \partial \dot{q}_n. \quad (\text{E.2})$$

Now it may turn out that not all the momenta may be expressed as independent functions of the velocities. If this is the case, the Legendre transformation that takes us from the Lagrangian to the Hamiltonian is not defined uniquely over the whole phase space (q, p) . There then exist a number of *constraints* connecting the q 's and p 's:

$$\phi_m(q, p) = 0, \quad m = 1, \dots, M. \quad (\text{E.3})$$

These constraints restrict the motion to a *subspace* of the full $2N$ -dimensional phase space defined by the (p, q) .

Eventually, we would like to formulate the dynamics in terms of Poisson brackets defined for any two dynamical quantities $A(q, p)$ and $B(q, p)$:

$$\{A, B\} = \frac{\partial A}{\partial q_n} \frac{\partial B}{\partial p_n} - \frac{\partial A}{\partial p_n} \frac{\partial B}{\partial q_n}. \quad (\text{E.4})$$

The Poisson bracket (PB) formulation is the stage from which we launch into quantum mechanics. Since the PB is defined over the whole phase space only for *independent* variables (q, p) , we are faced with the problem of extending the PB definition (among other things) onto a constrained phase space.

The constraints are a consequence of the form of the Lagrangian alone. Following Anderson and Bergmann [15], we will call the ϕ_m *primary constraints*. Now to develop the theory, consider the quantity $p_n \dot{q}_n - L$. If we make variations in the quantities q, \dot{q} and p we obtain

$$\delta(p_n \dot{q}_n - L) = \delta p_n \dot{q}_n - \dot{p}_n \delta q_n \quad (\text{E.5})$$

using Eq. (E.2) and the Lagrange equation $\dot{p}_n = \partial L / \partial q_n$. Since the right-hand side of Eq. (E.5) is independent of $\delta \dot{q}_n$ we will call $p_n \dot{q}_n - L$ the Hamiltonian H . Notice that this Hamiltonian is not unique. We can add to H any linear combination of the primary constraints and the resulting new Hamiltonian is just as good as the original one.

How do the primary constraints affect the equations of motion? Since not all the q 's and p 's are independent, the variations in Eq. (E.5) cannot be made independently. Rather, for Eq. (E.5) to hold, the variations must preserve the conditions Eq. (E.3). The result is [413]

$$\dot{q}_n = (\partial H / \partial p_n) + u_m \partial \phi_m / \partial p_n \quad (\text{E.6})$$

and

$$\dot{p}_n = -(\partial H / \partial q_n) - u_m \partial \phi_m / \partial q_n \quad (\text{E.7})$$

where the u_m are unknown coefficients. The N \dot{q} 's are fixed by the N q 's, the $N - M$ independent p 's and the M u 's. Dirac takes the variables q, p and u as the Hamiltonian variables.

Recalling the definition of the Poisson bracket Eq. (E.4) we can write, for any function g of the q 's and p 's

$$\dot{g} = \frac{\partial g}{\partial q_n} \dot{q}_n + \frac{\partial g}{\partial p_n} \dot{p}_n = \{g, H\} + u_m \{g, \phi_m\} \quad (\text{E.8})$$

using Eqs. (E.6) and (E.7). As mentioned already, the Poisson bracket has meaning only for two dynamical functions defined uniquely over the whole phase space. Since the ϕ_m restrict the independence of some of the p 's, we must not use the condition $\phi_m = 0$ within the PB. The PB should be evaluated based on the functional form of the primary constraints. After all PB's have been calculated, then we may impose $\phi_m = 0$. From now on, such restricted relations will be denoted with a squiggly equal sign:

$$\phi_m \approx 0. \quad (\text{E.9})$$

This is called a *weak equality*. The equation of motion for g is now

$$\dot{g} \approx \{g, H_T\} \quad (\text{E.10})$$

where

$$H_T = H + u_m \phi_m \quad (\text{E.11})$$

is the *total* Hamiltonian [126]. If we take g in Eq. (E.10) to be one of the ϕ 's we will get some consistency conditions since the primary constraints should remain zero throughout all time:

$$\{\phi_m, H\} + u_{m'} \{\phi_m, \phi_{m'}\} \approx 0. \quad (\text{E.12})$$

What are the possible outcomes of Eq. (E.12)? Unless they all reduce to $0 = 0$, i.e., are identically satisfied, we will get more conditions between the Hamiltonian variables q , p and u . We will exclude the case where an inappropriate Lagrangian leads to an inconsistency like $1 = 0$. There are then two cases of interest. The first possibility is that Eq. (E.12) provides no new information but imposes conditions on the u 's. The second possibility is that we get an equation independent of u_m but relating the p 's and q 's. This can happen if the $M \times M$ matrix $\{\phi_m, \phi_{m'}\}$ has any rows (or columns) which are linearly dependent. These new conditions between the q 's and p 's are called *secondary constraints*

$$\chi_{k'} \approx 0, \quad k' = 1, \dots, K' \quad (\text{E.13})$$

by Anderson and Bergmann [15]. Notice that primary constraints follow from the form of the Lagrangian alone whereas secondary constraints involve the equations of motion as well. These secondary constraints, like the primary constraints, must remain zero throughout all time so we can perform the same consistency operation on the χ 's:

$$\dot{\chi}_k = \{\chi_k, H\} + u_m \{\chi_k, \phi_m\} \approx 0. \quad (\text{E.14})$$

This equation is treated in the same manner as Eq. (E.12). If it leads to more conditions on the p 's and q 's the process is repeated again. We continue like this until either all the consistency conditions are exhausted or we get an identity.

Let us write all the constraints obtained in the above manner under one index as

$$\phi_j \approx 0, \quad j = 1, \dots, M + K \equiv J \quad (\text{E.15})$$

then we obtain the following matrix equation for the u_m :

$$\{\phi_j, H\} + u_m \{\phi_j, \phi_m\} \approx 0. \quad (\text{E.16})$$

The most general solution to Eq. (E.16) is

$$u_m = U_m + v_a V_{am}, \quad a = 1, \dots, A, \quad (\text{E.17})$$

where V_m is a solution of the homogeneous part of Eq. (E.16) and $v_a V_{am}$ is a linear combination of *all* such independent solutions. The coefficients v_a are arbitrary.

Substitute Eq. (E.17) into Eq. (E.11). This gives

$$H_T = H + U_m \phi_m + v_a V_{am} \phi_m = H' + v_a \phi_a, \quad (\text{E.18})$$

where

$$H' = H + U_m \phi_m \quad (\text{E.19})$$

and

$$\phi_a = V_{am}\phi_m. \quad (\text{E.20})$$

Note that the u 's must satisfy consistency requirements whereas the v 's are totally arbitrary functions of time. Later, we will have more to say about the appearance of these arbitrary features in our theory.

To further classify the quantities in our theory, consider the following definitions given by Dirac [124]. Any dynamical variable, $F(q, p)$, is called *first class* if

$$\{F, \phi_j\} \approx 0, \quad j = 1, \dots, J, \quad (\text{E.21})$$

i.e., F has zero PB with *all* the ϕ 's. If $\{F, \phi_j\}$ is not weakly zero F is called *second class*. Since the ϕ 's are the only independent quantities which are weakly zero, we can write the following *strong* equations when F is first class:

$$\{F, \phi_j\} = c_{jj'}\phi_{j'}. \quad (\text{E.22})$$

Any quantity which is weakly zero is strongly equal to some linear combination of the ϕ 's. Given Eqs. (E.21) and (E.22) it is easy to show that H' and ϕ_a (see Eqs. (E.19) and (E.20)) are first class quantities. Since ϕ_a is a linear combination of primary constraints Eq. (E.20), it too is a primary constraint. Thus, the total Hamiltonian Eq. (E.18), which is expressed as the sum of a first class Hamiltonian plus a linear combination of primary first class constraints, is a first class quantity.

Notice that the number of arbitrary functions of the time appearing in our theory is equivalent to the number of independent primary first class constraints. This can be seen by looking at Eq. (E.17) where all the independent first class primary constraints are included in the sum. This same number will also appear in the general equation of motion because of Eq. (E.18). Let us make a small digression on the role of these arbitrary functions of time.

The physical state of any system is determined by the q 's and p 's only and not by the v 's. However, if we start out at $t = t_0$ with fixed initial values (q_0, p_0) we arrive at different values of (q, p) at later times depending on our choice of v . The physical state does not uniquely determine a set of q 's and p 's but a given set of q 's and p 's must determine the physical state. We thus have the situation where there may be several sets of the dynamical variables which correspond to the same physical state.

To understand this better consider two functions A_{v_a} and $A_{v'_a}$ of the dynamical variables which evolve from some A_0 with different multipliers. Compare the two functions after a short time interval Δt by considering a Taylor expansion to first order in Δt :

$$A_{v_a}(t) = A_0 + \dot{A}_{v_a}\Delta t = A_0 + \{A_0, H_T\}\Delta t = A_0 + \Delta t[\{A_0, H'\} + v_a\{A_0, \phi_a\}]. \quad (\text{E.23})$$

Thus,

$$A_{v_a} - A_{v'_a} = \Delta t(v_a - v'_a)\{A_0, \phi_a\} \quad (\text{E.24})$$

or

$$\Delta A = \varepsilon_a\{A_0, \phi_a\} \quad (\text{E.25})$$

where

$$\varepsilon_a = \Delta t(v_a - v'_a) \quad (\text{E.26})$$

is a small, arbitrary quantity. This relationship between A_{v_a} and $A_{v'_a}$ tells us that the two functions are related by an infinitesimal canonical transformation (ICT) [186] whose generator is a first class primary constraint ϕ_a . This ICT leads to changes in the q 's and p 's which do not affect the physical state.

Furthermore, it can also be shown [126] that by considering successive ICTs that the generators need not be primary but can be secondary as well. To be completely general then, we should allow for such variations which do not change the physical state in our equations of motion. This can be accomplished by redefining H_T to include the first class secondary constraints with arbitrary coefficients. Since the distinction between first class primary and first class secondary is not significant [413] in what follows we will not make any explicit changes.

For future considerations, let us call those transformations which do not change the physical state *gauge transformations*. The ability to perform gauge transformations is a sign that the mathematical framework of our theory has some arbitrary features. Suppose we can add conditions to our theory that eliminate our ability to make gauge transformations. These conditions would enter as secondary constraints since they do not follow from the form of the Lagrangian. Therefore, upon imposing these conditions, all constraints become second class. If there *were* any more first class constraints we would have generators for gauge transformations which, by assumption, can no longer be made. This is the end of the digression although we will see examples of gauge transformations later.

In general, of the J constraints, some are first class and some are second class. A linear combination of constraints is again a constraint so we can replace the ϕ_j with independent linear combinations of them. In doing so, we will try to make as many of the constraints first class as possible. Those constraints which cannot be brought into the first class through appropriate linear combinations are labeled by ξ_s , $s = 1, \dots, S$. Now form the PBs of all the ξ 's with each other and arrange them into a matrix:

$$\Delta \equiv \begin{pmatrix} 0 & \{\xi_1, \xi_2\} & \cdots & \{\xi_1, \xi_S\} \\ \{\xi_2, \xi_1\} & 0 & \cdots & \{\xi_2, \xi_S\} \\ \vdots & \vdots & \ddots & \vdots \\ \{\xi_S, \xi_1\} & \{\xi_S, \xi_2\} & \cdots & 0 \end{pmatrix}. \quad (\text{E.27})$$

Dirac has proven that the determinant of Δ is non-zero (not even weakly zero). Therefore, the inverse of Δ exists:

$$(\Delta^{-1})_{ss'} \{\xi_{s'}, \xi_{ss'}\} = \delta_{ss'}. \quad (\text{E.28})$$

Define the Dirac bracket (DB) (Dirac called them “new Poisson brackets”) between any two dynamical quantities A and B to be

$$\{A, B\}^* = \{A, B\} - \{A, \xi_s\}(\Delta^{-1})_{ss'} \{\xi_{s'}, B\}. \quad (\text{E.29})$$

The DB satisfies all the same algebraic properties (anti-symmetry, linearity, product law, Jacobi identity) as the ordinary PB. Also, the equations of motion can be written in terms of the DB since for any $g(p, q)$,

$$\{g, H_T\}^* = \{g, H_T\} - \{g, \xi_s\}(\Delta^{-1})_{ss'} \{\xi_{s'}, H_T\} \approx \{g, H_T\}. \quad (\text{E.30})$$

The last step follows because H_T is first class.

Perhaps the most important feature of the DB is the way it handles second class constraints. Consider the DB of a dynamical quantity with one of the (remaining) ζ 's:

$$\{g, \zeta_{s'}\}^* = \{g, \zeta_{s'}\} - \{g, \zeta_s\}(\Lambda^{-1})_{ss'} \quad \{\zeta_{s'}, \zeta_{s'}\} = \{g, \zeta_{s'}\} - \{g, \zeta_s\}\delta_{ss'} = 0. \quad (\text{E.31})$$

The definition Eq. (E.28) was used in the second step above. Thus, the ζ 's may be set *strongly* equal to zero *before* working out the Dirac bracket. Of course, we must still be careful that we do not set ζ strongly to zero within a Poisson bracket. If we now replace all PBs by DBs (which is legitimate since the dynamics can be written in terms of DBs via Eq. (E.30)) any second class constraints in H_T will appear in the DB in Eq. (E.30). Eq. (E.31) then tells us that those constraints can be set to zero. Thus, all we are left with in our Hamiltonian are first class constraints:

$$\tilde{H}_T = H + v_i \Phi_i, \quad i = 1, \dots, I, \quad (\text{E.32})$$

where the sum is over the remaining constraints which are first class. It must be emphasized that this is possible only because we have reformulated the theory in terms of the Dirac brackets. Of course, this reformulation in terms of the DB does not uniquely determine the dynamics for us since we still have arbitrary functions of the time accompanying the first class constraints. If the Lagrangian is such it exhibits no first class constraints then the dynamics are completely defined.

Before doing an example from classical field theory, we should note some features of a field theory that differentiate it from point mechanics. In the classical theory with a finite number of degrees of freedom we had constraints which were functions of the phase space variables. Going over to field theory these constraints become *functionals* which in general may depend upon the spatial derivatives of the fields and conjugate momenta as well as the fields and momenta themselves:

$$\phi_m = \phi_m[\varphi(x), \pi(x), \partial_i \varphi, \partial_i \pi]. \quad (\text{E.33})$$

The square brackets indicate a functional relationship and $\partial_i \equiv \partial/\partial x^i$. A consequence of this is that the constraints are differential equations in general. Furthermore, the constraint itself is no longer the only independent weakly vanishing quantity. Spatial derivatives of ϕ_m and integrals of constraints over spatial variables are weakly zero also.

Since there are actually an infinite number of constraints for each m (one at each space-time point x) we write

$$H_T = H + \int d\mathbf{x} u_m(x) \phi_m(x). \quad (\text{E.34})$$

Consistency requires that the primary constraints be conserved in time:

$$0 \approx \{\phi_m(x), H_T\} = \{\phi_m, H\} + \int d\mathbf{y} u_n(y) \{\phi_m(x), \phi_n(y)\}. \quad (\text{E.35})$$

The field theoretical Poisson bracket for any two phase space functionals is given by

$$\{A, B\}_{x^0=y^0}(\mathbf{x}, \mathbf{y}) = \int d\mathbf{z} \left(\frac{\delta A}{\delta \varphi_i(\mathbf{z})} \frac{\delta B}{\delta \pi_i(\mathbf{z})} - \frac{\delta A}{\delta \pi_i(\mathbf{z})} \frac{\delta B}{\delta \varphi_i(\mathbf{z})} \right) \quad (\text{E.36})$$

with the subscript $x^0 = y^0$ reminding us that the bracket is defined for equal times only. Generally, there may be a number of fields present hence the discrete label i . The derivatives appearing in the

PB above are *functional* derivatives. If $F[f(x)]$ is a functional its derivative with respect to a function $f(y)$ is defined to be

$$\delta F[f(x)]/\delta f(y) = \lim_{\varepsilon \rightarrow 0} (1/\varepsilon) [F[f(x) + \varepsilon \delta(x - y)] - F[f(x)]] . \quad (\text{E.37})$$

Assuming Eq. (E.36) has a non-zero determinant we can define an inverse:

$$\int d\mathbf{y} P_{lm}(\mathbf{x}, \mathbf{y}) P_{mn}^{-1}(\mathbf{y}, \mathbf{z}) = \int d\mathbf{y} P_{lm}^{-1}(\mathbf{x}, \mathbf{y}) P_{mn}(\mathbf{y}, \mathbf{z}) = \delta_{ln} \delta(\mathbf{x} - \mathbf{z}) , \quad (\text{E.38})$$

where

$$P_{lm}(\mathbf{x}, \mathbf{y}) \equiv \{\phi_l(\mathbf{x}), \phi_m(\mathbf{y})\}_{x^0=y^0} . \quad (\text{E.39})$$

Unlike the discrete case, the inverse of the PB matrix above is not unique in general. This introduces an arbitrariness which was not present in theories with a finite number of degrees of freedom. The arbitrariness makes itself manifest in the form of *differential* (rather than algebraic) equations for the multipliers. We must then supply boundary conditions to fix the multipliers [413].

The Maxwell theory for the free electro-magnetic field is defined by the action

$$S = \int d^4x \mathcal{L}(x) , \quad (\text{E.40})$$

where \mathcal{L} is the Lagrangian *density*, Eq. (B.8). The action is invariant under local gauge transformations. The ability to perform such gauge transformations indicates the presence of first class constraints. To find them, we first obtain the momenta conjugate to the fields A_μ : $\pi^\mu = -F^{0\mu}$ as defined in Eq. (B.12). This gives us a primary constraint, namely $\pi^0(x) = 0$. Using Eq. (B.26), we can write the canonical Hamiltonian density as

$$P_{lm}(\mathbf{x}, \mathbf{y}) \equiv \{\phi_l(\mathbf{x}), \phi_m(\mathbf{y})\}_{x^0=y^0} , \quad (\text{E.41})$$

where the velocity fields \dot{A}_i have been expressed in terms of the momenta π_i . After a partial integration on the second term, the Hamiltonian becomes

$$\begin{aligned} H &= \int d^3x \left(\frac{1}{2} \pi_i \pi_i - A_0 \partial_i \pi_i + \frac{1}{4} F_{ik} F_{ik} \right) \\ &\Rightarrow H_T = H + \int d^3x v_1(x) \pi^0(x) . \end{aligned} \quad (\text{E.42})$$

Again, for consistency, the primary constraints must be constant in time so that

$$0 \approx \{\pi^0, H_T\} = - \left\{ \pi^0, \int d^3x A_0 \partial_i \pi_i \right\} = \partial_i \pi_i . \quad (\text{E.43})$$

Thus, $\partial_i \pi_i \approx 0$ is a secondary constraint. We must then check to see if Eq. (E.43) leads to further constraints by also requiring that $\partial_i \pi_i$ is conserved in time:

$$0 \approx \{\partial_i \pi_i, H_T\} . \quad (\text{E.44})$$

The PB above vanishes identically however so there are no more constraints which follow from consistency requirements. So we have our two *first class* constraints:

$$\phi_1 = \pi^0 \approx 0 \quad (\text{E.45})$$

and

$$\chi \equiv \phi_2 = \partial_i \pi_i \approx 0. \quad (\text{E.46})$$

In light of the above statements the first class *secondary* constraints should be included in H_T as well (Some authors call the Hamiltonian with first class secondary constraints included the *extended* Hamiltonian):

$$H_T = H + \int d^3x (v_1 \phi_1 + v_2 \phi_2). \quad (\text{E.47})$$

Notice that the fundamental PB's among the A_μ and π^μ ,

$$\{A_\mu(x), \pi^\nu(y)\}_{x^0=y^0} = \delta_\mu^\nu \delta(\mathbf{x} - \mathbf{y}) \quad (\text{E.48})$$

are incompatible with the constraint $\pi^0 \approx 0$ so we will modify them using the Dirac-Bergmann procedure. The first step towards this end is to impose certain conditions to break the local gauge invariance. Since there are two first class constraints, we need two gauge conditions imposed as second class constraints. The traditional way to implement this is by imposing the *radiation gauge* conditions:

$$\Omega_1 \equiv A_0 \approx 0 \quad \text{and} \quad \Omega_2 \equiv \partial_{iA_i} \approx 0. \quad (\text{E.49})$$

It can be shown [413] that the radiation gauge conditions completely break the gauge invariance thereby bringing all constraints into the second class.

The next step is to form the matrix of second class constraints with matrix elements $\Delta_{ij} = \{\Omega_i, \phi_j\}_{x^0=y^0}$ and $i, j = 1, 2$:

$$\Delta = \begin{pmatrix} 0 & 0 & 1 & 0 \\ 0 & 0 & 0 & -\nabla^2 \\ -1 & 0 & 0 & 0 \\ 0 & \nabla^2 & 0 & 0 \end{pmatrix} \delta(\mathbf{x} - \mathbf{y}). \quad (\text{E.50})$$

To get the Dirac bracket we need the inverse of Δ . Recalling the definition, Eq. (E.38), we have

$$\int d\mathbf{y} \Delta_{ij}(\mathbf{x}, \mathbf{y}) (\Delta^{-1})_{jk}(\mathbf{y}, \mathbf{z}) = \delta_{ik} \delta(\mathbf{x} - \mathbf{z}). \quad (\text{E.51})$$

With the help of $\nabla^2(1/|\mathbf{x} - \mathbf{y}|) = -4\pi\delta(\mathbf{x} - \mathbf{y})$ we can easily perform Eq. (2.11) element by element to obtain

$$\Delta^{-1} = \begin{pmatrix} 0 & 0 & -\delta(\mathbf{x} - \mathbf{y}) & 0 \\ 0 & 0 & 0 & -\frac{1}{4\pi|\mathbf{x} - \mathbf{y}|} \\ \delta(\mathbf{x} - \mathbf{y}) & 0 & 0 & 0 \\ 0 & \frac{1}{4\pi|\mathbf{x} - \mathbf{y}|} & 0 & 0 \end{pmatrix} \quad (\text{E.52})$$

Thus, the Dirac bracket in the radiation gauge is (all brackets are at equal times)

$$\{A(x), B(y)\}^* = \{A(x), B(y)\} - \iint d\mathbf{u} d\mathbf{v} \{A(x), \psi_i(\mathbf{u})\} (\Delta^{-1})_{ij}(\mathbf{u}, \mathbf{v}) \{\psi_j(\mathbf{v}), B(y)\}, \quad (\text{E.53})$$

where $\psi_1 = \Omega_1$, $\psi_2 = \Omega_2$, $\psi_3 = \phi_1$ and $\psi_4 = \phi_2$. The fundamental Dirac brackets are

$$\begin{aligned} \{A_\mu(x), \pi^\nu(y)\}^* &= (\delta_\mu^\nu + \delta_\mu^0 g^{\nu 0}) \delta(\mathbf{x} - \mathbf{y}) - \partial_\mu \partial^\nu (1/4\pi|\mathbf{x} - \mathbf{y}|) \\ \{A_\mu(x), A_\nu(y)\}^* &= 0 = \{\pi^\mu(x), \pi^\nu(y)\}^*. \end{aligned} \quad (\text{E.54})$$

From the first of the above equations we obtain,

$$\{A_i(x), \pi_j(y)\}^* = \delta_{ij} \delta(\mathbf{x} - \mathbf{y}) - \partial_i \partial_j (1/4\pi|\mathbf{x} - \mathbf{y}|). \quad (\text{E.55})$$

The right-hand side of the above expression is often called the “transverse delta function” in the context of canonical quantization of the electro-magnetic field in the radiation gauge. In nearly all treatments of that subject, however, the transverse delta function is introduced “by hand” so to speak. This is done after realizing that the standard commutation relation $[A_i(x), \pi_j(y)] = i\delta_{ij} \delta(\mathbf{x} - \mathbf{y})$ is in contradiction with Gauss’ law. In the Dirac–Bergmann approach the familiar equal-time commutator relation is obtained without any hand-waving arguments.

The choice of the radiation gauge in the above example most naturally reflects the splitting of A and π into transverse and longitudinal parts. In fact, the gauge condition $\partial_i A_i = 0$ implies that the longitudinal part of A is zero. This directly reflects the observation that no longitudinally polarized photons exist in nature.

Given this observation, we should somehow be able to associate the true degrees of freedom with the transverse parts of A and π . Sundermeyer [413] shows that this is indeed the case and that, for the true degrees of freedom, the DB and PB coincide.

We have up till now concerned ourselves with constrained dynamics at the classical level. Although all the previous developments have occurred quite naturally in the classical context, it was the problem of *quantization* which originally motivated Dirac and others to develop the previously described techniques. Also, more advanced techniques incorporating constraints into the path integral formulation of quantum theory have been developed.

The general problem of quantizing theories with constraints is very formidable especially when considering general gauge theories. We will not attempt to address such problems. Rather, we will work in the non-relativistic framework of the Schrödinger equation where quantum states are described by a wave function.

As a first case, let us consider a classical theory where all the constraints are first class. The Hamiltonian is written then as the sum of the canonical Hamiltonian $H = p_i \dot{q}_i - L$ plus a linear combination of the first class constraints:

$$H' = H + v_j \phi_j. \quad (\text{E.56})$$

Take the p 's and q 's to satisfy

$$\{q_i, p_j\} \Rightarrow (i/\hbar) [\hat{q}_i, \hat{p}_j] \quad (\text{E.57})$$

where the hatted variables denote quantum operators and $[\hat{q}_i, \hat{p}_j] = \hat{q}_i\hat{p}_j - \hat{p}_j\hat{q}_i$ is the commutator. The Schrödinger equation reads

$$i\hbar d\psi/dt = H'\psi, \quad (\text{E.58})$$

where ψ is the wavefunction on which the dynamical variables operate. For each constraint ϕ_j impose supplementary conditions on the wavefunction

$$\hat{\phi}_j\psi = 0. \quad (\text{E.59})$$

Consistency of the Eq. (E.59) with one another demands that

$$[\hat{\phi}_j, \hat{\phi}_{j'}]\psi = 0. \quad (\text{E.60})$$

Recall the situation in the classical theory where anything that was weakly zero could be written strongly as a linear combination of the ϕ 's:

$$\{\phi_j, \phi_{j'}\} = c_{jj'}^r \phi^{j'}. \quad (\text{E.61})$$

Now if we want Eq. (E.60) to be a *consequence* of Eq. (E.59), an analogous relation to Eq. (E.61) must hold in the quantum theory, namely,

$$[\hat{\phi}_j, \hat{\phi}_{j'}] = \hat{c}_{jj'}^r \hat{\phi}^{j'}. \quad (\text{E.62})$$

The problem is that the coefficients \hat{c} in the quantum theory are in general functions of the operators \hat{p} and \hat{q} and do not necessarily commute with the $\hat{\phi}$'s. In order for consistency then, we must have the coefficients in the quantum theory all appearing to the *left* of the $\hat{\phi}$'s.

The same conclusion follows if we consider the consistency of Eq. (E.59) with the Schrödinger equation. If we cannot arrange to have the coefficients to the left of the constraints in the quantum theory then as Dirac says “we are out of luck” [126].

Consider now the case where there are second class constraints, ξ_s . The problems encountered when there are second class constraints are similar in nature to the first class case but appear even worse. This statement follows simply from the definition of second class. If we try to impose a condition on ψ similarly to Eq. (E.59) but with a second class constraint we must get a contradiction since already $\{\xi_s, \phi_j\} \neq 0$ for all j at the *classical* level.

Of course if we imposed $\hat{\xi}_s = 0$ as an operator identity then there is no contradiction. In the classical theory, the analogous constraint condition is the strong equality $\xi = 0$. We have seen that strong equalities for second class constraints emerge in the classical theory via the Dirac–Bergmann method. Thus it seems quite suggestive to postulate

$$\{A, B\}^* \Rightarrow (i/\hbar) [\hat{A}, \hat{B}] \quad (\text{E.63})$$

as the rule for quantizing the theory while imposing $\hat{\xi}_s = 0$ as an operator identity. Any remaining weak equations are all first class and must then be treated as in the first case using supplementary conditions on the wave function. Hence, the operator ordering ambiguity still exists in general.

We have seen that there is no definite way to guarantee a well defined quantum theory given the corresponding classical theory. It is possible, since the Dirac bracket depends on the gauge constraints imposed by hand, that we can choose such constraints in such a way as to avoid any

problems. For a general system however, such attempts would at best be difficult to implement. We have seen that there is a consistent formalism for determining (at least as much one can) the dynamics of a generalized Hamiltonian system. The machinery is as follows:

- Obtain the canonical momenta from the Lagrangian.
- Identify the primary constraints and construct the total Hamiltonian.
- Require the primary constraints to be conserved in time.
- Require any additional constraints obtained by step 3 to also be conserved in time.
- Separate all constraints into first class or second class.
- Invert the matrix of second class constraints.
- Form the Dirac bracket and write the equations of motion in terms of them.
- Quantize by taking the DB over to the quantum commutator.

Of course, there are limitations throughout this program; especially in steps six and eight. If there are any remaining first class constraints it is a sign that we still have some gauge freedom left in our theory. Given the importance of gauge field theory in today's physics it is certainly worth one's while to understand the full implications of constrained dynamics. The material presented here is meant to serve as a primer for further study.

References

- [1] J. Abad, J.G. Esteve, A.F. Pacheco, *Phys. Rev. D* 32 (1985) 2729.
- [2] O. Abe, K. Tanaka, K.G. Wilson, *Phys. Rev. D* 48 (1993) 4856–4867.
- [3] O. Abe, G.J. Aubrecht, K. Tanaka, *Phys. Rev. D* 56 (1997) 2242–2249.
- [4] N.A. Aboud, J.R. Hiller, *Phys. Rev. D* 41 (1990) 937–945.
- [5] C. Acerbi, A. Bassetto, *Phys. Rev. D* 49 (1994) 1067–1076.
- [6] S. Adler, *Nucl. Phys. B* 415 (1994) 195.
- [7] A. Ali, V.M. Braun, H. Simma, *Z. Physik C* 63 (1994) 437–454.
- [8] E.A. Ammons, *Phys. Rev. D* 50 (1994) 980–990.
- [9] F. Antonuccio, S. Dalley, *Phys. Lett. B* 348 (1995) 55.
- [10] F. Antonuccio, S. Dalley, *Nucl. Phys. B* 461 (1996) 275.
- [11] F. Antonuccio, S. Dalley, *Phys. Lett. B* 376 (1996) 154.
- [12] F. Antonuccio, S.J. Brodsky, S. Dalley, *Phys. Lett. B* 412 (1997) 104.
- [13] F. Antonuccio, S. Pinsky, *Phys. Lett. B* 397 (1997) 42–50.
- [14] A.M. Annenkova, E.V. Prokhatilov, V.A. Franke, *Phys. Atom. Nucl.* 56 (1993) 813–825.
- [15] J.L. Anderson, P.G. Bergman, *Phys. Rev.* 83 (1951) 1018.
- [16] K. Bardakci, M.B. Halpern, *Phys. Rev.* 176 (1968) 1786.
- [17] W.A. Bardeen, R.B. Pearson, *Phys. Rev. D* 13 (1976) 547.
- [18] W.A. Bardeen, R.B. Pearson, E. Rabinovici, *Phys. Rev. D* 21 (1980) 1037.
- [19] V. Bargmann, *Proc. Natl. Acad. Sci. (USA)* 34 (1948) 211.
- [20] D. Bartoletta et al., *Phys. Rev. Lett.* 62 (1989) 2436.
- [21] A. Bassetto, G. Nardelli, R. Soldati, *Yang-Mills Theories in Algebraic Noncovariant Gauges*, World Scientific, Singapore, 1991.
- [22] A. Bassetto, *Phys. Rev. D* 47 (1993) 727–729.
- [23] A. Bassetto, M. Ryskin, *Phys. Lett. B* 316 (1993) 542–545.
- [24] A. Bassetto, I.A. Korchemskaya, G.P. Korchemsky, G. Nardelli, *Nucl. Phys. B* 408 (1993) 62–90.
- [25] A. Bassetto, *Nucl. Phys. Proc. Suppl. C* 51 (1996) 281–288.

- [27] A. Bassetto, L. Griguolo, G. Nardelli, *Phys. Rev. D* 54 (1996) 2845–2852.
- [28] A. Bassetto, G. Nardelli, *Int. J. Mod. Phys. A* 12 (1997) 1075–1090.
- [29] R. Bayer, H.C. Pauli, *Phys. Rev. D* 53 (1996) 939.
- [30] J.S. Bell, *Acta Phys. Austriaca (Suppl.)* 13 (1974) 395.
- [31] E. Belz, ANL preprint, 1994.
- [32] C.M. Bender, L.R. Mead, S.S. Pinsky, *Phys. Rev. Lett.* 56 (1986) 2445.
- [33] C.M. Bender, S.S. Pinsky, B. Van de Sande, *Phys. Rev. D* 48 (1993) 816.
- [34] H. Bergknoff, *Nucl. Phys. B* 122 (1977) 215.
- [35] C. Bloch, *Nucl. Phys.* 6 (1958) 329.
- [36] G. Bertsch, S.J. Brodsky, A.S. Goldhaber, J.F. Gunion, *Phys. Rev. Lett.* 47 (1981) 297.
- [37] H.A. Bethe, F. de Hoffman, *Mesons and Fields*, Vol. II, Row, Peterson and Company, Evanston, Ill, 1955.
- [38] G. Bhanot, K. Demeterfi, I.R. Klebanov, *Phys. Rev. D* 48 (1993) 4980.
- [39] J.D. Björken, S.D. Drell, *Relativistic Quantum Mechanics*, McGraw-Hill, New York, 1964; J.D. Björken, S.D. Drell, *Relativistic Quantum Fields*, McGraw-Hill, New York, 1965.
- [40] J.D. Björken, E.A. Paschos, *Phys. Rev.* 185 (1969) 1975.
- [41] J.D. Björken, J.B. Kogut, D.E. Soper, *Phys. Rev. D* 3 (1971) 1382.
- [42] B. Blaettel, G. Baym, L.L. Frankfurt, H. Heiselberg, M. Strikman, *Phys. Rev. D* 47 (1993) 2761.
- [43] R. Blankenbecler, S.J. Brodsky, J.F. Gunion, R. Savit, *Phys. Rev. D* 8 (1973) 4117.
- [44] G.T. Bodwin, D.R. Yennie, M.A. Gregorio, *Rev. Mod. Phys.* 56 (1985) 723.
- [45] A. Borderies, P. Grangé, E. Werner, *Phys. Lett. B* 319 (1993) 490–496.
- [46] A. Borderies, P. Grangé, E. Werner, *Phys. Lett. B* 345 (1995) 458–468.
- [47] J. Botts, *Nucl. Phys. B* 353 (1991) 20.
- [48] M. Brisudova, R.J. Perry, *Phys. Rev. D* 54 (1996) 1831–1843.
- [49] M. Brisudova, R.J. Perry, *Phys. Rev. D* 54 (1996) 6453–6458.
- [50] M. Brisudova, R.J. Perry, K.G. Wilson, *Phys. Rev. Lett.* 78 (1997) 1227–1230.
- [51] S.J. Brodsky, J.R. Primack, *Annals Phys.* 52 (1960) 315.
- [52] S.J. Brodsky, J.R. Primack, *Phys. Rev.* 174 (1968) 2071.
- [53] S.J. Brodsky, R. Roskies, R. Suaya, *Phys. Rev. D* 8 (1973) 4574.
- [54] S.J. Brodsky, G.R. Farrar, *Phys. Rev. D* 11 (1975) 1309.
- [55] S.J. Brodsky, B.T. Chertok, *Phys. Rev. D* 14 (1976) 3003.
- [56] S.J. Brodsky, S.D. Drell, *Phys. Rev. D* 22 (1980) 2236.
- [57] S.J. Brodsky, G.P. Lepage, S.A.A. Zaidi, *Phys. Rev. D* 23 (1981) 1152.
- [58] S.J. Brodsky, J.R. Hiller, *Phys. Rev. C* 28 (1983) 475.
- [59] S.J. Brodsky, C.-R. Ji, G.P. Lepage, *Phys. Rev. Lett.* 51 (1983) 83.
- [60] S.J. Brodsky, A.H. Mueller, *Phys. Lett. B* 206 (1988) 685.
- [61] S.J. Brodsky, G.F. de Teramond, *Phys. Rev. Lett.* 60 (1988) 1924.
- [62] S.J. Brodsky, G.P. Lepage, in: A.H. Mueller (Ed.), *Perturbative Quantum Chromodynamics*, World Scientific, Singapore, 1989.
- [63] S.J. Brodsky, I.A. Schmidt, *Phys. Lett. B* 234 (1990) 144.
- [64] S.J. Brodsky, G.F. de Teramond, I.A. Schmidt, *Phys. Rev. Lett.* 64 (1990) 1011.
- [65] S.J. Brodsky, I.A. Schmidt, *Phys. Rev. D* 43 (1991) 179.
- [66] S.J. Brodsky, H.C. Pauli, in: H. Mitter, H. Gausterer (Eds.), *Recent Aspect of Quantum Fields*, Lecture Notes in Physics, vol. 396, Springer, Berlin, 1991.
- [67] S.J. Brodsky, P. Hoyer, A.H. Mueller, W.-K. Tang, *Nucl. Phys. B* 369 (1992) 519.
- [68] S.J. Brodsky, G. McCartor, H.C. Pauli, S.S. Pinsky, *Particle World* 3 (1993) 109.
- [69] S.J. Brodsky, W.-K. Tang, C.B. Thorn, *Phys. Lett. B* 318 (1993) 203.
- [70] S.J. Brodsky, M. Burkardt, I. Schmidt, *Nucl. Phys. B* 441 (1994) 197.
- [71] S.J. Brodsky, F. Schlumpf, *Phys. Lett. B* 329 (1994) 111.
- [72] S.J. Brodsky, F. Schlumpf, *Prog. Part. Nucl. Phys.* 34 (1995) 69–86.
- [73] R.W. Brown, J.W. Jun, S.M. Shvartsman, C.C. Taylor, *Phys. Rev. D* 48 (1993) 5873–5882.
- [74] F. Buccella, E. Celeghin, H. Kleinert, C.A. Savoy, E. Sorace, *Nuovo Cimento A* 69 (1970) 133.

- [75] M. Burkardt, *Phys. A* 504 (1989) 762.
- [76] M. Burkardt, A. Langnau, *Phys. Rev. D* 44 (1991) 1187.
- [77] M. Burkardt, A. Langnau, *Phys. Rev. D* 44 (1991) 3857.
- [78] M. Burkardt, *Phys. Rev. D* 47 (1993) 4628.
- [79] M. Burkardt, *Phys. Rev. D* 49 (1994) 5446.
- [80] M. Burkardt, *Adv. Nucl. Phys.* 23 (1996) 1–74.
- [81] M. Burkardt, Light front hamiltonians and confinement, hep-ph/9512318.
- [82] M. Burkardt, H. El-Khozondar, *Phys. Rev. D* 55 (1997) 6514–6521.
- [83] M. Burkardt, *Phys. Rev. D* 54 (1996) 2913–2920.
- [84] M. Burkardt, B. Klindworth, *Phys. Rev. D* 55 (1997) 1001–1012.
- [85] M. Burkardt, *Phys. Rev. D* 57 (1998) 1136.
- [86] F. Cardarelli, I.L. Grach, I.M. Narodetskii, G. Salme, S. Simula, *Phys. Lett. B* 349 (1995) 393–399.
- [87] R. Carlitz, D. Heckathorn, J. Kaur, W.-K. Tung, *Phys. Rev. D* 11 (1975) 1234.
- [88] R. Carlitz, W.-K. Tung, *Phys. Rev. D* 13 (1976) 3446.
- [89] C.E. Carlson, J.L. Poor, *Phys. Rev. D* 38 (1988) 2758.
- [90] A. Carroll, Lecture at the Workshop on Exclusive Processes at High Momentum Transfer, Elba, Italy, 1993.
- [91] A. Casher, *Phys. Rev. D* 14 (1976) 452.
- [92] S. Chang, S. Ma, *Phys. Rev.* 180 (1969) 1506.
- [93] S.J. Chang, *Phys. Rev. D* 13 (1976) 2778.
- [94] S.J. Chang, T.M. Yan, *Phys. Rev. D* 7 (1973) 1147.
- [95] S.J. Chang, R.G. Root, T.M. Yan, *Phys. Rev. D* 7 (1973) 1133.
- [96] S.J. Chang, R.G. Root, T.M. Yan, *Phys. Rev. D* 7 (1973) 1133.
- [97] L. Chao, *Mod. Phys. Lett. A* 8 (1993) 3165–3172.
- [98] Z. Chen, A.H. Mueller, *Nucl. Phys. B* 451 (1995) 579.
- [99] H.Y. Cheng, C.Y. Cheung, C.W. Hwang, *Phys. Rev. D* 55 (1997) 1559–1577.
- [100] V.L. Chernyak, A.R. Zhitnitskii, *Phys. Rep.* 112 (1984) 173.
- [101] C.Y. Cheung, W.M. Zhang, G.-L. Lin, *Phys. Rev. D* 52 (1995) 2915–2925.
- [102] P.L. Chung, W.N. Polyzou, F. Coester, B.D. Keister, *Phys. Rev. C* 37 (1988) 2000.
- [103] P.L. Chung, F. Coester, *Phys. Rev. D* 44 (1991) 229.
- [104] F.E. Close, *An Introduction to Quarks and Partons*, Academic Press, New York, 1979.
- [105] F. Coester, W.N. Polyzou, *Phys. Rev. D* 26 (1982) 1349.
- [106] F. Coester, *Prog. Nuc. Part. Phys.* 29 (1992) 1.
- [107] F. Coester, W. Polyzou, *Found. Phys.* 24 (1994) 387–400.
- [108] S. Coleman, *Comm. Math. Phys.* 31 (1973) 259.
- [109] S. Coleman, R. Jackiw, L. Susskind, *Ann. Phys. (NY)* 93 (1975) 267.
- [110] S. Coleman, *Ann. Phys. (NY)* 101 (1976) 239.
- [111] J. Collins, *Renormalization*, Cambridge University Press, New York, 1984.
- [112] M.E. Convery, C.C. Taylor, J.W. Jun, *Phys. Rev. D* 51 (1995) 4445–4450.
- [113] D.P. Crewther, C.J. Hamer, *Nucl. Phys. B* 170 (1980) 353.
- [114] R.H. Dalitz, F.J. Dyson, *Phys. Rev.* 99 (1955) 301.
- [115] S. Dalley, I.R. Klebanov, *Phys. Rev. D* 47 (1993) 2517.
- [116] S. Dalley, B. van de Sande, *Nucl. Phys B Proc. Suppl.* 53 (1997) 827–830.
- [117] S.M. Dancoff, *Phys. Rev.* 78 (1950) 382.
- [118] R. Dashen, M. Gell-Mann, *Phys. Rev. Lett.* 17 (1966) 340.
- [119] S.P. De Alwis, *Nucl. Phys. B* 55 (1973) 427.
- [120] S.P. De Alwis, J. Stern, *Nucl. Phys. B* 77 (1974) 509.
- [121] K. Demeterfi, I.R. Klebanov, G. Bhanot, *Nucl. Phys. B* 418 (1994) 15.
- [122] N.B. Demchuk, P.Yu. Kulikov, I.M. Narodetskii, P.J. O'Donnell, *Phys. Atom. Nucl.* 60 (1997) 1292–1304.
- [123] P.A.M. Dirac, *Rev. Mod. Phys.* 21 (1949) 392.
- [124] P.A.M. Dirac, *Can. Jour. Math.* 2 (1950) 129.
- [125] P.A.M. Dirac, *The Principles of Quantum Mechanics*, 4th ed., Oxford Univ. Press, Oxford, 1958.

- [126] P.A.M. Dirac, Lectures on Quantum Mechanics, Belfer Graduate School of Science, Yeshiva University, 1964.
- [127] P.A.M. Dirac, in: D.W. Duke, J.F. Owens (Eds.), Perturbative Quantum Chromodynamics, Am. Inst. Phys., New York, 1981.
- [128] P.J. O'Donnell, Q.P. Xu, H.K.K. Tung, Phys. Rev. D 52 (1995) 3966–3977.
- [129] S.D. Drell, A.C. Hearn, Phys. Rev. Lett. 16 (1966) 908.
- [130] S.D. Drell, D. Levy, T.M. Yan, Phys. Rev. 187 (1969) 2159.
- [131] S.D. Drell, D. Levy, T.M. Yan, Phys. Rev. D 1 (1970) 1035.
- [132] S.D. Drell, D. Levy, T.M. Yan, Phys. Rev. D 1 (1970) 1617.
- [133] S.D. Drell, T.M. Yan, Phys. Rev. Lett. 24 (1970) 181.
- [134] A.Yu. Dubin, A.B. Kaidalov, Yu.A. Simonov, Phys. Lett. B 343 (1995) 310–314.
- [135] E. Eichten, F. Feinberg, J.F. Willemssen, Phys. Rev. D 8 (1973) 1204.
- [136] M.B. Einhorn, Phys. Rev. D 14 (1976) 3451.
- [137] T. Eller, H.C. Pauli, S.J. Brodsky, Phys. Rev. D 35 (1987) 1493.
- [138] T. Eller, H.C. Pauli, Z. Physik 42 C (1989) 59.
- [139] S. Elser, Hadron Structure '94, Kosice, Slovakia, 1994; Diplomarbeit, U. Heidelberg, 1994.
- [140] S. Elser, A.C. Kalloniatis, Phys. Lett. B 375 (1996) 285–291.
- [141] G. Fang et al., Presented at the INT -Fermilab Workshop on Perspectives of High Energy Strong Interaction Physics at Hadron Facilities, 1993.
- [142] F.L. Feinberg, Phys. Rev. D 7 (1973) 540.
- [143] T.J. Fields, K.S. Gupta, J.P. Vary, Mod. Phys. Lett. A 11 (1996) 2233–2240.
- [144] R.P. Feynman, Phys. Rev. Lett. 23 (1969) 1415.
- [145] R.P. Feynman, Photon–Hadron Interactions, Benjamin, Reading, MA, 1972.
- [146] V.A. Franke, Yu.A. Novozhilov, E.V. Prokhvatilov, Lett. Math. Phys. 5 (1981) 239.
- [147] V.A. Franke, Yu.A. Novozhilov, E.V. Prokhvatilov, Lett. Math. Phys. 5 (1981) 437.
- [148] V.A. Franke, Yu.A. Novozhilov, E.V. Prokhvatilov, in: Dynamical Systems and Microphysics, Academic Press, New York, 1982, pp. 389–400.
- [149] L. Frankfurt, T.S.H. Lee, G.A. Miller, M. Strikman, Phys. Rev. C 55 (1997) 909.
- [150] H. Fritzsche, M. Gell-Mann, Proc. 16th. Int. Conf. on HEP, Batavia, IL, 1972.
- [151] H. Fritzsche, Mod. Phys. Lett. A 5 (1990) 625.
- [152] H. Fritzsche, Constituent Quarks, Chiral Symmetry, the Nucleon Spin, talk given at the Leipzig Workshop on Quantum Field Theory Aspects of High Energy Physics CERN, September 1993, preprint TH. 7079/93.
- [153] S. Fubini, G. Furlan, Physics 1 (1965) 229.
- [154] S. Fubini, A.J. Hanson, R. Jackiw, Phys. Rev. D 7 (1973) 1732.
- [155] M.G. Fuda, Phys. Rev. C 36 (1987) 702–709.
- [156] M.G. Fuda, Phys. Rev. D 42 (1990) 2898–2910.
- [157] M.G. Fuda, Phys. Rev. D 44 (1991) 1880–1890.
- [158] M.G. Fuda, Nucl. Phys. A 543 (1992) 111c–126c.
- [159] M.G. Fuda, Ann. Phys. 231 (1994) 1–40.
- [160] M.G. Fuda, Phys. Rev. C 52 (1995) 1260–1269.
- [161] M.G. Fuda, Phys. Rev. D 54 (1996) 5135–5147.
- [162] T. Fujita, A. Ogura, Prog. Theor. Phys. 89 (1993) 23–36.
- [163] T. Fujita, C. Itoi, A. Ogura, M. Taki, J. Phys. G 20 (1994) 1143–1157.
- [164] T. Fujita, Y. Sekiguchi, Prog. Theor. Phys. 93 (1995) 151–160.
- [165] M. Fujita, Sh.M. Shvartsman, Role of zero modes in quantization of QCD in light-cone coordinates, CWRU-TH-95-11, hep-th/9506046, June 1995, 21pp.
- [166] T. Fujita, M. Hiramoto, H. Takahashi, Bound states of $(1 + 1)$ -dimensional field theories, hep-th/9609224.
- [167] T. Fujita, K. Yamamoto, Y. Sekiguchi, Ann. Phys. 255 (1997) 204–227.
- [168] M. Funke, V. Kaulfuss, H. Kummel, Phys. Rev. D 35 (1987) 621.
- [169] P. Gaete, J. Gamboa, I. Schmidt, Phys. Rev. D 49 (1994) 5621–5624.
- [170] M. Gari, N.G. Stephanis, Phys. Lett. B 175 (1986) 462.
- [171] A. Gasser, H. Leutwyler, Nucl. Phys. B 94 (1975) 269.

- [172] M. Gell-Mann, Phys. Lett. 8 (1964) 214.
- [173] M. Gell-Mann, Lectures given at the 1972 Schladming Winter School, Acta Phys. Austriaca 9 (Suppl.) 733 (1972).
- [174] S.B. Gerasimov, Yad. Fiz. 2 (1965) 598 [Sov. J. Nucl. Phys. 2 (1966) 430].
- [175] S.N. Ghosh, Phys. Rev. D 46 (1992) 5497–5503.
- [176] S. Głazek, Acta Phys. Pol. B 15 (1984) 889.
- [178] S. Głazek, R.J. Perry, Phys. Rev. D 45 (1992) 3734.
- [179] S. Głazek, R.J. Perry, Phys. Rev. D 45 (1992) 3740.
- [180] S. Głazek, K.G. Wilson, Phys. Rev. D 47 (1993) 4657.
- [181] S. Głazek, K.G. Wilson, Phys. Rev. D 48 (1993) 5863.
- [182] S. Głazek, A. Harindranath, S. Pinsky, J. Shigemitsu, K. Wilson, Phys. Rev. D 47 (1993) 1599.
- [183] S. Głazek, K.G. Wilson, Phys. Rev. D 49 (1994) 4214.
- [184] S. Głazek, K.G. Wilson, Phys. Rev. D 49 (1994) 6720.
- [185] S. Głazek (Ed.), Theory of Hadrons and Light-front QCD, World Scientific, Singapore, 1995.
- [186] H. Goldstein, Classical Mechanics, Addison-Wesley, Reading, MA, 1950.
- [187] I.L. Grach, I.M. Narodetskii, S. Simula, Phys. Lett. B 385 (1996) 317–323.
- [188] P. Grangé, A. Neveu, H.C. Pauli, S. Pinsky, E. Werner, (Eds.), New Non-perturbative Methods and Quantization on the Light Cone, “Les Houches Series”, Vol. 8, Springer, Berlin, 1997; Proc. Workshop at Centre de Physique des Houches, France, 24 February–7 March 1997.
- [189] V.N. Gribov, Nucl. Phys. B 139 (1978) 1.
- [190] P.A. Griffin, Nucl. Phys. B 372 (1992) 270.
- [191] P.A. Griffin, Phys. Rev. D 46 (1992) 3538–3543.
- [192] D. Gromes, H.J. Rothe, B. Stech, Nucl. Phys. B 75 (1974) 313.
- [193] D.J. Gross, I.R. Klebanov, A.V. Matytsin, A.V. Smilga, Nucl. Phys. B 461 (1996) 109–130.
- [194] E. Gubankova, F. Wegner, Exact renormalization group analysis in Hamiltonian theory: I. QED Hamiltonian on the light front, hep-th/9702162.
- [195] C.J. Hamer, Nucl. Phys. B 121 (1977) 159.
- [196] C.J. Hamer, Nucl. Phys. B 132 (1978) 542.
- [197] C.J. Hamer, Nucl. Phys. B 195 (1982) 503.
- [198] K. Harada, A. Okazaki, M. Taniguchi, M. Yahiro, Phys. Rev. D 49 (1994) 4226–4245.
- [199] K. Harada, A. Okazaki, M. Taniguchi, Phys. Rev. D 52 (1995) 2429–2438.
- [200] K. Harada, A. Okazaki, Phys. Rev. D 55 (1997) 6198–6208.
- [201] K. Harada, A. Okazaki, M. Taniguchi, Phys. Rev. D 54 (1996) 7656–7663.
- [202] K. Harada, A. Okazaki, M. Taniguchi, Phys. Rev. D 55 (1997) 4910–4919.
- [203] A. Harindranath, J.P. Vary, Phys. Rev. D 36 (1987) 1141.
- [204] A. Harindranath, J.P. Vary, Phys. Rev. D 37 (1988) 1064–1069.
- [205] A. Harindranath, R.J. Perry, J. Shigemitsu, Ohio State preprint, 1991.
- [206] T. Heinzl, S. Krusche, E. Werner, B. Zeller mann, Phys. Lett. B 272 (1991) 54.
- [207] T. Heinzl, S. Krusche, E. Werner, Phys. Lett. B 256 (1991) 55.
- [208] T. Heinzl, S. Krusche, E. Werner, Nucl. Phys. A 532 (1991) 4290.
- [209] T. Heinzl, S. Krusche, S. Simburger, E. Werner, Z. Phys. C 56 (1992) 415.
- [210] T. Heinzl, S. Krusche, E. Werner, Phys. Lett. B 275 (1992) 410.
- [211] T. Heinzl, E. Werner, Z. Phys. C 62 (1994) 521–532.
- [212] T. Heinzl, Nucl. Phys. Proc. Suppl. B 39C (1995) 217–219.
- [213] T. Heinzl, Hamiltonian formulations of Yang-Mills quantum theory, the Gribov problem, hep-th/9604018.
- [214] T. Heinzl, Phys. Lett. B 388 (1996) 129–136.
- [215] T. Heinzl, Nucl. Phys. Proc. Suppl. A 54 (1997) 194–197.
- [216] S. Heppelmann, Nucl. Phys. B Proc. Suppl. 12 (1990) 159 and references therein.
- [217] J.E. Hetrick, Nucl. Phys. B 30 (1993) 228–231.
- [218] J.E. Hetrick, Int. J. Mod. Phys. A 9 (1994) 3153.
- [219] M. Heyssler, A.C. Kalloniatis, Phys. Lett. B 354 (1995) 453.
- [220] J.R. Hiller, Phys. Rev. D 43 (1991) 2418.

- [221] J.R. Hiller, *Phys. Rev. D* 44 (1991) 2504.
- [222] J.R. Hiller, S.J. Brodsky, Y. Okamoto (in progress).
- [223] J. Hiller, S.S. Pinsky, B. van de Sande, *Phys. Rev. D* 51 (1995) 726.
- [224] L.C.L. Hollenberg, K. Higashijima, R.C. Warner, B.H.J. McKellar, *Prog. Theor. Phys.* 87 (1991) 3411.
- [225] L.C.L. Hollenberg, N.S. Witte, *Phys. Rev. D* 50 (1994) 3382.
- [226] K. Hornbostel, S.J. Brodsky, H.C. Pauli, *Phys. Rev. D* 38 (1988) 2363.
- [227] K. Hornbostel, S.J. Brodsky, H.C. Pauli, *Phys. Rev. D* 41 (1990) 3814.
- [228] K. Hornbostel, *Constructing Hadrons on the Light Cone*, Workshop on From Fundamental Fields to Nuclear Phenomena, Boulder, CO, 20–22 September 1990; Cornell preprint CLNS 90/1038, 1990.
- [229] K. Hornbostel, Cornell Preprint CLNS 91/1078, August 1991.
- [230] K. Hornbostel, *Phys. Rev. D* 45 (1992) 3781.
- [231] S. Hosono, S. Tsujimaru, *Int. J. Mod. Phys. A* 8 (1993) 4627–4648.
- [232] S.Z. Huang, W. Lin, *Ann. Phys.* 226 (1993) 248–270.
- [233] T. Hyer, *Phys. Rev. D* 49 (1994) 2074–2080.
- [234] M. Ida, *Prog. Theor. Phys.* 51 (1974) 1521.
- [235] M. Ida, *Prog. Theor. Phys.* 54 (1975) 1199.
- [236] M. Ida, *Prog. Theor. Phys.* 54 (1975) 1519.
- [237] M. Ida, *Prog. Theor. Phys.* 54 (1975) 1775.
- [238] N. Isgur, C.H. Llewellyn Smith, *Phys. Rev. B* 217 (1989) 2758.
- [239] K. Itakura, *Phys. Rev. D* 54 (1996) 2853–2862.
- [240] K. Itakura, *Dynamical symmetry breaking in light front Gross-Neveu model*, UT-KOMABA-96-15, August 1996, 12pp. hep-th/9608062.
- [241] K. Itakura, S. Maedan, *Prog. Theor. Phys.* 97 (1997) 635–652.
- [242] C. Itzykson, J.B. Zuber, *Quantum Field Theory*, McGraw-Hill, New York, 1985.
- [244] J. Jackiw, in: A. Ali, P. Hoodbhoy (Eds.), *M.A.B. Bég Memorial Volume*, World Scientific, Singapore, 1991.
- [245] R. Jackiw, N.S. Manton, *Ann. Phys. (NY)* 127 (1980) 257.
- [246] W. Jaus, *Phys. Rev. D* 41 (1990) 3394.
- [247] J. Jersák, J. Stern, *Nucl. Phys. B* 7 (1968) 413.
- [248] J. Jersák, J. Stern, *Nuovo Cimento* 59 (1969) 315.
- [249] C.R. Ji, S.J. Brodsky, *Phys. Rev. D* 34 (1986) 1460; *D* 33 (1986) 1951, 1406, 2653.
- [250] X.D. Ji, *Comments Nucl. Part. Phys.* 21 (1993) 123–136.
- [251] C.R. Ji, *Phys. Lett. B* 322 (1994) 389–396.
- [252] C.R. Ji, G.H. Kim, D.P. Min, *Phys. Rev. D* 51 (1995) 879–889.
- [253] C.R. Ji, S.J. Rey, *Phys. Rev. D* 53 (1996) 5815–5820.
- [254] C.R. Ji, A. Pang, A. Szczepaniak, *Phys. Rev. D* 52 (1995) 4038–4041.
- [255] B.D. Jones, R.J. Perry, *Phys. Rev. D* 55 (1997) 7715–7730.
- [256] B.D. Jones, R.J. Perry, S.D. Glazek, *Phys. Rev. D* 55 (1997) 6561–6583.
- [257] J.W. Jun, C.K. Jue, *Phys. Rev. D* 50 (1994) 2939–2941.
- [258] A.C. Kalloniatis, H.C. Pauli, *Z. Phys. C* 60 (1993) 255.
- [259] A.C. Kalloniatis, H.C. Pauli, *Z. Phys. C* 63 (1994) 161.
- [260] A.C. Kalloniatis, D.G. Robertson, *Phys. Rev. D* 50 (1994) 5262.
- [261] A.C. Kalloniatis, H.C. Pauli, S.S. Pinsky, *Phys. Rev. D* 50 (1994) 6633.
- [262] A.C. Kalloniatis, *Phys. Rev. D* 54 (1996) 2876.
- [263] A.C. Kalloniatis, D.G. Robertson, *Phys. Lett. B* 381 (1996) 209–215.
- [264] M. KaluRza, H.C. Pauli, *Phys. Rev. D* 45 (1992) 2968.
- [265] M. KaluRza, H.-J. Pirner, *Phys. Rev. D* 47 (1993) 1620.
- [266] G. Karl, *Phys. Rev. D* 45 (1992) 247.
- [267] V.A. Karmanov, *Nucl. Phys. B* 166 (1980) 378.
- [268] V.A. Karmanov, *Nucl. Phys. A* 362 (1981) 331.
- [269] B.D. Keister, *Phys. Rev. C* 43 (1991) 2783–2790.
- [270] B.D. Keister, *Phys. Rev. D* 49 (1994) 1500–1505.

- [271] Y. Kim, S. Tsujimaru, K. Yamawaki, *Phys. Rev. Lett.* 74 (1995) 4771–4774; Erratum-ibid. 75 (1995) 2632.
- [272] D. KlabuRcar, H.C. Pauli, *Z. Phys. C* 47 (1990) 141.
- [273] J.R. Klauder, H. Leutwyler, L. Streit, *Nuovo Cimento* 59 (1969) 315.
- [274] J.B. Kogut, D.E. Soper, *Phys. Rev. D* 1 (1970) 2901.
- [275] J.B. Kogut, L. Susskind, *Phys. Rep. C* 8 (1973) 75.
- [276] S. Kojima, N. Sakai, T. Sakai, *Prog. Theor. Phys.* 95 (1996) 621–636.
- [277] J. Kondo, *Solid State Physics* 23 (1969) 183.
- [278] V.G. Koures, *Phys. Lett. B* 348 (1995) 170–177.
- [279] M. Krautgärtner, H.C. Pauli, F. Wölz, *Phys. Rev. D* 45 (1992) 3755.
- [280] A.D. Krisch, *Nucl. Phys. B (Proc. Suppl.) B* 25 (1992) 285.
- [281] H.R. Krishnamurthy, J.W. Wilkins, K.G. Wilson, *Phys. Rev. B* 21 (1980) 1003.
- [282] H. Kröger, R. Girard, G. Dufour, *Phys. Rev. D* 35 (1987) 3944.
- [283] H. Kröger, H.C. Pauli, *Phys. Lett. B* 319 (1993) 163–170.
- [284] A.S. Kronfeld, B. Nizic, *Phys. Rev. D* 44 (1991) 3445.
- [285] S. Krusche, *Phys. Lett. B* 298 (1993) 127–131.
- [286] W. Kwong, P.B. Mackenzie, R. Rosenfeld, J.L. Rosner, *Phys. Rev. D* 37 (1988) 3210.
- [289] P.V. Landshoff, *Phys. Rev. D* 10 (1974) 10241.
- [290] E. Langmann, G.W. Semenoff, *Phys. Lett. B* 296 (1992) 117.
- [291] A. Langnau, S.J. Brodsky, *J. Comput. Phys.* 109 (1993) 84–92.
- [292] A. Langnau, M. Burkardt, *Phys. Rev. D* 47 (1993) 3452–3464.
- [293] T.D. Lee, *Phys. Rev.* 95 (1954) 1329.
- [294] P. Lenz, F.J. Wegner, cond-mat/9604087; *Nucl. Phys. B* 482 (1996) 693.
- [295] F. Lenz, in: D. Vautherin, F. Lenz, J.W. Negele (Eds.), *Nonperturbative Quantum Field Theory*, Plenum Press, New York, 1990.
- [296] F. Lenz, M. Thies, S. Levit, K. Yazaki, *Ann. Phys.* 208 (1991) 1.
- [297] G.P. Lepage, S.J. Brodsky, *Phys. Lett. B* 87 (1979) 359.
- [298] G.P. Lepage, S.J. Brodsky, *Phys. Rev. Lett.* 43 (1979) 545, 1625 (E).
- [299] G.P. Lepage, S.J. Brodsky, *Phys. Rev. D* 22 (1980) 2157.
- [300] G.P. Lepage, S.J. Brodsky, T. Huang, P.B. Mackenzie, in: A.Z. Capri, A.N. Kamal (Eds.), *Particles and Fields 2*, Plenum Press, New York, 1983.
- [301] G.P. Lepage, B.A. Thacker, CLNS-87, 1987.
- [302] H. Leutwyler, *Acta Phys. Austriaca* 5 (Suppl.) (1968) 320.
- [303] H. Leutwyler, in: *Springer Tracts in Modern Physics*, Vol. 50, Springer, New York, 1969, p. 29.
- [304] H. Leutwyler, *Phys. Lett. B* 48 (1974) 45.
- [305] H. Leutwyler, *Phys. Lett. B* 48 (1974) 431.
- [306] H. Leutwyler, *Nucl. Phys. B* 76 (1974) 413.
- [307] H. Leutwyler, *J. Stern, Ann. Phys.* 112 (1978) 94.
- [308] H. Li, G. Sterman, *Nucl. Phys. B* 381 (1992) 129.
- [309] N.E. Ligterink, B.L.G. Bakker, *Phys. Rev. D* 52 (1995) 5917–5925.
- [310] N.E. Ligterink, B.L.G. Bakker, *Phys. Rev. D* 52 (1995) 5954–5979.
- [311] J. Lowenstein, A. Swieca, *Ann. Phys. (NY)* 68 (1971) 172.
- [312] W. Lucha, F.F. Schöberl, D. Gromes, *Phys. Rep.* 200 (1991) 127.
- [313] M. Luke, A.V. Manohar, M.J. Savage, *Phys. Lett. B* 288 (1992) 355.
- [314] M. Lüscher, *Nucl. Phys. B* 219 (1983) 233.
- [315] Y. Ma, J.R. Hiller, *J. Comp. Phys.* 82 (1989) 229.
- [316] B.Q. Ma, *J. Phys. G* 17 (1991) L53.
- [317] B.Q. Ma, Qi-Ren Zhang, *Z. Phys. C* 58 (1993) 479.
- [318] B.Q. Ma, *Z. Physik A* 345 (1993) 321–325.
- [319] B.Q. Ma, The proton spin structure in a light cone quark spectator diquark model, hep-ph/9703425.
- [320] N. Makins et al., NE-18 Collaboration, MIT preprint, 1994.

- [321] N.S. Manton, *Ann. Phys. (NY)* 159 (1985) 220.
- [322] G. Martinelli, C.T. Sachrajda, *Phys. Lett. B* 217 (1989) 319.
- [323] J.C. Maxwell, *Treatise on Electricity and Magnetism*, 3rd ed., 2 Vols., reprint by Dover, New York, 1954.
- [324] T. Maskawa, K. Yamawaki, *Prog. Theor. Phys.* 56 (1976) 270.
- [325] G. McCartor, *Z. Phys. C* 41 (1988) 271.
- [326] G. McCartor, *Z. Phys. C* 52 (1991) 611.
- [327] G. McCartor, D.G. Robertson, *Z. Phys. C* 53 (1992) 679.
- [328] G. McCartor, D.G. Robertson, *Z. Physik C* 62 (1994) 349–356.
- [329] G. McCartor, *Z. Physik C* 64 (1994) 349–354.
- [330] G. McCartor, D.G. Robertson, *Z. Physik C* 68 (1995) 345–351.
- [331] G. McCartor, D.G. Robertson, S. Pinsky, Vacuum structure of 2D gauge theories on the light front, hep-th/96112083.
- [332] H.J. Melosh, *Phys. Rev. D* 9 (1974) 1095.
- [333] A. Messiah, *Quantum Mechanics*, 2 Vols., North-Holland, Amsterdam, 1962.
- [334] G.A. Miller, *Phys. Rev. C* 56 (1997) 8–11.
- [335] J.A. Minahan, A.P. Polychronakos, *Phys. Lett. B* 326 (1994) 288.
- [336] A. Misra, *Phys. Rev. D* 53 (1996) 5874–5885.
- [337] P.M. Morse, H. Feshbach, *Methods of Theoretical Physics*, 2 Vols., McGraw-Hill, New York, 1953.
- [338] Y. Mo, R.J. Perry, *J. Comp. Phys.* 108 (1993) 159.
- [339] D. Mustaki, S. Pinsky, J. Shigemitsu, K. Wilson, *Phys. Rev. D* 43 (1991) 3411.
- [340] D. Mustaki, S. Pinsky, *Phys. Rev. D* 45 (1992) 3775.
- [341] D. Mustaki, Bowling Green State Univ. preprint, 1994.
- [342] T. Muta, *Foundations of Quantum Chromodynamic: Lecture Notes in Physics*, vol. 5, World Scientific, Singapore, 1987.
- [343] O. Nachtmann, *Elementarteilchenphysik*, Vieweg, Braunschweig, 1986.
- [344] T. Nakatsu, K. Takasaki, S. Tsujimaru, *Nucl. Phys. B* 443 (1995) 155–200.
- [345] J.M. Namyslowski, *Prog. Part. Nuc. Phys.* 74 (1984) 1.
- [346] E. Noether, *Kgl. Ges. d. Wiss. Nachrichten, Math.-phys. Klasse*, Göttingen, 1918.
- [347] Y. Nakawaki, *Prog. Theor. Phys.* 70 (1983) 1105.
- [348] H.W.L. Naus, H.J. Pirner, T.J. Fields, J.P. Vary, QCD near the light cone, hep-th/9704135
- [349] A. Ogura, T. Tomachi, T. Fujita, *Ann. Phys.* 237 (1995) 12–45.
- [350] H. Osborn, *Nucl. Phys. B* 80 (1974) 90.
- [351] Particle Data Group, *Phys. Rev. D* 45 (1992) 1.
- [352] H.C. Pauli, *Nucl. Phys. A* 396 (1981) 413.
- [353] H.C. Pauli, *Z. Phys. A* 319 (1984) 303.
- [354] H.C. Pauli, S.J. Brodsky, *Phys. Rev. D* 32 (1985) 1993.
- [355] H.C. Pauli, S.J. Brodsky, *Phys. Rev. D* 32 (1985) 2001.
- [356] H.C. Pauli, *Nucl. Phys. A* 560 (1993) 501.
- [357] H.C. Pauli, in: B. Geyer, E.M. Ilgenfritz (Eds.), *Quantum Field Theoretical Aspects of High Energy Physics*, Naturwissenschaftlich Theoretisches Zentrum der Universität, Leipzig, 1993.
- [358] H.C. Pauli, A.C. Kalloniatis, S.S. Pinsky, *Phys. Rev. D* 52 (1995) 1176.
- [359] H.C. Pauli, J. Merkel, *Phys. Rev. D* 55 (1997) 2486–2496.
- [360] H.C. Pauli, R. Bayer, *Phys. Rev. D* 53 (1996) 939.
- [361] H.C. Pauli, Solving gauge field theory by discretized light-cone quantization, Heidelberg Preprint MPIH-V25-1996, hep-th/9608035.
- [362] H.C. Pauli, in: B.N. Kursunoglu, S. Mintz, A. Perlmutter (Eds.), *Neutrino Mass, Monopole Condensation, Dark matter, Gravitational waves, Light-Cone Quantization*, Plenum Press, New York, 1996, pp. 183–204.
- [363] R.J. Perry, A. Harindranath, K.G. Wilson, *Phys. Rev. Lett.* 65 (1990) 2959.
- [364] R.J. Perry, A. Harindranath, *Phys. Rev. D* 43 (1991) 4051.
- [365] R.J. Perry, *Phys. Lett. B* 300 (1993) 8.

- [366] R.J. Perry, K.G. Wilson, *Nucl. Phys. B* 403 (1993) 587.
- [367] R.J. Perry, Hamiltonian light-front field theory and quantum chromodynamics, *Hadron 94*, Gramado, Brasil, April 1994.
- [368] R.J. Perry, *Ann. Phys.* 232 (1994) 116–222.
- [369] V.N. Pervushin, *Nucl. Phys. B* 15 (1990) 197.
- [370] I. Pesando, *Mod. Phys. Lett. A* 10 (1995) 525–538.
- [371] I. Pesando, *Mod. Phys. Lett. A* 10 (1995) 2339–2352.
- [372] S.S. Pinsky, *Proc. 4th Conf. on the Intersections between Particle and Nuclear Physics*. Tucson, AZ, May 1991, World Scientific, Singapore, 1991.
- [373] S.S. Pinsky, *Proc. Division of Particles and Fields of the APS*, Vancouver, B.C., Canada, 18–22 August 1991, World Scientific, Singapore.
- [374] S.S. Pinsky, in: J. Tran Thanh Van (Ed.), *Proc. 27th Rencontre de Moriond*, Les Arcs, Savoie, France, 22–28 March, 1992, Editions Frontieres, Dreux.
- [375] S.S. Pinsky, *Proc. Orbis Scientiae*, 25–27 January 1993, Coral Gables, FL, Nova Science.
- [376] S.S. Pinsky, in: S. Dubnicka, A. Dubnickova (Eds.), *Proc. “Hadron Structure ’93”* Banska Stiavnica Slovakia, 5–10 September 1993, Institute of Physics, Slovak Academy of Science.
- [377] S.S. Pinsky, in: St. Glazek (Ed.), *Proc. Theory of Hadrons and Light-Front QCD* Polona Zgorzelisko Poland, August 1994, World Scientific, Singapore.
- [378] S.S. Pinsky, *Proc. Orbis Scientiae*, 25–28 January 1996, Coral Gables FL, Nova Science.
- [379] S.S. Pinsky, R. Mohr, *Proc. Conf. on Low Dimensional Field Theory*, Telluride Summer Research Institute, August 1996; *Int. J. of Mod. Phys. A*, to appear.
- [380] S.S. Pinsky, Wilson loop on a Light-cone cylinder, hep-th/9702091.
- [381] S. Pinsky, *Phys. Rev. D* 56 (1997) 5040–5049.
- [382] S.S. Pinsky, B. van de Sande, *Phys. Rev. D* 49 (1994) 2001.
- [383] S.S. Pinsky, A.C. Kalloniatis, *Phys. Lett. B* 365 (1996) 225–232.
- [384] S.S. Pinsky, D.G. Robertson, *Phys. Lett. B* 379 (1996) 169–178.
- [385] E.V. Prokhvatilov, V.A. Franke, *Sov. J. Nucl. Phys.* 49 (1989) 688.
- [386] J. Przeszowski, H.W.L. Naus, A.C. Kalloniatis, *Phys. Rev. D* 54 (1996) 5135–5147.
- [387] S.G. Rajeev, *Phys. Lett. B* 212 (1988) 203.
- [388] D.G. Robertson, G. McCartor, *Z. Phys. C* 53 (1992) 661.
- [389] D.G. Robertson, *Phys. Rev. D* 47 (1993) 2549–2553.
- [390] F. Rohrlich, *Acta Phys. Austriaca VIII (Suppl.)* (1971) 2777.
- [391] R.E. Rudd, *Nucl. Phys. B* 427 (1994) 81–110.
- [392] M. Sawicki, *Phys. Rev. D* 32 (1985) 2666.
- [393] M. Sawicki, *Phys. Rev. D* 33 (1986) 1103.
- [394] H. Sazdjian, *J. Stern, Nucl. Phys. B* 94 (1975) 163.
- [395] F. Schlumpf, *Phys. Rev. D* 47 (1993) 4114.
- [396] F. Schlumpf, *Phys. Rev. D* 48 (1993) 4478.
- [397] F. Schlumpf, *Mod. Phys. Lett. A* 8 (1993) 2135.
- [398] F. Schlumpf, *J. Phys. G* 20 (1994) 237.
- [399] N.C.J. Schoonderwoerd, B.L.G. Bakker, Equivalence of renormalized covariant and light front perturbation theory, 11pp. hep-ph/9702311, February 1997.
- [400] S. Schweber, *Relativistic Quantum Field Theory*, Harper and Row, New York, 1961.
- [401] J. Schwinger, *Phys. Rev.* 125 (1962) 397.
- [402] J. Schwinger, *Phys. Rev.* 128 (1962) 2425.
- [403] M.A. Shifman, A.I. Vainshtein, V.I. Zakharov, *Nucl. Phys. B* 147 (1979) 38.
- [404] S. Simula, *Phys. Lett. B* 373 (1996) 193–199.
- [405] C.M. Sommerfield, Yale preprint July, 1973.
- [406] D.E. Soper, Ph.D Thesis, 1971; SLAC Report No. 137, 1971.
- [407] M.G. Sotiropoulos, G. Sterman, *Nucl. Phys. B* 425 (1994) 489.
- [408] P.P. Srivastava, *Nuovo Cim. A* 107 (1994) 549–558.

- [409] P. Stoler, *Phys. Rev. Lett.* 66 (1991) 1003.
- [410] T. Sugihara, M. Matsuzaki, M. Yahiro, *Phys. Rev. D* 50 (1994) 5274–5288.
- [411] T. Sugihara, M. Yahiro, *Phys. Rev. D* 53 (1996) 7239–7249.
- [412] T. Sugihara, M. Yahiro, *Phys. Rev. D* 55 (1997) 2218–2226.
- [413] K. Sundermeyer, *Constrained Dynamics*, Springer, New York, 1982.
- [414] L. Susskind, G. Frye, *Phys. Rev.* 164 (1967) 2003.
- [415] L. Susskind, *Phys. Rev.* 165 (1968) 1535.
- [416] L. Susskind, Stanford preprint SU-ITP-97-11, April 1997, hep-th/9704080; hep-th/9611164.
- [418] A. Szczepaniak, E.M. Henley, S.J. Brodsky, *Phys. Lett. B* 243 (1990) 287.
- [419] A. Szczepaniak, L. Mankiewicz, Univ. of Florida Preprint, 1991.
- [420] A. Tam, C.J. Hamer, C.M. Yung, *J. Phys. G* 21 (1995) 1463–1482.
- [421] I. Tamm, *J. Phys. (USSR)* 9 (1945) 449.
- [422] A.C. Tang, S.J. Brodsky, H.C. Pauli, *Phys. Rev. D* 44 (1991) 1842.
- [423] M. Tachibana, *Phys. Rev. D* 52 (1995) 6008–6015.
- [424] G. 't Hooft, Published in *Erice Subnucl. Phys.* (1975) 261.
- [425] M. Thies, K. Ohta, *Phys. Rev. D* 48 (1993) 5883–5894.
- [426] C.B. Thorn, *Phys. Rev. D* 19 (1979) 639.
- [427] C.B. Thorn, *Phys. Rev. D* 20 (1979) 1934.
- [428] T. Tomachi, T. Fujita, NUP-A-91-10, September 1991, 45pp.
- [429] U. Trittmann, H.C. Pauli, Heidelberg preprint MPI H-V4-1997, January. 1997, hep-th/9704215.
- [430] U. Trittmann, H.C. Pauli, Heidelberg preprint MPI H-V7-1997, April 1997, hep-th/9705021.
- [431] U. Trittmann, Heidelberg preprint MPI H-V17-1997, April 1997, hep-th/9705072.
- [432] W.K. Tung, *Phys. Rev.* 176 (1968) 2127.
- [433] W.K. Tung, *Group Theory in Physics*, World Scientific, Singapore, 1985.
- [434] P. van Baal, *Nucl. Phys. B* 369 (1992) 259.
- [435] B. van de Sande, S. Pinsky, *Phys. Rev. D* 46 (1992) 5479.
- [436] B. van de Sande, S.S. Pinsky, *Phys. Rev. D* 49 (1994) 2001.
- [437] B. van de Sande, M. Burkardt, *Phys. Rev. D* 53 (1996) 4628.
- [438] B. van de Sande, *Phys. Rev. D* 54 (1996) 6347.
- [439] B. van de Sande, S. Dalley, *Orbis Scientiae: Neutrino Mass, Dark Matter, Gravitational Waves, Condensation of Atoms, Monopoles, Light-Cone Quantization*, Miami Beach, FL, 25–28 January 1996.
- [440] J.B. Swenson, J.R. Hiller, *Phys. Rev. D* 48 (1993) 1774.
- [441] S. Tsujimaru, K. Yamawaki, MPI H-V19-1997, April 1997, 47pp., hep-th/9704171.
- [442] J.P. Vary, T.J. Fields, H.J. Pirner, ISU-NP-94-14, August 1994. 5pp., hep-ph/9411263.
- [443] J.P. Vary, T.J. Fields, H.-J. Pirner, *Phys. Rev. D* 53 (1996) 7231–7238.
- [444] F.J. Wegner, *Phys. Rev. B* 5 (1972) 4529.
- [445] F.J. Wegner, *Phys. Rev. B* 6 (1972) 1891.
- [446] F.J. Wegner, in: C. Domb, M.S. Green (Eds.), *Phase Transitions and Critical Phenomena*, vol. 6, Academic Press, London, 1976.
- [447] F.J. Wegner, *Annalen Physik* 3 (1994) 77.
- [448] S. Weinberg, *Phys. Rev.* 150 (1966) 1313.
- [449] H. Weyl, *Z. Phys.* 56 (1929) 330.
- [450] E. Wigner, *Ann. Math.* 40 (1939) 149.
- [451] K.G. Wilson, *Phys. Rev. B* 140 (1965) 445.
- [452] K.G. Wilson, *Phys. Rev. D* 2 (1970) 1438.
- [453] K.G. Wilson, *Rev. Mod. Phys.* 47 (1975) 773.
- [454] K.G. Wilson, in: A. Perlmutter (Ed.), *New Pathways in High Energy Physics*, vol. II, Plenum Press, New York, 1976, pp. 243–264.
- [455] K.G. Wilson, in: R. Petronzio et al. (Eds.) *Proc. Int. Symp. Capri, Italy, 1989* [*Nucl. Phys. B (Proc. Suppl.)* 17 (1989)].
- [456] K.G. Wilson, T.S. Walhout, A. Harindranath, W.M. Zhang, R.J. Perry, S.D. Glazek, *Phys. Rev. D* 49 (1994) 6720–6766.

- [457] R.S. Wittman, in: M.B. Johnson, L.S. Kisslinger (Eds.), *Nuclear and Particle Physics on the Light Cone*, World Scientific, Singapore, 1989.
- [458] J.J. Wivoda, J.R. Hiller, *Phys. Rev. D* 47 (1993) 4647.
- [459] P.M. Wort, Carleton University preprint, February 1992.
- [460] C.M. Yung, C.J. Hamer, *Phys. Rev. D* 44 (1991) 2598.
- [461] W.M. Zhang, A. Harindranath, *Phys. Rev. D* 48 (1993) 4868–4880.
- [462] W.M. Zhang, A. Harindranath, *Phys. Rev. D* 48 (1993) 4881.
- [463] W.M. Zhang, A. Harindranath, *Phys. Rev. D* 48 (1993) 4903.
- [464] W.M. Zhang, *Phys. Lett. B* 333 (1994) 158–165.
- [465] W.M. Zhang, G.L. Lin, C.Y. Cheung, *Int. J. Mod. Phys. A* 11 (1996) 3297–3306.
- [466] W.M. Zhang, *Phys. Rev. D* 56 (1997) 1528–1548.
- [467] D.C. Zheng, J.P. Vary, B.R. Barret, *Nucl. Phys. A* 560 (1993) 211.
- [468] A.R. Zhitnitskii, *Phys. Lett. B* 165 (1985) 405.
- [469] G. Zweig, CERN Reports Th. 401 and 412, 1964; in: A. Zichichi (Ed.), *Proc. Int. School of Phys. Ettore Majorana*, Erice, Italy, 1964, Academic, New York, p. 192.